

Resilient Repair Guide Source Report: Case Study Annex

Prepared by

APPLIED TECHNOLOGY COUNCIL
201 Redwood Shores Parkway, Suite 240
Redwood City, California 94065
www.ATCouncil.org

Prepared for

FEDERAL EMERGENCY MANAGEMENT AGENCY
Michael Mahoney, Project Officer
William T. Holmes, Technical Monitor
Washington, D.C.

APPLIED TECHNOLOGY COUNCIL
Jon A. Heintz, Project Executive and Project Manager
Chiara McKenney, Assistant Project Manager

PROJECT TECHNICAL COMMITTEE

Ken Elwood (Project Tech. Director)
Nic Brooke
Gregory G. Deierlein
Abbie Liel
Santiago Pujol Llano
James Malley
Jack P. Moehle
Bill Tremayne
John Wallace

PROJECT REVIEW PANEL

Santiago Pujol Llano
James Malley

WORKING GROUP

Saman Abdullah
Vishvendra (Jay) Bhanu
Ryo Kuwabara
Donovan Llanes
Kai Marder
Gonzalo Munoz
Polly Murray
Eyitayo Opabola
Matias Rojas Leon
Amir Safiey
Mehdi Sarrafzadeh
Prateek Shah
Tomomi Suzuki



FEMA



Notice

Any opinions, findings, conclusions, or recommendations expressed in this publication do not necessarily reflect the views of the Applied Technology Council (ATC), the Department of Homeland Security (DHS), or the Federal Emergency Management Agency (FEMA). Additionally, neither ATC, DHS, FEMA, nor any of their employees, makes any warranty, expressed or implied, nor assumes any legal liability or responsibility for the accuracy, completeness, or usefulness of any information, product, or process included in this publication. Users of information from this publication assume all liability arising from such use.

Cover photograph – N/A

Table of Contents

ES.	Executive Summary	ES-1
ES.0	Overview	ES-1
ES.1	Case Study 1: Five-Story Building, E-Defense	ES-1
ES.2	Case Study 2: Eight-Story Building, Wellington	ES-2
ES.3	Findings and Recommendations.....	ES-2
Case Study 1: Five-Story Building, E-Defense	1-1	
1	Introduction	1-1
2	Building Description	2-1
2.1	Configurations and Material Properties.....	2-1
3	Test Details.....	3-1
3.1	Input ground motion.....	3-1
3.2	Repair Methodology.....	3-3
3.3	Response of the Structure.....	3-6
4	Inspection and Analysis Phase	4-1
4.1	Preliminary Inspection	4-2
4.2	Analysis.....	4-9
4.3	Summary	4-27
5	Safety-assessment Phase	5-1
5.1	System Check.....	5-2
5.2	Component Check	5-2
5.3	Fatigue Check.....	5-4
5.4	Concentrated Damage Check	5-14
5.5	Summary	5-14
6.	Serviceability Assessment.....	6-1
6.1	Drift Estimate	6-2
6.2	Repair Recommendations.....	6-4
7.	Conclusions and Recommendations.....	7-1
7.1	Inspection Locations.....	7-1
7.2	Drift Estimation of a Damaging Earthquake	7-1
7.3	System and Component Check for the Safety Assessment	7-2
7.4	Fatigue Check.....	7-2
7.5	Drift Estimation of a Damaged and Repaired Structure	7-2
Appendix A	Repair Technique	A-1
Appendix B	Material Properties	B-1
Appendix C	Hysteresis Response of the building	C-1
Appendix D	Visual Inspection.....	D-1
D.1	Crack Patterns	D-1
D.2	Maximum Residual Crack Width.....	D-6
Appendix E	ATC-38 Completed Form	E-1
Appendix F	Detail Assumptions for the Analysis Procedure.....	F-1
F.1	Material Properties	F-1

F.2	Stiffness	F-1
F.3	Joint Model	F-4
F.4	Spring Model	F-7
F.5	Damping	F-10
F.6	Modification Factor for the Linear Dynamic Procedure (LDP).....	F-10
F.7	Equivalent Ductility.....	F-14
Appendix G	DCR Estimates	G-1
G.1	Linear Model	G-1
G.2	Modified Linear Model.....	G-8
Appendix H	Ductility demand and m-factors	H-1
H.1	Linear Model	H-1
H.2	Modified Linear Model.....	H-17
Appendix I	Stiffness Reduction Factors	I-1
Appendix J	Visual Inspection After Run4	J-1
Appendix K	Damping Identification.....	K-1
K.1	Singular Value	K-1
K.2	SDOF PSD Bell Function.....	K-3
K.3	Correlation Function.....	K-5
K.4	Damping Ratio.....	K-7
Appendix L	Alternative Approach of Inspection Locations.....	L-1
Appendix M	FEMA P-58 Fragility Database	M-1
References	N-1

Case Study 2: Eight-Story Building, Wellington 1-1

1	Introduction.....	1-1
1.1	Summary.....	1-1
2	Building Description.....	2-1
3	Seismic Event	3-1
3.1	Ground Motion Recording Sources	3-1
4	Inspection and Analysis Phase.....	4-1
4.1	Preliminary Inspection.....	4-1
5	Safety Assessment Phase.....	5-1
5.1	System Check	5-1
5.2	Component Checks.....	5-1
6	Serviceability Assessment	6-1
6.1	Drift Check	6-1
6.2	Repair Recommendations.....	6-5
7	Conclusions and Recommendations	7-1
7.1	Recommendations for Future Study	7-2
Appendix A	ATC-38 Completed Form.....	A-1
Appendix B	Frame Damage Elevations.....	B-1
Appendix C	Frame Visual Inspections	C-1
References	D-1

Executive Summary

ES.0 Overview

The two case study buildings have completed an iteration through the ATC-145-1 Source Report (ATC, 2020) assessment framework, including inspection, analysis, safety-assessment and serviceability-assessment phases. Both buildings are classified as essentially conforming reinforced concrete special moment resisting frames. A summary of key findings for each building, recommendations and next steps are as follow.

ES.1 Case Study 1: Five-Story Building, E-Defense

The building was subjected to a peak story drift demand of approximately 2% on the E-Defense shake table. The moment frames generally exhibited strong-column/weak-beam response, with typical beam ductility demands in the damaged bays ranging from 3 to 4.

A reasonable agreement between the recorded and estimated (by analysis) drifts was achieved. The estimated ductility demands on individual components (beams and columns) suggested more extensive damage than was observed. This resulted in a conservative number of Inspection Locations.

The FEMA P-58, *Seismic Performance Assessment of Buildings*, fragility curves (FEMA, 2019) for special reinforced concrete moment frames are not sufficiently refined to correlate observed component damage with estimated and measured drifts when drift demands are less than 2%. Improvements have been subsequently developed and evaluated in Case Study 2 (see ES.2).

The building satisfied the safety-assessment checks, including the Simplified and Detailed fatigue assessment procedures per Appendix C of the Source Report.

The damaged building did not satisfy the 1% serviceability drift limit, although this was readily satisfied in the pre-damage condition. Thus, repair was triggered per the framework. Epoxy injection reduced the estimated serviceability drift by approximately 40%, and the building was found to

comply with the 1% serviceability drift limit. This was generally consistent with the observed performance from testing.

ES.2 Case Study 2: Eight-Story Building, Wellington

The building was subjected to estimated peak story drift demands of 1.3 to 2% by the 2016 Kaikoura earthquake. The moment frames generally exhibited strong-column/weak-beam response, with typical beam ductility demands in the damaged bays ranging from 3 to 5.

No ground motion data was available at the building site, and demands were estimated by applying the response spectra from the two nearest strong ground motion recording stations with similar soil classification.

Fragility curves were used to infer drift demands based upon the observed damage at each beam-column joint. As identified by Case Study 1, modification of the FEMA P-58 concrete moment frame fragility curve (FEMA, 2019) was recommended. The curve was modified by adding DS 0.5 to fill the gap between “no observed damage” (0% drift) and DS 1 (2% drift). This modified approach gave drift estimates that were in reasonable agreement with those estimated by analysis and overall damage patterns observed by inspection.

Similar to Case Study 1, the estimated ductility demands by analysis on individual components (beams and columns) suggested more extensive damage than was observed by inspection, particularly on the longitudinal frames. This resulted in a conservative number of Inspection Locations. The ductility demands indicated that many of the beams were between the Immediate Occupancy and primary Life Safety acceptance criteria per ASCE/SEI 41 (ASCE, 2017).

Further modification of the Inspection Location triggers was developed to ensure that components with relatively high strength DCR's (i.e., ductility demand) but low story drifts (i.e., < 1%) were not missed from the visual inspection scope.

The building satisfied the safety-assessment checks, including the Simplified fatigue assessment procedure per Appendix C of the Source Report.

Serviceability drift demands on the damaged frames increased by 50 to 100%, based on the reduced frame stiffness accounting for estimated ductility demand on each component. This was primarily influenced by the extensive beam hinging. The damaged building did not satisfy the NZS 1170.5 (Standard New Zealand, 2004) serviceability drift limit of 0.5%; however, it should be noted that the building did not satisfy this limit in the

pre-damage condition and it was unlikely to have been a requirement at the time of the building's design and construction.

Epoxy injection was estimated to reduce the maximum serviceability drifts to approximately 0.8% (approximately 25% higher than the pre-damage condition.) As the undamaged building did not satisfy the drift limit; thus, epoxy injection alone was insufficient to achieve compliance with the serviceability drift limit specified by the applicable building regulations. Thus, more complex repair or strengthening measures are required if the building is to satisfy the serviceability drift limit.

There was limited opportunity to test the use of non-structural damage to infer drift demand. Based on limited documentation of partition damage and FEMA P-58 fragility functions (FEMA, 2019), drifts at the center of building were estimated in the range of 0.7 to 1.0%. This was slightly lower than the drift demands estimated by analysis.

ES.3 Findings and Recommendations

A summary of findings and recommendations with regard to the ATC-145-1 Source Report assessment framework for conforming reinforced concrete moment frames are as follow:

1. ASCE/SEI 41 analysis methods can be used to achieve a reasonable estimate of peak deformation demands and identification of where yielding is likely to have occurred. At least one round of reconciliation between observation and analysis results should be assumed to improve correlation.
2. Where ground motion input is not available at the base of structure, the user should consider applying nearby recordings with similar soil site characteristics and estimating results based on a combination of demands (e.g., average).
3. Demand-capacity ratio (DCR) based on strength is a very conservative means of determining the onset of visual damage for deformation-controlled actions. This arrives at a conservative estimate of visual Inspection Locations.
4. The Inspection Location criteria should be updated to include drift and ductility criteria, as proposed via Case Study 2, to reduce the number of Inspection Locations in areas where damage is unlikely to have occurred for a conforming reinforced concrete special moment resisting frame.
5. The FEMA P-58 fragility function for conforming reinforced concrete frames is too coarse to effectively estimate drift demands when the

damage is less than Damage State 1 (2% drift.) No damage is rationally expected at 0% drift.

6. To address this issue, it is proposed to define an intermediate damage state: DS 0.5. This damage state has an expected drift of 1% and covers the range between “no observed damage” (0% drift) and DS 1 (2% drift.) Note that 1% drift is also associated with a low probability (10%) of the component being at DS 1. This intermediate damage state was found to improve the correlation between estimated drift and observed damage for Case Study 1 and 2.
7. The fatigue assessment procedures will benefit from the development of a spreadsheet tool to help with the implementation of the Simplified method per Appendix C of the Source Report.
8. Structures subject to moderate and extensive ductility demands (i.e., distributed hinging) can be expected to exhibit significantly more flexible response at future service level earthquakes. Epoxy repair alone may not be sufficient to restore serviceability performance; however, this is highly dependent upon the serviceability criteria, including hazard and drift criteria, specified by the Authority Having Jurisdiction or applicable building regulations.

Case Study 1

Chapter 1

Introduction

This case study report is intended to provide detailed guidance for application of ATC-145 (ATC, 2020) post-earthquake assessment procedure. The reliability of ATC-145 assessment procedures were investigated using a test building, a five-story reinforced concrete building. At the end of this report, recommendations on use of ATC-145 assessment procedure are provided in a conclusion section. Additionally, improved approaches are also discussed in this report. Brief descriptions of each chapter are shown as below.

Chapter 2: Building Description

This chapter describes detailed information of a test building, such as configuration of a building, sectional configuration of components, reinforcement details and material properties.

Chapter 3: Test Details

Input ground motions, repair methodology and test results are described in this chapter.

Chapter 4: Inspection and Analysis Phase

In this chapter, approaches for visual inspection and story drift estimation are investigated. For the inspection phase, a definition of damage state is illustrated to determine damage level of structures. For drift estimate, visual-inspection-based approach and analytical approaches were discussed.

Chapter 5: Safety Assessment Phase

System check procedure was applied to a test building in this chapter. Detailed fatigue assessment procedures were discussed in addition to drift and component rotation check.

Chapter 6: Serviceability Assessment Phase

Serviceability assessment procedure was applied to a test building in this chapter. Drift estimates of both a damaged and a repaired structure were

investigated. Numerical modelling procedure of a repaired building is also provided.

Chapter 7: Conclusions and Recommendations

Conclusions and recommendations found through this case study are provided.

Building Description

An experiment used in this study was a shake table test conducted at the E-Defense facility in Japan in 2020. A specimen was a five-story reinforced concrete moment-resisting frame structure and tested dynamically. Once it was tested, the specimen was repaired with the epoxy injection and mortar patching and tested again. This test shows the difference in the performance of structure between the undamaged state and repaired state. Further detailed information of the test is described in the following section.

2.1 Configurations and Material Properties

The configuration of the specimen is shown in Figure 2-2. The specimen was designed following the Japanese design standard (AIJ, 2010), but was scaled down to 80% in order to fit on the shake table. The lateral force resisting system of the building consists of three 6.0 m wide two bay frames in the X direction, and three 3.0 m wide two bay frames in the Y direction. The frames had detailing equivalent to special moment frames in ACI 318 (ACI, 2014) and the section and reinforcement detailing for the columns is shown in Table 2-1 and the section and reinforcement detailing for the beams is shown in Table 2-2. The material properties are shown in Table 2-3 and Table 2-4 Table B-2. The design strength of concrete was 33 MPa for all the parts of structure. The material tests were conducted 28 days following concrete casting as well as 2 weeks before the test.



Figure 2-1 Overall view of the specimen.

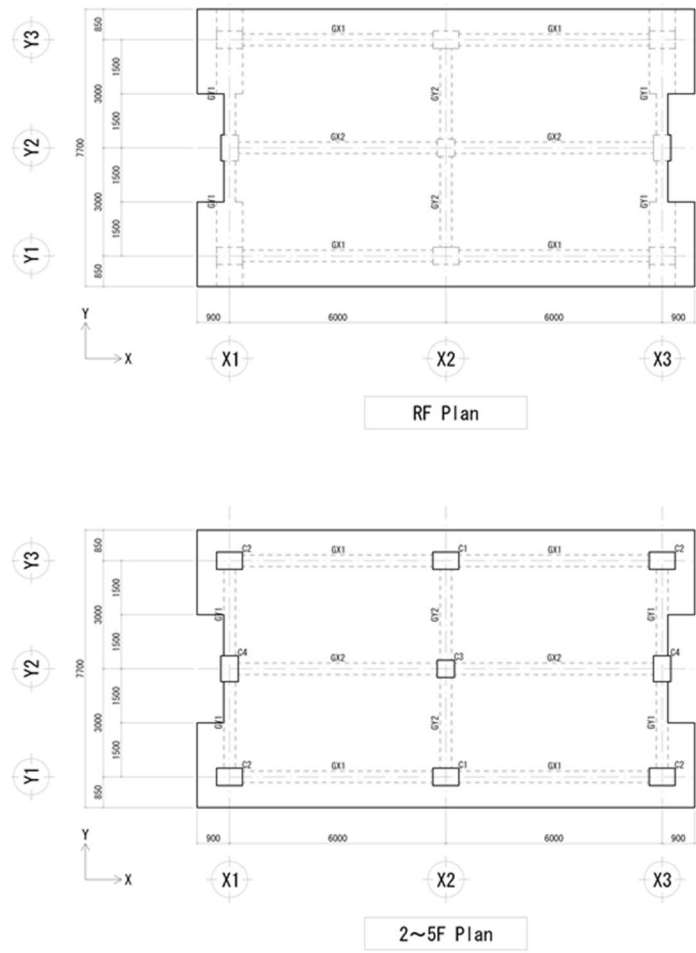
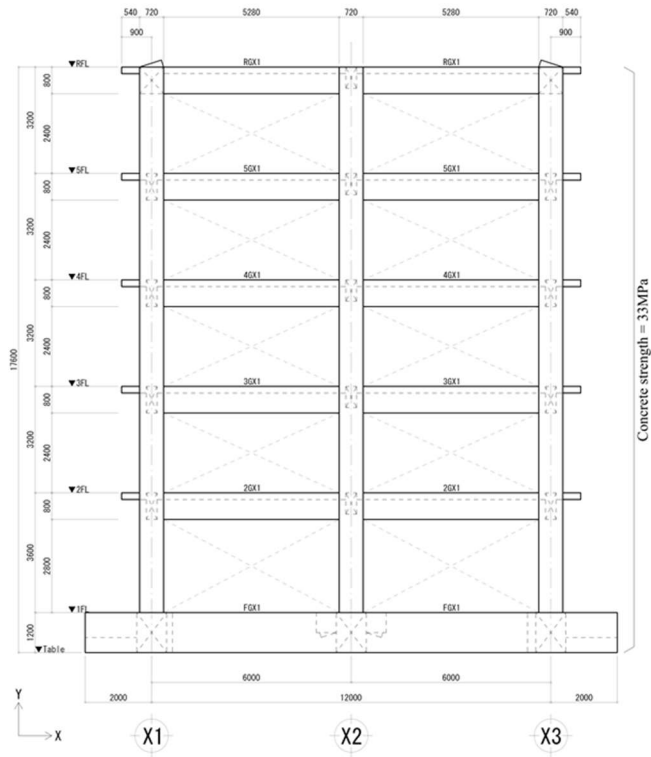
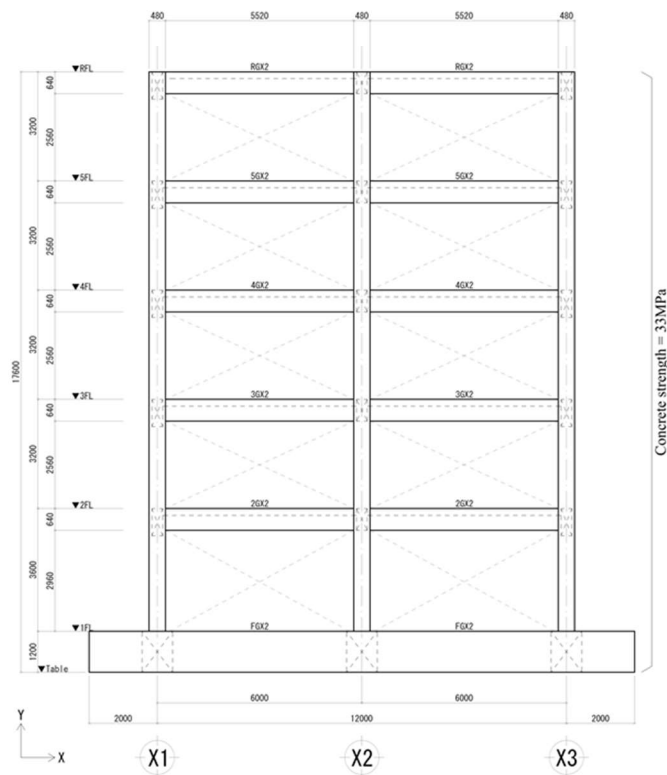


Figure 2-2 Configuration of the specimen.



Y1, Y3 Frame



Y2 Frame

Figure 2-2(cont.) Configuration of the specimen.

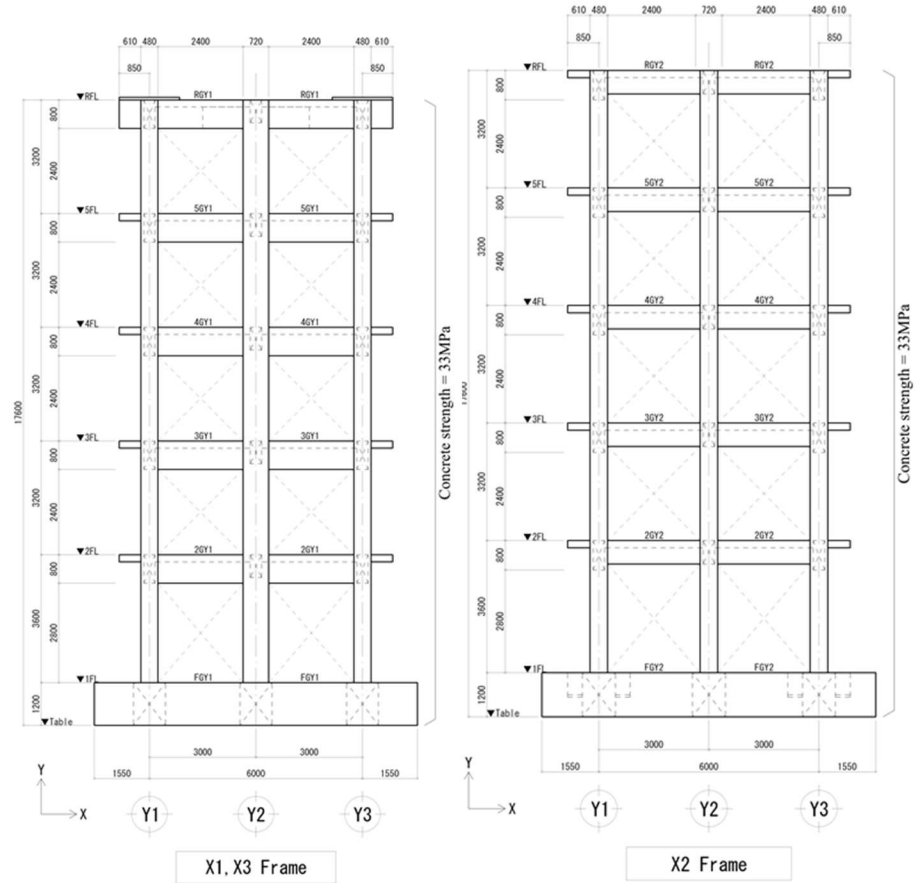


Figure 2-2(cont.) Configuration of the specimen.

Table 2-1 Cross Section (Column)

	GX1	GX2	GY1		GY2	
RF	▼RFL			Outside 	Inside 	
	b × D	320 × 800	320 × 640	720 × 800	320 × 800	320 × 640
	Top bar	2 - D19	2 - D19	6 - D19	2 - D19	2 - D19
	Bottom bar	2 - D19	2 - D19	4 - D19	2 - D19	2 - D19
	Stirrup	2 - D10 @200	2 - D10 @200	2 - D10 @200	2 - D10 @200	2 - D10 @200
5F	▼5FL					
	b × D	320 × 800	320 × 640	720 × 800	320 × 640	
	Top bar	3 - D19	3 - D19	6 - D19	2 - D19	
	Bottom bar	3 - D19	3 - D19	4 - D19	2 - D19	
	Stirrup	2 - D10 @200	2 - D10 @200	2 - D10 @200	2 - D10 @200	
4F	▼4FL					
	b × D	320 × 800	320 × 640	720 × 800	320 × 640	
	Top bar	6 - D19	4 - D19	6 - D19	2 - D19	
	Bottom bar	6 - D19	4 - D19	4 - D19	2 - D19	
	Stirrup	2 - D10 @200	2 - D10 @200	2 - D10 @200	2 - D10 @200	
3F	▼3FL					
	b × D	320 × 800	320 × 640	720 × 800	320 × 640	
	Top bar	8 - D19	4 - D19	6 - D19	2 - D19	
	Bottom bar	8 - D19	4 - D19	4 - D19	2 - D19	
	Stirrup	2 - D10 @200	2 - D10 @200	2 - D10 @200	2 - D10 @200	
2F	▼2FL					
	b × D	320 × 800	320 × 640	720 × 800	320 × 640	
	Top bar	8 - D19	4 - D19	6 - D19	2 - D19	
	Bottom bar	8 - D19	4 - D19	4 - D19	2 - D19	
	Stirrup	2 - D10 @200	2 - D10 @200	2 - D10 @200	2 - D10 @200	

Table 2-2 Cross Section (Beam)

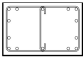
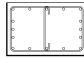
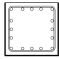
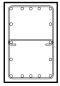
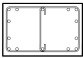
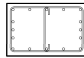
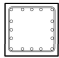

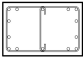
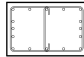
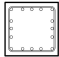
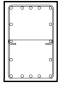
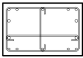
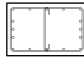
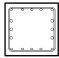
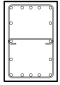
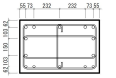
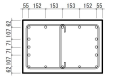
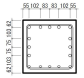
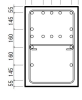
	C1	C2	C3	C4
5F				
Dx × Dy	720 × 480	720 × 480	480 × 480	480 × 720
Long. bar	12 - D25, 2 - D22	16 - D22	16 - D25	16 - D22
Hoop (X)	2 - D10 @75	2 - D10 @75	2 - D10 @75	3 - D10 @75
Hoop (Y)	3 - D10 @75	3 - D10 @75	2 - D10 @75	2 - D10 @75
4F				
Dx × Dy	720 × 480	720 × 480	480 × 480	480 × 720
Long. bar	12 - D25, 2 - D22	16 - D22	16 - D25	16 - D22
Hoop (X)	2 - D10 @75	2 - D10 @75	2 - D10 @75	3 - D10 @75
Hoop (Y)	3 - D10 @75	3 - D10 @75	2 - D10 @75	2 - D10 @75
3F				
Dx × Dy	720 × 480	720 × 480	480 × 480	480 × 720
Long. bar	12 - D25, 2 - D22	16 - D22	16 - D25	16 - D22
Hoop (X)	2 - D10 @75	2 - D10 @75	2 - D10 @75	3 - D10 @75
Hoop (Y)	3 - D10 @75	3 - D10 @75	2 - D10 @75	2 - D10 @75
2F				
Dx × Dy	720 × 480	720 × 480	480 × 480	480 × 720
Long. bar	12 - D25, 2 - D22	16 - D22	16 - D25	16 - D22
Hoop (X)	3 - D10 @75	2 - D10 @75	2 - D10 @75	3 - D10 @75
Hoop (Y)	3 - D10 @75	3 - D10 @75	2 - D10 @75	2 - D10 @75
1F				
Dx × Dy	720 × 480	720 × 480	480 × 480	480 × 720
Long. bar	12 - D25, 2 - D22	16 - D22	16 - D25	16 - D22
Hoop (X)	4 - D10 @75	2 - D10 @75	2 - D10 @75	3 - D10 @75
Hoop (Y)	3 - D10 @75	3 - D10 @75	2 - D10 @75	2 - D10 @75

Table 2-3 Mechanical Properties of Concrete

Compression Strength f'_c (MPa)	Tensile Strength f_t (MPa)	Young's Modulus E_c (MPa)	Shear Modulus G (MPa)	Poisson's ratio ν	Weight γ_c (t/m ³)
41.2	3.98	30168	12067	0.2	2.3

Table 2-4 Mechanical Properties of Steel

Steel grade	Diameter	Yield Strength f_y (MPa)	Ultimate Strength f_u (MPa)	Young's Modulus E_s (MPa)	Shear Modulus G (MPa)	Poisson's ratio ν	Weight γ_s (t/m ³)
SD295A	D10	376.1	514.8	205000	79000	0.3	7.85
	D13	338.7	477.9				
SD345	D19	401.2	567.6				
	D22	404.2	573.8				
	D25	396.5	567.3				
SD390	D38	450.6	642.5				

The basic concept of the excitation plan and input ground motion is described in this section and shown in Figure 3-3. The intensity of ground motion of each Run was determined to obtain target behavior in both the original and repair tests. Four ground motions in the original specimen and three ground motions in the repair test were applied. The main concept of the original test was to make the structure damaged with four input ground motions, ranging from service-level to design level. Run 1 was intended for the cracking point of the members, Run 2 was for the yielding point, and Run 3 was intended to replicate design level shaking. Run 4 was then applied to measure the response of the damaged structure if subjected to a second time to the design level input ground motion. After Run 4, the specimen was repaired and tested again. Run 5 and Run 6 were also targeted cracking and yielding of the structure, respectively. Run 7 was intended for the ultimate state of the structure (Figure 3-3).

3.1 Input Ground Motion

The input ground motion used during testing was the El Centro NS component, which was fitted to the design spectra in Japanese standard. The time step was then multiplied by $\sqrt{0.8}$ considering the scaling of the specimen. The input wave was applied uni-directionally in the longitudinal direction (X direction) only. The time history and the acceleration spectra of the input motion with 5.0% damping are shown in Figure 3-1 and Figure 3-2, respectively.

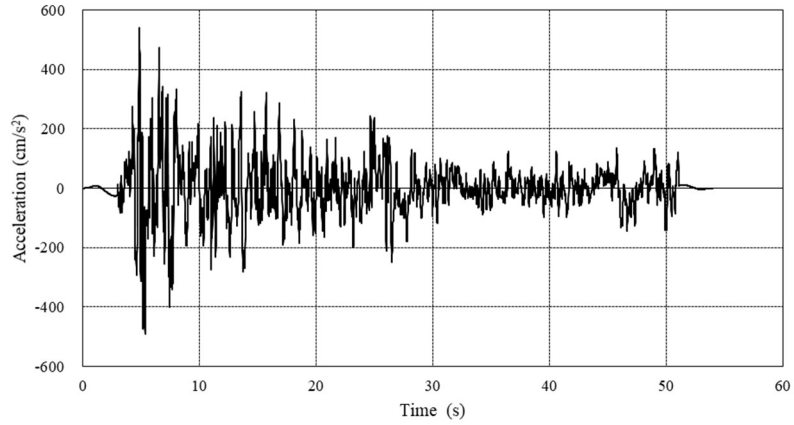


Figure 3-1 Time history of fitted El Centro NS wave (100%).

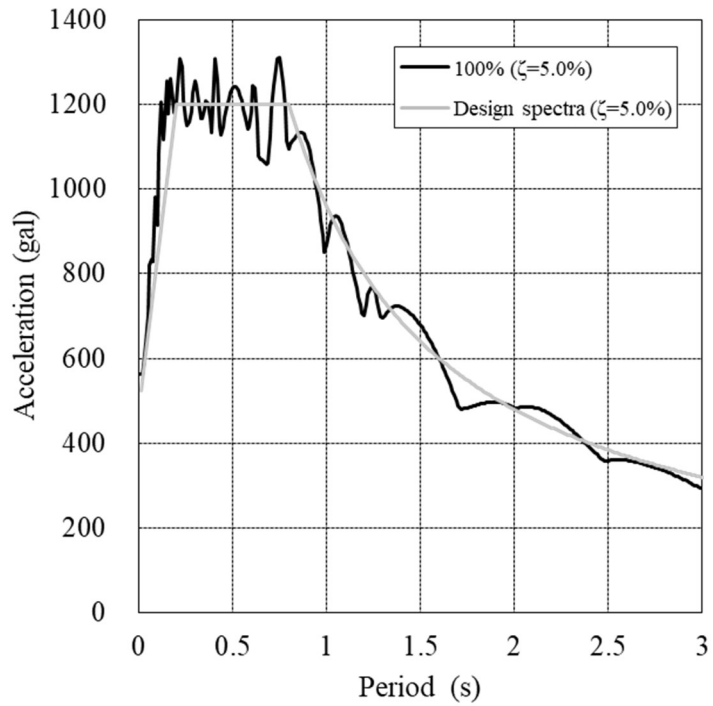


Figure 3-2 Acceleration spectrum of the input motion with 5.0% damping.

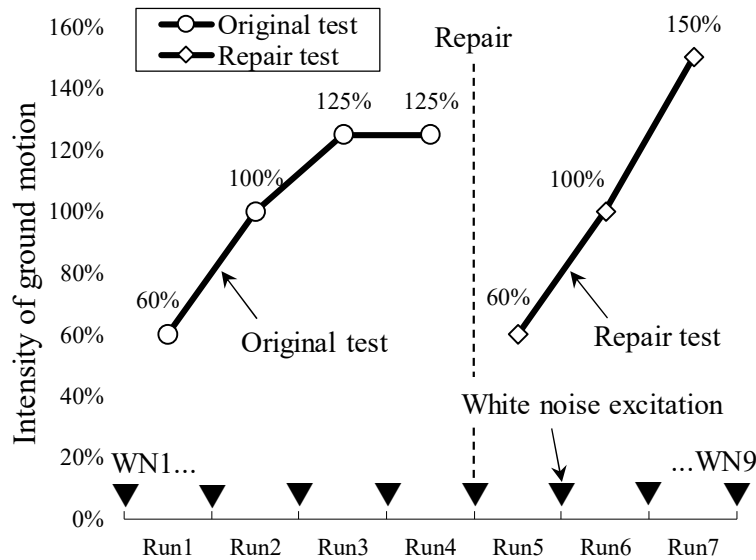


Figure 3-3 Excitation plan.

3.2 Repair Methodology

The concept of the repair was to determine the ability of a simple repair methodology to recover the original structural capacity. In this test, the specimen was repaired with epoxy injection and mortar patching. The scope of the repair was the plastic hinge zone of each component and beam-column joints. In order to simplify the repair work, the plastic hinge length of each member was defined as 1.0 m from the face of the beam-column joint. However, repair was not always contained to this 1.0 m distance because if the cracks straddle the plastic hinge region, the epoxy resin also penetrated into the cracks out of this range.

The repair technique was able to inject down to 0.05 mm cracks. Therefore, basically all the cracks in the plastic hinge zone and the beam-column joint were repaired.

Figure 3-4 illustrates the areas where the repair was applied. Each beam, column and beam-column joint was repaired up to the third floor level. On the fourth floor level, beams were repaired only at the critical section, and beam-column joints were repaired in the same way as the lower floors. Due to the time restriction between tests, the fourth and fifth stories were not repaired. As the drift demands in these stories were less 1.0% during the previous Runs, it was deemed acceptable to leave these stories un-repaired.

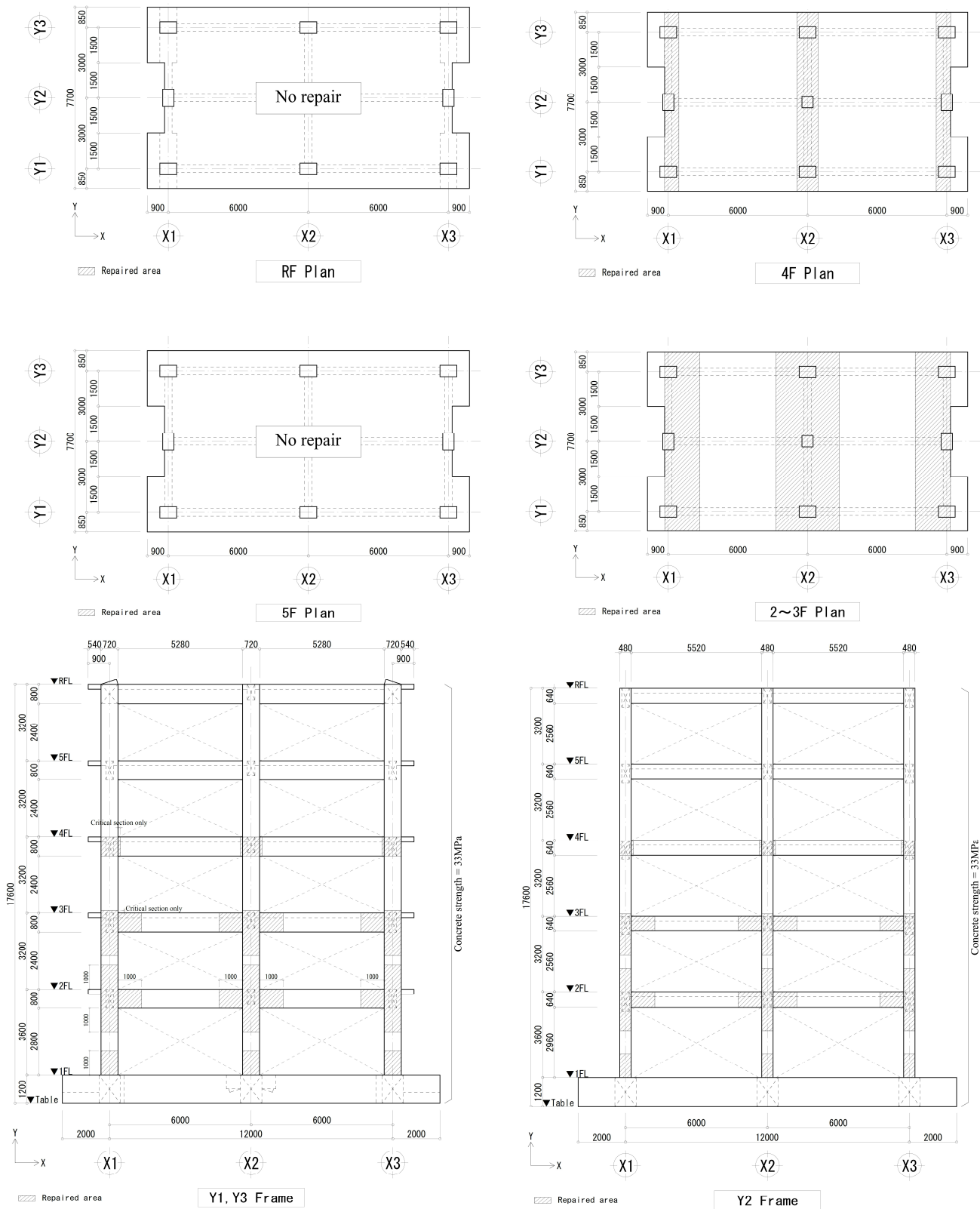


Figure 3-4 Repaired area in test building.

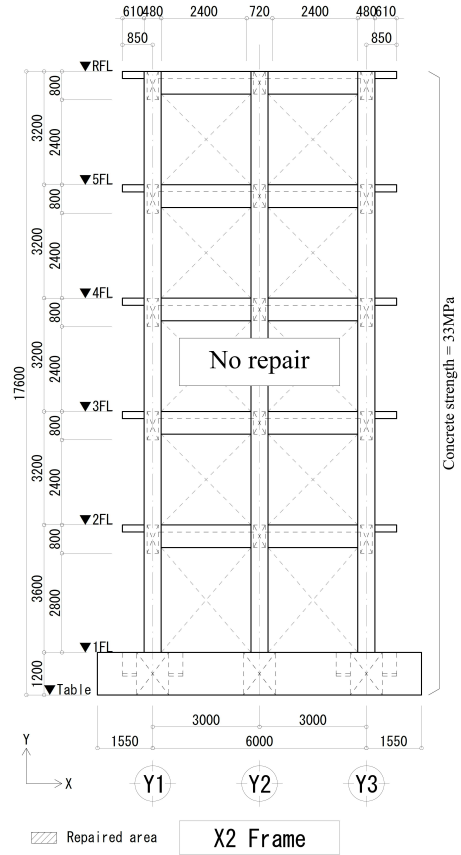
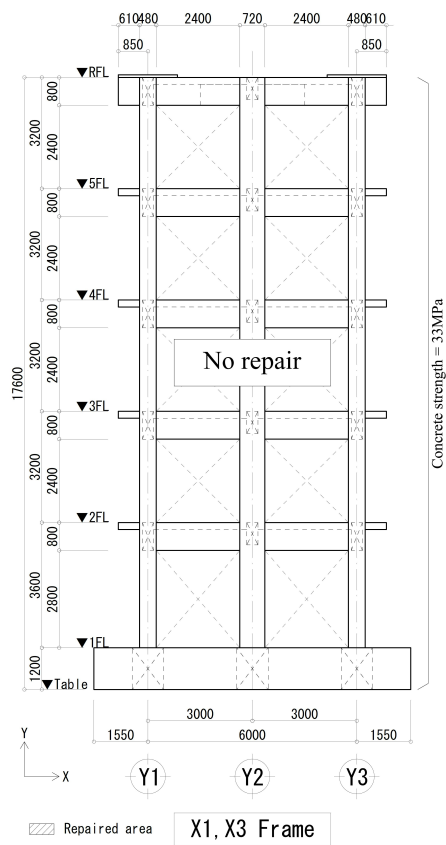


Figure 3-4(cont) Repaired area in test building.

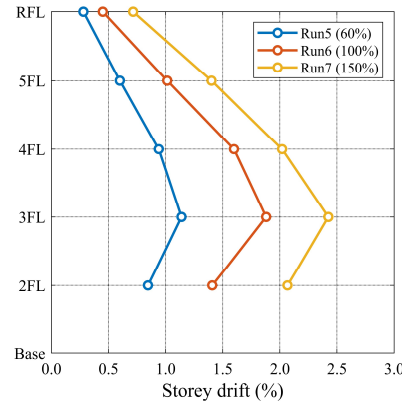
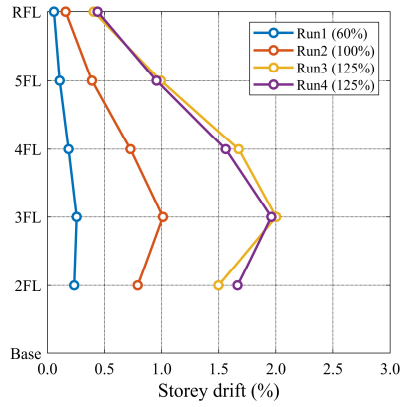


Figure 3-5 Epoxy injection and mortar patch.

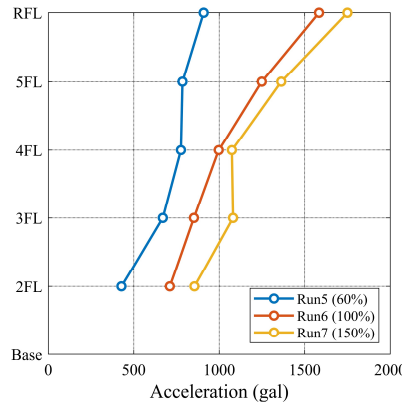
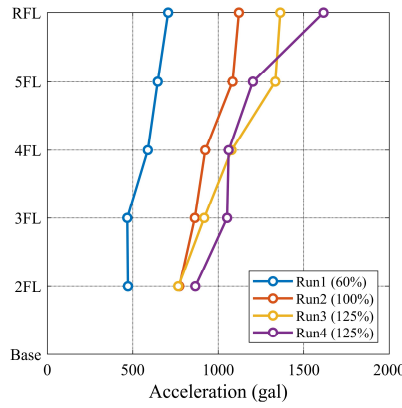
3.3 Response of the Structure

This section provides peak story responses of the building to each excitation. Figure 3-6 shows peak system-level response profiles in both the original and repair test. Figure 3-6 (a) shows peak story drift profiles. The original test started with 60% input (service-level) and experienced up to 125% (Design-level). The maximum peak story drift was 2.0% at 2FL with 125% input. The building was then repaired and 60% input was applied to start off the repair test. Peak story drift against 60% was approximately 1.1% at 2FL. Comparing peak story drifts of both the original and repaired buildings, it was obvious that peak story drift of the repaired building was significantly increased due to stiffness degradation. Subsequently, 100% and 150% input were applied, and peak story drifts were approximately 1.9% and 2.4%, respectively. Interestingly, peak story drift of the repaired building with 150% was not such significant compared to that of the original building with 125%. Figure 3-6 (b) shows peak acceleration responses. In the original test, peak floor acceleration increased with increase of intensity of ground motion and reached at approximately 1600 gal at RFL with 125% input. In the repair

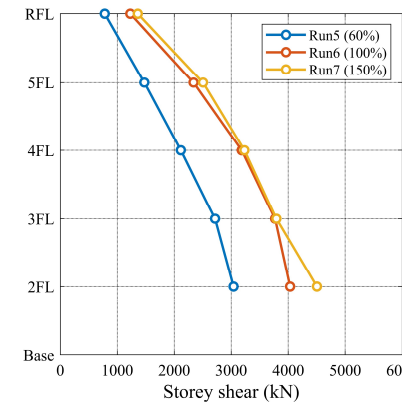
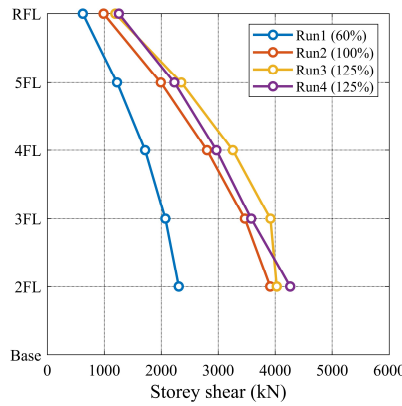
test, peak floor acceleration reached at 1600 gal at RFL with 100% and reached at 1800 gal at RFL with 150%. Figure 3-6 (c), (d) show peak story shear and story shear coefficient, respectively. In the original test, similar story shear distributions were observed after Run 1. This result means the building started yielding with Run 2 (100%). Similarly, this story shear of Run 6 (100%) and Run 7 (100%) as the building started showing inelastic response. In the story shear coefficient profile, it was observed that base shear coefficient of the original building was approximately 0.5 and increased up to 0.9. Run 2-4 exhibited the approximately same base shear coefficient of 0.9. Story shear coefficient of the original building was mostly inverse triangle distribution in Run 2-3. In the repair test, base shear coefficient was 0.6 in Run 5, and close to 1.0 in Run 6 and 7. In Run 6 and 7, it was seen that story shear coefficient increased on especially upper stories. Hysteresis responses of the building are provided in Appendix C.



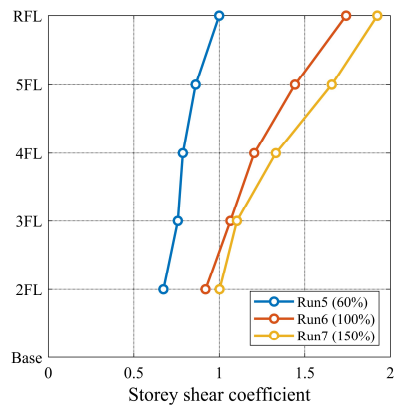
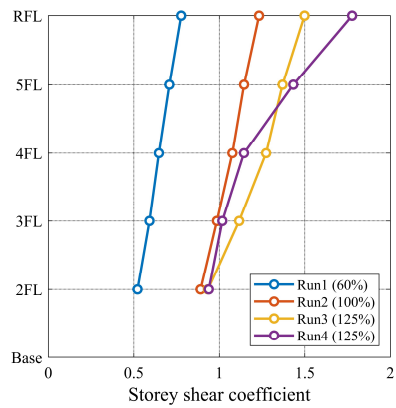
(a) Peak story drift



(b) Peak floor acceleration



(c) Peak story shear



(d) Peak story shear coefficient

Figure 3-6 System responses in each excitation.

Case Study 1
Chapter 4

Inspection and Analysis Phase

The proposed Inspection and Analysis Phase, per ATC-145-1 (ATC, 2020), illustrated in the flowchart in Figure 4-1, was used to evaluate the case study specimen in order to benchmark the procedure and provide detailed feedback on its use. The tested building was assessed with the damage inspection criteria to estimate the damage level of the building, and the estimated damage level was used for validation of the analytical drift estimation by using fragility functions.

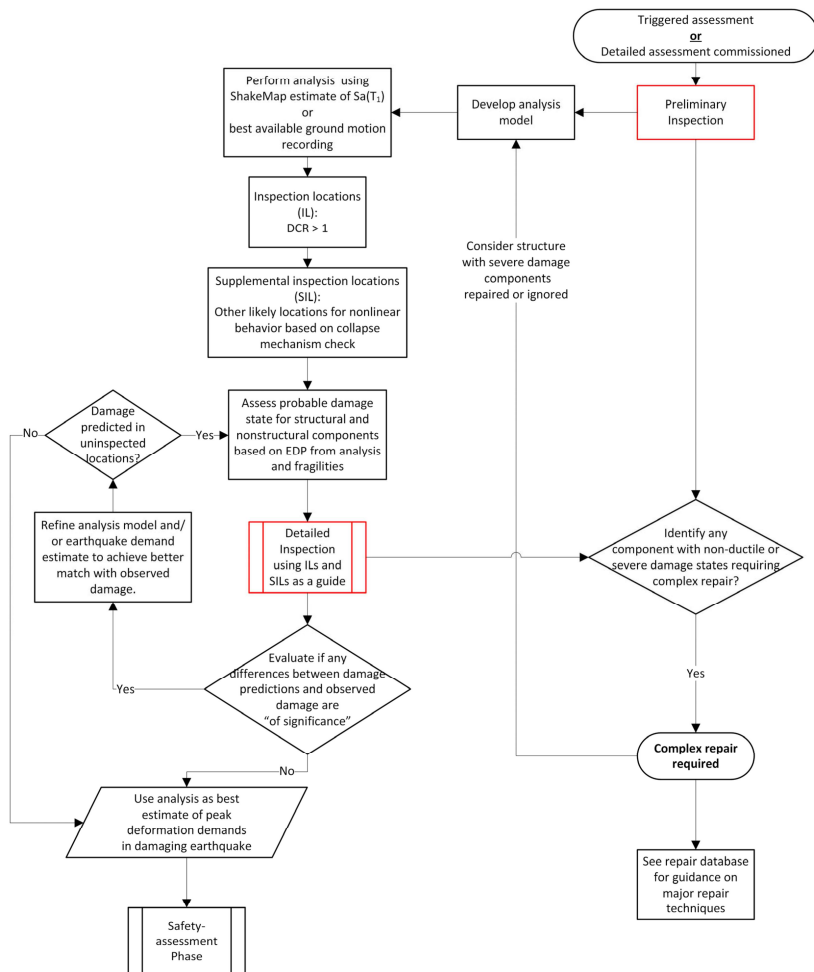


Figure 4-1 Inspection and analysis phase.

4.1 Preliminary Inspection

As the frame of the test specimen was detailed similarly to the Special Moment Frame requirement ACI 318 (ACI, 2014), damage states were evaluated in accordance with the damage indices in FEMA-P58-3 (FEMA, 2019) as shown in Table 4-1. Damage State 0 (DS0) is defined as essentially undamaged. Once maximum crack width exceeds 1.5mm, damage state is categorized as Damage State 1 (DS1). Damage State 2-4 (DS2-4) are defined by the degree of concrete spalling/ crushing and reinforcing bars. It is important to note that DS3 and DS4 are mutually exclusive and that either may occur following DS2, with the main difference being the fracture or buckling of longitudinal reinforcement and crushing of core concrete in present in DS3 but not in DS4.

Additionally, DS0.5 was introduced during the development of the case study, as an intermediate damage state between DS0 and DS1, since the gradation of damage and median drift between DS0 (un-damaged, 0% drift) and DS1 (crack widths > 1.5 mm, 2% drift) is quite coarse. Median drift corresponding to DS0.5 is assumed equal to 1.0%, with crack widths less than or equal to 1.5 mm.

	DS0	DS0.5	DS1	DS2	DS3	DS4
Median drift	0%	1.00%	2.00%	2.50%	2.75%	2.75%
Residual crack width	← ≤ 1.5mm →			← > 1.5mm →		
Cover spalling				← →		
Exposure of trasverse reinforcement				← →		
Exposure of longitudinal reinforcement				← →		
Core cruching/ Bar buckling/ Bar fracture				← →		
Damage description			"Beams or joints exhibit residual crack width > 1.5 mm. No significant spalling. No fracture or buckling of reinforcing"	"Beams and joints exhibits residual crack width > 1.5 mm. Spalling of cover concrete exposes beam and joint transverse reinforcement but not longitudinal reinforcement. No fracture or buckling of reinforcing."	"Beams and joints exhibits residual crack width > 1.5 mm. Spalling of cover concrete exposes a significant length of beam longitudinal reinforcement. Crushing of core concrete may occur. Fracture or buckling of reinforcing requiring replacement may occur."	"Beams and joints exhibits residual crack width > 1.5 mm. Spalling of cover concrete exposes beam and joint transverse reinforcement but not longitudinal reinforcement. No fracture or buckling of reinforcing."

Figure 4-2 shows FEMA P-58 fragility function and corresponding damage state. This fragility function is used for drift estimation based on visual

inspection. Once the damage state of a component is established, peak story drift demand is estimated as the average of the median drifts for each inspected component on a common frame line at the same story (i.e., DS1 for all components of a frame line at the same story, implies a story drift of 2.0%).

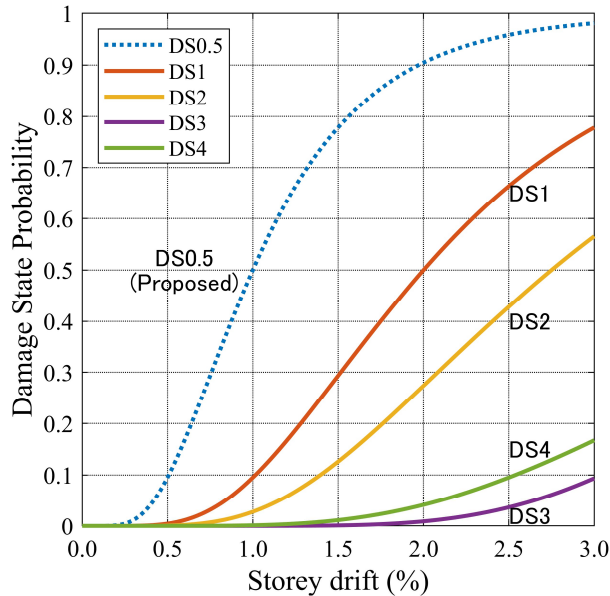
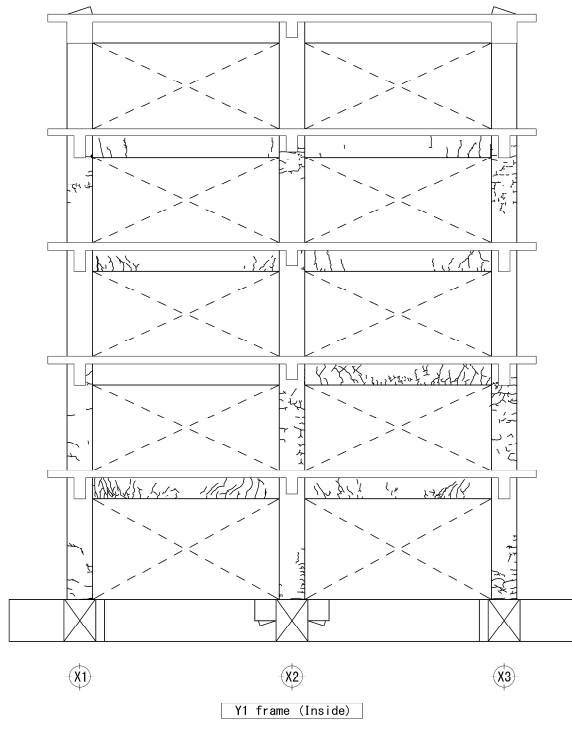


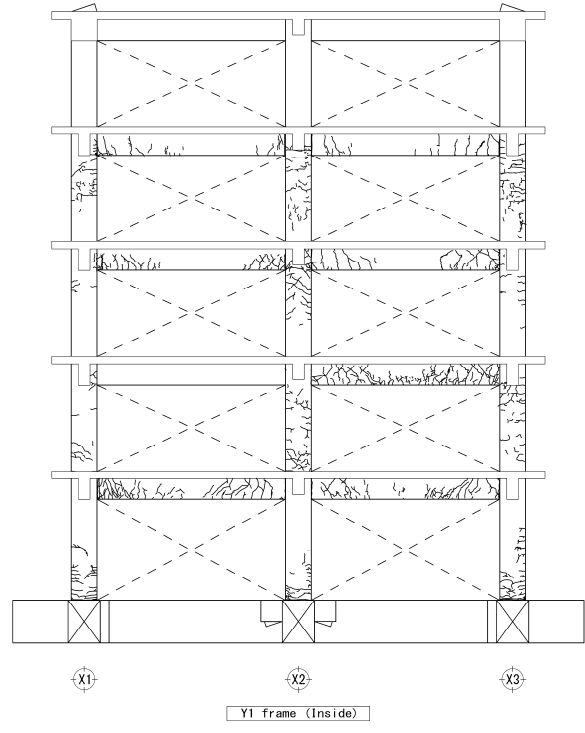
Figure 4-2 FEMA P-58 fragility curves and proposed intermediate damage state.

4.1.1 Visual Observation

Figure 4-3 shows crack patterns observed in the test and Figure 4-4 shows maximum residual crack width in the test. Crack width highlighted represents crack width exceeding DS1 crack width criterion (1.5 mm). In the Figure 4-4, story drift demand measured in the test and story drift estimated with the fragility function is also shown. Damage State shown in the joints are estimated by taking the maximum Damage State of beams and columns around the joint. Median story drifts of each joint’s Damage States were then averaged at each floor level. This averaged drift was taken as the estimated story drift demand. As seen, the figure indicates that story drift demands per fragility function reasonably correlates with measured story drift demands in the test.

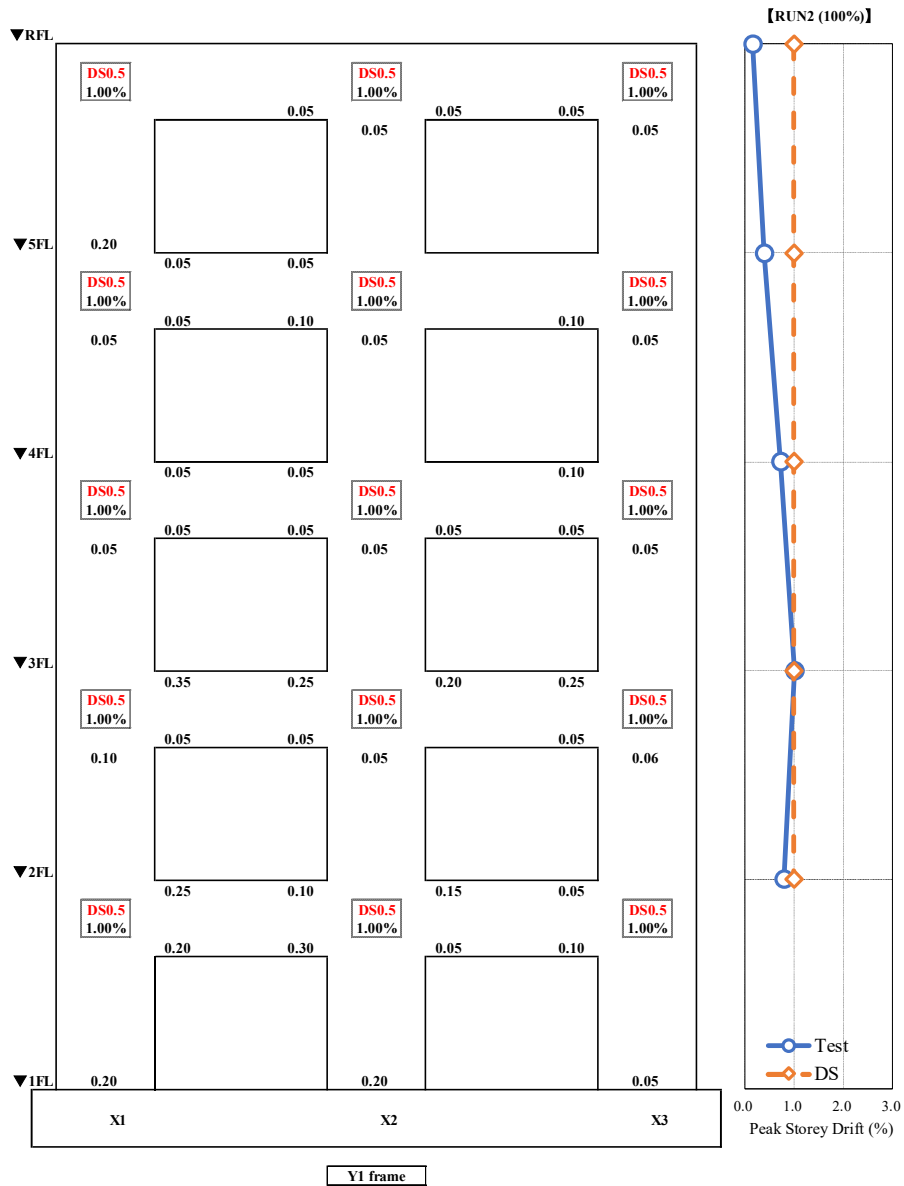


(a) Run 2



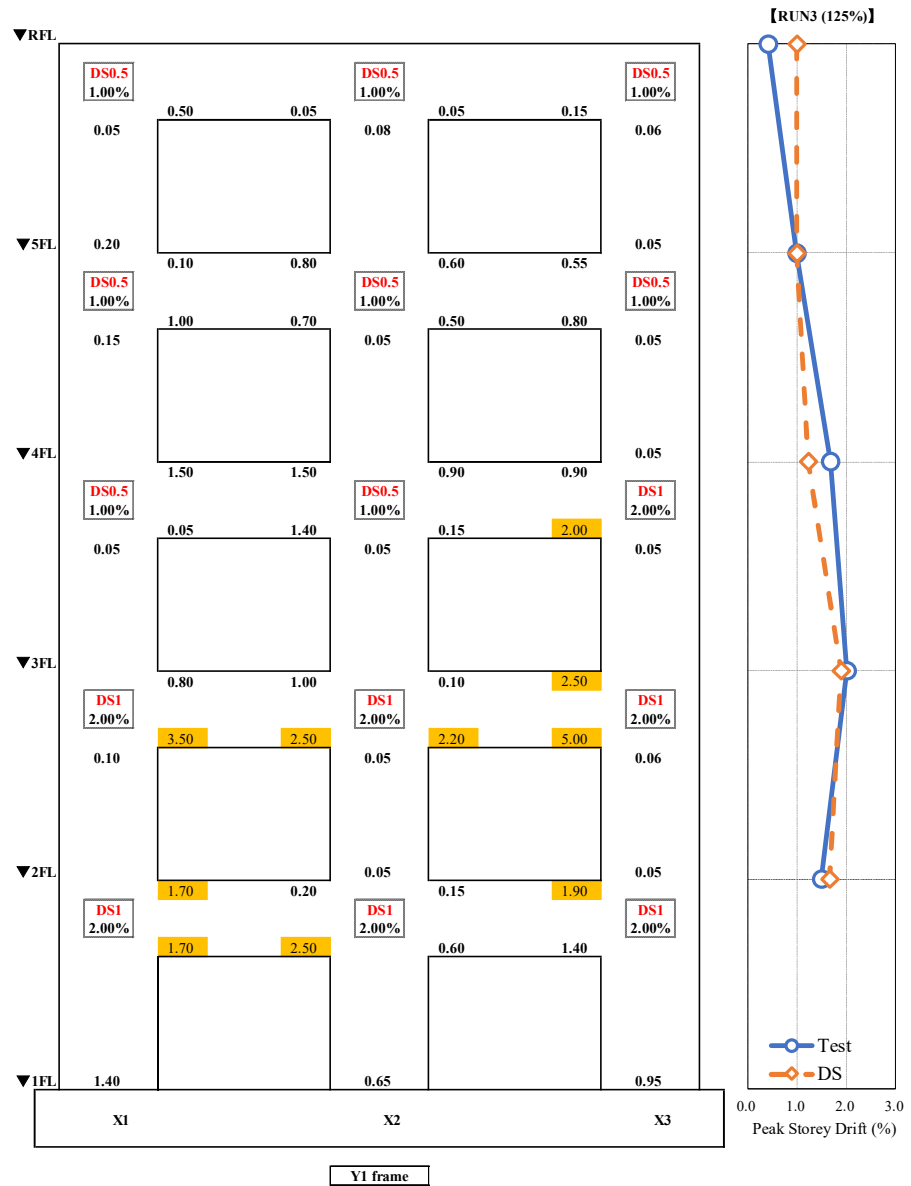
(b) Run 3

Figure 4-3 Crack patterns of the Y1 frame.



(a) Run 2

Figure 4-4 Maximum residual crack width. Crack width colored represents crack width exceeding DS1 criterion (1.5 mm).



(b) Run 3

Figure 4-4(cont) Maximum residual crack width. Crack width colored represents crack width exceeding DS1 criterion (1.5 mm).

Table 4-2 summarizes the degree of damage and damage state of each excitation. The specimen was observed only after Run 2 and Run 3, since no damage from Run 1 was observed. In Run 2, maximum crack width of 0.8mm was observed in the beam in the third story (3GX1). As no other damage except this light cracking was observed, the damage state of Run 2 was classified as DS0. In Run 3, a maximum crack width of 5.0mm was measured in the beam in the third story (3GX1), and some minor spalling was also observed. Based on this damage the damage state of Run 3 was determined as DS1.

Table 4-2 The Degree of Damage and Damage State in Each Excitation

Damage indices	Run 1 (60%)	Run 2 (100%)	Run 3 (125%)
Maximum crack width	-	0.8mm	5.0mm
Minor cover spalling	-	NO	YES
Exposure of transverse bars	-	NO	NO
Exposure of longitudinal bars	-	NO	NO
Core crushing/ Bar buckling • fracture	-	NO	NO
Damage State (maximum)	(DS0)	DS0	DS1

4.1.2 ATC-38 Form

The ATC-38 form (ATC, 2000) provides a brief description of a damaged structure following visual inspections. A complete form is shown in Appendix E. With this form the damage state of a building can be estimated using a damage probability matrix of ATC-38 (ATC, 2000) The damage state is determined by Mean Damage Factor (MDF) as shown in equation 3.3. MDF can be calculated as the product of the Modified Mercalli Intensity (MMI) (USGS) vector and Central Damage Factor (CDF) vector. MMI is defined with corresponding damage level observed in visual inspections (Table 4-4).

Mean Damage Factor (MDF) can be estimated as follows.

$$\begin{aligned}
 MDF_i &= \sum_{DS=1}^7 P_{DS}^i \cdot CDF_{DS} \\
 &= \overline{P^i} \cdot \overline{CDF}
 \end{aligned}
 \tag{3-1}$$

Where: MDF_i : mean damage factor at given intensity MMI of i , P_{DS}^i : probability of a single damage state given a MMI of i per Damage Probability Matrix, CDF_{DS} : central damage factor for a single damage state per Damage Probability Matrix.

According to the visual inspection in 3.1.1, the damage observed was not significant with only the occurrence of minor spalling and cracking. Since, the MMI of the input ground motion can be classified MMI of VI.

Thus, MDF is calculated as follows.

$$MDF_{VI} = \overline{P^{VI}} \cdot \overline{CDF}$$

$$= 0.4 \cdot \begin{bmatrix} 95 \\ 3 \\ 1.5 \\ 0.1 \\ 0 \\ 0 \end{bmatrix} \begin{bmatrix} 0 \\ 0.5 \\ 5 \\ 20 \\ 45 \\ 80 \\ 100 \end{bmatrix}$$

$$= 21.5\%$$

Damage State of the building is therefore “Moderate” per the Damage Probability matrix of Table 4-3.

Table 4-3 Damage Probability Matrix (Table 3.1 of ATC-38 (ATC, 2000))

Damage State	Damage Factor Range (%)	Central Damage Factor (%)	Probability of Damage in Percent By MMI and Damage State						
			VI	VII	VIII	IX	X	XI	XII
1 - NONE	0	0	95	49	30	14	3	1	0.4
2 - SLIGHT	0 - 1	0.5	3	38	40	30	10	3	0.6
3 - LIGHT	1 - 10	5	1.5	8	16	24	30	10	1
4 - MODERATE	10 - 30	20	0.4	2	8	16	26	30	3
5 - HEAVY	30 - 60	45	0.1	1.5	3	10	18	30	18
6 - MAJOR	60 - 100	80	-	1	2	4	10	18	39
7 - DESTROYED	100	100	-	0.5	1	2	3	8	38

The following definitions can be used as a guideline:

- 1 - NONE: No damage.
- 2 - SLIGHT: Limited localized minor damage not requiring repair.
- 3 - LIGHT: Significant localized damage of some components generally not requiring repair.
- 4 - MODERATE: Significant localized damage of many components warranting repair.
- 5 - HEAVY: Extensive damage requiring major repairs.
- 6 - MAJOR: Major widespread damage that may result in the facility being razed, demolished, or repaired.
- 7 - DESTROYED: Total destruction of the majority of the facility.

Table 4-4 Modified Mercalli Intensity (MMI) (USGS)

Intensity	Shaking	Description/Damage
I	Not felt	Not felt except by a very few under especially favorable conditions.
II	Weak	Felt only by a few persons at rest, especially on upper floors of buildings.
III	Weak	Felt quite noticeably by persons indoors, especially on upper floors of buildings. Many people do not recognize it as an earthquake. Standing motor cars may rock slightly. Vibrations similar to the passing of a truck. Duration estimated.
IV	Light	Felt indoors by many, outdoors by few during the day. At night, some awakened. Dishes, windows, doors disturbed; walls make cracking sound. Sensation like heavy truck striking building. Standing motor cars rocked noticeably.
V	Moderate	Felt by nearly everyone; many awakened. Some dishes, windows broken. Unstable objects overturned. Pendulum clocks may stop.
VI	Strong	Felt by all, many frightened. Some heavy furniture moved; a few instances of fallen plaster. Damage slight.
VII	Very strong	Damage negligible in buildings of good design and construction; slight to moderate in well-built ordinary structures; considerable damage in poorly built or badly designed structures; some chimneys broken.
VIII	Severe	Damage slight in specially designed structures; considerable damage in ordinary substantial buildings with partial collapse. Damage great in poorly built structures. Fall of chimneys, factory stacks, columns, monuments, walls. Heavy furniture overturned.
IX	Violent	Damage considerable in specially designed structures; well-designed frame structures thrown out of plumb. Damage great in substantial buildings, with partial collapse. Buildings shifted off foundations.
X	Extreme	Some well-built wooden structures destroyed; most masonry and frame structures destroyed with foundations. Rails bent.

4.2 Analysis

Following the visual inspection, the response of the specimen was simulated with a numerical analysis to obtain the best estimation of the peak response. Figure 4-5 illustrates the configuration of the numerical model of the specimen. The specimen was modeled with a three-dimensional frame model.

The analysis procedure started with a linear model in accordance with ATC-145-1 procedure in order to estimate reasonable drift demands. The linear model was updated into a modified linear model and a nonlinear model once the analysis result implied a discrepancy against the visual inspection result.

Material properties of concrete and steel used for the analysis are as shown in Table 2-3, Table 2-4. Further information on model of members (beams, columns and beam-column joints) are described in Appendix F. Also, as shown in Figure F-3, the structure has a strong-column/weak-beam mechanism.

P- Δ effect was incorporated in a linear and nonlinear model in accordance with ASCE/SEI 41 7.2.6 (ASCE, 2017).

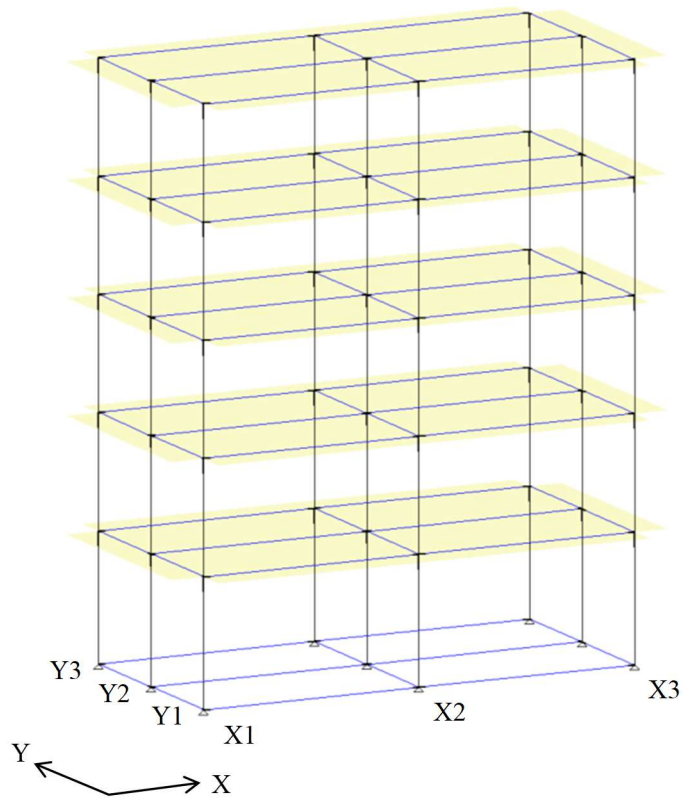


Figure 4-5 Configuration of a numerical model.

4.2.1 Linear Analysis

Figure 4-6 shows the backbone curve of a linear model. The Initial stiffness of beam and column element was defined as effective stiffness per ASCE/SEI 41 (ASCE, 2017) (Figure F-2). Equivalent viscous damping was assumed 2.0% in accordance with the recommendation per ASCE/SEI 41 (ASCE, 2017) (Table F-3) for bare frame structures. Other detail assumptions and calculations are shown in Appendix F.

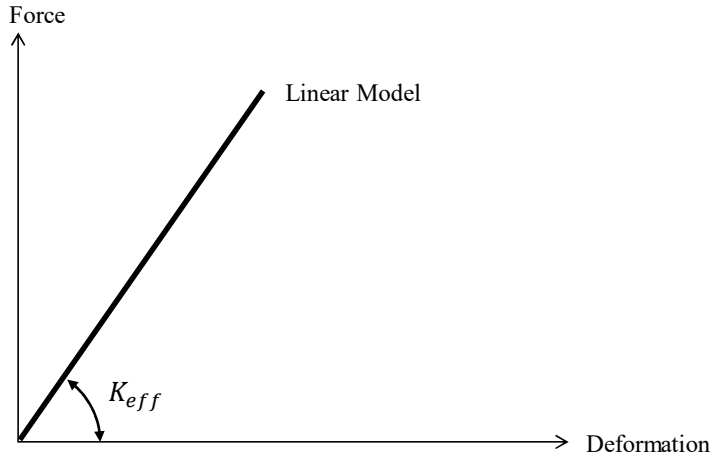


Figure 4-6 Backbone curve of a linear model.
 K_{eff} : Effective stiffness per ASCE/SEI 41 (ASCE, 2017).

4.2.1.1 Drift Estimate

Figure 4-7 shows peak story drift demand estimation with a linear model for Run 1, Run 2 and Run 3. Run 1 and Run 2 closely matched the experimental data as Run 1 and Run 2 correspond to the minor or moderate level earthquake that is less than design level. For Run 3, the linear model significantly underestimates the peak story drift response. This is because that the structure began showing limited inelastic behavior with Run 2 (Figure 4-3 and Figure 4-8), and it indicates that the model should be refined to simulate the nonlinear response.

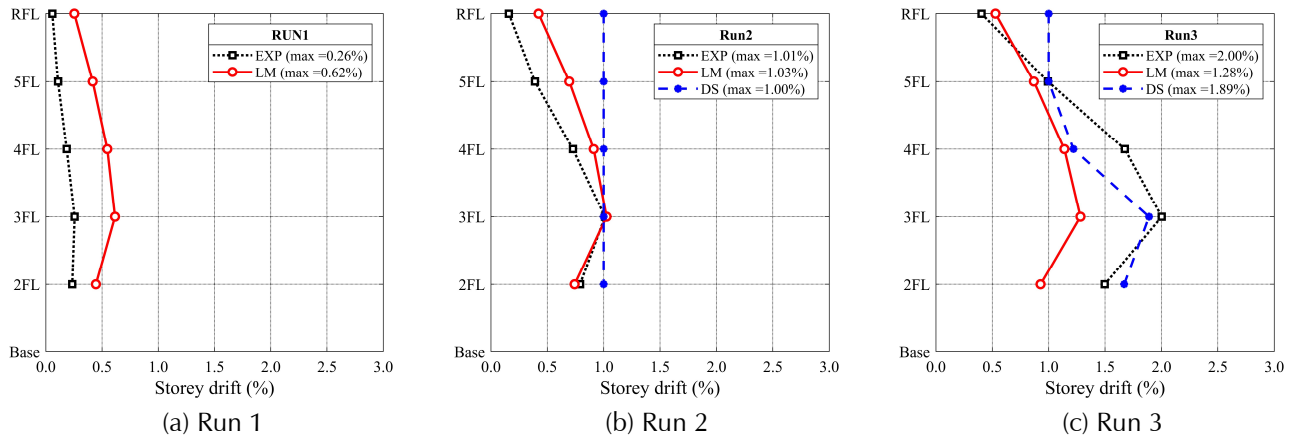


Figure 4-7 Peak story drift estimation with a linear model.

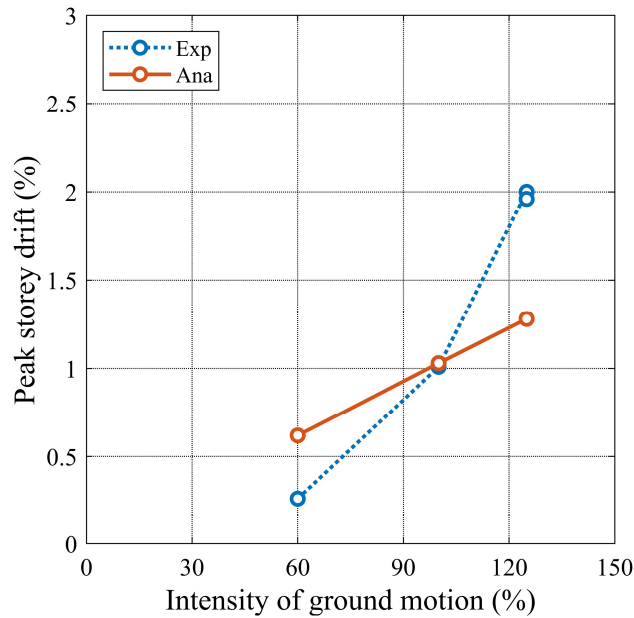
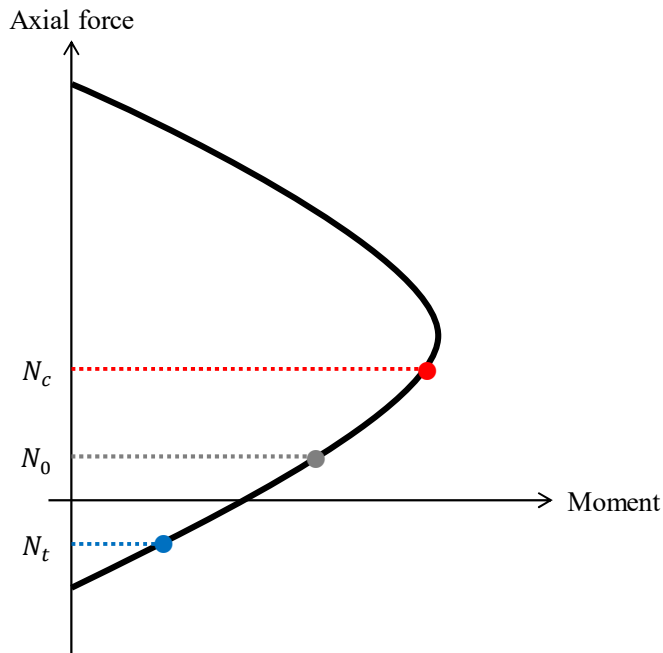


Figure 4-8 Intensity of ground motion versus peak drift with a linear model.

4.2.1.2 Demand-Capacity Ratio (DCR) Estimate

With the linear analysis, it is important to estimate the probability of inelastic response and damage progression with demand-capacity ratio (DCR). This section describes the procedure on the model update and identification of Inspection Locations (IL) with DCR of the linear model.

In order to identify maximum DCR, moment capacity and moment demand are compared in this section. DCR is identified in both positive and negative directions. Moment capacity of the beams was calculated with fiber analysis, considering effective flange width, and the details of this calculation are described in Appendix F. As expected, the moment capacity of columns varies depending on axial force level (Figure 4-9). Moment capacity of the columns were calculated by maximum compression force since axial tension force typically gives lower capacity and it leads to significantly conservative DCR estimates.



N_0 : Axial force by dead load and live load
 N_c : Compression axial force at peak response
 N_t : Tension axial force at peak response

Figure 4-9 Moment capacity of columns.

Figure 4-10 describes moment capacity demand ratio in each frame and for each Run. A significant number of plastic hinges exceed 1.0 in DCR in all Runs. Especially, an excessive number of hinges was flagged compared to the visual inspection results. Moreover, the DCR of columns is relatively high because of the tension axial force effect. It should be noted that considering the axial force effect for the DCR check leads to a conservative check.

Figure 4-11 is a comparison of displacement ductility and m-factors of Primary Collapse Prevention (CP) of beams and columns. The m-factors of beams and columns were determined per Table 4-5 in accordance with ASCE/SEI 41 (ASCE, 2017). As seen in this figure, a couple of columns exceeded their Primary CP m-factor. Thus, strength degradation can be anticipated with these columns.

Table 4-5 m-Factors of Beams and Columns

Conditions	m-Factors ^a						
	Performance Level						
	Component Type						
	IO	Primary		Secondary			
	LS	CP	LS	CP			
Condition i. Beams controlled by flexure ^b							
$\rho - \rho'$							
ρ_{bal}	Transverse reinforcement ^c	$\frac{V^d}{b_w d \sqrt{f'_{cE}}}$					
≤ 0.0	C	≤ 3 (0.25)	3	6	7	6	10
≤ 0.0	C	≥ 6 (0.5)	2	3	4	3	5
≥ 0.5	C	≤ 3 (0.25)	2	3	4	3	5
≥ 0.5	C	≥ 6 (0.5)	2	2	3	2	4
≤ 0.0	NC	≤ 3 (0.25)	2	3	4	3	5
≤ 0.0	NC	≥ 6 (0.5)	1.25	2	3	2	4
≥ 0.5	NC	≤ 3 (0.25)	2	3	3	3	4
≥ 0.5	NC	≥ 6 (0.5)	1.25	2	2	2	3
Condition ii. Beams controlled by shear ^b							
Stirrup spacing $\leq d/2$			1.25	1.5	1.75	3	4
Stirrup spacing $> d/2$			1.25	1.5	1.75	2	3
Condition iii. Beams controlled by inadequate development or splicing along the span ^b							
Stirrup spacing $\leq d/2$			1.25	1.5	1.75	3	4
Stirrup spacing $> d/2$			1.25	1.5	1.75	2	3
Condition iv. Beams controlled by inadequate embedment into beam-column joint ^b							
			2	2	3	3	4

Note: f'_{cE} in lb/in.² (MPa) units.
^a Values between those listed in the table shall be determined by linear interpolation.
^b Where more than one of conditions i, ii, iii, and iv occurs for a given component, use the minimum appropriate numerical value from the table.
^c "C" and "NC" are abbreviations for conforming and nonconforming transverse reinforcement. Transverse reinforcement is conforming if, within the flexural plastic hinge region, hoops are spaced at $\leq d/3$, and if, for components of moderate and high ductility demand, the strength provided by the hoops (V_s) is at least $3/4$ of the design shear. Otherwise, the transverse reinforcement is considered nonconforming.
^d V is the shear force calculated using limit-state analysis procedures in accordance with Section 10.4.2.4.1.

$\left(\frac{N_{UD}}{A_g f'_{cE}}\right)$	m-Factors ^a					
	Performance Level					
	Component Type					
	IO	Primary		Secondary		
	ρ_t	V_{YE}/V_{CoIOE}	LS	CP	LS	CP
Columns not controlled by inadequate development or splicing along the clear height ^b						
≤ 0.1	≥ 0.0175	≥ 0.2	1.7	3.4	4.2	8.9
		< 0.6	1.2	1.4	1.7	1.7
≥ 0.7	≥ 0.0175	≥ 0.2	1.5	2.6	3.2	3.2
		< 0.6	1.0	1.0	1.0	1.0
≤ 0.1	≤ 0.0005	≥ 0.2	1.5	2.7	3.3	8.9
		< 0.6	1.0	1.0	1.0	1.0
≥ 0.7	≥ 0.0175	≥ 0.6	1.0	1.0	1.0	1.0
		< 1.0	1.3	1.9	2.3	2.3
≤ 0.1	≤ 0.0005	≥ 0.6	1.0	1.0	1.0	1.0
		< 1.0	1.3	1.8	2.2	8.9
≥ 0.7	≥ 0.0175	≥ 1.0	1.0	1.0	1.0	1.0
≤ 0.1	≤ 0.0005	≥ 1.0	1.1	1.0	1.1	2.1
≥ 0.7	≤ 0.0005	≥ 1.0	1.0	1.0	1.0	1.0
Columns controlled by inadequate development or splicing along the clear height ^b						
≤ 0.1	≥ 0.0075	≥ 1.0	1.0	1.7	2.0	6.8
≥ 0.7	≥ 0.0075	≥ 1.0	1.0	1.0	1.0	3.5
≤ 0.1	≤ 0.0005	≥ 1.0	1.0	1.0	1.0	1.6
≥ 0.7	≤ 0.0005	≥ 1.0	1.0	1.0	1.0	1.0

^a Values between those listed in the table shall be determined by linear interpolation.
^b Columns are considered to be controlled by inadequate development or splicing where the calculated steel stress at the splice exceeds the steel stress specified by Eq. (10-1a) or (10-1b). Acceptance criteria for columns controlled by inadequate development or splicing shall never exceed those of columns not controlled by inadequate development or splicing.

4.2.1.3 Inspection Locations

In this section, the procedure of Inspection Location phase was investigated with the linear model and the modified linear model per ATC-145-1 procedure. The number of IL identified with analysis was then compared to the visual inspection result. An alternative approach on the IL procedure is discussed in Appendix L.

Table 4-6 shows the number of plastic hinges flagged as Inspection Locations (IL). With experimental data, plastic hinges evaluated greater than DS1 are defined as an IL, and with the analysis result, any plastic hinges with a DCR greater than 1.0 was defined as an IL.

On both beams and columns, there is a significant discrepancy between the number of IL determined from analysis and the visual inspection results. The analysis significantly overestimates the number of IL. In the comparison of beams, no beam hinges were flagged in Run 1 and Run 2, and 20% of the beam hinges were flagged as IL in Run 3 based on post-test visual inspection; However, the Analysis result shows about 80% in Run 1 and over 90% in Runs 2 and 3 were judged as IL. Furthermore, none of column hinges were flagged as ILs with visual inspection, versus up to 60% of the column hinges were required to be inspected based upon the analysis for Run 3. This result shows that a DCR greater than 1.0 is an overly-conservative criterion for IL. In order to resolve this discrepancy, further refinement is discussed in Appendix L.

Table 4-6 The Number of Inspection Locations with a linear Model

			The No. of hinges	Visual Inspection	ATC-145-1 approach
Criteria				$DS > 1$	$DCR > 1.0$
Run 1	LM	Beam	60	-* ¹	47 (78%)
		Column	90	-* ¹	6 (7%)
		Total	150	-* ¹	53 (35%)
Run 2	LM	Beam	60	0 (0%)	57 (95%)
		Column	90	0 (0%)	18 (20%)
		Total	150	0 (0%)	75 (50%)
Run 3	LM	Beam	60	11 (18%)	57 (95%)
		Column	90	0 (0%)	51 (57%)
		Total	150	11 (7%)	108 (72%)

*¹ Visual inspection was not performed in Run 1.

4.2.1.4 Reconciliation with Inspection Result

Figure 4-12 shows a fragility curve and peak story drift demand predicted with linear model. The fragility curve is obtained with FEMA-P58 (FEMA, 2019) database in accordance with an ACI 318-conforming concrete special moment frame category.

Table 4-7 summarizes damage state predicted by linear analysis and damage observation. Damage state with linear procedure is determined with the fragility curve. Predicted peak story demand in each Run shows the highest probability of DS0. Therefore, all the Runs are classified into DS0. Run 1 and Run 2 were classified into DS0 based on the damage observation as well. Therefore, Run 1 and Run 2 have good agreement between the predicted damage state and the damage observation, and as such are regarded as the best estimation. On the other hand, the damage state predicted with linear model in Run 3 (DS0) does not match damage state defined with damage observation (DS1). Thus, the linear model is required to be refined.

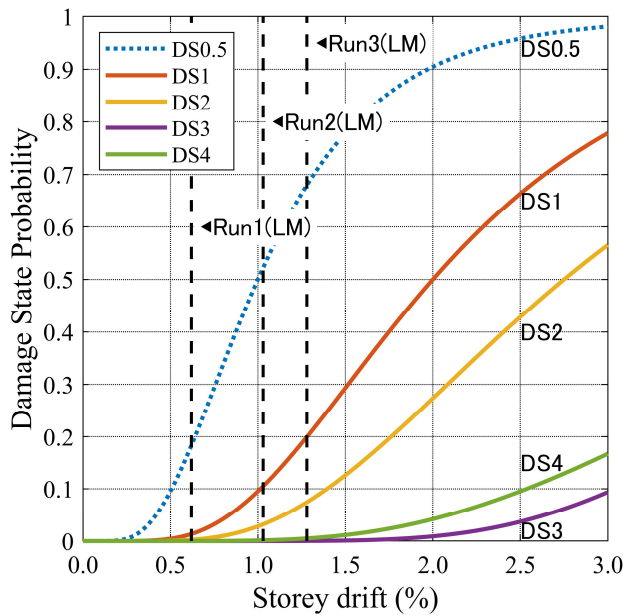


Figure 4-12 Fragility curve and drift estimation with a linear model.

Table 4-7 Summary of Drift Estimation with a Linear Model and Damage State

Case	Model	Drift estimation	Damage State probability						Most probable DS	DS from Visual inspection	DS matches?
			DS0	DS0.5	DS1	DS2	DS3	DS4			
Run 1	Linear model	0.61%	80%	18%	2%	0%	0%	0%	DS0	DS0	OK
Run 2	Linear model	1.03%	53%	37%	6%	4%	0%	0%	DS0	DS0	OK
Run 3	Linear model	1.28%	32%	48%	12%	8%	0%	0%	DS0.5	DS1	NG

4.2.1.4.1 Linear Model Modification

In order to improve the drift prediction of the linear model, it was refined with stiffness reduction factors based on maximum ductility in each member from Run 2 (initial onset of damage.) Figure 4-13 shows the basic concept of a linear model with stiffness reduction to predict nonlinear response. This model aims to generate peak-oriented behavior with a linear model based on equal-displacement theory (F.7). With equal-displacement theory, peak displacement of the original linear model is converted to peak displacement of equivalent nonlinear model. Ductility of this structure can be estimated assuming yield displacement. The estimated ductility is then used to obtain a stiffness reduction factor and this is applied to a linear model to get a damaged linear model.

Figure 4-14 describes empirical relationship between stiffness reduction and maximum ductility. Basically, the stiffness decays with the increase of ductility. However, in the range of $\mu = 1$ to 2, stiffness reduction is defined as 0.5, which avoids overestimation of stiffness reduction.

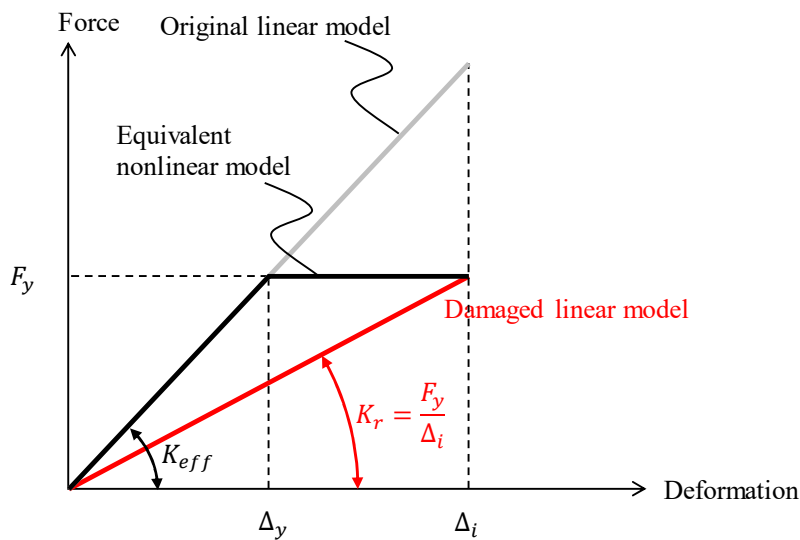


Figure 4-13 Basis of equal-displacement theory and stiffness modification for an original linear model considering ductility demand in a previous shaking (Marder, 2018).

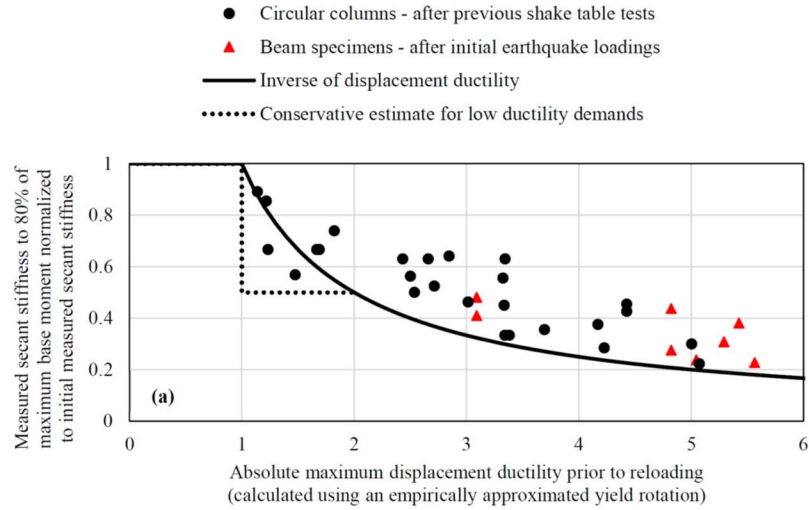


Figure 4-14 Ductility demand and stiffness reduction factors (Marder, 2018).

$$\lambda_k = \frac{K_r}{K_y} = \begin{cases} 1.0 & \mu < 1.0 \\ 0.5 & 1.0 \leq \mu \leq 2.0 \\ 1/\mu & 2.0 \leq \mu \end{cases}$$

4.2.1.4.2 Stiffness Reduction Factor for Modified Linear Model

The stiffness reduction factor identified by the maximum ductility demand of each plastic hinge from Run 2 was applied to the original linear model. Figure 4-15 (a) illustrates the stiffness reduction factor for each plastic hinge of components. In this study, the average of both stiffness reduction factors of plastic hinges in one component (Figure 4-15 (b)) was applied to the model.

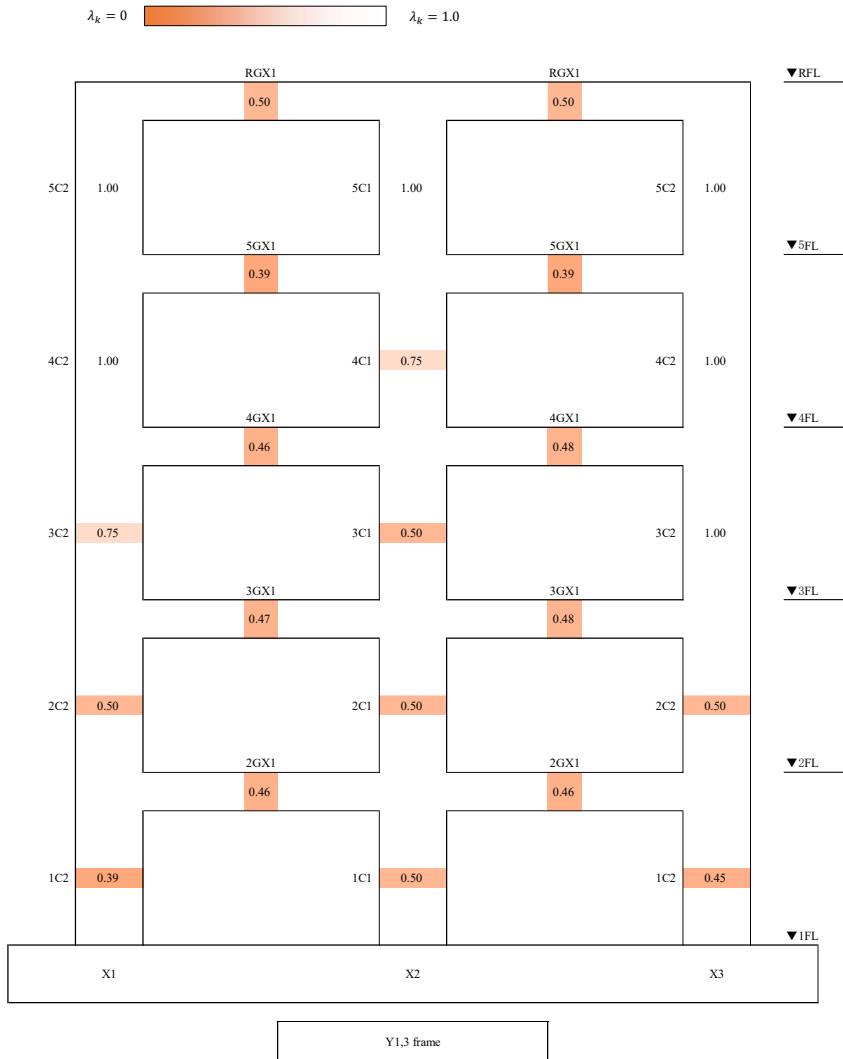


Figure 4-15 Averaged stiffness reduction factors for beams and columns.

4.2.2 Modified Linear Model Response

Following the model modification process aforementioned, a modified linear model was developed by applying stiffness reduction factors to the original linear model. The modified linear model response was compared to Run 3 to determine its ability to capture better the drift profile of the test building at design level shaking as is shown in following sections.

4.2.2.1 Drift Estimate

Figure 4-16 represents peak story drift demand estimation with the modified linear model and peak drift demand measured in the test. The peak story drift in each story was reasonably well simulated with a modified linear model, and the drift estimation being fairly conservative. Also, peak drift estimate with Damage State was close to the test result.

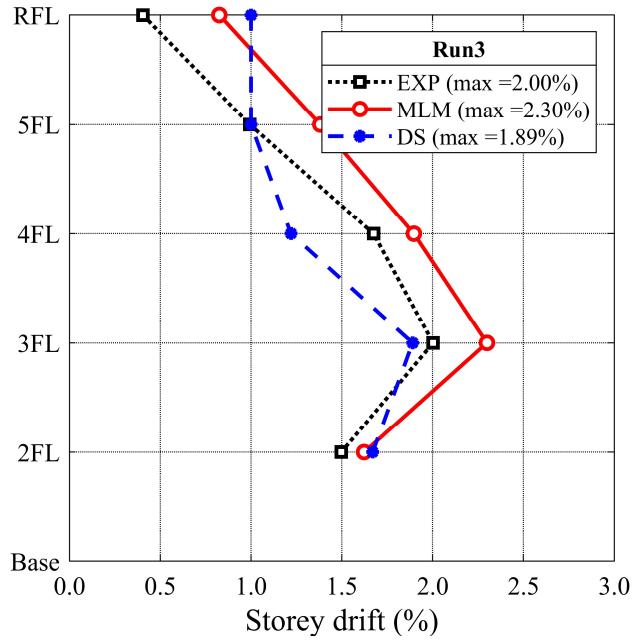


Figure 4-16 Peak story drift demand with the modified linear model (Run 3).

Figure 4-17 summarizes the result of the drift estimation with the linear model and the modified linear model on the intensity of ground motion (i.e., drift estimation of Run 1 and Run 2 are from the linear model (LM) and Run 3 is from the modified linear model (MLM)). The three excitations (Run1-3) are simulated well, and all provide a fairly conservative estimation.

A dashed green line represents crude estimation of peak-oriented response in the future, smaller earthquake. Given that 60% input ground motion is service-level earthquake, this structure is likely to be subjected to 1.1% drift. Further discussion of the response of the damaged building is found in 5.1.1.

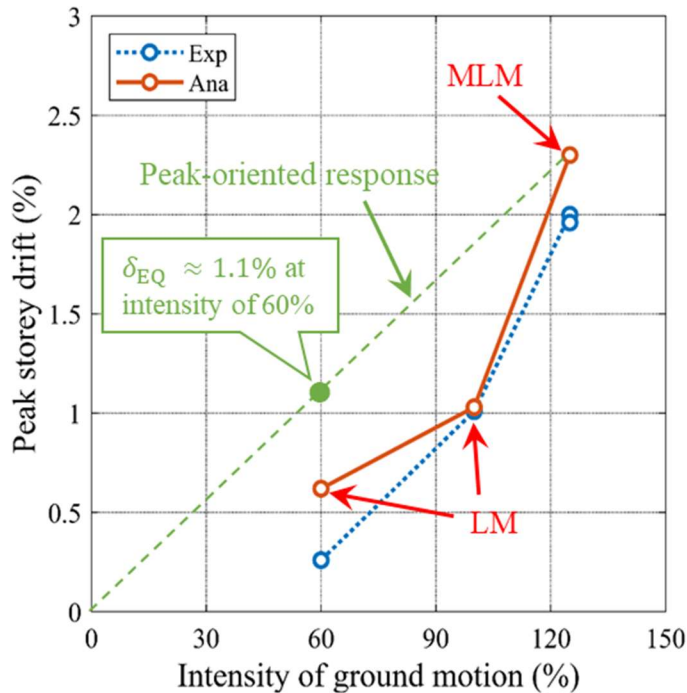


Figure 4-17 Intensity of ground motion versus peak drift demand.

4.2.2.2 DCR Estimate

Figure 4-18 shows DCR of each component with the modified linear model on the exterior and interior frame. As can be seen, most of the beams show DCRs of nearly 2.0 – 3.0, which implies these beams are subjected to moderate ductility demand compared to prior ductility demand. In the columns, DCRs are nearly 2.0 other than the bottom of columns in the first story. These outputs indicate that most of beams and columns were likely to experience inelastic response and be severely damaged. However, in the visual inspection, no severe damage was observed. This discrepancy might lead to significantly conservative estimation on ductility demand and damage level.

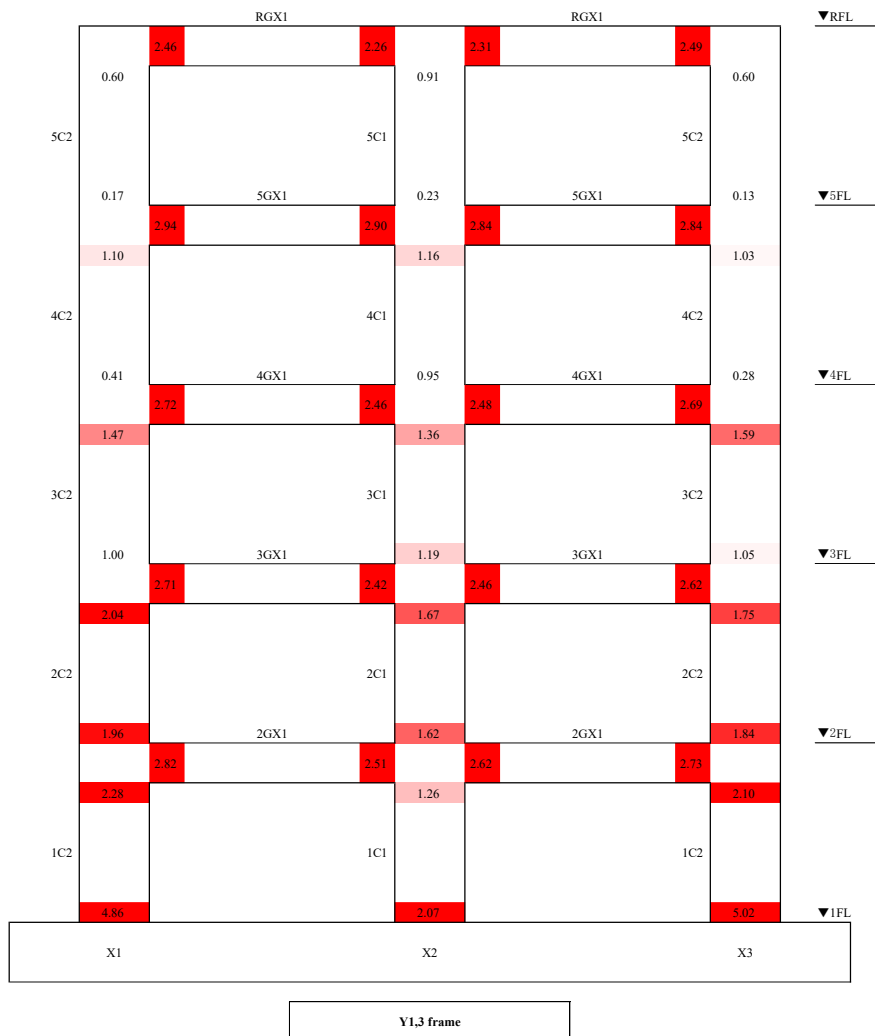


Figure 4-18 DCR with the modified linear model (Run 3).

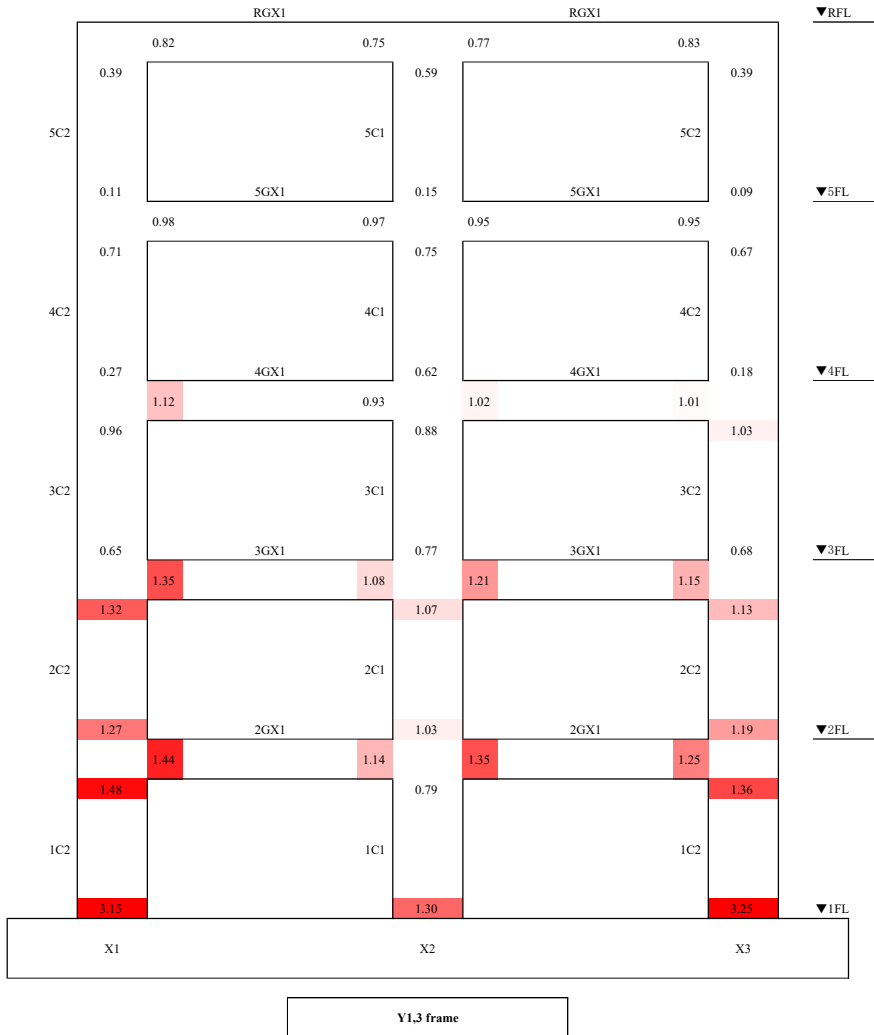


Figure 4-19 Ductility and m-factor (IO) ratio with the modified linear model (Run 3).

4.2.2.3 Inspection Locations

Table 4-8 indicates the number of IL with the linear model and the modified linear model. ILs for Run 1 and Run 2 were estimated with the original linear model and Run 3 was estimated with the modified linear model. As with the linear model, a significant number of plastic hinges were flagged as ILs with the modified linear model.

Table 4-8 The Number of Inspection Locations with a Linear Model and Nonlinear Model

			The No. of hinges	Visual Inspection	ATC-145-1 approach
Criteria				$DS > 1$	$DCR > 1.0$
Run 3	MLM	Beam	60	11 (18%)	60 (100%)
		Column	90	0 (0%)	51 (57%)
		Total	150	11 (73%)	111 (74%)

*1 Visual inspection was not performed in Run 1.

4.2.2.4 Reconciliation with Inspection Results

The drift estimation of the modified linear model was compared to the fragility curve in Figure 4-20. The maximum story drift of the modified linear model was 2.3%. This resulted in the probability of the DS1-4 to be approximately 60%, and the most probable Damage State is likely to be DS0-2, at the story with maximum drift. Table 4-9 summarizes Damage States estimated with analysis and by visual inspection. Comparing Damage State with the modified linear model to Damage State based on visual inspection, these Damage States are consistent. Thus, the drift estimation with the modified linear model was determined to be an improved DS estimation procedure.

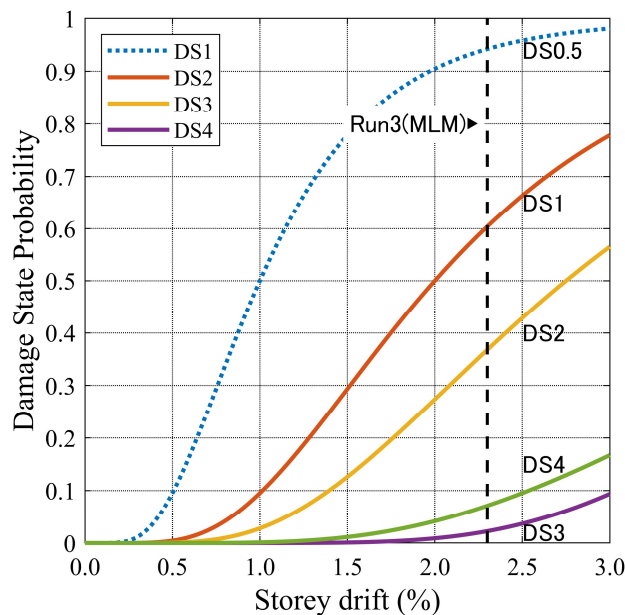


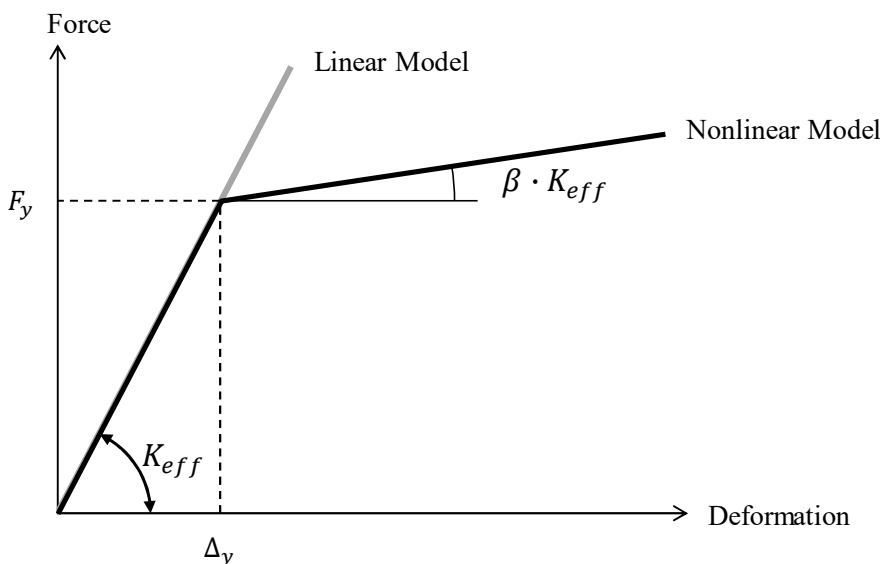
Figure 4-20 Fragility curve and drift estimation with the modified linear model.

Table 4-9 Summary of Damage State Predicted by Analysis and Damage Observation

Case	Model	Drift estimation	Damage State probability						Most probable DS	DS from Visual inspection	DS matches?
			DS0	DS0.5	DS1	DS2	DS3	DS4			
Run 3	Modified linear model	2.30%	5%	35%	23%	30%	3%	4%	DS0-2	DS1	OK

4.2.3 Nonlinear Analysis

This section examines the ability of a nonlinear model for drift estimation as a possible model refinement. With the comparison between the estimation of the linear model and visual inspection, the model was refined into a nonlinear model for the drift estimation of Run 3. Figure 4-21 illustrates the backbone curve of a nonlinear model. Nonlinear behavior was assumed as bi-linear response herein. The initial stiffness was defined as effective stiffness which is consistent with the original linear model. The post-yield stiffness was defined as beta times effective stiffness in which beta is the ratio of post-yield stiffness to the initial stiffness, and beta was assumed as 0.05. The viscous damping ratio for the nonlinear model was assumed as 1.0% considering hysteretic damping is explicitly accounted for in the analysis. Further details on viscous damping are provided in F.5.



K_{eff} : Effective stiffness per Table F-2, Δ_y : Yield deformation, F_y : Yield capacity

Figure 4-21 Backbone curve of a nonlinear model. β is assumed as 0.05.

4.2.3.1 Drift Estimate

Figure 4-22 shows the peak drift estimation with the nonlinear model. Although the nonlinear model slightly underestimated the test result, it has

reasonable agreement. The error was within 20% and is considered a reasonable level of accuracy.

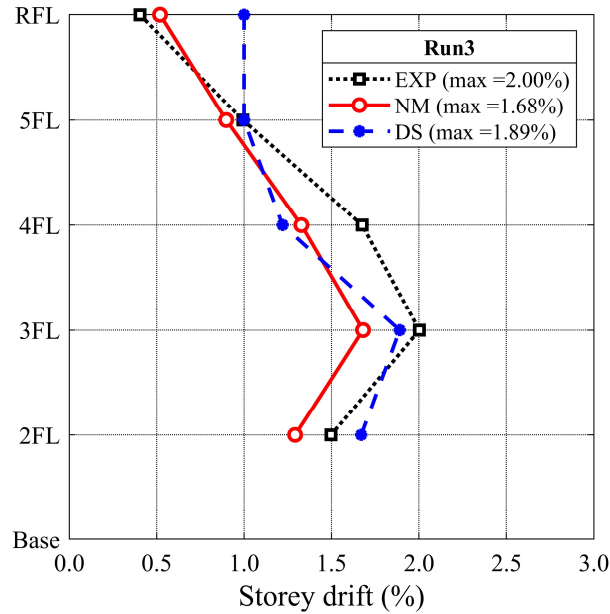


Figure 4-22 Peak story drift estimation with a nonlinear model.

4.2.3.2 Reconciliation with Inspection Results

In order to determine the ability of the nonlinear model predict the damage state of the building, the peak drift estimate of the nonlinear model was compared to the fragility curves as shown in Figure 4-23. The peak story drift from the nonlinear model was 1.68% and the most probable damage state is then DS0.5 with approximately 83% probability. This result is not consistent with the test result and the model would be required to be updated. It should be noted that the damage state can be underestimated with the fragility function, even if the drift estimation has good enough agreement with the drift imposed during an earthquake. This sensitivity between drift and damage state should be noted around the threshold of DS1 (2.0%) as the slight difference of drift estimation generates a different damage state.

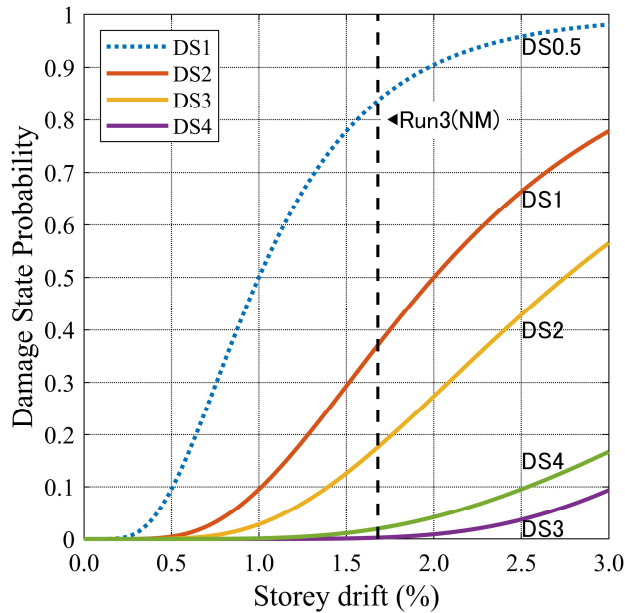


Figure 4-23 Fragility curve with the nonlinear model.

Table 4-10 Summary of Damage State Predicted by Nonlinear Model

Case	Model	Drift estimation	Damage State probability						Most probable DS	DS from Visual inspection	DS matches?
			DS0	DS0.5	DS1	DS2	DS3	DS4			
Run 3	Nonlinear model	1.68%	17%	46%	19%	17%	0%	1%	DS0.5	DS1	NG

4.3 Summary

A five-story reinforced concrete building was assessed with the ATC-145-1 (ATC, 2020) procedure per Inspection and Analysis Phase. The damaged building was evaluated with FEMA P-58 (FEMA, 2019) damage evaluation criteria. In order to estimate the story drift demand during the shaking, both linear and nonlinear models were employed. The key findings through the visual inspection and analysis are listed below.

Preliminary Inspection

- The current recommendation for Inspection Location per ATC-145-1 (ATC, 2020), components showing $DCR > 1.0$ should be inspected as Inspection Locations, is likely to be conservative compared to visual inspection results. With $DCR > 1.0$ criterion, a significant number of plastic hinges were required to be inspected, although no significant damage was observed at these locations. To address this issue, an alternate approach for Inspection Location is provided in Appendix L.

Analysis phase

- The linear model was able to predict the peak story drift of the structure fairly accurately when subjected to shaking less than the design level. The linear model reasonably predicted the peak story drift demand in Run 1 and Run 2 that reached around yield point. However, the linear model was not able to simulate the response of design-level ground motion as the structure showed inelastic behavior. For the drift estimation with design-level earthquake, a refined model, a linear or nonlinear model was required.
- In the DCR estimate, DCR of beams was typically consistent with the location of damages observed in the test. However, DCR of columns is likely overestimated. Even if a significant DCR was found, the degree of damage observed was minor.
- It is shown that the reduced stiffness approach based upon element ductility demand can be an option of model refinement where prior damage has occurred. In order to predict the peak drift demand during the design-level earthquake (Run 3), the linear model was refined with stiffness reduction based on equivalent ductility of the prior excitation (Run 2). The modified linear model was able to predict peak story drift in Run 3. It is recommended to use a modified linear model before updating it to a nonlinear model.
- It was demonstrated that the drift estimation with a nonlinear model has reasonable agreement with the test result of design-level ground motion (Run 3). This result indicates a nonlinear model is a reasonable refinement to estimate the story drift demand with design level shaking.
- Use of fragility curves to validate damage state of analytical prediction against the observed damage is likely to be conservative. Nevertheless, drift estimation with a nonlinear model had good agreement with measured drift in the test, the damage state prediction per fragility curves was not consistent with that of observed damage, due to the drifts being slightly underestimated. Thus, it should be noted that the fragility functions are sensitive to the drift inputs; however, using the functions in the other direction, it was also observed that reasonable story drift estimates could be obtained based on observed damage state.

Case Study 1
Chapter 5

Safety-Assessment Phase

In this chapter, the damaged specimen is assessed with the Safety-assessment procedure shown in Figure 5-1. The damaged specimen goes through system check whether or not it exceeds safety drift limit. If it passes the system check, the serviceability assessment procedure can be initiated. If it does not pass, component level as well as low-cycle fatigue check is required. In this study, the specimen went through every assessment, system check, component check and fatigue check. For the fatigue check, two approaches: simplified method and detailed method are presented.

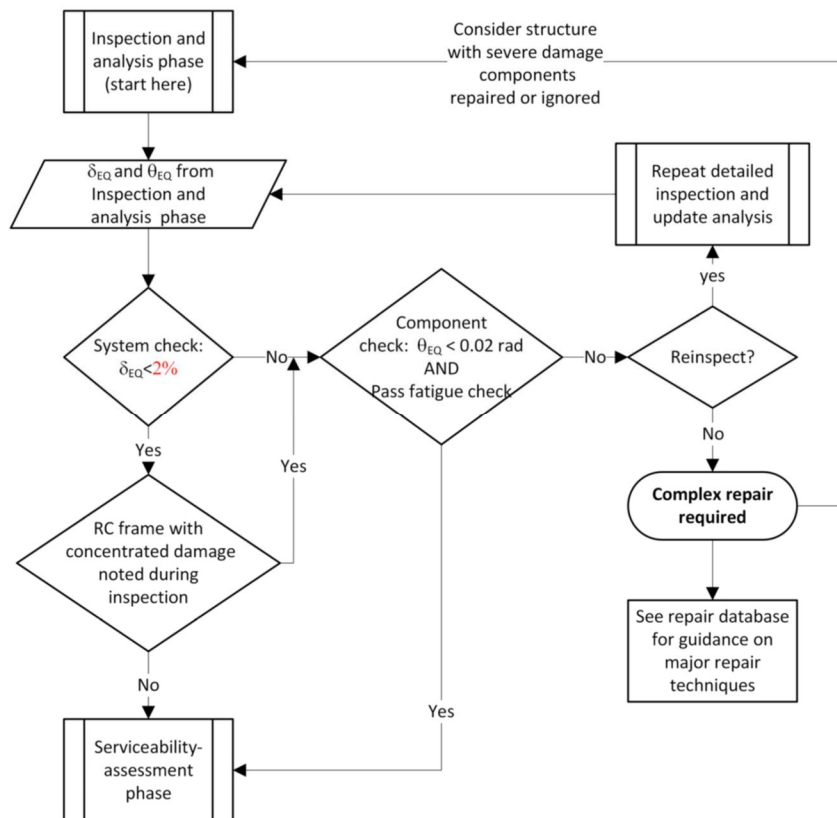


Figure 5-1 Safety-assessment procedure.

5.1 System Check

In the system check, the peak story drift is assessed as to whether it exceeds the safety drift limit assumed to be 2.0%. Figure 5-2 indicates the peak drift estimation with the modified linear model and the nonlinear model from Inspection and Analysis phase. The test result is also plotted in this figure. The modified linear model, the nonlinear model and the test result show peak story drift of 2.30%, 1.79%, and 2.00%, respectively. Thus, only the modified linear model would trigger component and the fatigue check. However, for completeness, each of these cases went through the component and the fatigue check in this study.

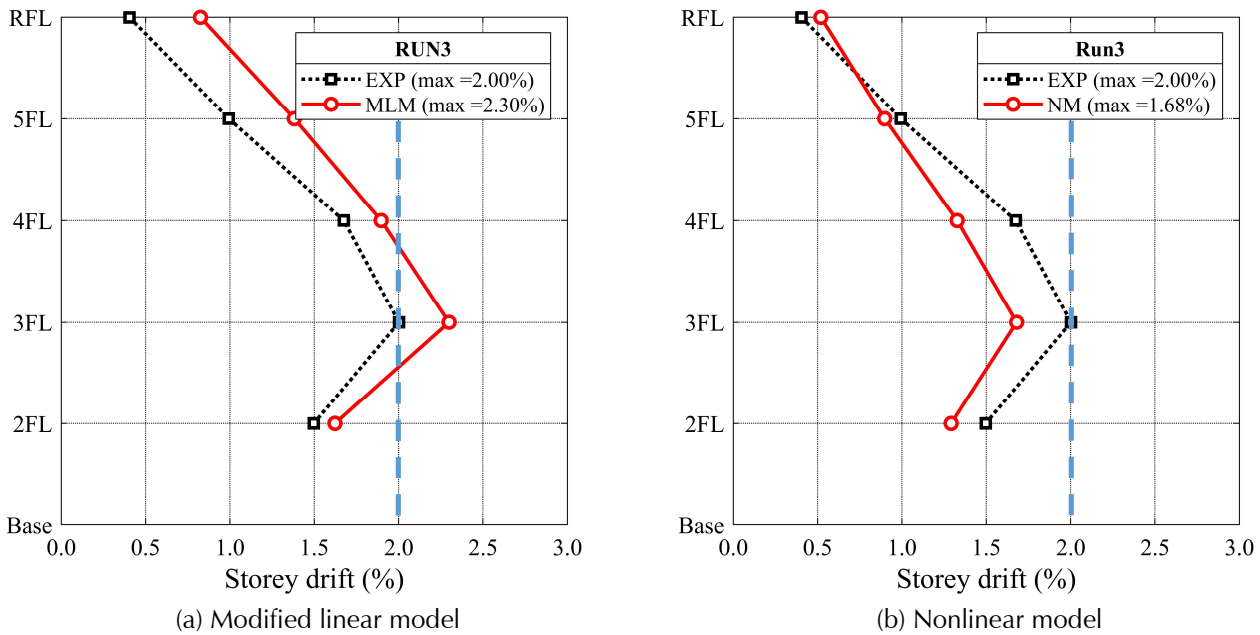


Figure 5-2 Peak story drift distribution. A dashed-line represents 2.0% criterion.

5.2 Component Check

Component level checks were performed for each of the three demand cases: the modified linear model, nonlinear model and test results, in which the rotation at each component was compared against the rotation limit. It should be noted that rotation of the test result represents hinge rotation as only the plastic hinge region (200 mm from column face for beams) was measured with LVDT. On the other hand, rotations of the modified linear model and nonlinear model represent chord rotation in accordance with ATC-145-1 (ATC, 2020)

Figure 5-3 illustrates the location of the beam hinges, and Figure 5-4 shows the peak chord rotation demand of beams. For each demand case, the peak

rotations were less than 2.0%, meaning that these beams pass the rotation check.

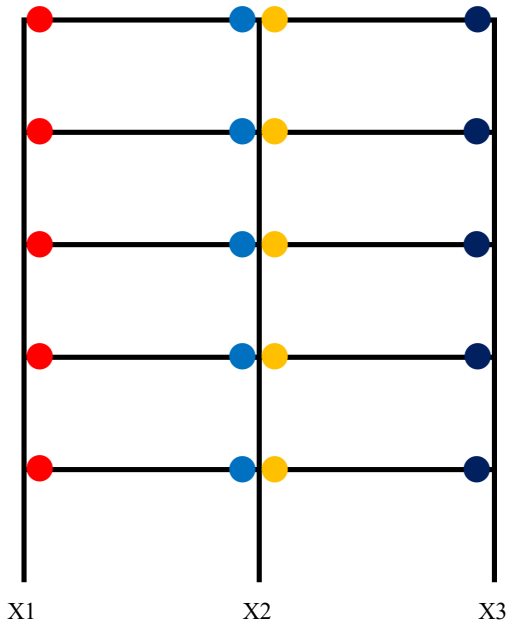
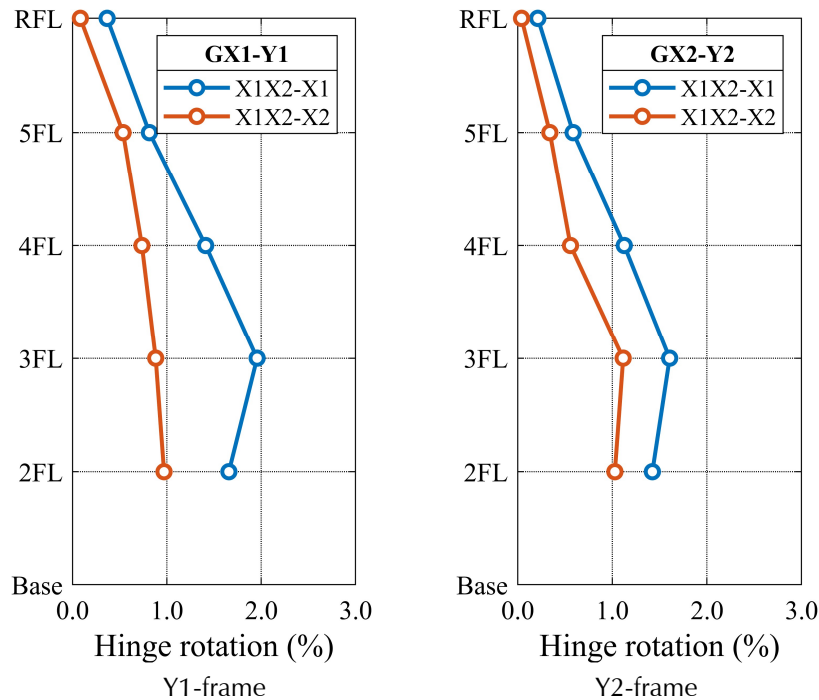
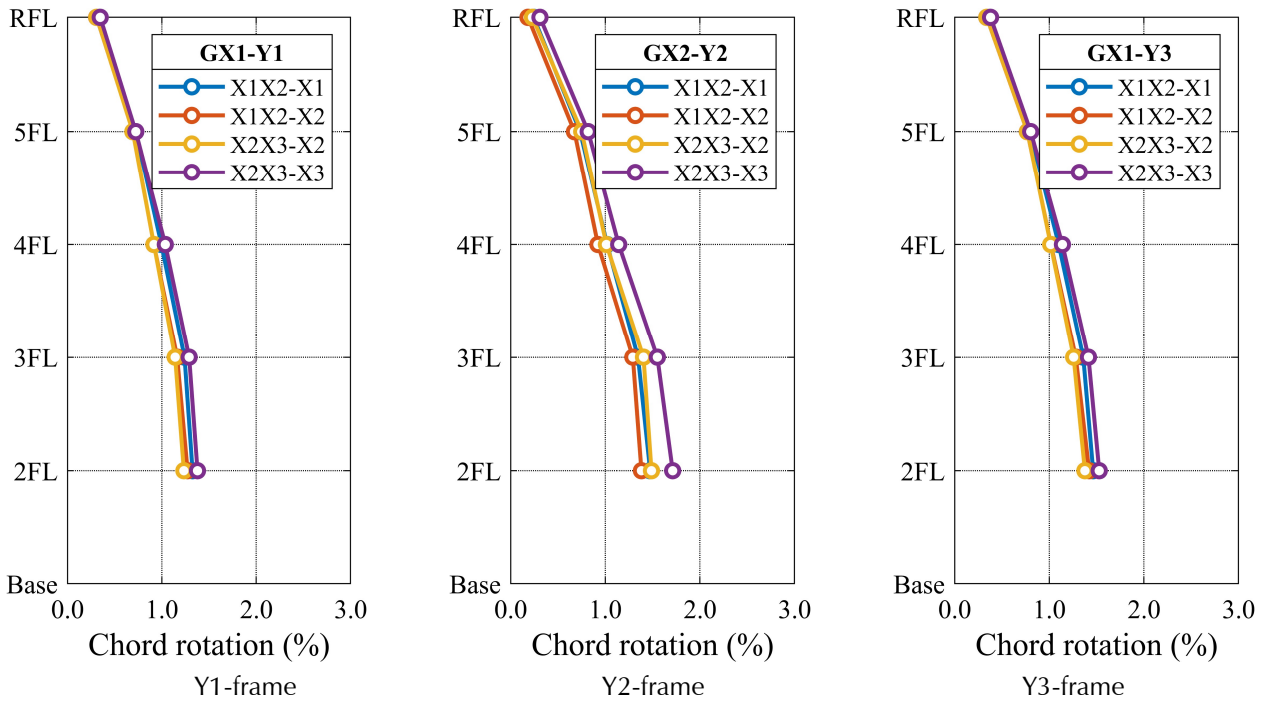


Figure 5-3 Location of beam hinges. In the test, only the rotation of beams in the X1X2 bay were measured. Colors correspond to plot colors in Figure 5-4.

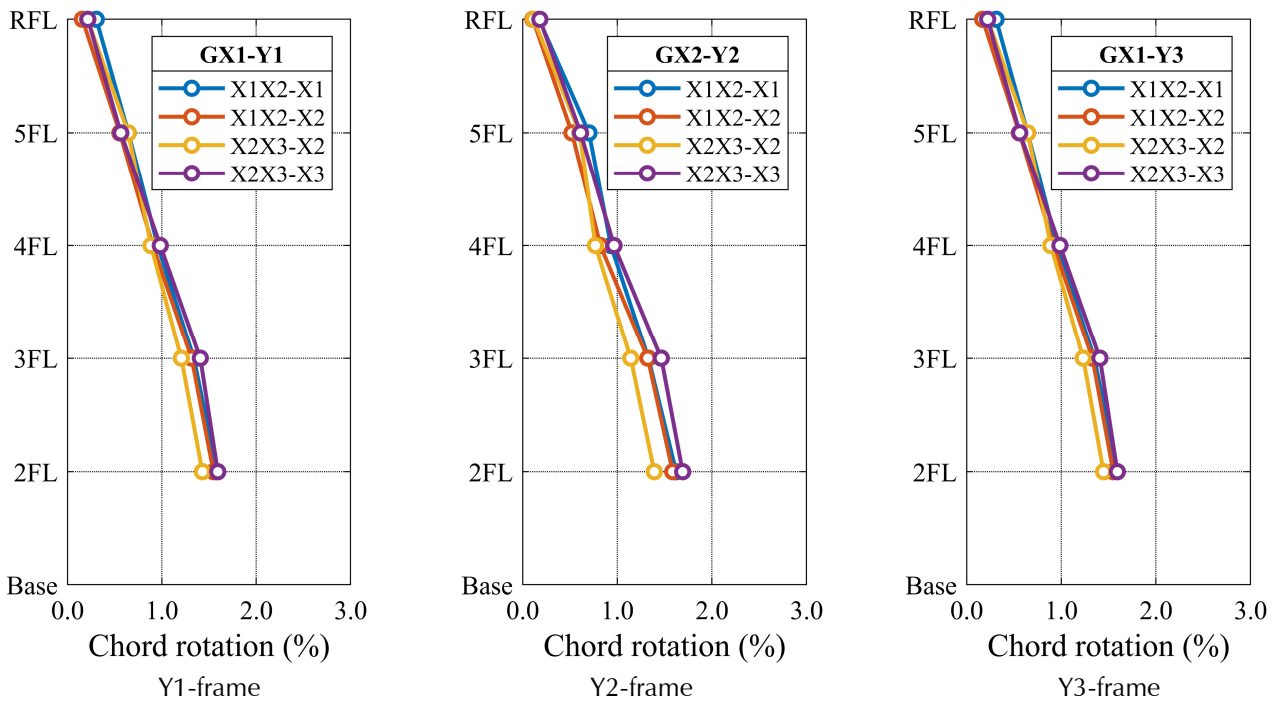


(a) Test result (hinge rotation)

Figure 5-4 Peak chord rotation (Analysis) and hinge rotation (Test) of beams.



(b) Modified linear model (chord rotation)



(c) Nonlinear model (chord rotation)

Figure 5-4(cont) Peak chord rotation (Analysis) and hinge rotation (Test) of beams.

5.3 Fatigue Check

In this section, two options for how to conduct the fatigue check are presented. The first method is the simplified fatigue life assessment. This

method is to assess the fatigue life of the reinforcement, assuming a simplified loading history. The second method is the detailed fatigue damage assessment. This approach is to identify the fatigue damage of reinforcement with a dynamic analysis procedure.

5.3.1 Fatigue Check Exception Criteria

The ATC-145-1 (ATC, 2020) provides three criteria for exception of fatigue check, thus fatigue check is not necessary when all three conditions below are met.

- The maximum chord rotation is less than 0.02 rad.
- The significant duration ($D_{5.95}$) of the damaging earthquake was less than 45 sec.
- The effective plastic hinge length of an element is greater than 0.4 times the member depth

It was confirmed that the maximum chord rotation demands of the test result, the linear model and nonlinear model were less than 0.02 rad as shown in 4.2. Therefore, this structure meets the chord rotation criterion.

Figure 5-5 shows a time history of acceleration of Run 2+3 and its significant duration (SD) per Arias intensity. Subsequent ground motion, Run 2+3, is evaluated since these ground motions caused damage. Arias intensity is defined as follows.

$$I_a = \frac{\pi}{2g} \int_0^{T_d} a(t)^2 dt$$

Where g : gravitational acceleration, T_d : duration of a ground acceleration, $a(t)$: ground acceleration at time t .

According to Figure 5-5, SD is 84.22 sec, therefore it **does not satisfy the second criterion.**

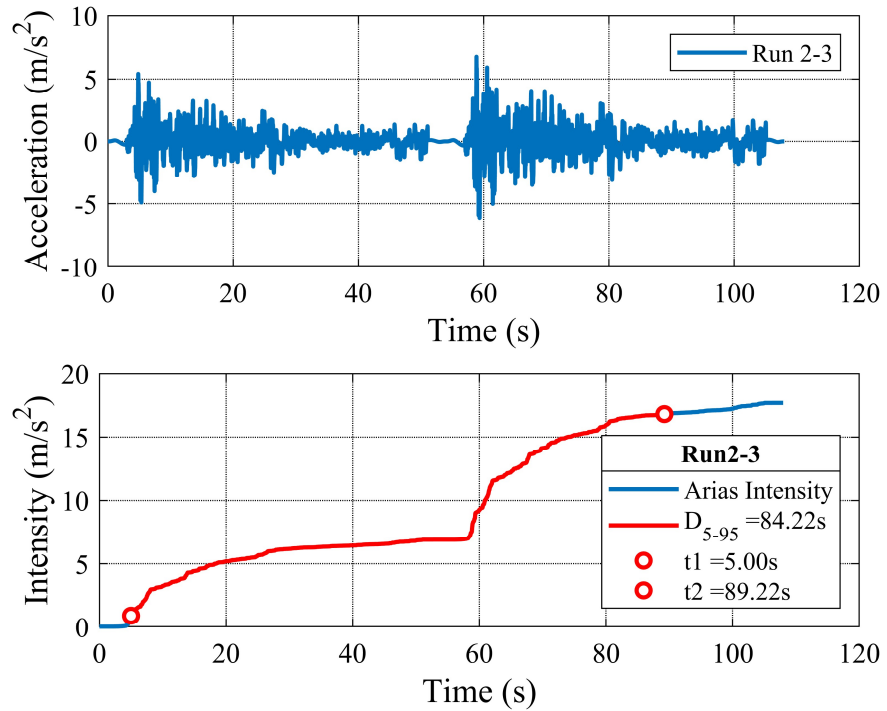


Figure 5-5 Time history of acceleration and significant duration per Arias intensity.

The effective hinge length can be calculated by the following equations.

$$L_p = k_{lp} \cdot a + L_{sp} \geq 2L_{sp}$$

where,

$$k_{lp} = 0.2(f_u/f_y - 1) \leq 0.08$$

a : shear span, L_{sp} : strain penetration length = $0.022f_y d_b$ where the f_y is in MPa, f_y : probable yield strength of longitudinal reinforcement, d_b : diameter of longitudinal reinforcement, f_u : probable ultimate strength of the longitudinal reinforcement.

Shear span, a , was assumed as a half of the clear span of members. Material test result (Table B-2) was used for f_y and f_u . A summary of the calculation of the effective plastic hinge length is provided in Table 5-1. As shown in the table, the effective plastic hinge length of all the beams satisfies the third criterion.

Table 5-1 Summary of the Calculation of the Effective Plastic Hinge Length

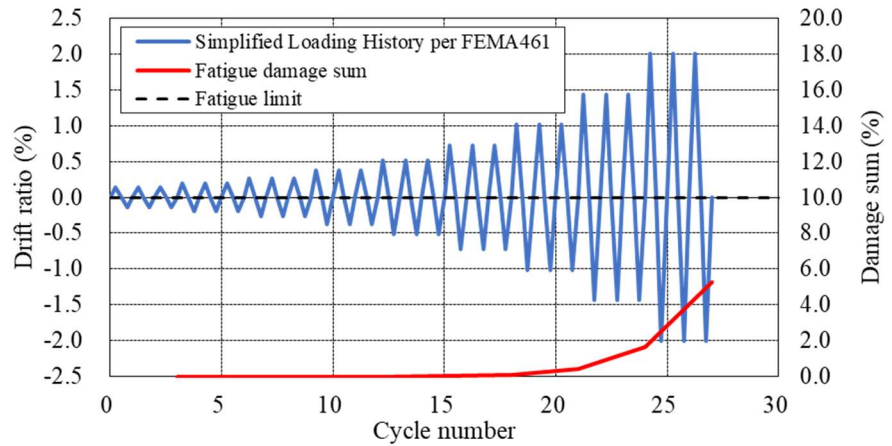
Depth	Shear span	Bar diameter	Yield strength	Ultimate strength	Strain penetration length	Effective plastic hinge length			
D (mm)	a (mm)	d_b (mm)	f_y (MPa)	f_u (MPa)	L_{sp} (mm)	k_{lp}	L_p (mm)	$0.4D$ (mm)	
GX1	800	2640	19	401	568	168	0.08	379	320 ...OK
GX2	640	2760	19	401	568	168	0.08	388	256 ...OK

For the investigations above, the first and third criteria were met, yet the second criterion was not satisfied. Therefore, the fatigue check is required.

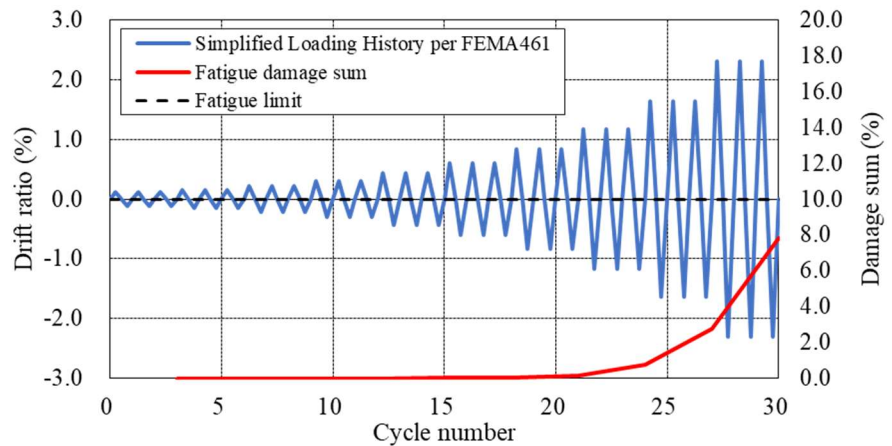
5.3.2 Simplified Fatigue Life Assessment

The simplified fatigue life assessment procedure is intended to make a rough estimation of the fatigue damage imposed during an earthquake. The fatigue damage is calculated with simplified loading history as per FEMA 461 (FEMA, 2007). The entire loading history is defined by the maximum story drift estimation with the analysis.

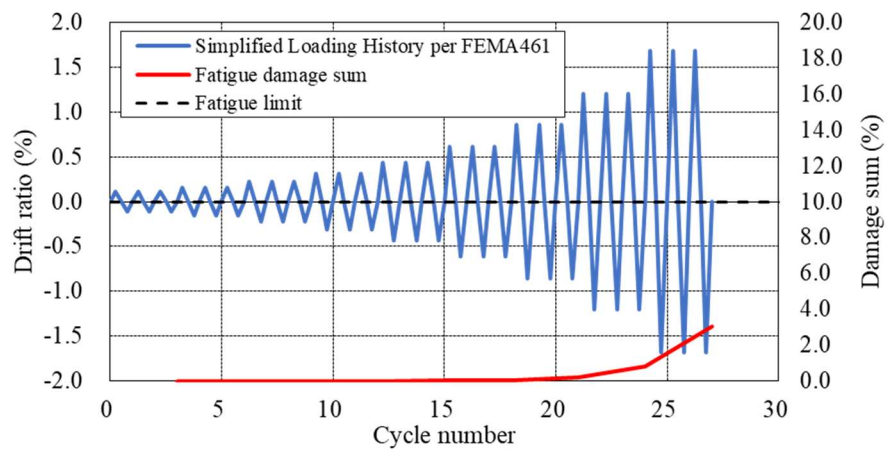
Figure 5-6 shows the simplified loading history and fatigue damage sum for the test result, the modified linear model and nonlinear model. The fatigue damage of these three cases is less than 10%, which is also less than the fatigue assessment criterion. Given that this simplified approach provides reasonable estimation of fatigue damage, these three cases do not require longitudinal bar replacement. The fatigue estimation is verified by comparing to the detailed estimation in 4.3.3.



(a) Test



(b) Modified linear model



(c) Nonlinear model

Figure 5-6 Simplified loading history per FEMA 461.

5.3.3 Detailed Method

This section explains how to assess the fatigue damage of longitudinal reinforcement with a detailed method per Appendix C in ATC-145-1 (ATC, 2020). The detailed method herein is to identify the fatigue damage with a dynamic analysis that was used in the Inspection and Analysis phase. A dynamic analysis typically provides rotation demand of the components, and strain demand can be estimated by rotation of the components. The fatigue damage was estimated from the test data, the linear model and the nonlinear model.

5.3.3.1 Strain Demand Estimation

In both the test and the analysis, strain demand can be obtained from the rotation demand of the components, assuming plain-sections-remain-plane. The strain demand of longitudinal reinforcement of the beams is estimated in this section.

Figure 5-7 illustrates the arrangement of LVDTs and longitudinal reinforcement of one of the beam hinges. LVDTs were placed on the end of the beam, and the measuring length was 200 mm from the column face. Also, these LVDTs were 50 mm away from the slab or bottom of the beam. From the output of the LVDTs, the strain distribution can be estimated, and the hysteretic response of longitudinal reinforcement was estimated. It is important to note that this output of the LVDTs includes the pull-out deformation of the longitudinal bar within the joint. Figure 5-8 indicates the actual strain distribution and average strain distribution within the measuring length. The average strain is then used for fatigue damage assessment. The average tensile strain is calculated, considering strain penetration length and average compression strain is calculated as the average strain within measuring length of LVDT. The average strain is estimated by the following equation.

$$\varepsilon_{ave} = \begin{cases} \frac{\delta_{LVDT}}{l_{sp} + l_{LVDT}} & (\delta_{LVDT} \geq 0) \\ \frac{\delta_{LVDT}}{l_{LVDT}} & (\delta_{LVDT} < 0) \end{cases}$$

Where: δ_{LVDT} : Deformation of LVDT, ε_{ave} : Average strain, l_{sp} : Strain penetration length, l_{LVDT} : Measuring length of LVDT.

According to Brown and Kunnath (Brown & Kunnath, 2000), strain amplitude for the fatigue assessment can be assumed as follows.

$$\varepsilon_a = \varepsilon_{ave}/2$$

Strain penetration length is calculated by the following equation (ATC, 2020).

$$l_{sp} = 0.022f_yd_b$$

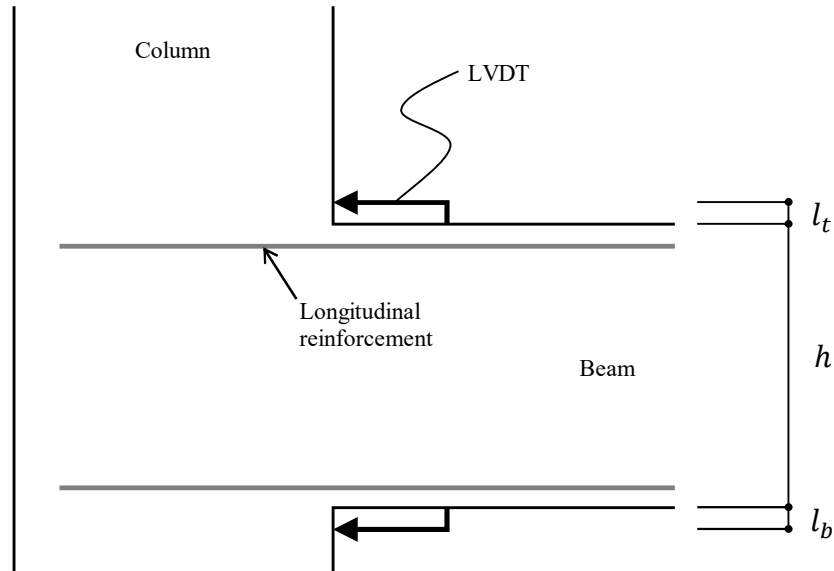


Figure 5-7 Arrangement of LVDTs and longitudinal reinforcement.

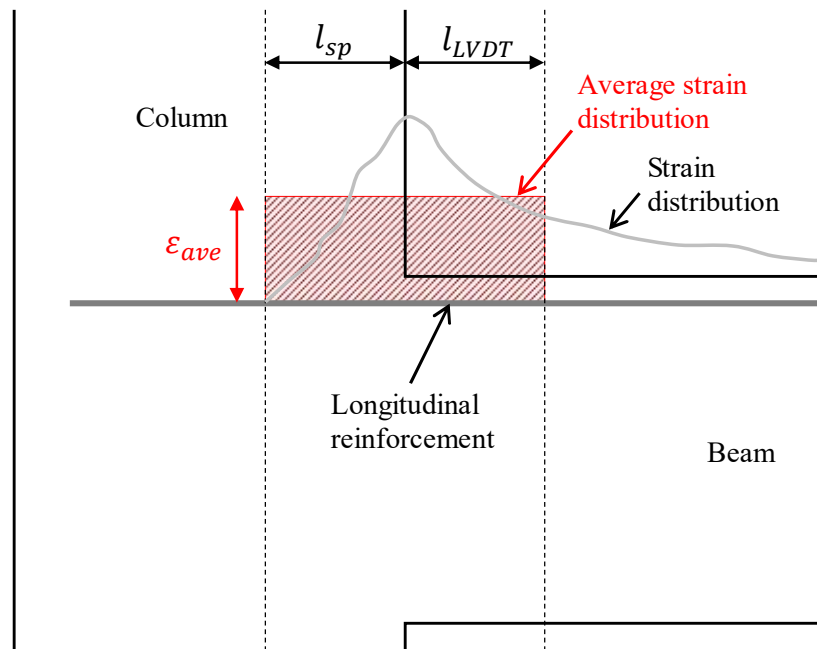


Figure 5-8 Average tensile strain in a longitudinal reinforcement.

On the other hand, the output with the analysis is only the rotation demand on the member, and it is not possible to estimate strain demand by only rotation demand. Therefore, the neutral axis depth is assumed, depending on

curvature. The idealized neutral axis depth-curvature relationship is expressed as follows.

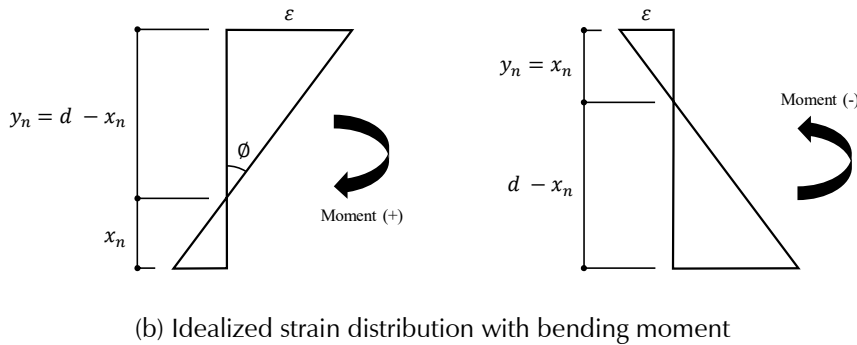
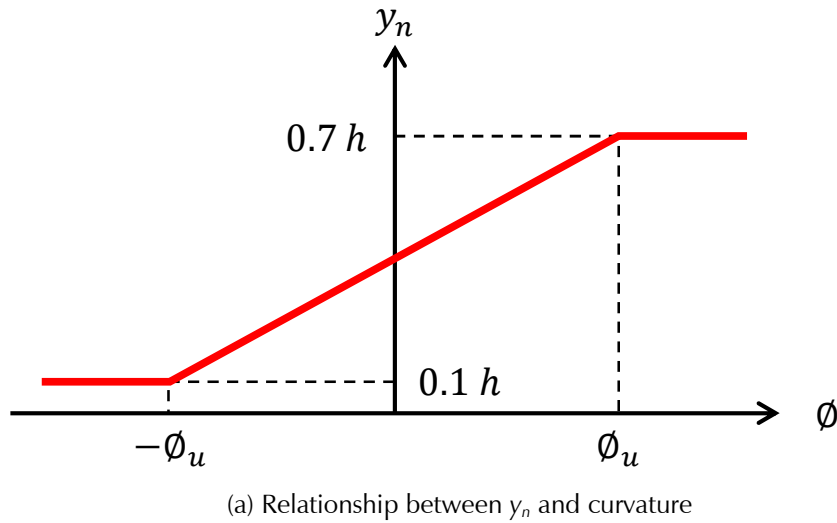


Figure 5-9 Idealized neutral axis depth-curvature relationship.

Effective depth of the member is calculated as follows.

$$d = 0.8h$$

where, h : Section height

Neutral axis depth with ultimate curvature is assumed as follows.

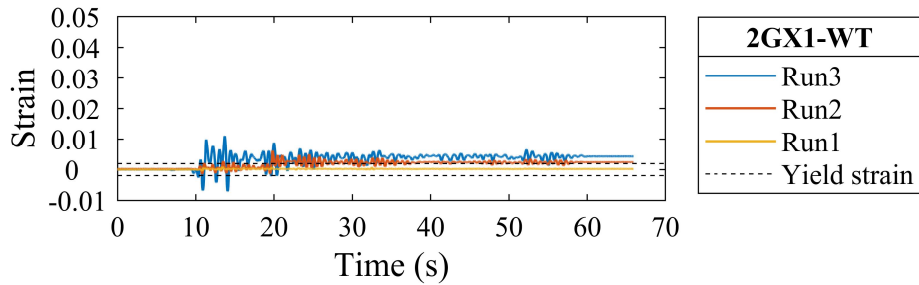
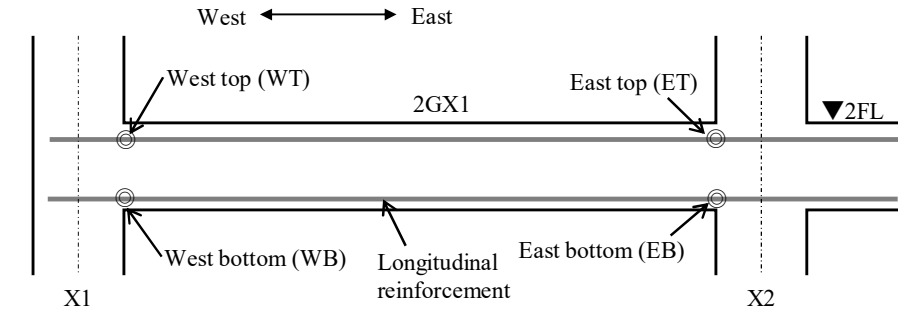
$$x_n = 0.1h$$

Ultimate curvature can be assumed by the following equation.

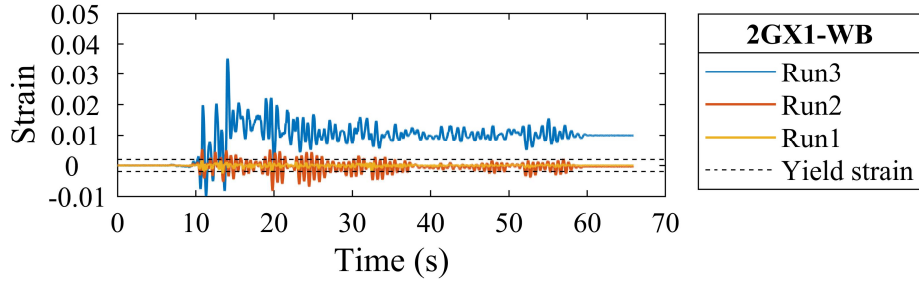
$$\phi_u = \frac{\epsilon_u}{x_n}$$

Where: ϵ_u : Ultimate strain of the extreme compression fiber (= 0.004).

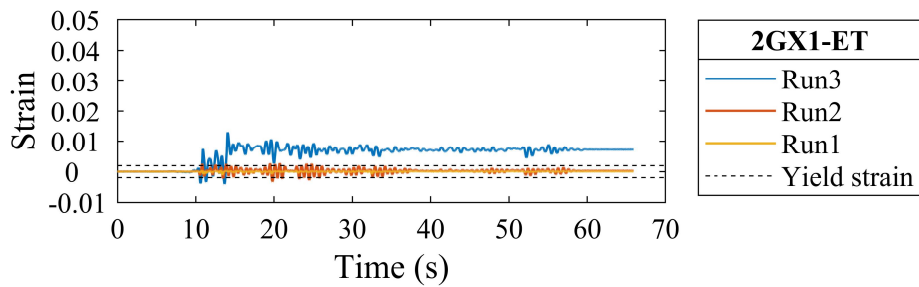
Figure 5-10 shows time history of strain in longitudinal reinforcements measured with LVDTs in the test. With these estimated strain demands, the fatigue damage of each of these longitudinal reinforcements was predicted in the following section.



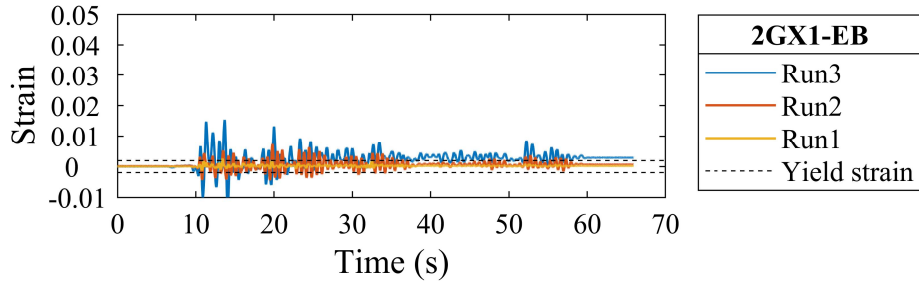
(a) West-top (WT) bar



(b) West-bottom (WB) bar



(c) East-top (ET) bar



(d) East-bottom (EB) bar

Figure 5-10 Time history of strain in longitudinal reinforcements.

5.3.3.2 Fatigue Damage Assessment

The estimated strain history is then used for cycle counting calculation. The cycle counting method employed in this study is the rainflow counting method (Endo et al., 1974), with the number of cycles and strain amplitude, the fatigue damage sum can be calculated with the Minor's sum. Figure 5-11 shows the cumulative fatigue damage of longitudinal reinforcements in beams up to Run 3 based on strain measured with LVDTs in the test. The cumulative fatigue damage is less than 2.0%. Therefore, the reinforcement does not suffer significant fatigue damage in the test. Comparing the fatigue damage estimation with the simplified method, while the simplified method provides fatigue damage estimate of 4 to 8 %, the detailed method indicates less than 1.0% fatigue damage. This result substantiates that the simplified method provides conservative fatigue damage estimate, and the detailed method can be used for detailed investigation of the fatigue assessment.

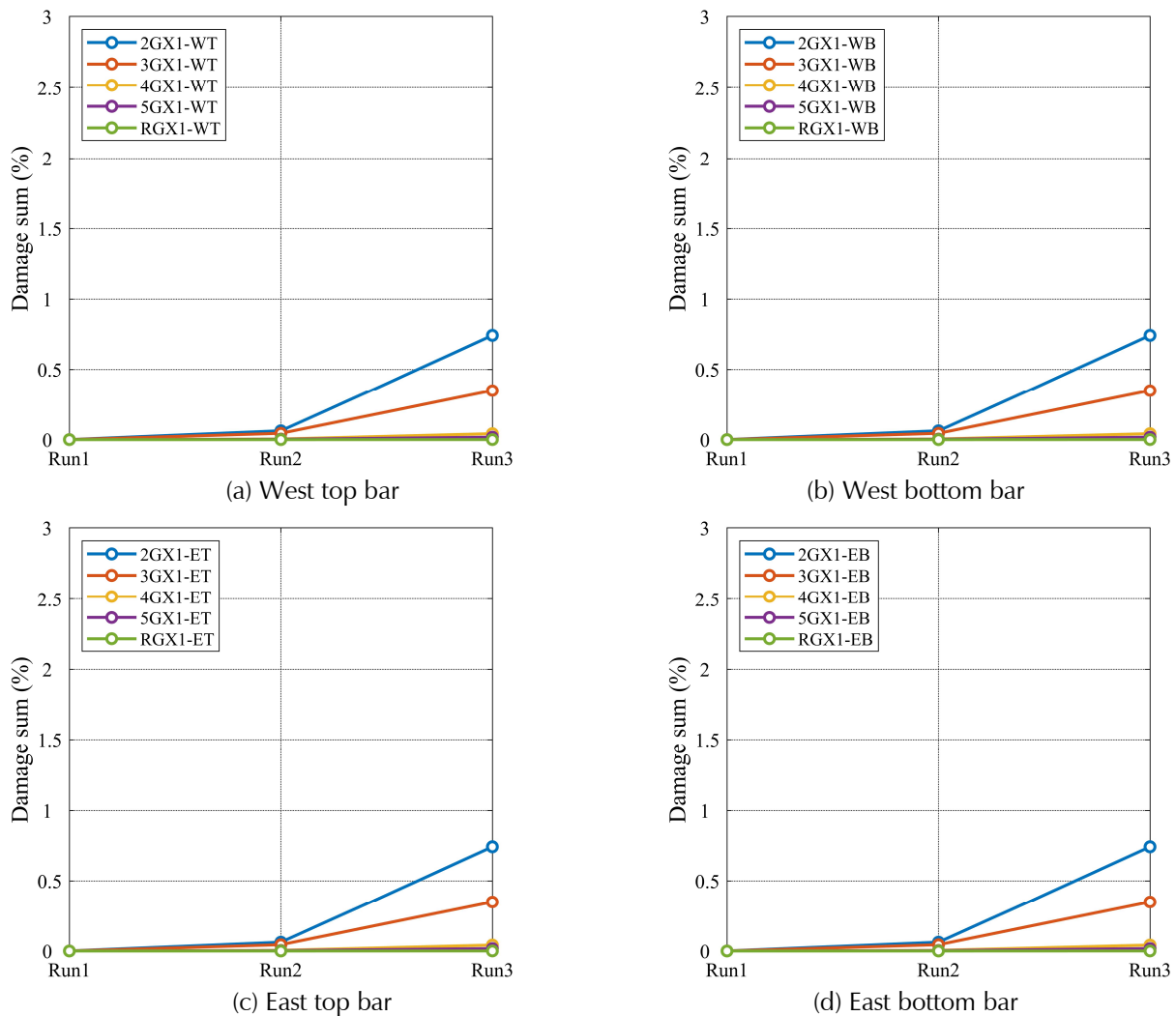


Figure 5-11 Cumulative fatigue damage of beams. Legends correspond to locations in Figure 5-10.

5.4 Concentrated Damage Check

Figure 5-12 shows photos of damaged members during Run 4, and supplemental damage photos are provided in Figure J-1. After Run 4 (125%), the specimen reached the mechanism of the structure. The cracks occurred mainly in the plastic hinge zone of the members forming plastic hinges. Only minor spalling was observed on the bottom of the columns in 1st story and plastic hinge zone in the beams. There was no severe spalling or crushing of core concrete, so it does not appear that bar buckling occurred with Run 4. Overall, this specimen passed the Concentrated damage check and goes to Serviceability assessment.



Column (1F X3Y1)



Beam (2F X2Y3)

Figure 5-12 Damage occurred during Run 4.

5.5 Summary

In this chapter, the specimen was assessed with the safety assessment criteria. The safety assessment includes system check, component check and fatigue check. The main findings through the assessment are listed below.

System Check

- The test result, the modified linear model and the nonlinear model were compared to the safety drift limit. The modified linear model and test both exceeded the 2.0% safety drift limit and triggered the component and fatigue checks.

Component Check

- The chord rotation of beams with analysis and the plastic hinge rotation measured in the test were assessed. The chord rotations of analysis and plastic hinge rotation of the test result passed the chord rotation limit of the component check. It should be noted that plastic rotation of the test are not supposed to be compared to chord rotation limit in ATC-145-1 (ATC, 2020), but, it can be assumed that

components with plastic rotations less than 2.0% are not prone to significant fatigue damage as hinge rotation is typically greater than chord rotation. Provided that there is not a significant difference between measured plastic hinge rotation and chord rotation in the test, beams could meet the rotation criterion. Furthermore, this result supports the assumption that the structure with less than 2.0% story drift is unlikely to be imposed significant rotation demand.

Fatigue Check

- The simplified fatigue check was conducted with the test result, the modified linear model and the nonlinear model, respectively. In all the cases, the estimated fatigue damages were 4 to 8%, and these results meet the fatigue criterion.
- The fatigue damage estimate with the detailed method was less than 1.0% based on strain demand measured in the test. This result implies that the detailed method can provide more accurate estimation compared to the simplified method. On the other hand, the simplified method can provide a conservative estimate of fatigue damage.

Case Study 1

Chapter 6

Serviceability Assessment

In the serviceability assessment phase, the damaged structure is assessed to determine whether or not epoxy or more significant repair is needed. Figure 6-1 illustrates the serviceability assessment procedure. Serviceability assessment starts with drift estimation of a damaged structure. The drift estimation is then compared to the drift limit of serviceability of the structure. The serviceability limit is defined by drift sensitive nonstructural components (e.g., partition walls). The drift limit for serviceability was assumed 1.0% herein, as recommended in ATC-145-1 (ATC, 2020). Once the drift estimation exceeds the serviceability limit, the structure is required to be repaired. Finally, the repaired structure is assessed for drift demand to determine whether or not it meets the serviceability limit for a future earthquake.

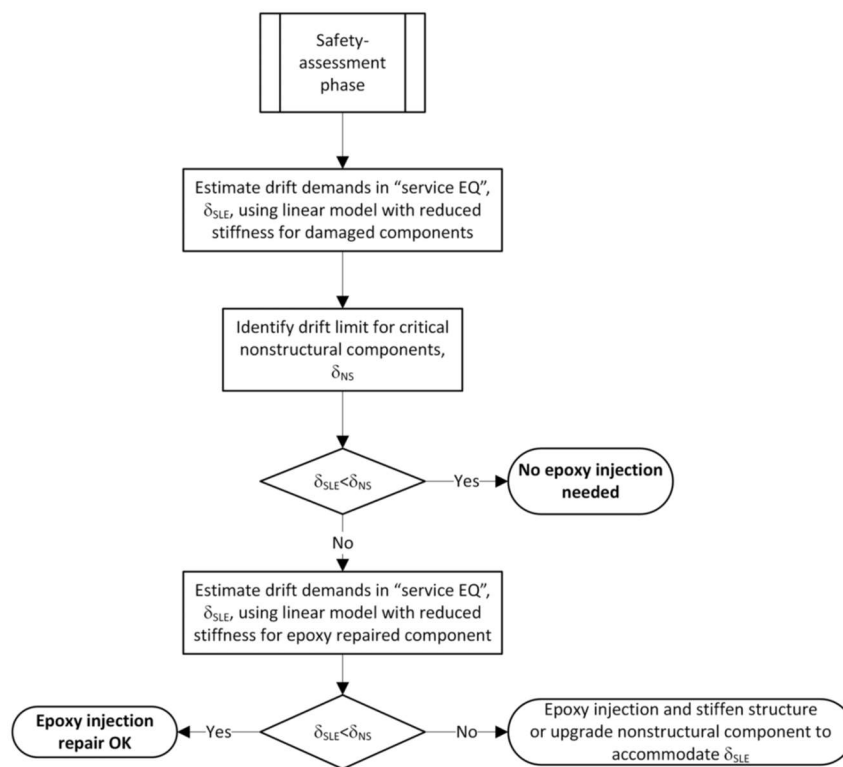


Figure 6-1 Serviceability assessment procedure.

6.1 Drift Estimate

6.1.2 Damaged Structure

Peak story drift demand can be estimated by a linear model with the stiffness reduction described in 3.2.1.4.1. Equivalent ductility was estimated by DCR of the original linear model for Run 3. Equivalent ductility is then converted to stiffness reduction factor.

Figure 6-2 shows the drift estimation with a damaged linear model. Although it can be slightly high, 60% El Centro NS wave was applied as a service-level earthquake. 60% seems relatively high as a “service-level” earthquake. Further discussion might be needed on if this scaling is appropriate for “service-level” earthquake. In most of the stories, story drift exceeds the serviceability limit of 1.0%, triggering structural repaired to satisfy serviceability criteria. This result indicates that this structure needs to be repaired as to achieve serviceability criterion. Also, this result was consistent with the secant stiffness type approach in Figure 4-17.

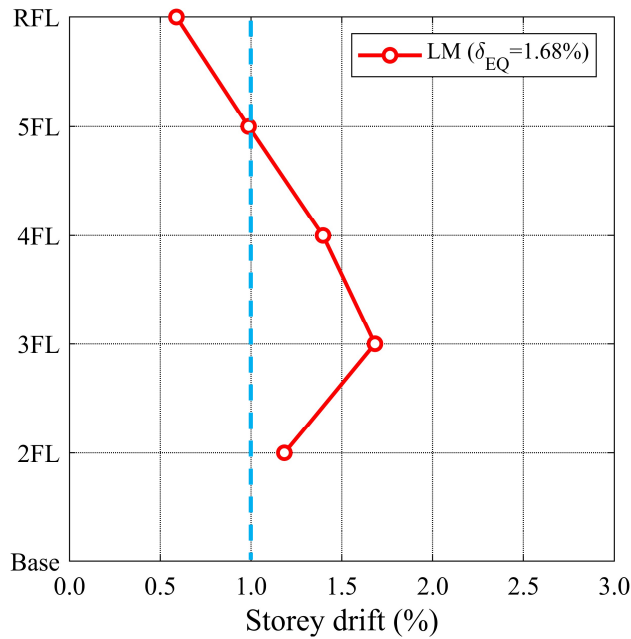


Figure 6-2 Peak drift demand with a damaged linear model.

6.1.2 Repaired Structure

Response of the repaired structure can be predicted with a linear model with stiffness reduction factor as shown in Figure 6-3. Stiffness reduction factor for epoxy-repaired components was assumed 0.8 as recommended in ATC-145-1 (ATC, 2020). In addition, no stiffness recovery was assumed for the columns, so were modeled using their damaged state. Table 6-2 summarizes effective rigidity for repaired beams and columns. As shown in Figure 3-4,

the specimen was repaired up to the fourth-floor level, which means beams in the fourth and fifth story was left damaged.

Figure 6-4 shows peak drift estimation with a repaired linear model and test result in Run 5. The analysis result slightly underestimated the test result but was generally well estimated. One of the probable reasons for this underestimation is that beams on the fourth-floor level were repaired only in the range of the critical section. This repair could cause a lower recovery than 0.8. Overall, the response of the repaired structure was reasonably well estimated. Hence, it can be said that the repaired linear model provides a reasonable drift estimation.

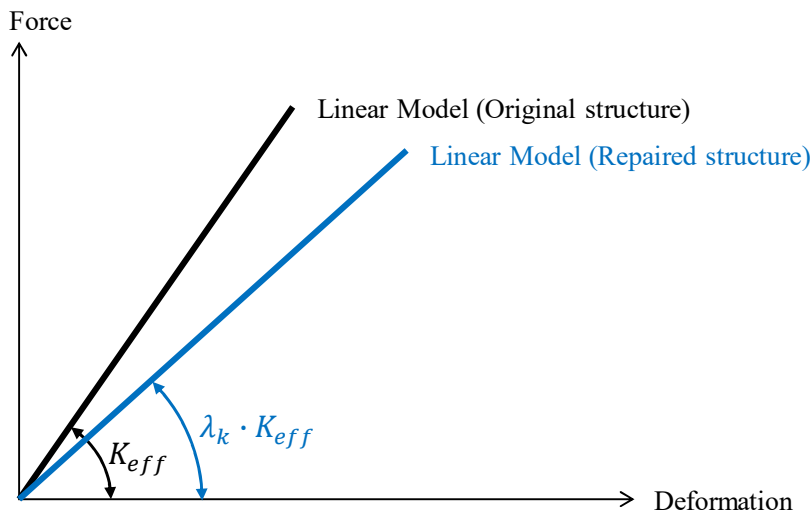


Figure 6-3 Repaired linear model.

Table 6-2 Stiffness of Linear Model of the Repaired Structure

	Stiffness modification, λ_k	Flexural rigidity		Shear rigidity	Axial rigidity
Beam	0.8	$0.3E_cI_g \times \lambda_k$		$0.4E_cA_w$	$1.0E_cA_g$
Column	No stiffness recovery assumed	$0.7E_cI_g \times \lambda_k$	$(0.5 \leq \eta_0)$		
		$(\eta_0 - 0.2) E_cI_g \times \lambda_k$	$(0.1 < \eta_0 < 0.5)$		
		$0.3E_cI_g \times \lambda_k$	$(\eta_0 \leq 0.1)$		

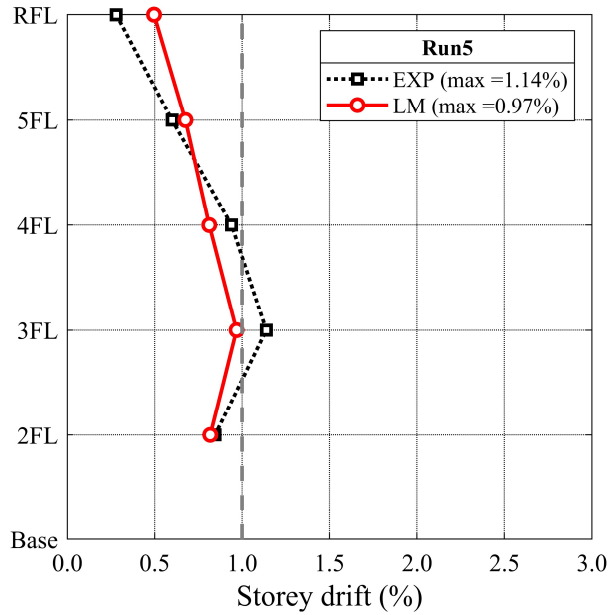


Figure 6-4 Peak story drift estimation with a repaired linear model.

6.2 Repair Recommendations

In the test, the specimen was repaired with epoxy injection and mortar patching as this is a well-established and widely-used methodology. The peak story drift demand of the repaired specimen during the 60% input ground motion was 1.14%, and it is feasible to ensure the serviceability of moderately damaged ductile concrete moment frame buildings using this repair methodology. Furthermore, considering that the repaired area was limited within the ends of components and the upper stories were not repaired, it may be reasonable to ensure serviceability of structures without repairing the entire building. However, epoxy repair of all the damage in the building could have a better outcome. Moreover, 60% input is relatively high as a service-level earthquake, so the drift response in a more frequent, smaller earthquake could be smaller.

Conclusions and Recommendations

The main objective of this case study is to provide an application example of post-earthquake assessment using ATC-145-1 (ATC, 2020) procedure and to investigate its validity. A five-story reinforced concrete building tested on a shake table at the E-Defense facility was assessed with ATC-145-1 (ATC, 2020). It was found that the post-earthquake assessment approach per ATC-145-1 (ATC, 2020) can reasonably estimate the damage level and the response of the structure. Several limitations on the use of the ATC-145-1 (ATC, 2020) were also discussed.

7.1 Inspection Locations

Inspection Location (IL) is one of the important phases in the assessment procedure as it defines the damage state of the building and is used to validate the analytical model. IL is typically defined as the plastic hinge with that DCR is greater than 1.0, and a significant number of plastic hinges are flagged in accordance with this criterion. On the other hand, given that plastic hinges with DS1 or greater should be defined as IL, the number of plastic hinges that were actually found with DS1 (or greater) was quite limited compared to the analytical estimation. Therefore, it was found that the default criterion, DCR greater than 1.0, is conservative. The more locations are specified as IL, the higher the time and cost to inspect, and this would be a disadvantage on visual inspection. Further refinement may be needed on the criterion of IL.

7.2 Drift Estimation of a Damaging Earthquake

As a method of drift estimation of a damaging earthquake, it is recommended to start with a simple linear model and update it depending on the agreement with visual inspection. It was shown that a linear model was able to simulate the peak story drift demand in the test within the elastic range. However, the linear model underestimates the inelastic response of the structure. For the refinement of the analysis, there are two way to update; update of the model or update of a damaging earthquake demand. Yet, only the analytical model was updated as the damaging earthquake was already known. In order to refine the model, the

modified linear model and nonlinear model were investigated. The modified linear model was the linear model with the initial stiffness reduction by maximum ductility imposed in the past earthquake, and this model provided a good prediction of the test result. The nonlinear model, using a bilinear backbone characteristic was found that also reasonably predict the test result; however, estimated drifts were lower which led to an underestimation of the damage state. It should be noted that the modified linear model can be employed only in the case that the structure was already damaged by an earthquake. Thus, in most cases, the nonlinear model will likely be adopted for added analysis refinement.

7.3 System and Component Check for the Safety Assessment

Based on the peak story drift of the test result and analysis result, the System check and Component check were investigated. The component check should have been exempted for the structure with less than 2.0% story drift, but all the cases were assessed with Component check in this study. In the case of less than 2.0% story drift, rotation demands of the components were less than 0.02 rad, and those components were unlikely to be subjected to a significant degree of deformation demands. Also, in the case of more than 2.0% story drift, rotation demands of the components did not exceed 0.02 rad. Hence, it can be said that 2.0% for story drift criterion is reasonably conservative for Component check.

7.4 Fatigue Check

The simplified method and the detailed method of the low-cycle fatigue check were investigated and compared. On both cases, test result and analysis result, the fatigue damage was estimated with the simplified method and the detailed method. The simplified method was based on the simplified loading history per FEMA 461 defined by maximum story drift. The cumulative damage estimations with the simplified method were less than 10%, and this result indicates that these structures were unlikely to be compromised by fatigue damage. On the other hand, the damage sums with the detailed method were less than 1.0% in all the beam hinges. Thus, it is concluded that the simplified method is likely to give conservative and quicker result compared to the detailed method.

7.5 Drift Estimation of a Damaged and Repaired Structure

For the assessment of necessity of repair, a damaged model and a repaired model were investigated. Both a damaged and repaired structure were modelled as a linear model with stiffness reduction. It was found that the damaged structure was likely to exceed the serviceability limit of 1.0% story drift and trigger repair. Thus, the damaged structure was required to be repaired with epoxy injection. In a repaired model, the stiffness recovery was only assumed for the beams, which meant no stiffness recovery was assumed for the columns. The repaired model

matched the story drift demand of repaired specimen well. Thus, it was demonstrated that a repaired linear model can be valid for the drift estimation of repaired structures. Additionally, epoxy injection and mortar patching can be an effective means of restoring the serviceability performance of light to moderately damaged concrete moment frames.

Case Study 1

Appendix A

Repair Technique

Figure A-1 describes repair process applied to the test building. After the building was damaged, initially, cracks were drilled to make holes to inject epoxy resin (Figure A-1 (a)). Then all the cracks other than the drilled holes and spalled area were sealed with caulking compound and mortar not to get leaking of epoxy and put base of syringes (Figure A-1 (b-c)). Set syringes on the bases and inject epoxy resin into cracks. The design injecting pressure was $0.06 \pm 0.01 \text{ N/mm}^2$. Figure A-2 shows those repair process on each component.

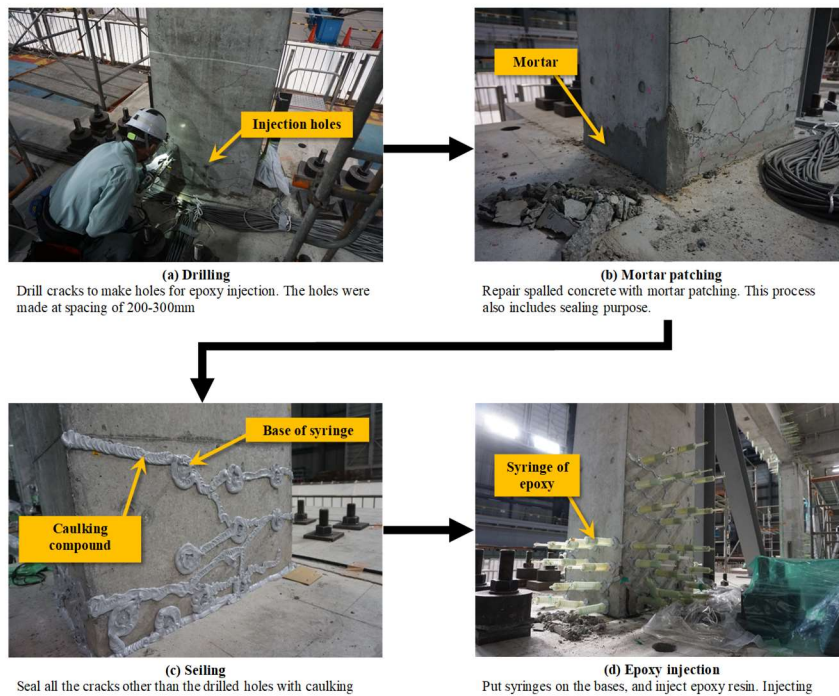
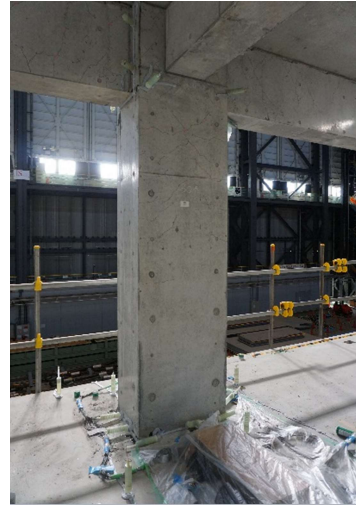


Figure A-1 Repair process.



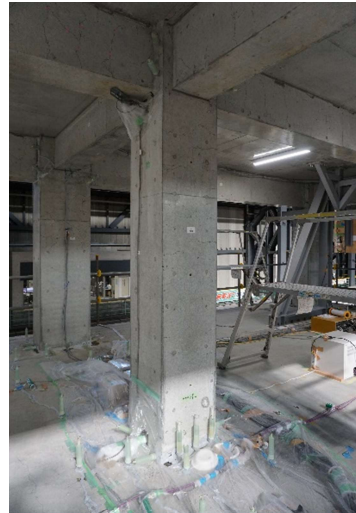
4FL X1Y1



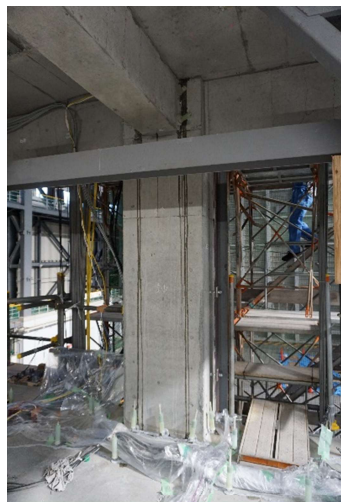
4FL X2Y1



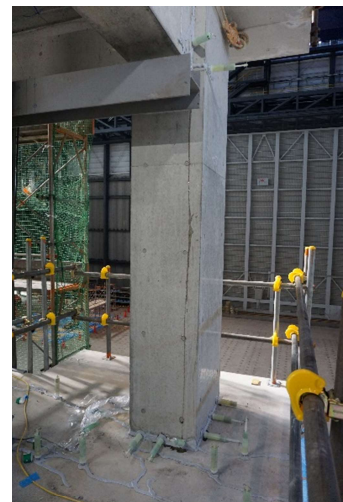
4FL X3Y1



4FL X2Y2



4FL X3Y2



4FL X1Y3

Figure A-2 Photos of epoxy injection.



4FL X2Y3



3FL X1Y1



3FL X2Y1



3FL X3Y1



3FL X1Y2

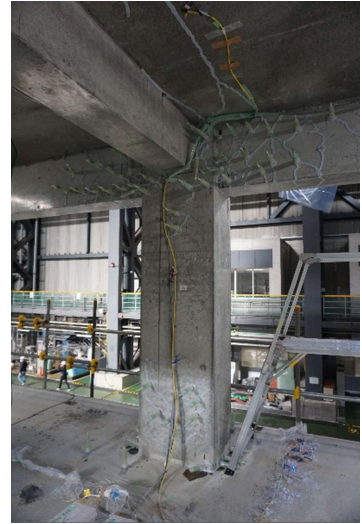


3FL X2Y2

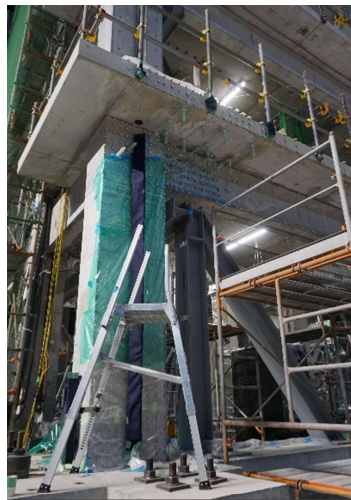
Figure A-2(cont) Photos of epoxy injection.



3FL X3Y2



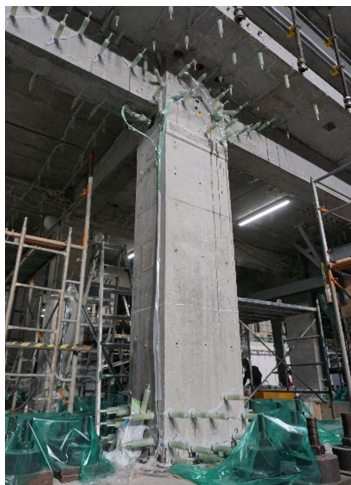
3FL X2Y3



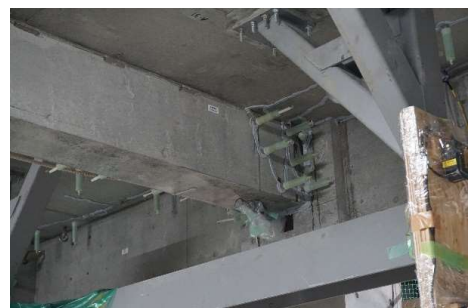
2FL X1Y1



2FL X2Y1



2FL X3Y1



2FL X1Y2

Figure A-2(cont) Photos of epoxy injection.



2FL X2Y2



2FL X1Y3



2FL X2Y3



2FL X3Y3

Figure A-2(cont) Photos of epoxy injection.

Case Study 1

Appendix B

Material Properties

Table B-1 shows the mechanical properties of concrete. The design strength of concrete was 33 MPa. Concrete samples were collected when casted. The compression tests and split tension tests were performed on these concrete samples at four-weeks after casting and before the shake table test.

Table B-1 Mechanical Properties of Concrete

Storey	Date of cast	Design strength	Four weeks test		Compression test			Tension test	
			Date	Compression strength	Date	Compression strength	Young's modulus	Date	Tesion strength
		F_c		f'_c (MPa)		f'_c (MPa)	E_c (MPa)		f_t (MPa)
5F	2020/07/21	33	2020/08/18	41.0	2020/10/01	38.2	30700	2020/09/30	3.14
4F	2020/07/02		2020/07/30	33.6	2020/10/01	37.4	30100	2020/09/30	3.13
3F	2020/06/16		2020/07/14	36.0	2020/10/01	42.2	31700	2020/09/30	2.90
2F	2020/05/25		2020/06/22	36.1	2020/10/01	39.2	30000	2020/09/30	3.13
1F	2020/03/17		2020/04/14	37.8	2020/10/01	49.0	33100	2020/09/30	3.43
Foundation	2020/02/10		2020/03/09	39.0	2020/10/01	49.2	34000	2020/09/30	3.33
Average				37.3		42.5	31600.0		3.2

Table B-2 shows the mechanical properties of reinforcing bars. The Tension tests were performed on each grade of steels.

Table B-2 Mechanical Properties of Reinforcing Bars

Bar	Member	Steel grade	Tension test			
			Yield strength		Ultimate strength	
			(Sample) (MPa)	(Average) (MPa)	(Sample) (MPa)	(Average) (MPa)
D38	Foundation beam	SD390	446.6		642.1	
			453.0		641.9	
			452.2	450.6	643.5	642.5
					642.6	
D25	Column	SD345	391.3		567.8	
			402.4		570.4	
			395.8	396.5	566.3	567.3
					564.7	
D22	Column	SD345	404.3		571.9	
			403.5		571.9	
			404.9	404.2	573.8	573.8
					577.4	
D19	Beam	SD345	403.3		566.6	
			404.3		568.8	
			396.1	401.2	568.0	567.7
					567.2	
D13	Slab	SD295A	340.8		474.3	
			334.5		479.7	
			340.9	338.7	478.9	477.9
					478.8	
D10 (Lot A)	Hoop Stirrup	(1-2F) (2-3F) SD295A	350.4		474.4	
			376.4		514.6	
			377.3	368.0	517.0	495.6
					476.4	
		516.7				
D10 (Lot B)	Hoop Stirrup	(3-4F) (4-5F) SD295A	380.4		518.6	
			375.6		518.9	
			375.6	377.2	515.5	517.7
					517.8	
D10 (Lot C)	Hoop Stirrup	(5F) (RF) SD295A	380.4		527.5	
			386.7		529.3	
			382.5	383.2	526.5	526.9
					524.4	

Case Study 1

Appendix C

Hysteresis Response of the Building

Figure C-1 shows hysteresis response of the original and repaired specimen.

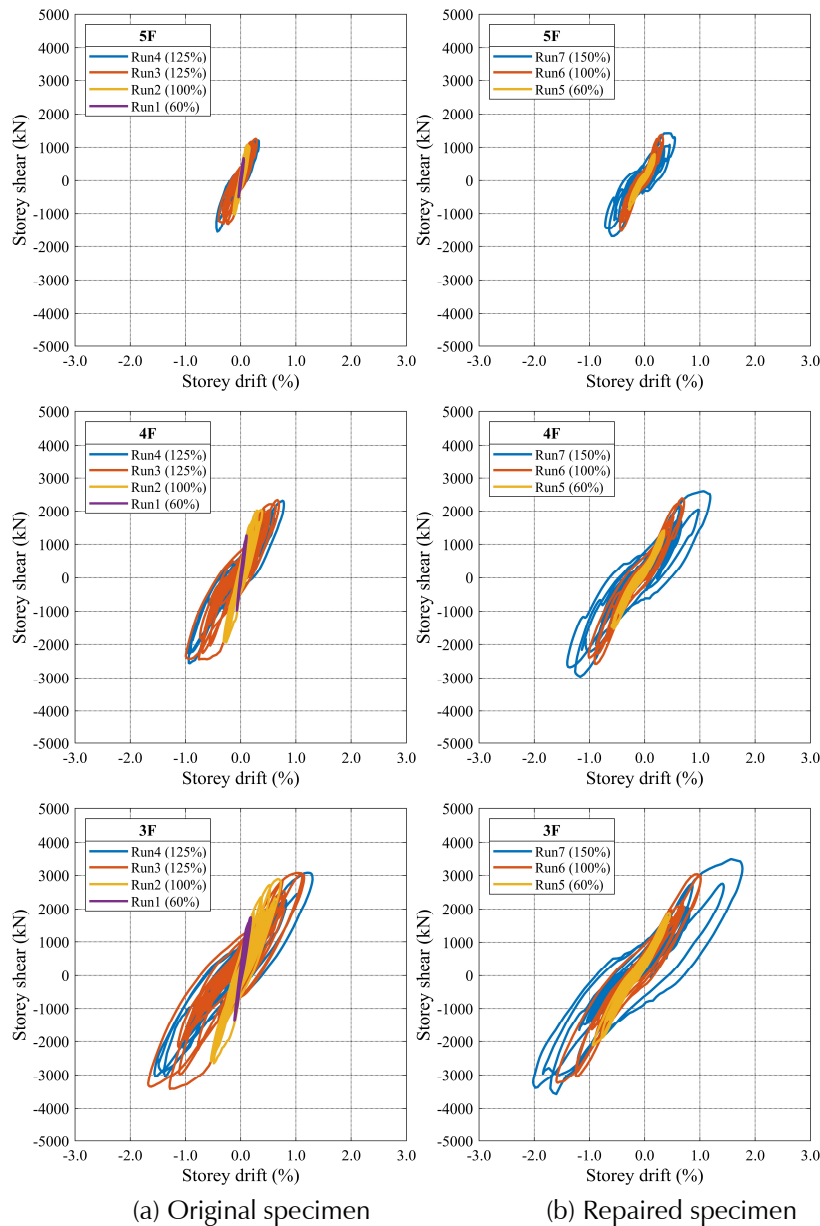


Figure C-1 Hysteresis response of the specimen.

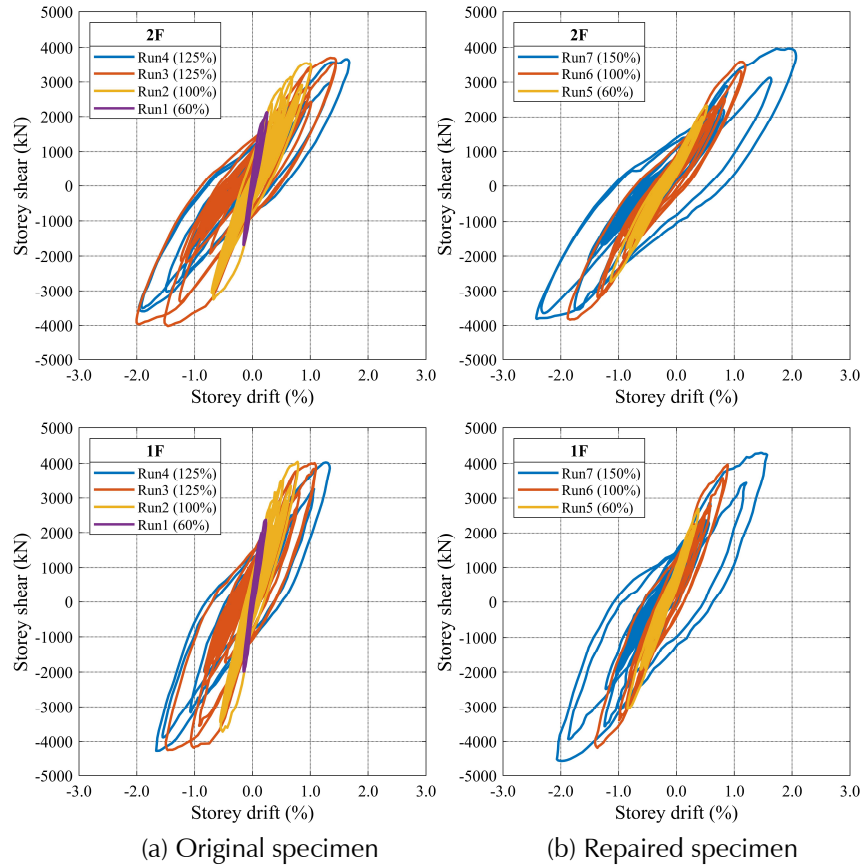
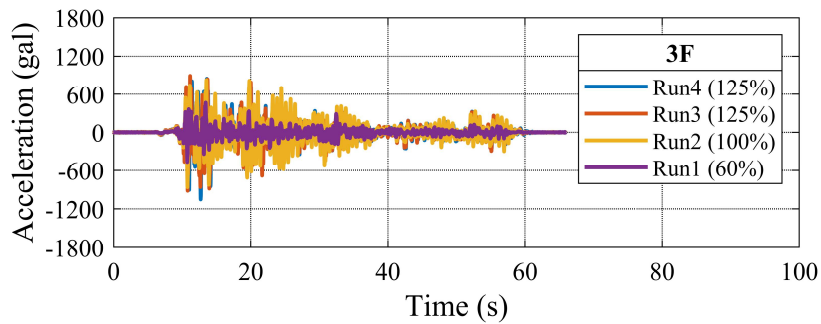
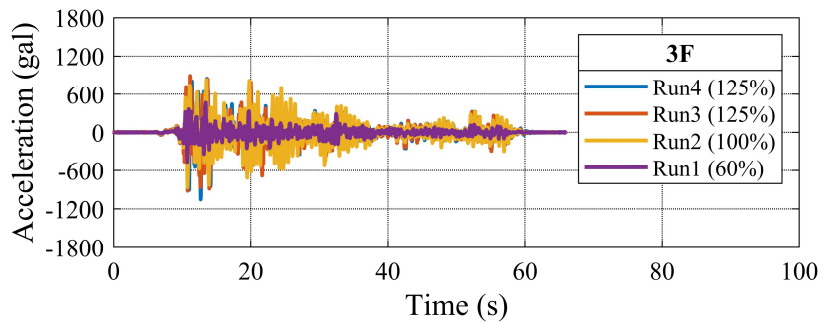
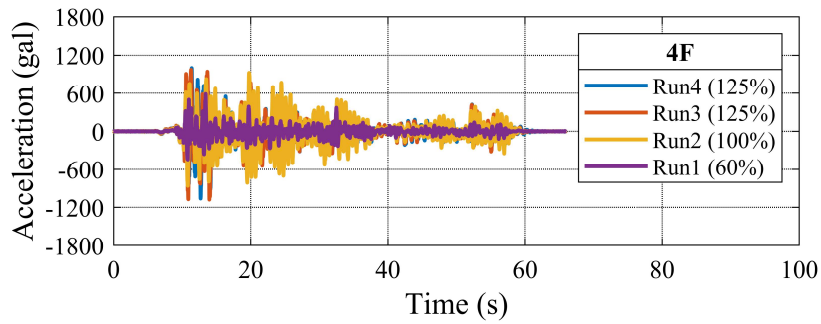
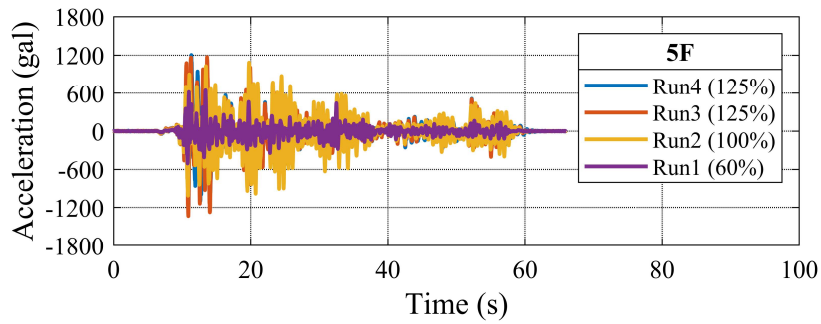
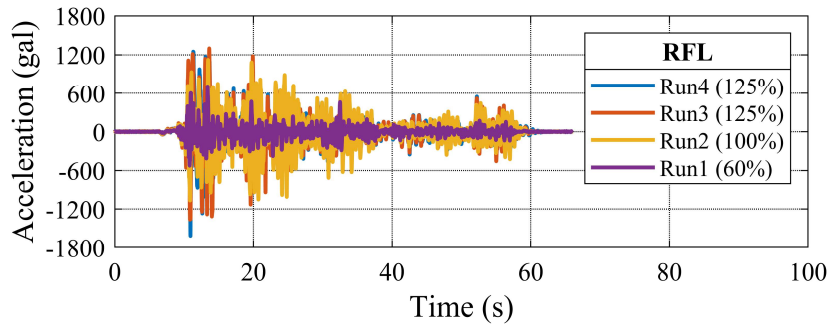


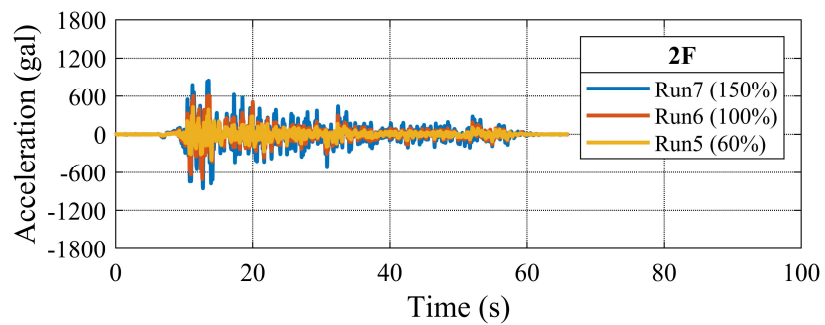
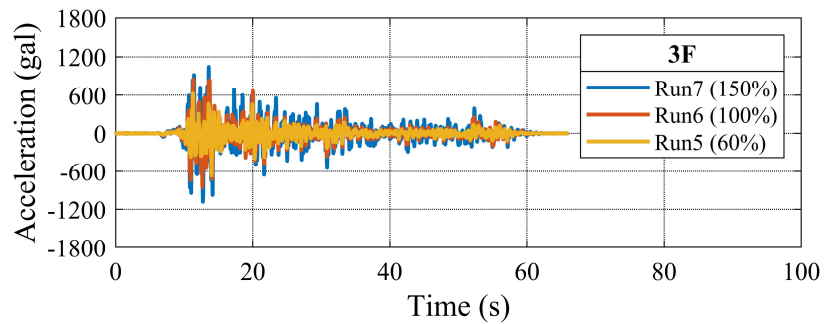
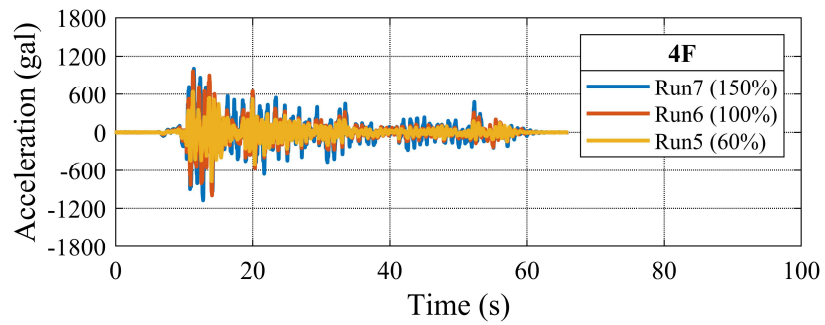
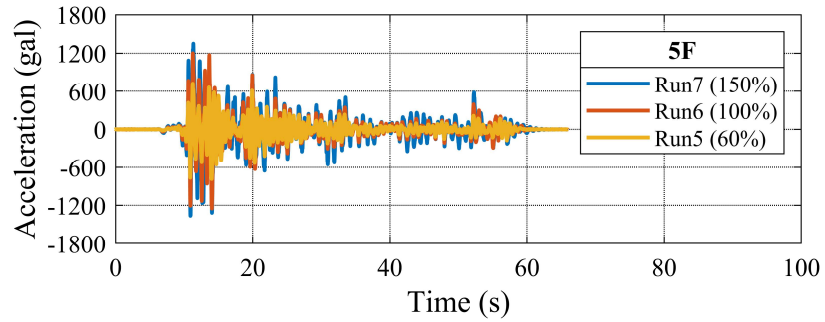
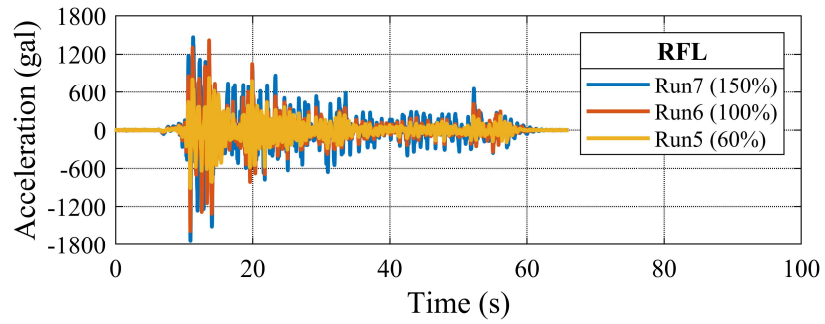
Figure C-1(cont) Hysteresis response of the specimen.

Figure C-2 shows time history of acceleration response of the original and repaired specimen at each floor-level.



(a) Original specimen

Figure C-2 Time history of acceleration response.



(b) Repaired specimen

Figure C-2(cont) Time history of acceleration response.

Case Study 1

Appendix D

Visual Inspection

D.1 Crack Patterns

Figure D-1 shows crack mapping of the original specimen after Run 2 and Run 4.

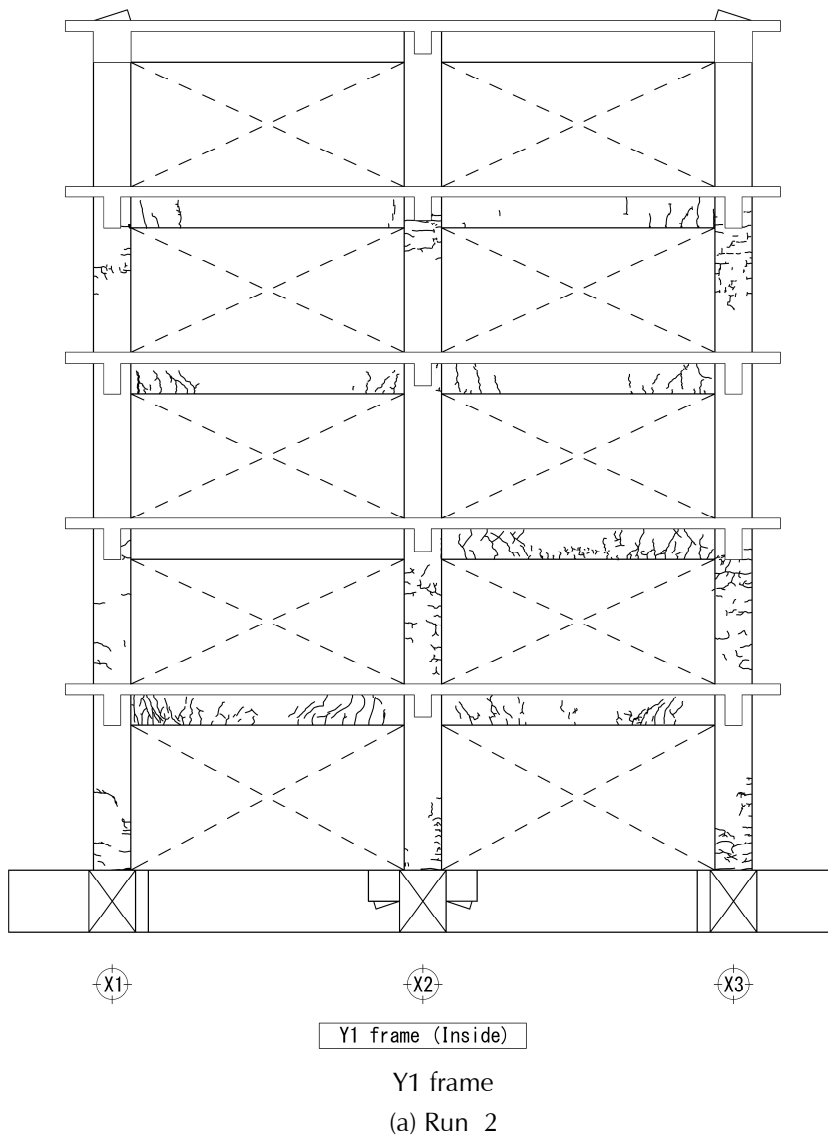


Figure D-1 Crack patterns.

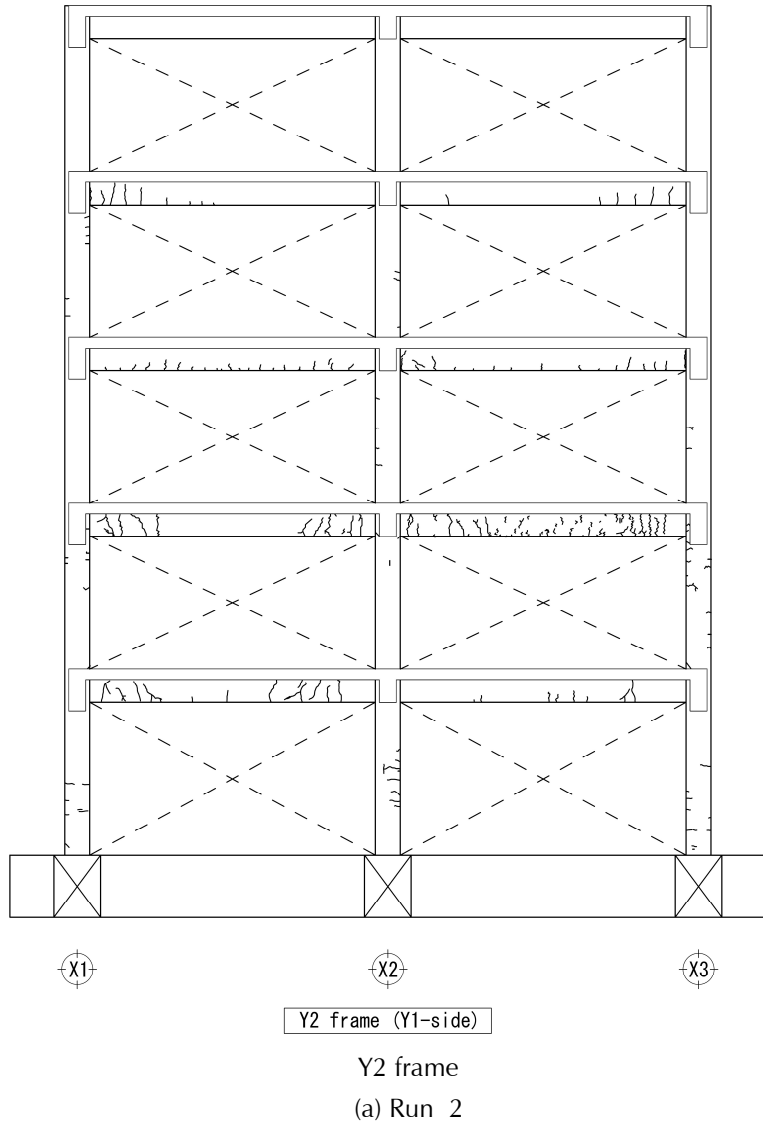


Figure D-1(cont) Crack patterns.

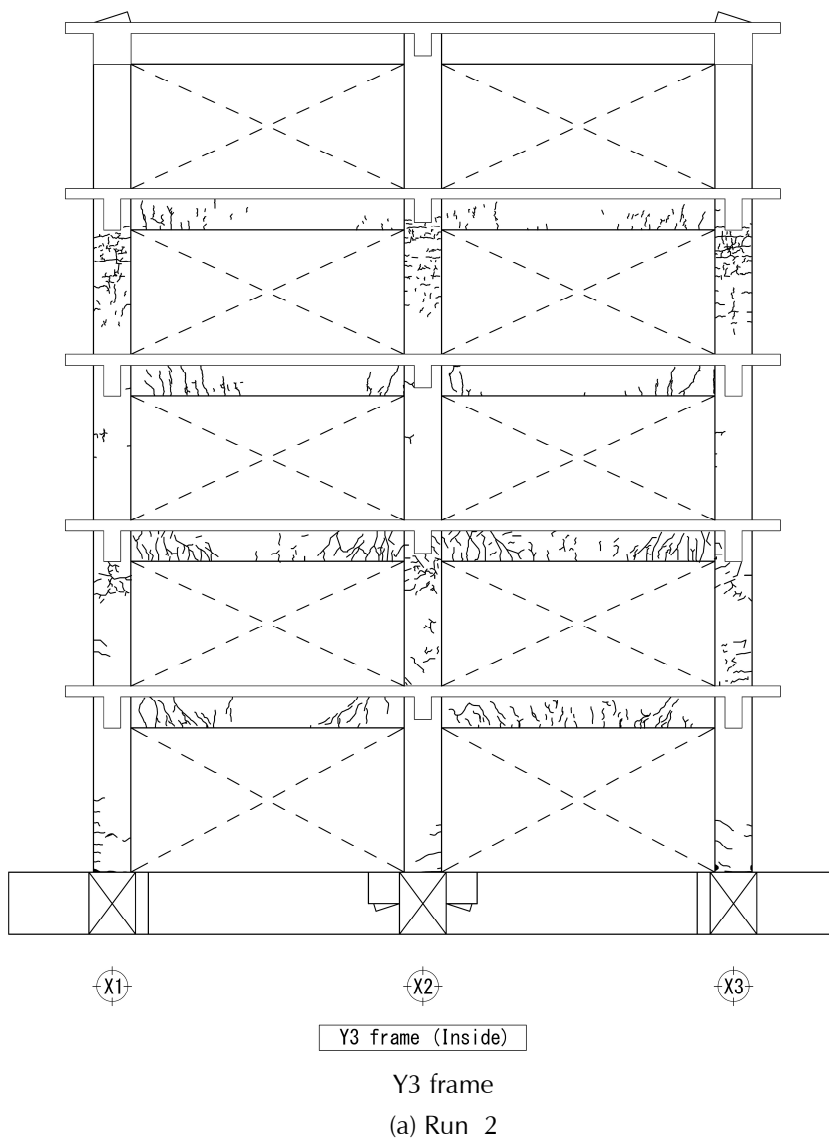
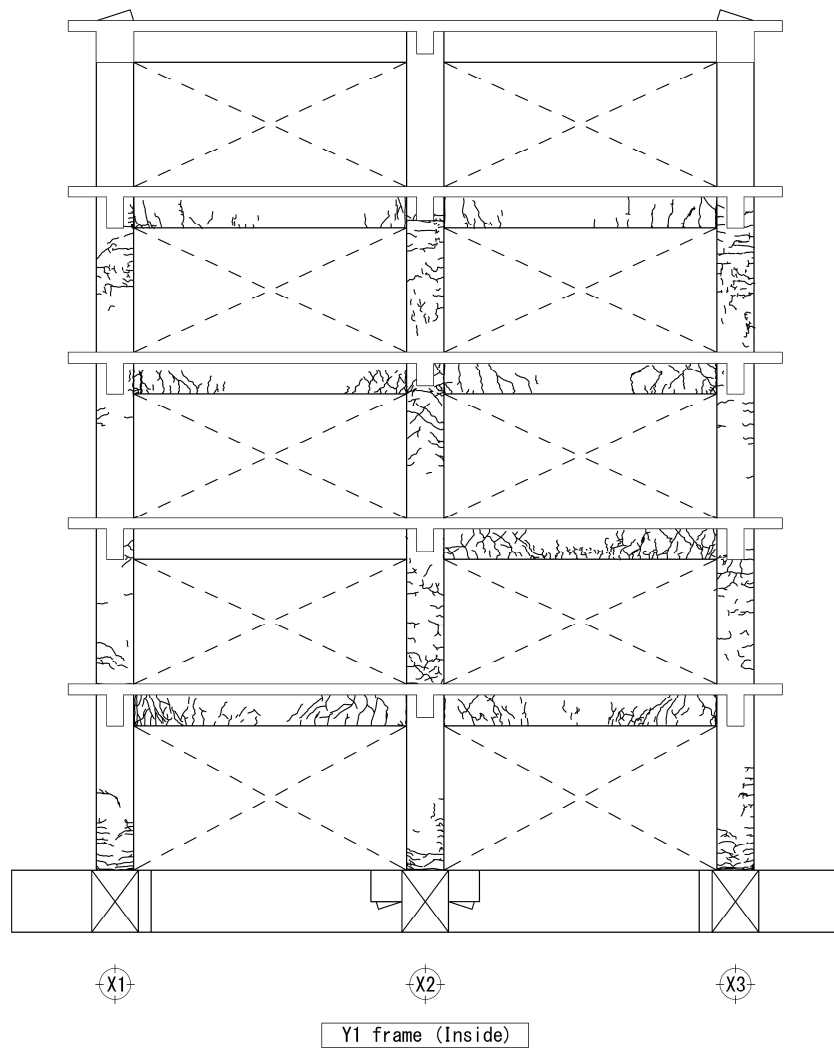
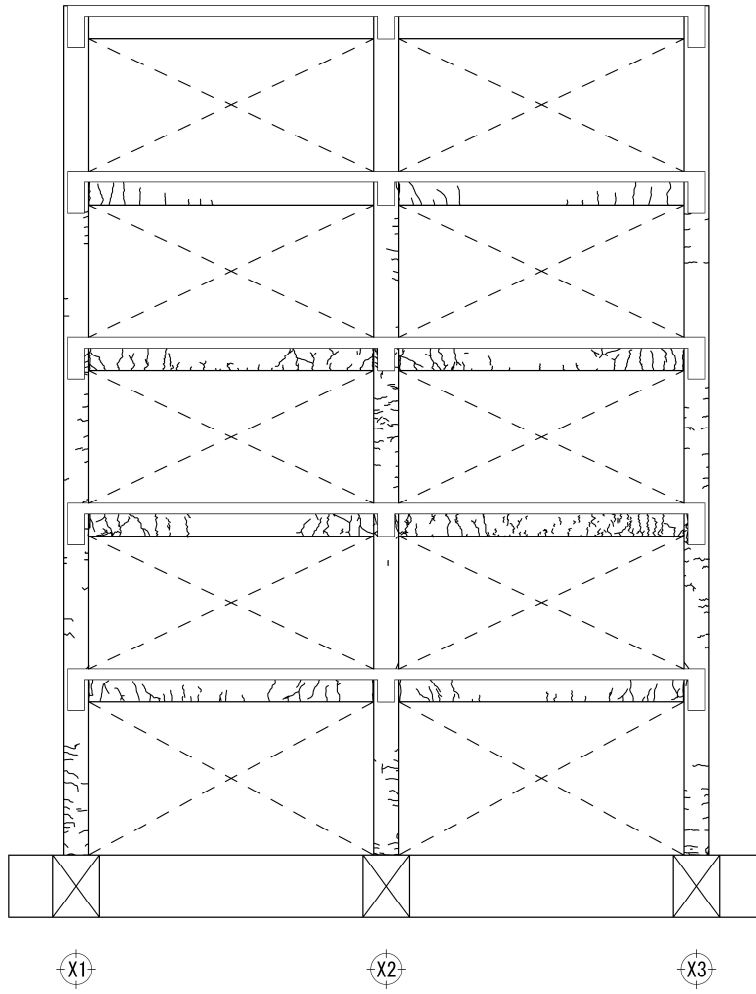


Figure D-1(cont) Crack patterns.



(b) Run 3

Figure D-1(cont) Crack patterns.

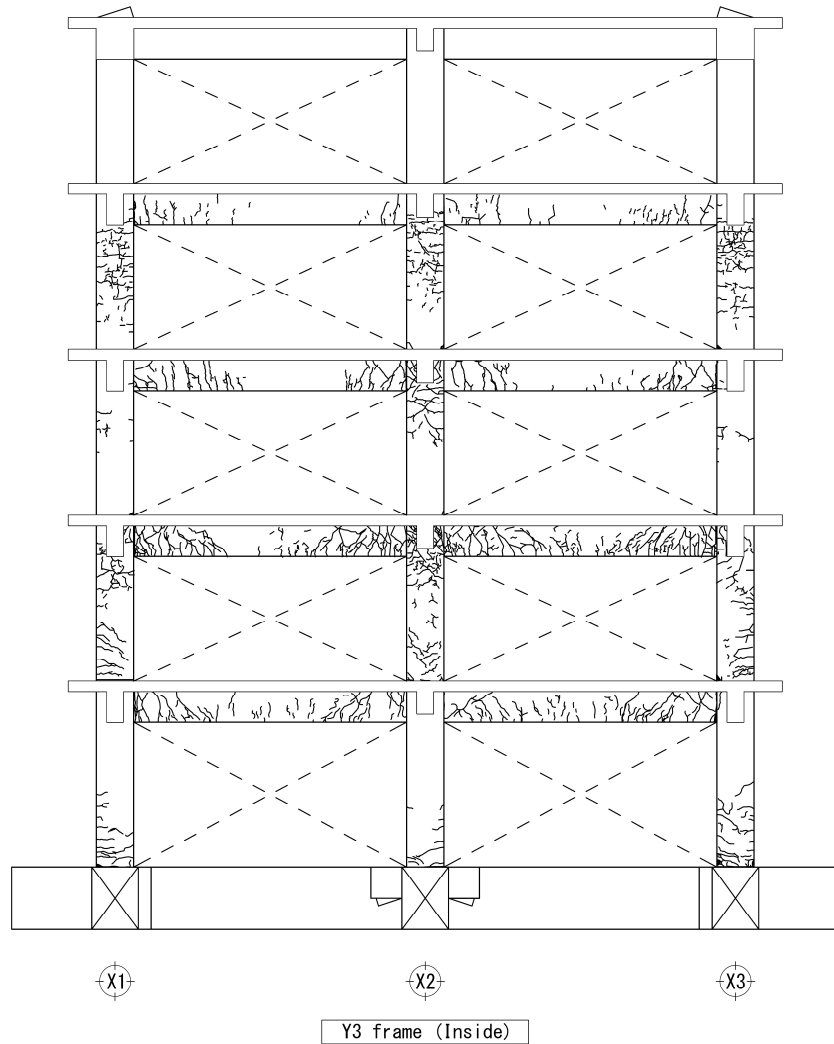


Y2 frame (Y1-side)

Run 3

(b)

Figure D-1(cont) Crack patterns.

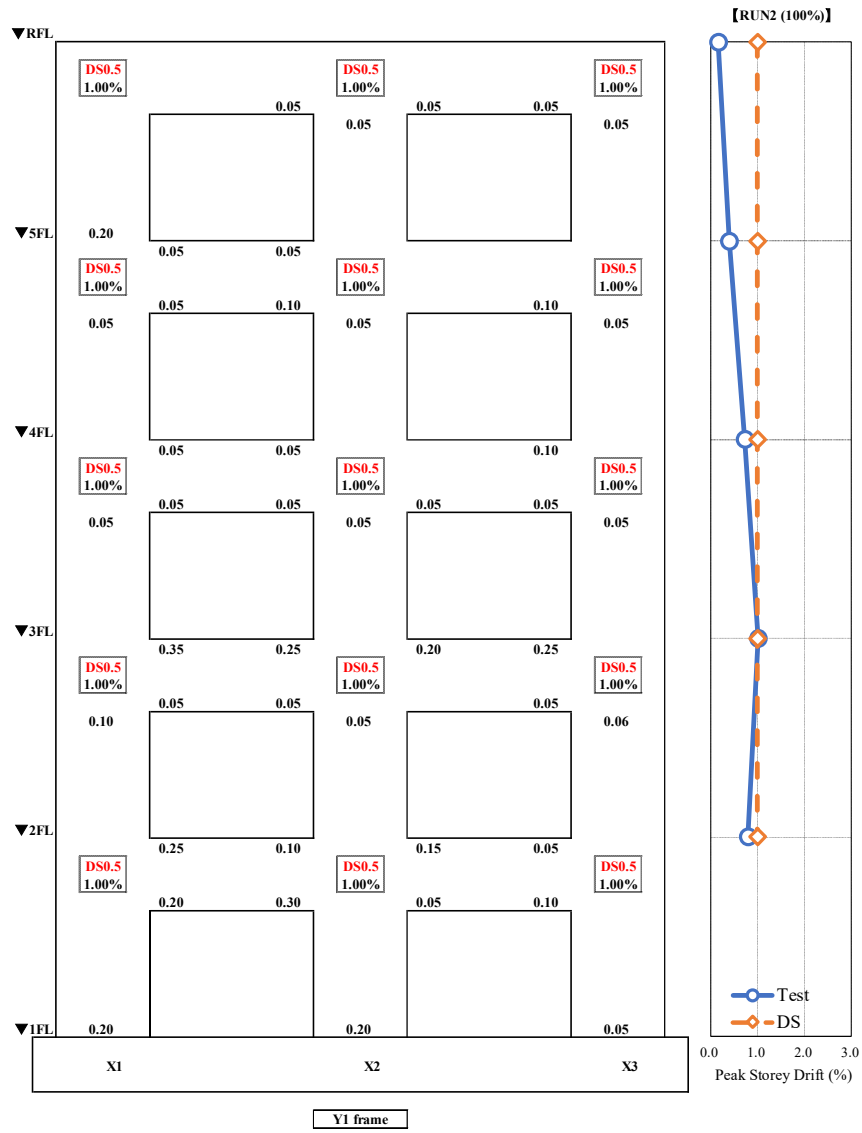


(b) Run 3

Figure D-1(cont) Crack patterns.

D.2 Maximum Residual Crack Width

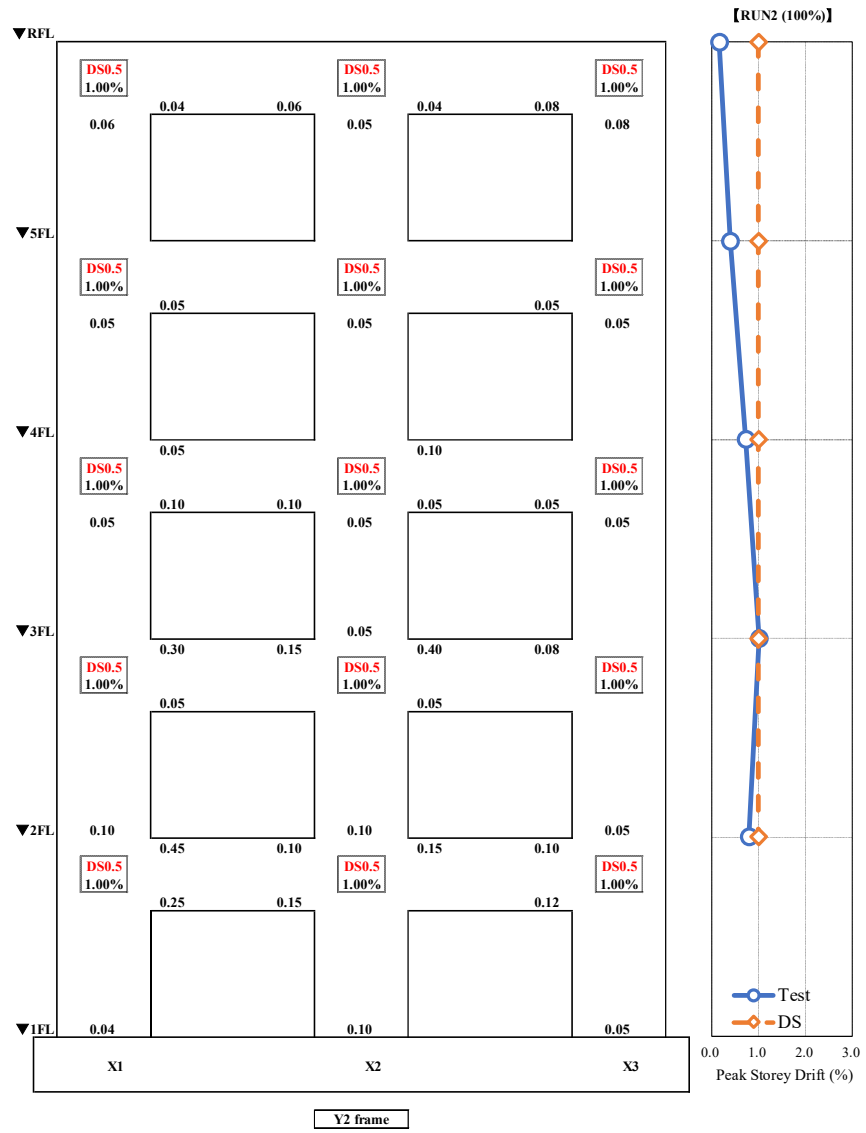
Figure D-2 shows the maximum residual crack width in Run 2 and Run 3, and story drift demand measured in the test and averaged median story drift estimated with Damage State.



Y1 frame

(a) Run 2

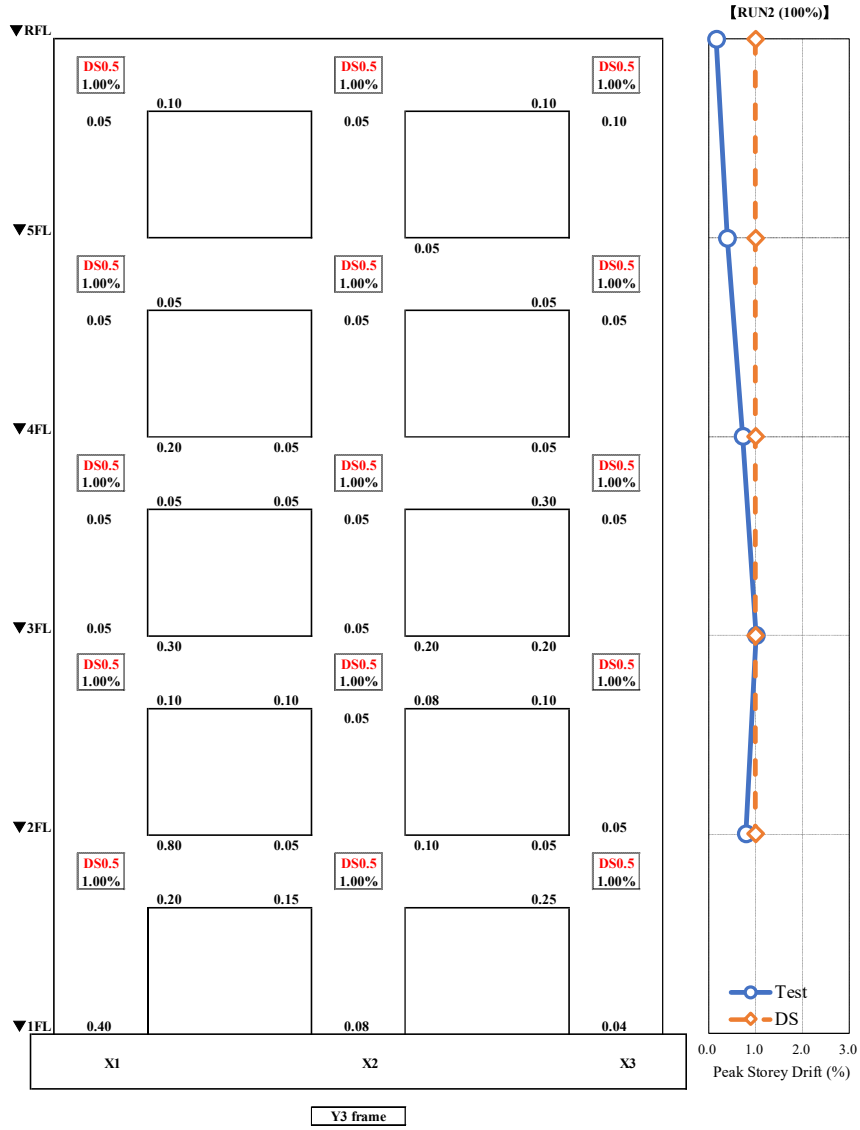
Figure D-2 Maximum residual crack width. Crack width colored represents crack width exceeding DS1 criterion (1.5mm).



Y2 frame

(a) Run 2

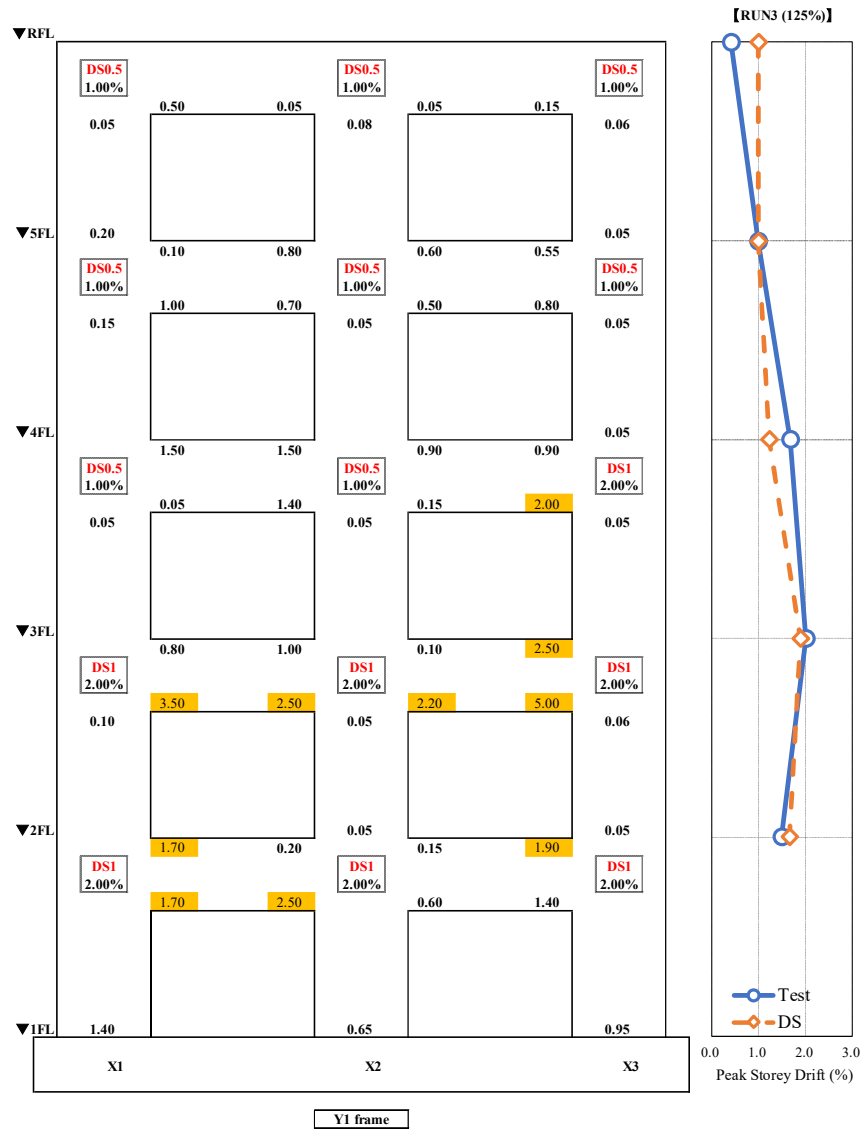
Figure D-2(cont) Maximum residual crack width. Crack width colored represents crack width exceeding DS1 criterion (1.5mm).



Y3 frame

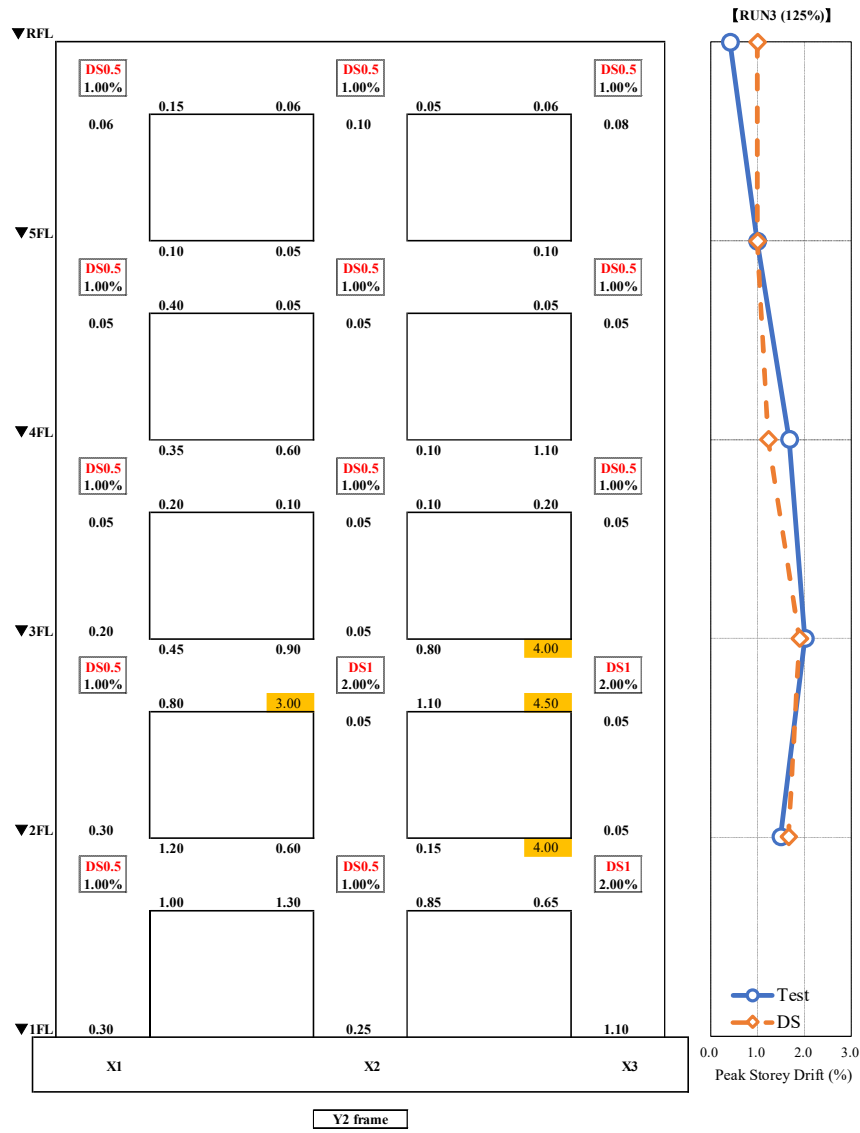
(a) Run 2

Figure D-2(cont) Maximum residual crack width. Crack width colored represents crack width exceeding DS1 criterion (1.5mm).



Y1 frame
 (b) Run 3

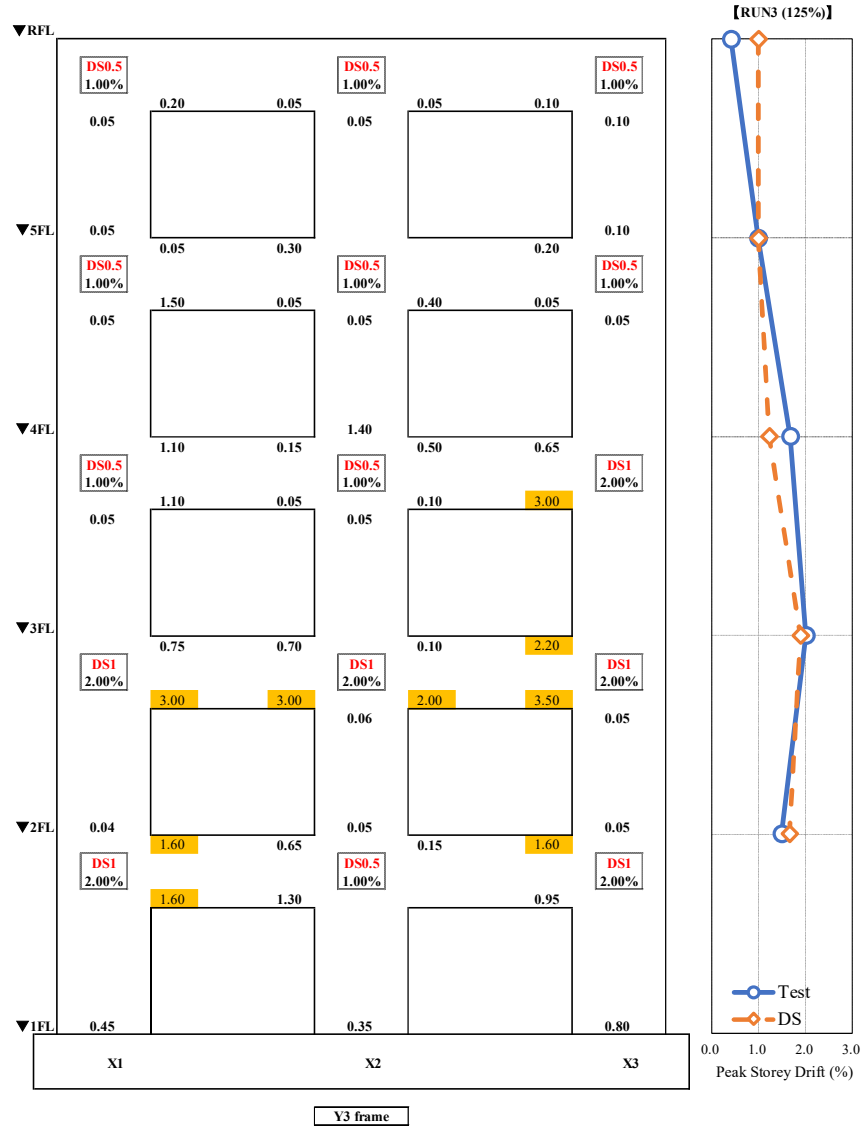
Figure D-2(cont) Maximum residual crack width. Crack width colored represents crack width exceeding DS1 criterion (1.5mm).



Y2 frame

(b) Run 3

Figure D-2(cont) Maximum residual crack width. Crack width colored represents crack width exceeding DS1 criterion (1.5mm).



Y3 frame

(b) Run 3

Figure D-2(cont) Maximum residual crack width. Crack width colored represents crack width exceeding DS1 criterion (1.5mm).

Case Study 1

Appendix E

ATC-38 Competed Form

The following form shows an assessment result with the ATC-38 (ATC, 2000) form.

Note: DO NOT LEAVE ANY BLANK SPACES!
Indicate Unknown (UNK), Not Applicable (NA), or None if necessary.

Building Site Information [1]

Inspector(s):	Date: Oct. 2020	Bldg. ID#: WG1a Case Study 1	Page 1 of 6
Address: E-Defense, Japan		Building Name: E-Defense Test Specimen 2020	
Type of Survey: <input type="checkbox"/> Interior Only <input type="checkbox"/> Exterior and Interior <input checked="" type="checkbox"/> Exterior Only		Recording Station ID:	
Existing Posting Placard: <input type="checkbox"/> Red <input type="checkbox"/> Yellow <input type="checkbox"/> Green <input type="checkbox"/> None		Photo ID#s:	
Building Owner/Manager Contact – Name:		Phone:	
Civil/Structural Engineer for Repair – Name:		Phone:	
General Damage Classification (see Glossary): <input type="checkbox"/> None (N) <input type="checkbox"/> Insignificant (I) <input type="checkbox"/> Moderate (M) <input type="checkbox"/> Heavy (H) [Note: For “M” or “H” classification, fill out Detailed Damage Description Section]			

Building Construction Data [2]

Construction Date: 2020	Design Date: 2020	Sloped Site: <input type="checkbox"/> Yes <input checked="" type="checkbox"/> No
Number of Stories Above Ground: 5 stories	Number of Basement Levels: None	
Number of Living Units:	Foundation Type: Rigid	
Plan Width (ft): 6m	Plan Length (ft): 12m	Approximate Building Area (sq.ft.): 72m2
Occupancy Type (see Glossary):	Occupied Prior to Earthquake: <input checked="" type="checkbox"/> Yes <input type="checkbox"/> No <input type="checkbox"/> UNK	

Model Building Type [3]

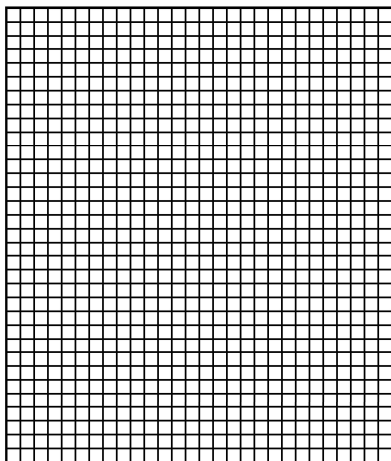
Predominant Model Building Type (see Glossary): C1	Seismic Retrofit: <input type="checkbox"/> Yes <input checked="" type="checkbox"/> No <input type="checkbox"/> UNK
Describe Building if More Than One Model Building Type Present: NA	
Describe Retrofit if Present: NA	

Performance Modifiers [4]

Bldg. ID#: WG1a Case Study 1 Page 2 of 6

Discontinuous Columns: <input type="checkbox"/> Y <input checked="" type="checkbox"/> N <input type="checkbox"/> UNK <input type="checkbox"/> NA		Facade Setbacks: <input type="checkbox"/> Y <input checked="" type="checkbox"/> N <input type="checkbox"/> UNK <input type="checkbox"/> NA	
Pounding Potential: <input type="checkbox"/> Y <input checked="" type="checkbox"/> N <input type="checkbox"/> UNK <input type="checkbox"/> NA		Seismic Expansion Joints: <input type="checkbox"/> Y <input checked="" type="checkbox"/> N <input type="checkbox"/> UNK <input type="checkbox"/> NA	
Open Front Plan: <input type="checkbox"/> Y <input checked="" type="checkbox"/> N <input type="checkbox"/> UNK <input type="checkbox"/> NA		Other Torsional Imbalance: <input type="checkbox"/> Y <input checked="" type="checkbox"/> N <input type="checkbox"/> UNK <input type="checkbox"/> NA	
Plan Irregularities: <input type="checkbox"/> Y <input checked="" type="checkbox"/> N <input type="checkbox"/> UNK <input type="checkbox"/> NA		Deterioration of Structure: <input type="checkbox"/> Y <input checked="" type="checkbox"/> N <input type="checkbox"/> UNK <input type="checkbox"/> NA	
Previous Earthquake Damage: <input checked="" type="checkbox"/> Yes <input type="checkbox"/> No <input type="checkbox"/> UNK <input type="checkbox"/> NA			
Describe Other Vertical Conditions: NA			
Describe Other Plan Vulnerabilities: NA			
Describe Other Pre-Earthquake Building Conditions: NA			

Plan Sketch of Building [5]



[Note: Include North arrow]

Nonstructural Elements [6]

Exterior Cladding/Glazing Code (see Glossary):
Partitions Code (see Glossary):
Ceilings Code (see Glossary):
Fire Protection: <input type="checkbox"/> Yes <input type="checkbox"/> No <input type="checkbox"/> UNK <input type="checkbox"/> NA
Elevators: <input type="checkbox"/> Yes <input type="checkbox"/> No <input type="checkbox"/> UNK <input type="checkbox"/> NA
Chimneys: <input type="checkbox"/> Yes <input type="checkbox"/> No <input type="checkbox"/> UNK <input type="checkbox"/> NA
Standard Plumbing, Electrical, Lighting, HVAC: <input type="checkbox"/> Yes <input type="checkbox"/> No <input type="checkbox"/> UNK <input type="checkbox"/> NA
Describe Major Fixed Equipment:
Describe Unusual Contents:

General Damage [7]Bldg. ID#: [WG1a Case Study 1](#)Page [3](#) of [6](#)

General Damage Classification (repeated from Section [1] on page 1): <input type="checkbox"/> None (N) <input type="checkbox"/> Insignificant (I) <input checked="" type="checkbox"/> Moderate (M) <input type="checkbox"/> Heavy (H)	
[Note: See Glossary for ATC-13 Damage State Definitions]	
ATC-13 Damage State, Structural: 4. Moderate	ATC-13 Damage State, Nonstructural: NA
ATC-13 Damage State, Equipment: NA	ATC-13 Damage State, Contents: NA
Percent of Floor Area Collapsed: <u>0</u> % <input type="checkbox"/> UNK <input type="checkbox"/> NA	
Building off Foundation: <input type="checkbox"/> Y <input type="checkbox"/> N <input type="checkbox"/> UNK <input checked="" type="checkbox"/> NA	Story out of Plumb: <input type="checkbox"/> Y <input type="checkbox"/> N <input type="checkbox"/> UNK <input checked="" type="checkbox"/> NA
Damage to Structural Members: <input checked="" type="checkbox"/> Y <input type="checkbox"/> N <input type="checkbox"/> UNK <input type="checkbox"/> NA	Hazmat: <input type="checkbox"/> Y <input type="checkbox"/> N <input type="checkbox"/> UNK <input checked="" type="checkbox"/> NA
Parapet Damage: <input type="checkbox"/> Y <input type="checkbox"/> N <input type="checkbox"/> UNK <input checked="" type="checkbox"/> NA	Chimney Damage: <input type="checkbox"/> Y <input type="checkbox"/> N <input type="checkbox"/> UNK <input checked="" type="checkbox"/> NA
Exterior Non-building Damage: <input type="checkbox"/> Y <input type="checkbox"/> N <input type="checkbox"/> UNK <input checked="" type="checkbox"/> NA	Pounding Damage: <input type="checkbox"/> Y <input type="checkbox"/> N <input type="checkbox"/> UNK <input checked="" type="checkbox"/> NA
Comments about General Damage: NA	

Nonstructural Damage [8]

Cladding Separation or Damage: ___% of wall area <input type="checkbox"/> UNK <input type="checkbox"/> NA
Partitions Damage: <input type="checkbox"/> None (N) <input type="checkbox"/> Insignificant (I) <input type="checkbox"/> Moderate (M) <input type="checkbox"/> Heavy (H) <input type="checkbox"/> UNK <input checked="" type="checkbox"/> NA
Windows Damage: ___% of windows <input type="checkbox"/> UNK <input type="checkbox"/> NA
Lights and Ceilings Damage: <input type="checkbox"/> None (N) <input type="checkbox"/> Insignificant (I) <input type="checkbox"/> Moderate (M) <input type="checkbox"/> Heavy (H) <input type="checkbox"/> UNK <input type="checkbox"/> NA
Buildings Contents Damage: <input type="checkbox"/> None (N) <input type="checkbox"/> Insignificant (I) <input type="checkbox"/> Moderate (M) <input type="checkbox"/> Heavy (H) <input type="checkbox"/> UNK <input type="checkbox"/> NA
Comments about Nonstructural Damage:

Injuries or Fatalities [9]

No. of Minor Injuries: ___ <input type="checkbox"/> UNK	No. of Major Injuries: ___ <input type="checkbox"/> UNK	No. of Fatalities: ___ <input type="checkbox"/> UNK
Comments about Injuries or Fatalities:		

Functionality [10]		Bldg. ID#: WG1a Case Study 1	Page 4 of 6
Percent Usable Space Immediately: ___% <input type="checkbox"/> UNK	Percent Usable Space in 1-3 Days: ___% <input type="checkbox"/> UNK		
Percent Usable Space within 1 Week: ___% <input type="checkbox"/> UNK	Percent Usable Space within 1 Mo.: ___% <input type="checkbox"/> UNK		
Percent Usable Space in 1-6 Months: ___% <input type="checkbox"/> UNK	Time Until Full Occupancy: _____ <input type="checkbox"/> UNK <input type="checkbox"/> NA		
Comments about Functionality:			

Geotechnical Failures [11]	
Lateral Ground Movement: <input type="checkbox"/> Y <input type="checkbox"/> N <input type="checkbox"/> UNK <input type="checkbox"/> NA	Buckled Sidewalks: <input type="checkbox"/> Y <input type="checkbox"/> N <input type="checkbox"/> UNK <input type="checkbox"/> NA
Ground Settlement: <input type="checkbox"/> Y <input type="checkbox"/> N <input type="checkbox"/> UNK <input type="checkbox"/> NA	Liquefaction Indicators: <input type="checkbox"/> Y <input type="checkbox"/> N <input type="checkbox"/> UNK <input type="checkbox"/> NA
Separation Between Building and Ground: <input type="checkbox"/> Y <input type="checkbox"/> N <input type="checkbox"/> UNK <input type="checkbox"/> NA	
Comments about Geotechnical Features:	

Additional Comments

Additional Comments Pertaining to Any Section of Survey Form (use additional pages if necessary):

[NA](#)

DETAILED DAMAGE DESCRIPTION

Bldg. ID#: WG1a Case Study 1	Page 5 of 6
--	---

Vertical Elements

Racking of Main Walls: <input type="checkbox"/> None (N) <input type="checkbox"/> Insignificant (I) <input type="checkbox"/> Moderate (M) <input type="checkbox"/> Heavy (H) <input type="checkbox"/> UNK <input checked="" type="checkbox"/> NA
Racking of Cripple Walls: <input type="checkbox"/> None (N) <input type="checkbox"/> Insignificant (I) <input type="checkbox"/> Moderate (M) <input type="checkbox"/> Heavy (H) <input type="checkbox"/> UNK <input checked="" type="checkbox"/> NA
Buckling, Crippling, Tearing of Steel Beams, Columns, or Braces: <input type="checkbox"/> None (N) <input type="checkbox"/> Insignificant (I) <input type="checkbox"/> Moderate (M) <input type="checkbox"/> Heavy (H) <input type="checkbox"/> UNK <input checked="" type="checkbox"/> NA
Spalling or Cracking of Concrete Columns or Beams: <input type="checkbox"/> None (N) <input type="checkbox"/> Insignificant (I) <input checked="" type="checkbox"/> Moderate (M) <input type="checkbox"/> Heavy (H) <input type="checkbox"/> UNK <input type="checkbox"/> NA
Column Crushing Due to Overturning or Discontinuous Lateral Resisting Elements: <input type="checkbox"/> None (N) <input checked="" type="checkbox"/> Insignificant (I) <input type="checkbox"/> Moderate (M) <input type="checkbox"/> Heavy (H) <input type="checkbox"/> UNK <input type="checkbox"/> NA
Shear Cracking in Columns: <input checked="" type="checkbox"/> None (N) <input type="checkbox"/> Insignificant (I) <input type="checkbox"/> Moderate (M) <input type="checkbox"/> Heavy (H) <input type="checkbox"/> UNK <input type="checkbox"/> NA
Cracked Shear Walls: <input type="checkbox"/> None (N) <input type="checkbox"/> Insignificant (I) <input type="checkbox"/> Moderate (M) <input type="checkbox"/> Heavy (H) <input type="checkbox"/> UNK <input checked="" type="checkbox"/> NA
Percentage of Shear Walls with Cracks: ___ % <input type="checkbox"/> UNK <input checked="" type="checkbox"/> NA
Rocking of Shear Walls: <input type="checkbox"/> None (N) <input type="checkbox"/> Insignificant (I) <input type="checkbox"/> Moderate (M) <input type="checkbox"/> Heavy (H) <input type="checkbox"/> UNK <input checked="" type="checkbox"/> NA
Damage to Shear Wall Boundary Elements: <input type="checkbox"/> None (N) <input type="checkbox"/> Insignificant (I) <input type="checkbox"/> Moderate (M) <input type="checkbox"/> Heavy (H) <input type="checkbox"/> UNK <input checked="" type="checkbox"/> NA
Damage to Shear Wall Coupling Beams: <input type="checkbox"/> None (N) <input type="checkbox"/> Insignificant (I) <input type="checkbox"/> Moderate (M) <input type="checkbox"/> Heavy (H) <input type="checkbox"/> UNK <input checked="" type="checkbox"/> NA
/ % of Tiltup Wall Panels Leaning or Fallen Out: ___ / ___ % <input type="checkbox"/> UNK <input checked="" type="checkbox"/> NA
Infill Walls Damaged or Fallen Out: <input type="checkbox"/> None (N) <input type="checkbox"/> Insignificant (I) <input type="checkbox"/> Moderate (M) <input type="checkbox"/> Heavy (H) <input type="checkbox"/> UNK <input checked="" type="checkbox"/> NA

Horizontal Elements

Roof Collapse: <u>0</u> % of Diaphragm <input type="checkbox"/> UNK <input type="checkbox"/> NA	Floor Collapse: <u>0</u> % of Diaphragm <input type="checkbox"/> UNK <input type="checkbox"/> NA
Loss of Vertical Roof Support: <u>0</u> % of Roof Area Affected <input type="checkbox"/> UNK <input type="checkbox"/> NA	
Tearing of Diaphragms at Other Points of High Stress: <u>0</u> % of Diaphragm <input type="checkbox"/> UNK <input type="checkbox"/> NA	
Damage at Re-entrant Corners: <input type="checkbox"/> None (N) <input type="checkbox"/> Insignificant (I) <input type="checkbox"/> Moderate (M) <input checked="" type="checkbox"/> Heavy (H) <input type="checkbox"/> UNK <input type="checkbox"/> NA	
Damage to Collectors at Walls: <input type="checkbox"/> None (N) <input type="checkbox"/> Insignificant (I) <input type="checkbox"/> Moderate (M) <input type="checkbox"/> Heavy (H) <input type="checkbox"/> UNK <input checked="" type="checkbox"/> NA	
Cross Grain Bending Damage at Roof-to-Wall Connections: ___ % of Connection Length <input type="checkbox"/> UNK <input checked="" type="checkbox"/> NA	

DETAILED DAMAGE DESCRIPTION (Continued)

Bldg. ID#: WG1a Case Study 1

Page 6 of 6

Connections

Girder-Column Connection Damage Including Panel Zones: <input type="checkbox"/> None (N) <input type="checkbox"/> Insignificant (I) <input type="checkbox"/> Moderate (M) <input type="checkbox"/> Heavy (H) <input type="checkbox"/> UNK <input checked="" type="checkbox"/> NA
Column Splice Damage: <input type="checkbox"/> None (N) <input type="checkbox"/> Insignificant (I) <input type="checkbox"/> Moderate (M) <input type="checkbox"/> Heavy (H) <input type="checkbox"/> UNK <input checked="" type="checkbox"/> NA
Damage to Brace Connections: <input type="checkbox"/> None (N) <input type="checkbox"/> Insignificant (I) <input type="checkbox"/> Moderate (M) <input type="checkbox"/> Heavy (H) <input type="checkbox"/> UNK <input checked="" type="checkbox"/> NA
Damage to Column-to-Foundation Connections: <input type="checkbox"/> None (N) <input type="checkbox"/> Insignificant (I) <input type="checkbox"/> Moderate (M) <input type="checkbox"/> Heavy (H) <input type="checkbox"/> UNK <input checked="" type="checkbox"/> NA
Damage to Connections of Precast Elements that are Part of the Lateral Force Resisting System: <input type="checkbox"/> None (N) <input type="checkbox"/> Insignificant (I) <input type="checkbox"/> Moderate (M) <input type="checkbox"/> Heavy (H) <input type="checkbox"/> UNK <input checked="" type="checkbox"/> NA

Foundations

Foundations Cracked or Otherwise Damaged: <input type="checkbox"/> None (N) <input type="checkbox"/> Insignificant (I) <input type="checkbox"/> Moderate (M) <input type="checkbox"/> Heavy (H) <input type="checkbox"/> UNK <input checked="" type="checkbox"/> NA
Slabs-on-Grade Cracked or Otherwise Damaged: <input type="checkbox"/> None (N) <input type="checkbox"/> Insignificant (I) <input type="checkbox"/> Moderate (M) <input type="checkbox"/> Heavy (H) <input type="checkbox"/> UNK <input checked="" type="checkbox"/> NA

Equipment and Systems

Electrical Equipment Damage Including Backup Generators: <input type="checkbox"/>None (N) <input type="checkbox"/>Insignificant (I) <input type="checkbox"/>Moderate (M) <input type="checkbox"/>Heavy (H) <input type="checkbox"/>UNK <input type="checkbox"/>NA
Damage to Boilers, Chillers, Tanks, etc.: <input type="checkbox"/>None (N) <input type="checkbox"/>Insignificant (I) <input type="checkbox"/>Moderate (M) <input type="checkbox"/>Heavy (H) <input type="checkbox"/>UNK <input type="checkbox"/>NA
HVAC Damage (Fans, Ducts): <input type="checkbox"/>None (N) <input type="checkbox"/>Insignificant (I) <input type="checkbox"/>Moderate (M) <input type="checkbox"/>Heavy (H) <input type="checkbox"/>UNK <input type="checkbox"/>NA
Damage to Water and Sprinkler Lines and Fire Pumps: <input type="checkbox"/>None (N) <input type="checkbox"/>Insignificant (I) <input type="checkbox"/>Moderate (M) <input type="checkbox"/>Heavy (H) <input type="checkbox"/>UNK <input type="checkbox"/>NA
Elevator Equipment Damage (Car and Counterweight Rails, Cars, Penthouse Equipment): <input type="checkbox"/>None (N) <input type="checkbox"/>Insignificant (I) <input type="checkbox"/>Moderate (M) <input type="checkbox"/>Heavy (H) <input type="checkbox"/>UNK <input type="checkbox"/>NA

Additional Comments (use additional pages if necessary): NA
--

Case Study 1

Appendix F

Detail Assumptions for the Analysis Procedure

This appendix provides detail assumptions and calculations used in the case study.

F.1 Material Properties

Young's modulus can be calculated by the following equation

$$E_c = 4700 \sqrt{f'_c} \quad (\text{F-1})$$

Tension strength of concrete can be estimated as follows.

$$f_t = 0.62 \sqrt{f'_c} \quad (\text{F-2})$$

Shear modulus can be calculated as follows.

$$G = 0.4E_c \quad (\text{F-3})$$

F.2 Stiffness

The gross stiffness of the members is obtained by the following equation

$$I_g = \phi \cdot I_0$$

where ϕ is amplification factor considering effective flange width obtained by the requirement below, I_0 is the moment of inertia and calculated by the following equation.

$$I_0 = \frac{bD^3}{12}$$

Where b and D are the width and depth of rectangular cross section, respectively.

In the ASCE/SEI 41 (ASCE, 2017), the stiffness of members with effective flange for flexure and axial loading is calculated following the requirements below. The effective flange width is the minimum of

1. The provided flange width
2. $8h$

3. $s_w/2$
4. $l_n/5$

Where h is slab width, s_w is the distance to the adjacent web, l_n is the clear span of the beam. According to this requirement, each value is calculated as follows.

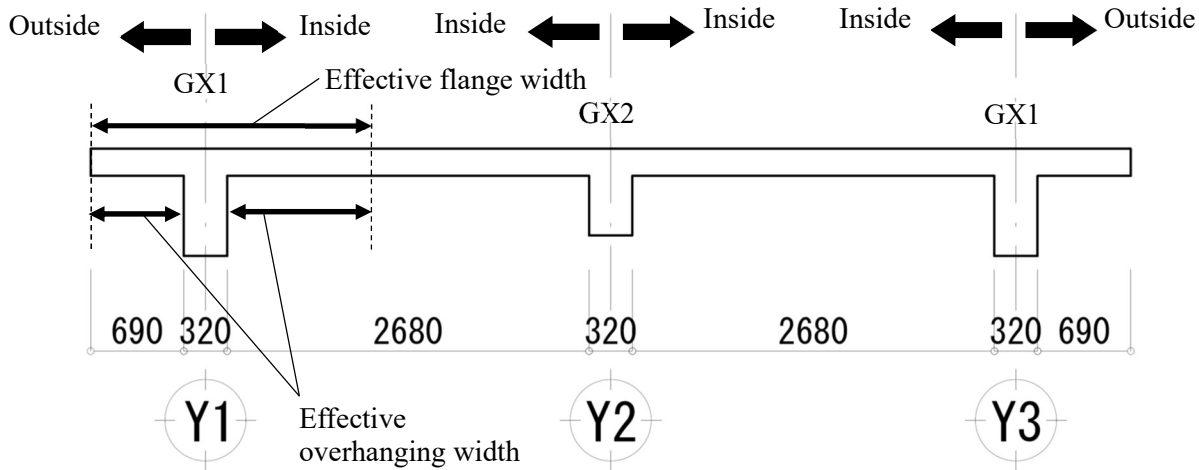


Figure F-1 Configuration of the beam effective flange width

Table F-1 Effective Flange Width for T-shaped Beams

Beam	Beam width b_w (mm)		Requirements				Overhanging flange width b_o (mm)	Effective flange width $b_f = b_w + b_o$ (mm)
			Provided width (mm)	$8h$ (mm)	$s_w/2$ (mm)	$l_n/5$ (mm)		
GX1	320	Inside	-	1600	1340	1056	1056+690 =1746	320+1746 =2066
		Outside	690	1600	-	1056		
GX2	320	Inside	-	1600	1340	1104	$1104 \times 2 = 2208$	$320 + 2208 = 2528$

Table F-2 shows the effective rigidities of beam and column. The initial stiffness of linear model, the modified linear model and nonlinear model used in the case study was based on these values. Effective rigidities of each components are shown in Figure F-2.

Table F-2 Effective Rigidity for Flexural, Shear and Axial Stiffness

	Flexural rigidity	Shear rigidity	Axial rigidity
Beam	$0.3E_c I_g$	$0.4E_c A_w$	$1.0E_c A_g$
Column	$0.7E_c I_g$ ($0.5 \leq \eta_0$)		
	$(\eta_0 - 0.2) E_c I_g$ ($0.1 < \eta_0 < 0.5$)		
Column	$0.3E_c I_g$ ($\eta_0 \leq 0.1$)		

η_0 : Axial force ratio by dead load and live load

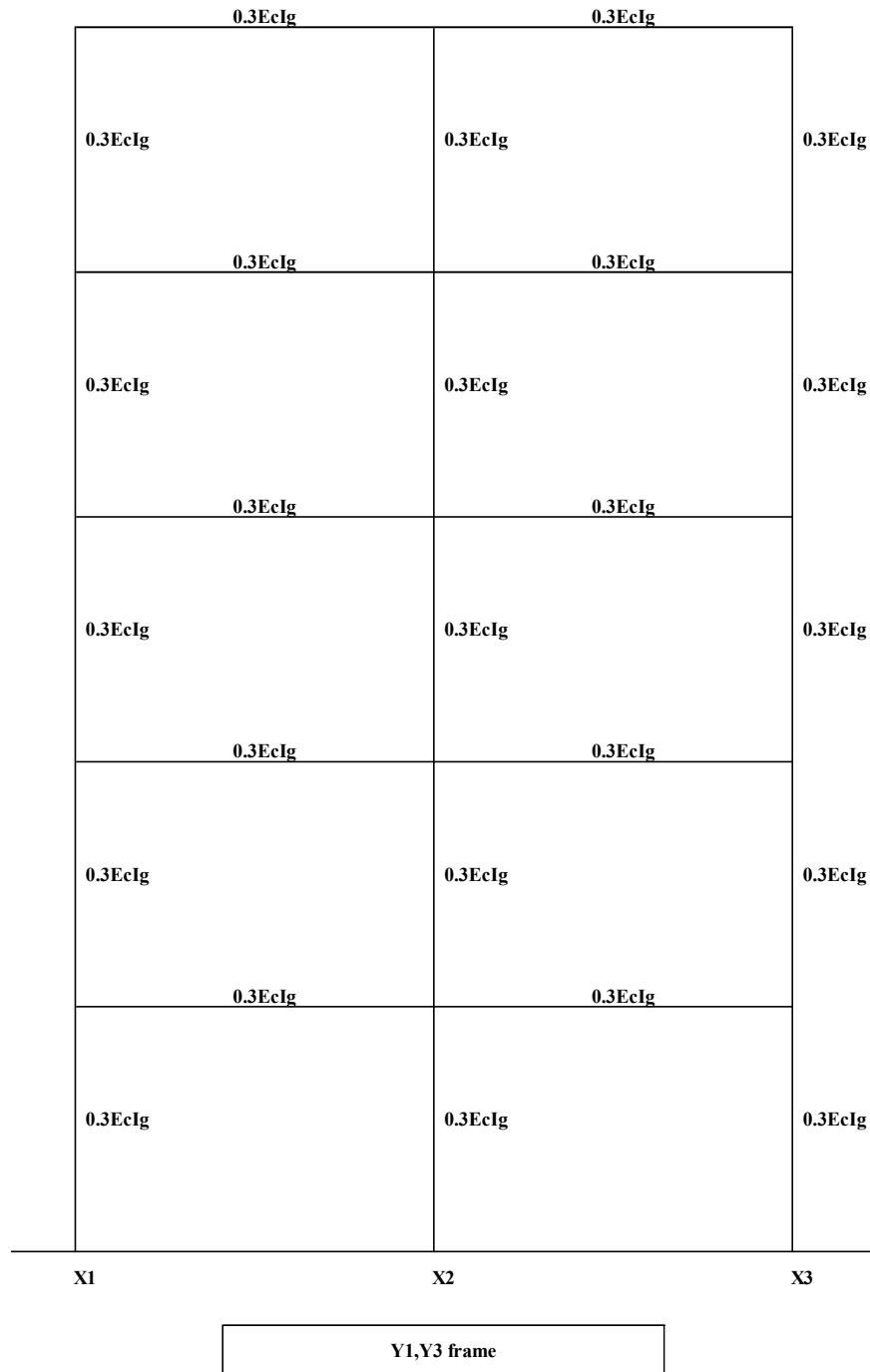


Figure F-2 Effective rigidity.

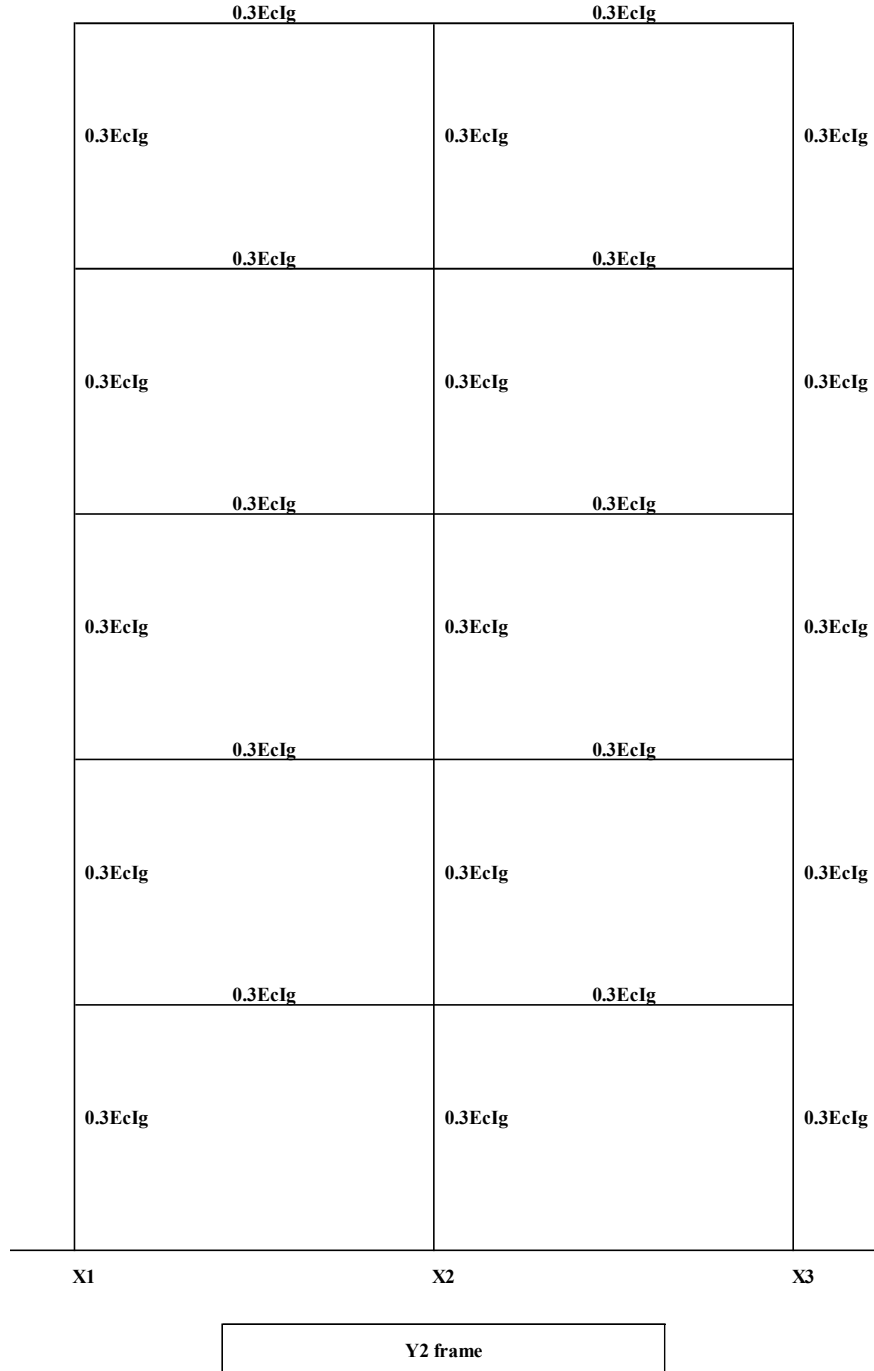


Figure F-2(cont) Effective rigidity.

F.3 Joint Model

Joint model provided in ASCE/SEI 41 (ASCE, 2017) are illustrated in Figure F-3. Beam-column joint were modeled implicitly assuming rigid zone in the joint. Rigid zone is defined based on yield moment capacity of beam and column. M_{nc} and M_{nb} represent yield moment capacity of column and beam,

respectively. Figure F-4 shows spring offset of one of the joints in the analysis model. Spring elements were placed at the beam or column face regardless of joint model. Joint models used in the analysis model of case study are provided in Figure F-5.

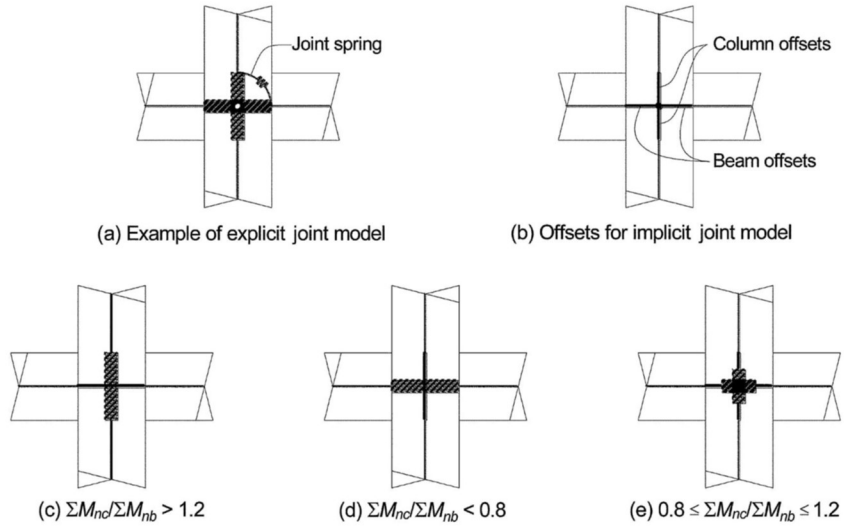


Figure F-3 Beam-column joint modeling. Hatched portion indicates rigid element.

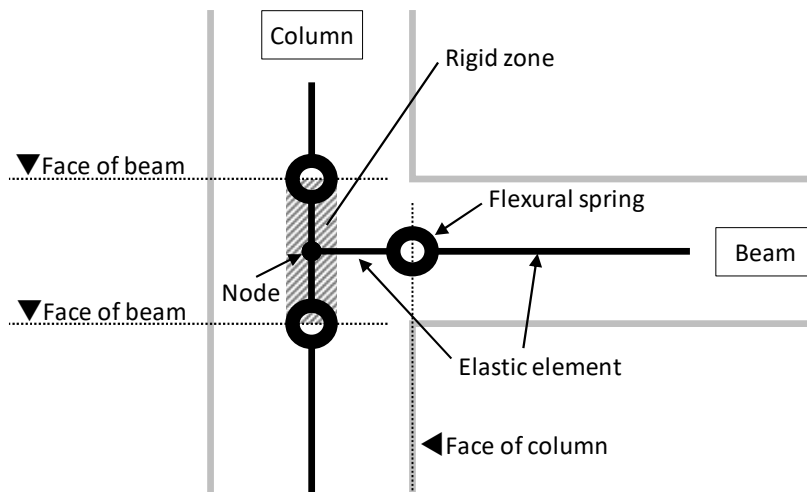


Figure F-4 Spring offset.

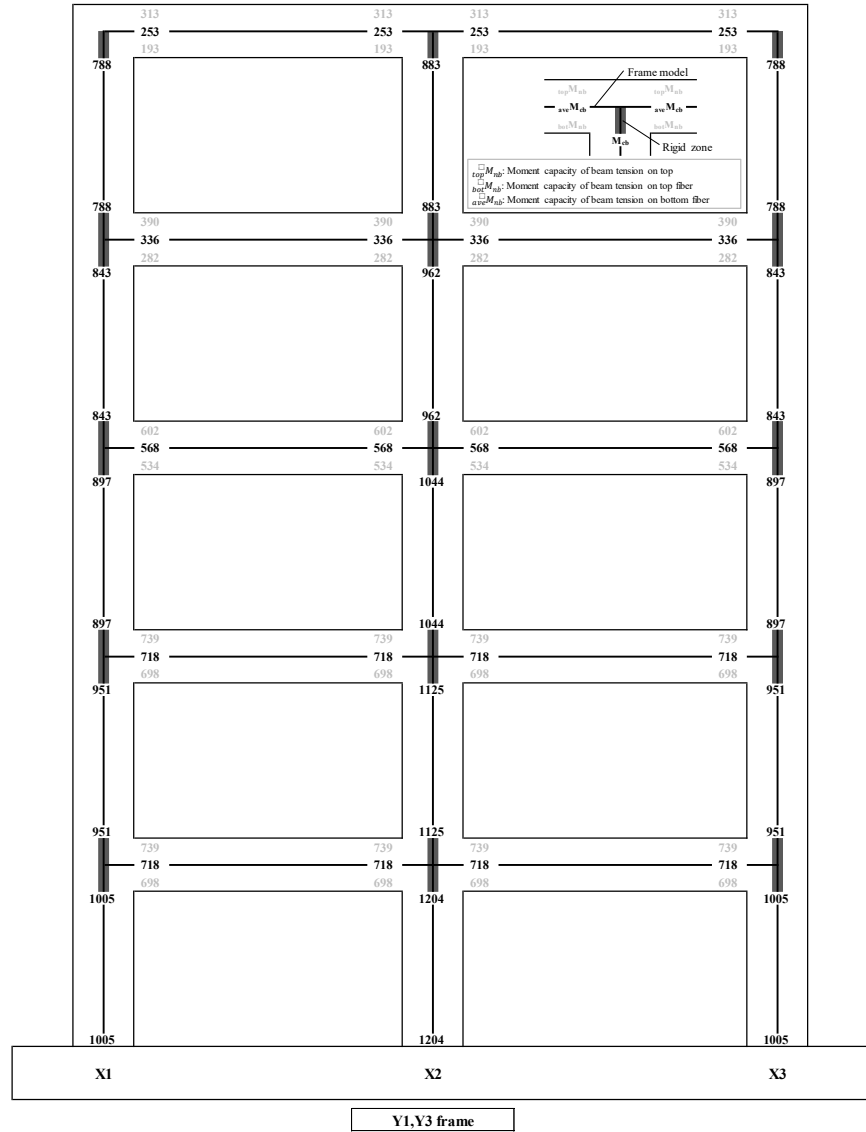


Figure F-5 Moment capacity and Joint model.

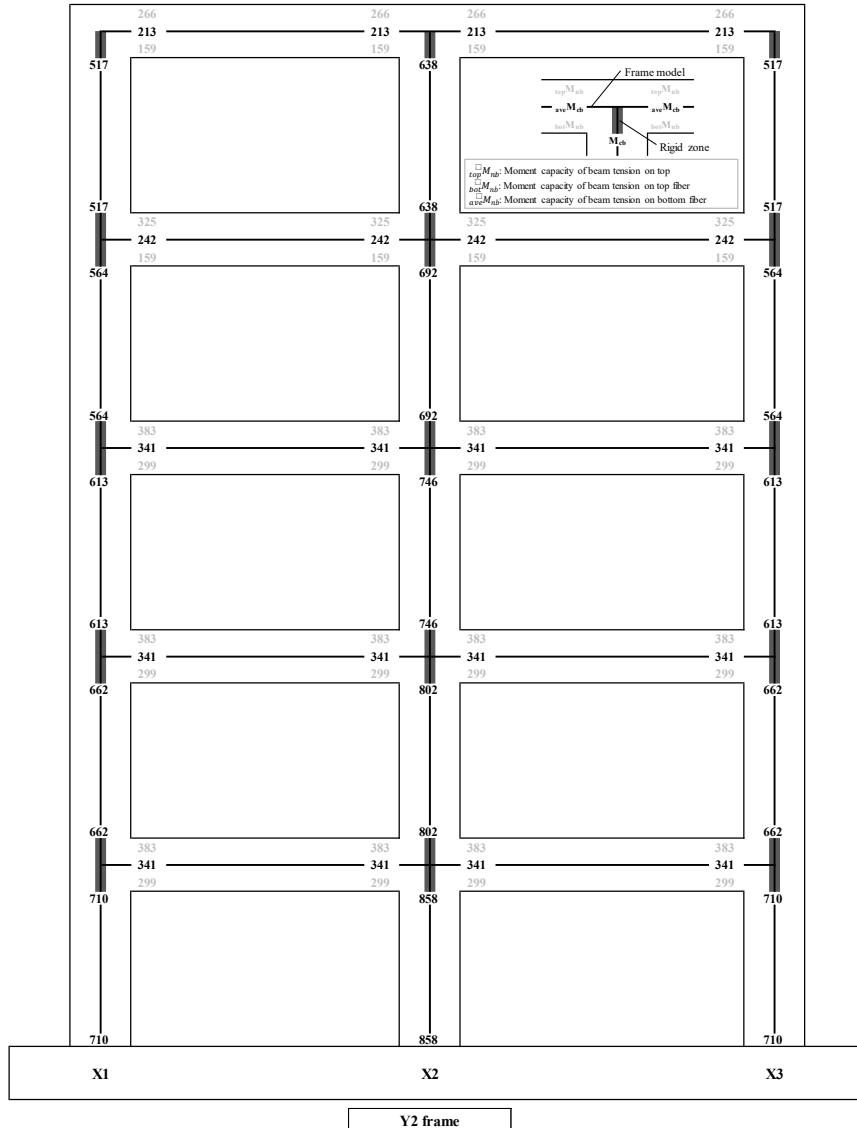


Figure F-5(cont) Moment capacity and Joint model.

F.4 Spring Model

Figure F-6 shows the uniaxial spring model used for beams in the analysis model. Beam elements consist of three uniaxial springs, flexural, shear and axial spring. The initial stiffness of these spring were defined in accordance with Figure F-2.

Force-deformation characteristic of flexural spring were defined by using fiber analysis based on the plane-sections-remain-plane assumption. Figure F-7 shows hysteresis model used for the nonlinear model. The force-deformation characteristic of nonlinear flexural spring was modeled as bilinear curve, determining cracking point (f_c, f_c') at yielding point (f_y, f_y') in Figure F-7. Shear spring and axial spring were defined as elastic element.

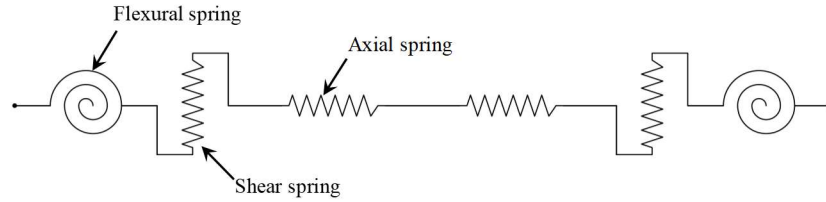


Figure F-6 Uniaxial spring model.

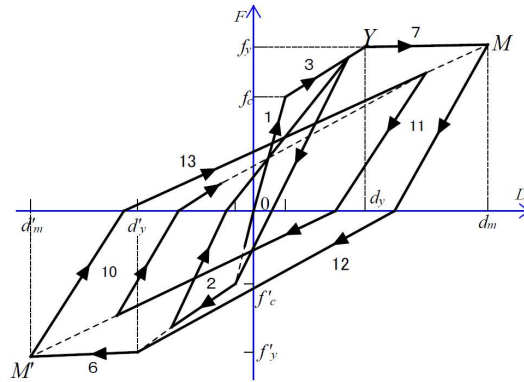


Figure F-7 Hysteresis model for flexural spring (Takeda model).

Figure F-8 shows the multi-spring (MS) model used for columns in the analysis model of the case study. Column element was modeled with multi-spring model, uniaxial shear spring and uniaxial axial spring. MS model consists of concrete element and steel element, and each element has individual stress-strain relationship. Therefore, MS model is able to take effect of axial force into flexural response. Figure F-9 shows hysteresis model of steel and concrete element. Mechanical properties were determined in accordance with material test result provided in Table 1-3, Table 1-4. In concrete, stress degradation was considered.

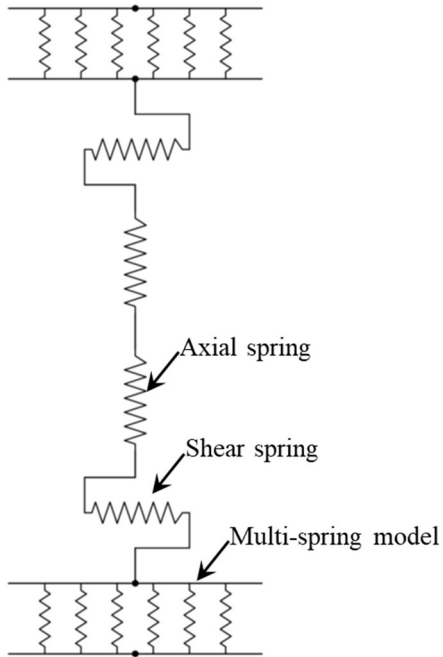
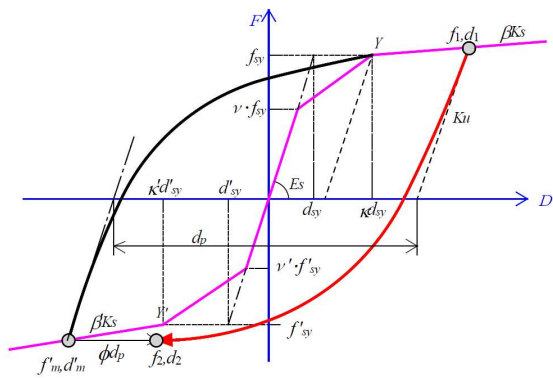
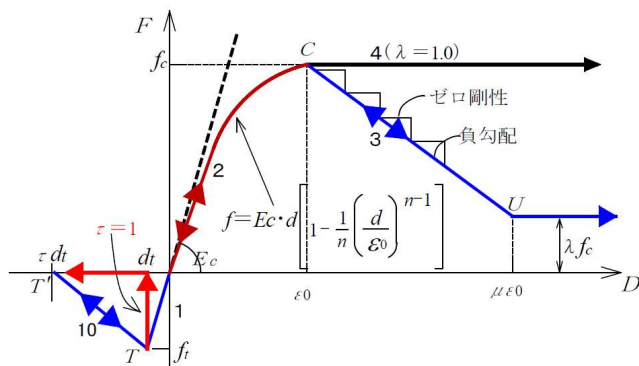


Figure F-8 Multi-spring (MS) model.



(a) Steel (Modified Ramberg-Osgood model)



(b) Concrete

Figure F-9 Hysteresis model of material element

F.5 Damping

Viscous damping ratio was assumed in accordance with ASCE/SEI 41 7.2.3.6. (ASCE, 2017). As the test building was bare moment frame (= Building without nonstructural components), 2.0% viscous damping was adopted. For the nonlinear dynamic analysis, 1.0% was assumed considering hysteresis damping.

Table F-3 Viscous Damping Ratio for Analysis Procedures

Analysis procedure	Building category	Viscous damping ratio
LS/ LD/ NS	Typical building*	5.0%
	Building without nonstructural components	2.0%
ND	Typical building*	3.0%
	Building without nonstructural components	1.0%

* All the building except the buildings meeting the criteria in ASCE/SEI 41 7.2.3.6 (ATC, 2020)

F.6 Modification Factor for the Linear Dynamic Procedure (LDP)

According to the ASCE/SEI 41 (ASCE, 2017), all forces and deformation demands computed by LDP should be modified by multiplying C_1 , C_2 factors. C_1 factor represents modification of the expected maximum inelastic response displacement to computed linear response displacement. Thus, the modified drift demand is denoted as below.

$$\Delta_{modified} = C_1 \cdot C_2 \cdot \Delta_0$$

where,

- C_1 : Modification factor to relate expected maximum inelastic displacements to displacements calculated for linear elastic response. For fundamental periods less than 0.2s, C_1 needs not to be taken as greater than the value at $T = 0.2$ s. For fundamental period greater than 1.0s, $C_1 = 1.0$.
- C_2 : Modification factor to represents the effect of pinched hysteresis shape, cyclic stiffness degradation, and strength deterioration on maximum displacement response. For fundamental period greater than 0.7s, $C_2 = 1.0$.
- Δ_0 : Original peak drift demand

$$C_1 = 1 + \frac{\mu_{strength} - 1}{\alpha T^2}$$

$$C_2 = 1 + \frac{1}{800} \left(\frac{\mu_{strength} - 1}{T} \right)^2$$

Where: α : Site factor shown in Table F-4, $\mu_{strength}$: Ratio of elastic strength demand to yield strength coefficient calculated by following equation, T : Fundamental period of the building in the direction under consideration.

Table F-4 Site Factor α

Site class	Site class A	Site class B	Site class C	Site class D
a	130	130	90	60

Note: Bolded value is selected herein

The fundamental period is determined by following equation.

$$T = C_t h_n^\beta$$

where: h_n : Height above the base to roof level (ft)

Table F-5 C_t Values

Frame type	Steel moment-resisting frame system	Concrete moment-resisting frame system	Steel eccentrically braced frame systems	All other framing system
C_t	0.035	0.018	0.030	0.020

Note: Bolded value is selected herein

Table F-6 β Values

Frame type	Steel moment-resisting frame system	Concrete moment-resisting frame system	All other framing system
β	0.80	0.90	0.75

Note: Bolded value is selected herein

$$\mu_{strength} = \frac{S_a}{V_y/W} \cdot C_m$$

Where: S_a : Response spectrum acceleration and it is taken as a response acceleration at the fundamental period in Figure 2-2, V_y : Yield strength on idealized base shear and roof drift relationship obtained by a nonlinear pushover analysis, C_m : Effective mass factor in Table F-7.

Table F-7 Effective Mass Factor C_m

No. of Stories	Concrete Moment frame	Concrete Shear wall	Concrete Pier-spandrel	Steel Moment frame	Steel Concentrically Braced frame	Steel Eccentrically Braced frame	Other
1-2	1.0	1.0	1.0	1.0	1.0	1.0	1.0
3-	0.9	0.8	0.8	0.9	0.9	0.9	1.0

Note: Bolded value is selected herein

The idealized force-deformation curve is described in ASCE/SEI 41 (ASCE, 2017) per section 7.4.3. V_d is the maximum base shear demand in the pushover analysis and Δ_d is the roof drift at V_d . V_y is calculated by assuming $\alpha_l=0.01$. Analysis result and idealized curve are shown in Figure F-10 and Figure F-11, respectively.

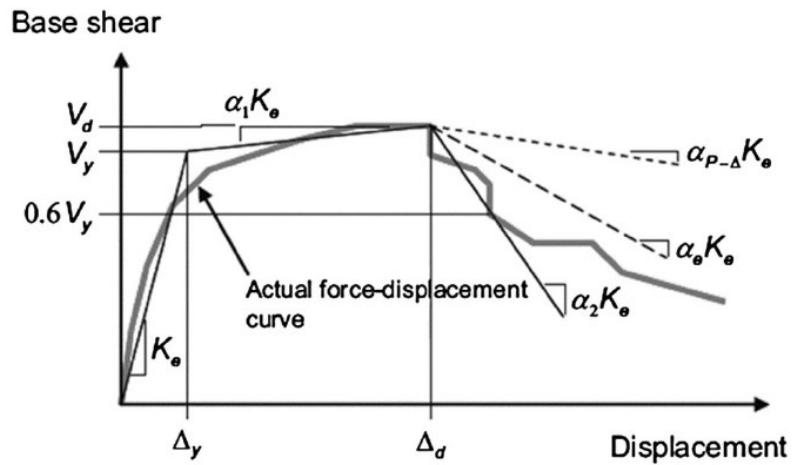


Figure F-10 Idealized Force-Deformation curve per ASCE/SEI 41 (ASCE, 2017).

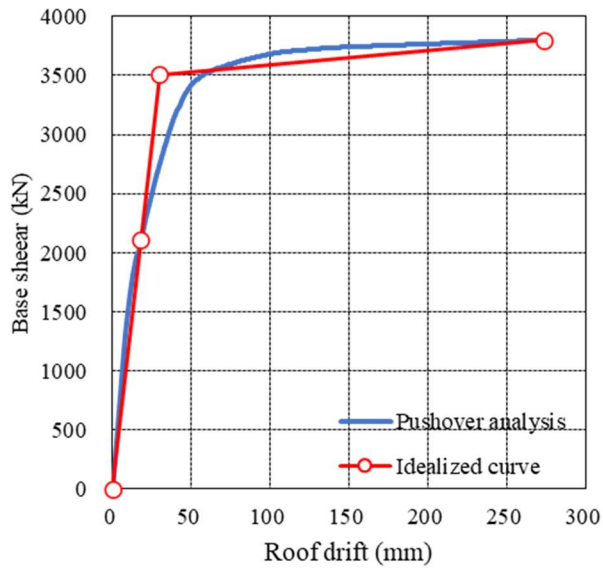


Figure F-11 Pushover analysis and idealized curve.

Table F-8 summarizes C_1C_2 calculation. In each excitation case, C_1C_2 is approximately 1.0.

Table F-8 Summary of C_1 , C_2 Calculation

		Original	60%	100%	125%	150%
Height	h_n (ft)	53.8				
Coefficient	C_t	0.018				
Coefficient	β	0.9				
Fundamental period	T (s)	0.65				
Analytical model period*	T_{ana} (s)	0.49	0.60	0.64	-	-
Site Class	a	C: 90				
Response spectrum acceleration	S_a (m/s)		7.2	12	15	18
Effective seismic weight	W (t)	463.7				
Yield strength	V_y (kN)	3509				
Effective mass factor	C_m	0.9				
Ratio of elastic strength demand to yield strength	$\mu_{strength}$		0.86	1.43	1.78	2.14
Modification factor	C_1		1.00	1.01	1.02	1.03
	C_2		1.00	1.00	1.00	1.00

* First mode period with an eigen analysis with stiffness reduction based on maximum ductility after shaking.

F.7 Equivalent Ductility

The equal-displacement theory is introduced to estimate ductility with a linear analysis. Figure F-12 shows the concept of equal-displacement theory. The maximum displacement of the linear model (Δ_{max}) is assumed equal to the maximum displacement with equivalent nonlinear model (Δ_{eq}). Since the equivalent ductility (μ_{eq}) is obtained by yield displacement. The equivalent ductility is then converted to DCR to estimate the stiffness reduction factor for damaged components.

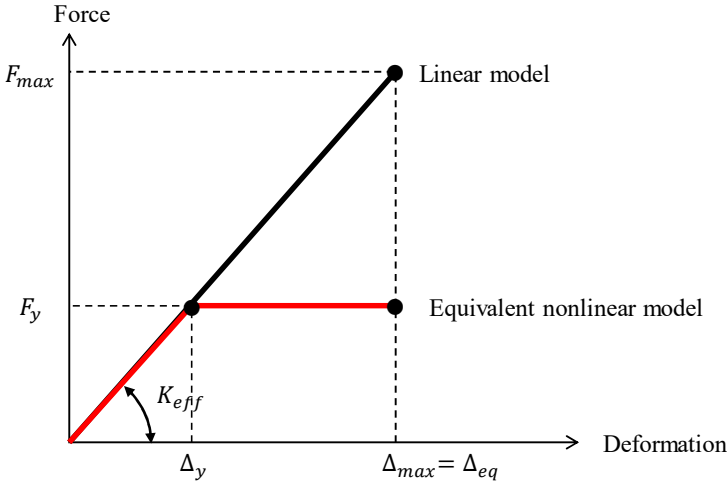


Figure F-12 Equal-displacement theory.

Equivalent ductility is defined by the following equation

$$\mu_{eq} = \frac{\Delta_{eq}}{\Delta_y}$$

The demand capacity ratio (DCR) is expressed as below

$$DCR = \frac{F_{max}}{F_y}$$

The equivalent ductility is calculated with the following equation

$$\begin{aligned} K_{eff} &= \frac{F_y}{\Delta_y} = \frac{F_{max}}{\Delta_{max}} = \frac{F_{max}}{\Delta_{eq}} \\ \Leftrightarrow \frac{F_y}{\Delta_y} &= \frac{F_{max}}{\Delta_{eq}} \\ \frac{\Delta_{eq}}{\Delta_y} &= \frac{F_{max}}{F_y} \\ \therefore \mu &= DCR \end{aligned}$$

Case Study 1

Appendix G

DCR Estimates

This appendix provides DCRs with the linear model and the modified linear model on all the frame in shaking direction.

G.1 Linear Model

Figure G-1 shows DCRs on Y1-3 frame with the linear model in Run 1-3.

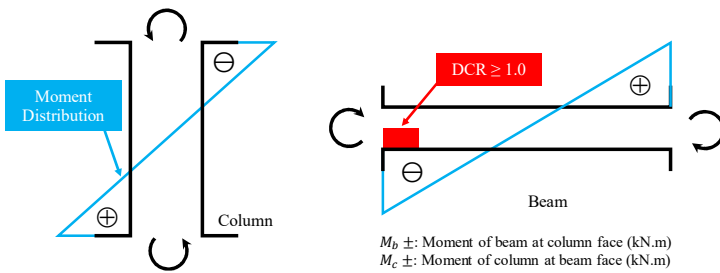
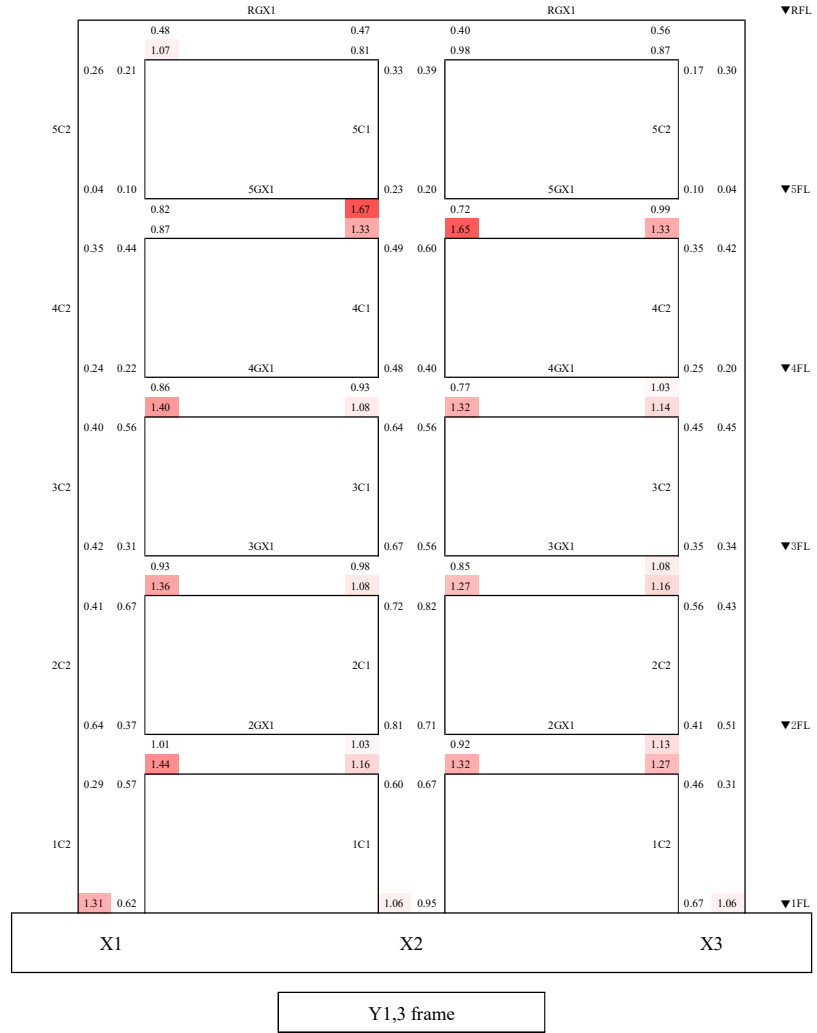
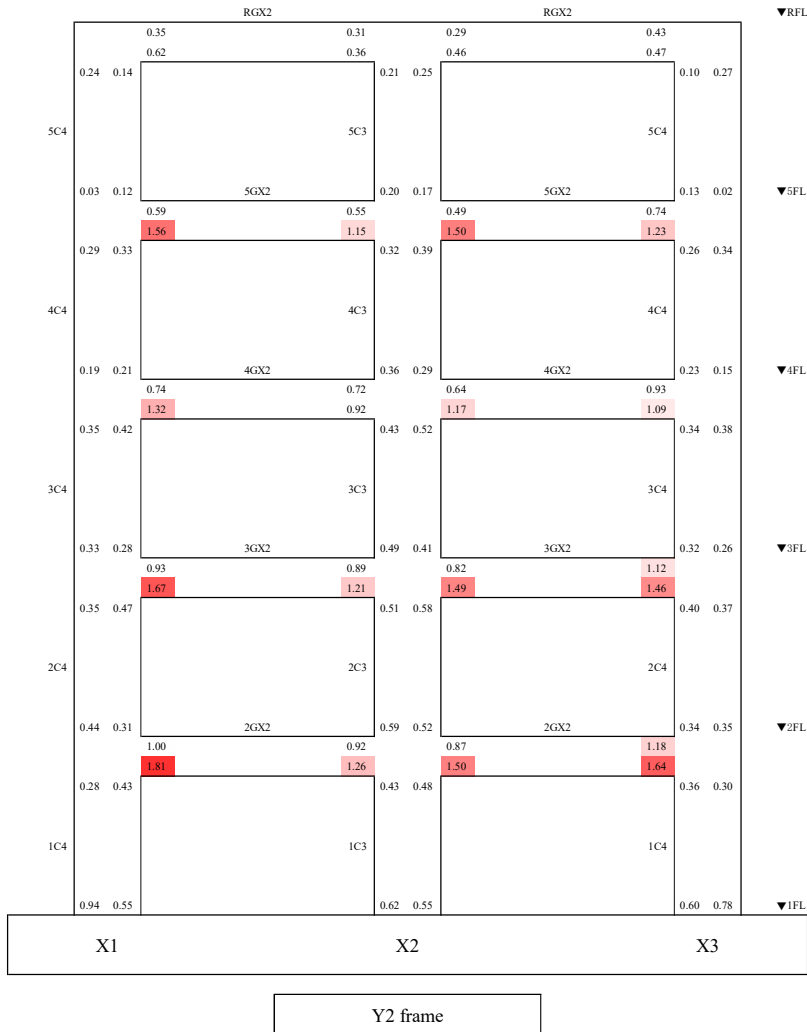


Figure G-1 DCRs with the linear model.



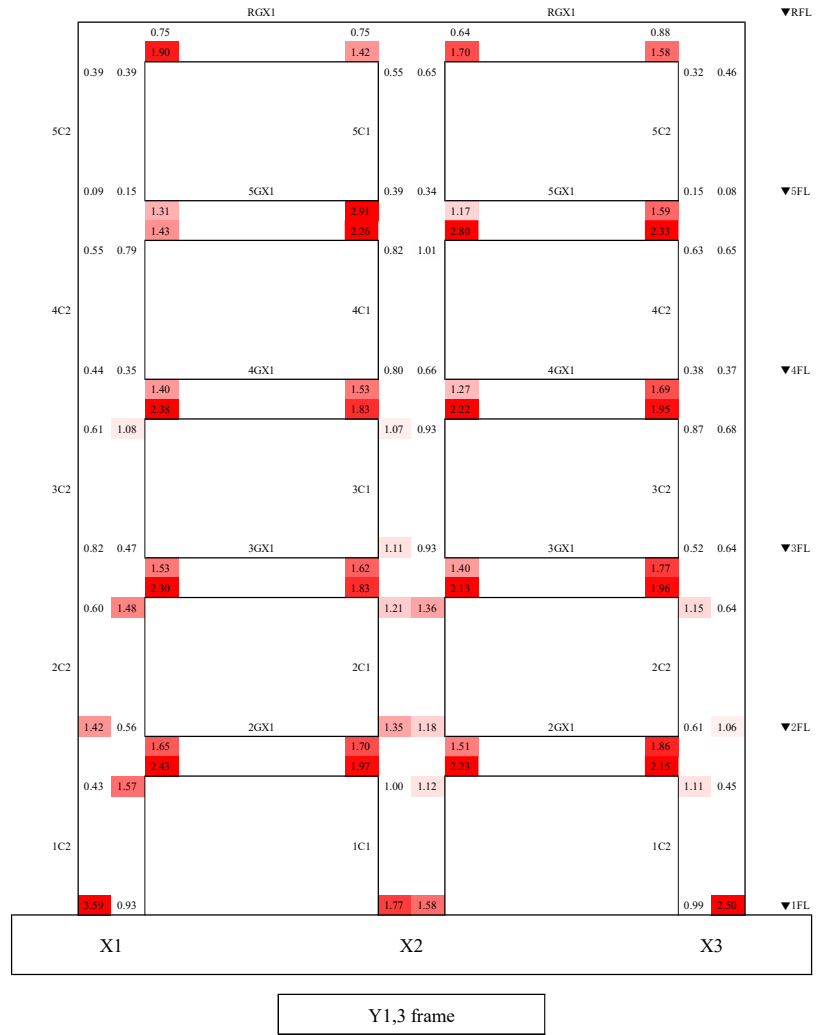
(a) Run 1

Figure G-1(cont) DCRs with the linear model.



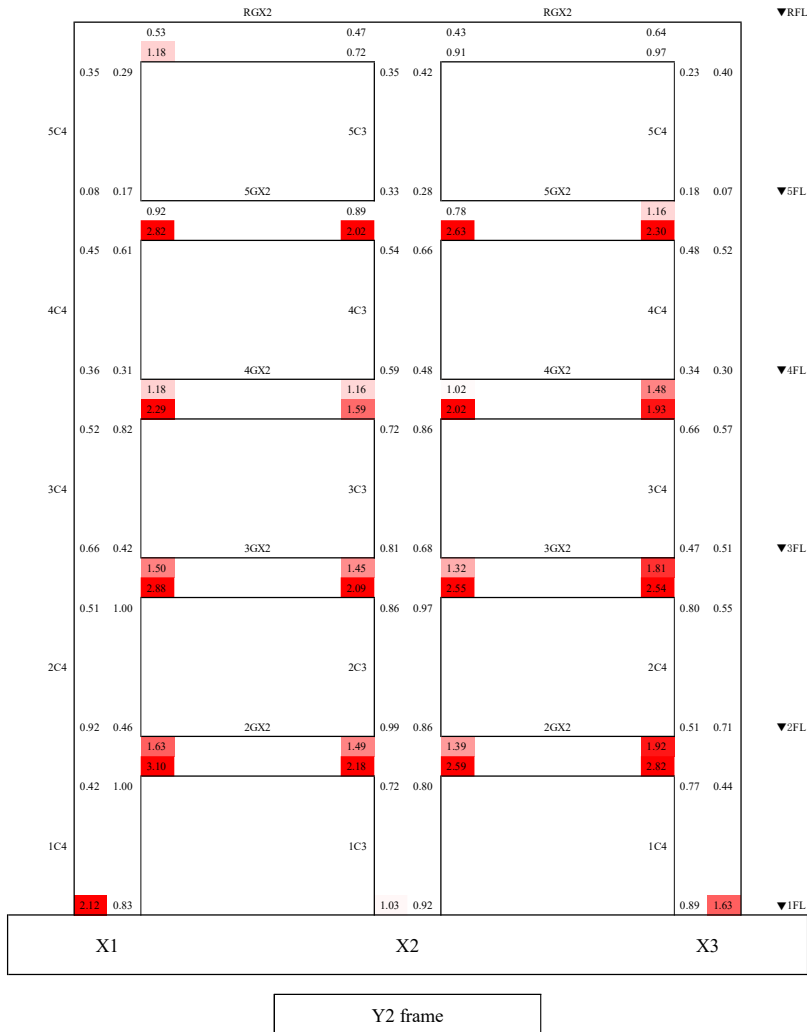
(a) Run 1

Figure G-1(cont.)DCRs with the linear model.



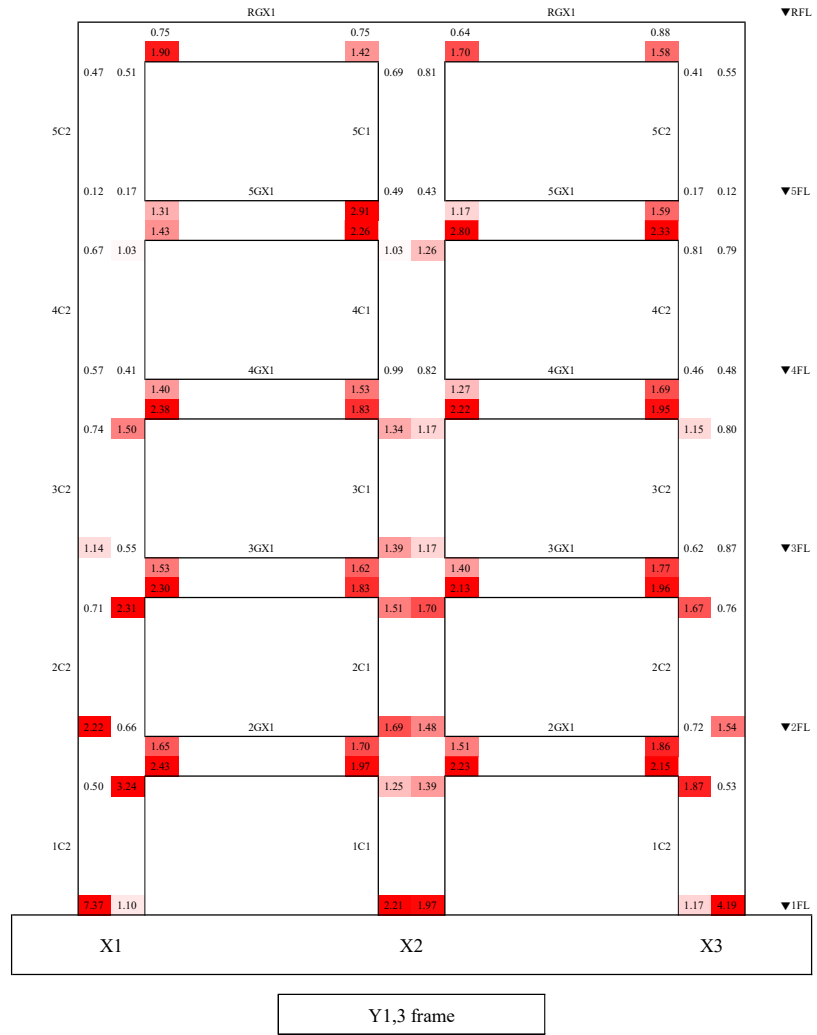
(b) Run 2

Figure G-1(cont) DCRs with the linear model.



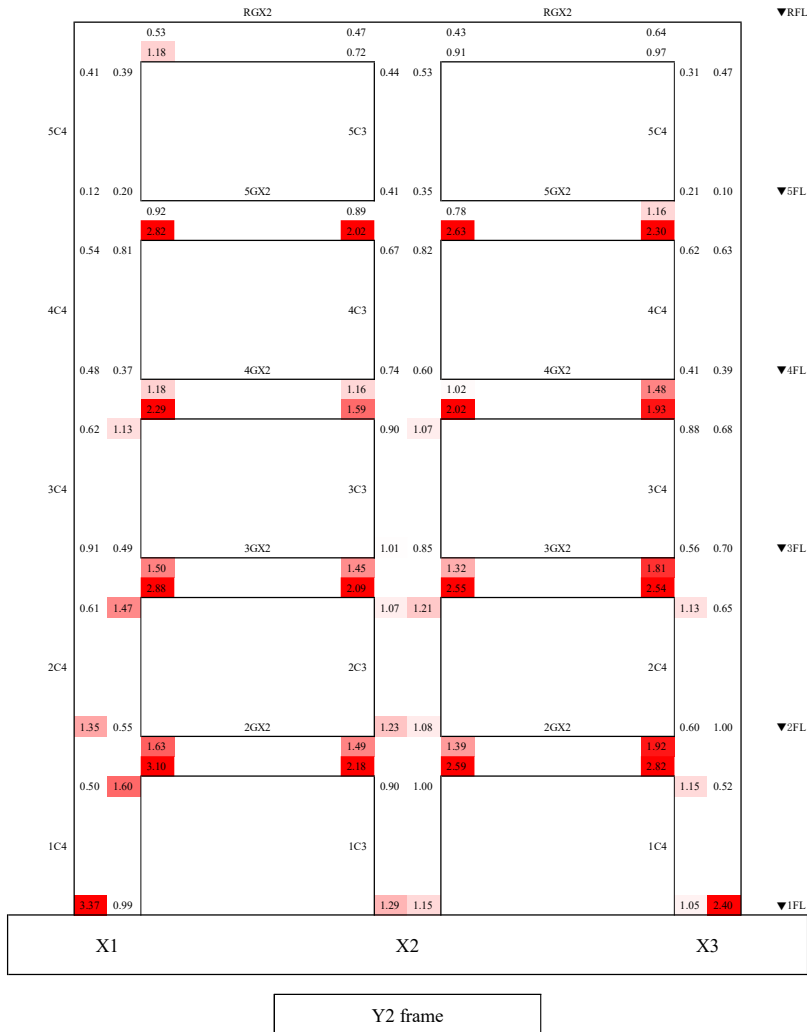
(b) Run 2

Figure G-1(cont) DCRs with the linear model.



(c) Run 3

Figure G-1(cont) DCRs with the linear model.



(c) Run 3

Figure G-1(cont) DCRs with the linear model.

G.2 Modified Linear Model

Figure G-2 shows DCRs with the modified linear model in Run 3.

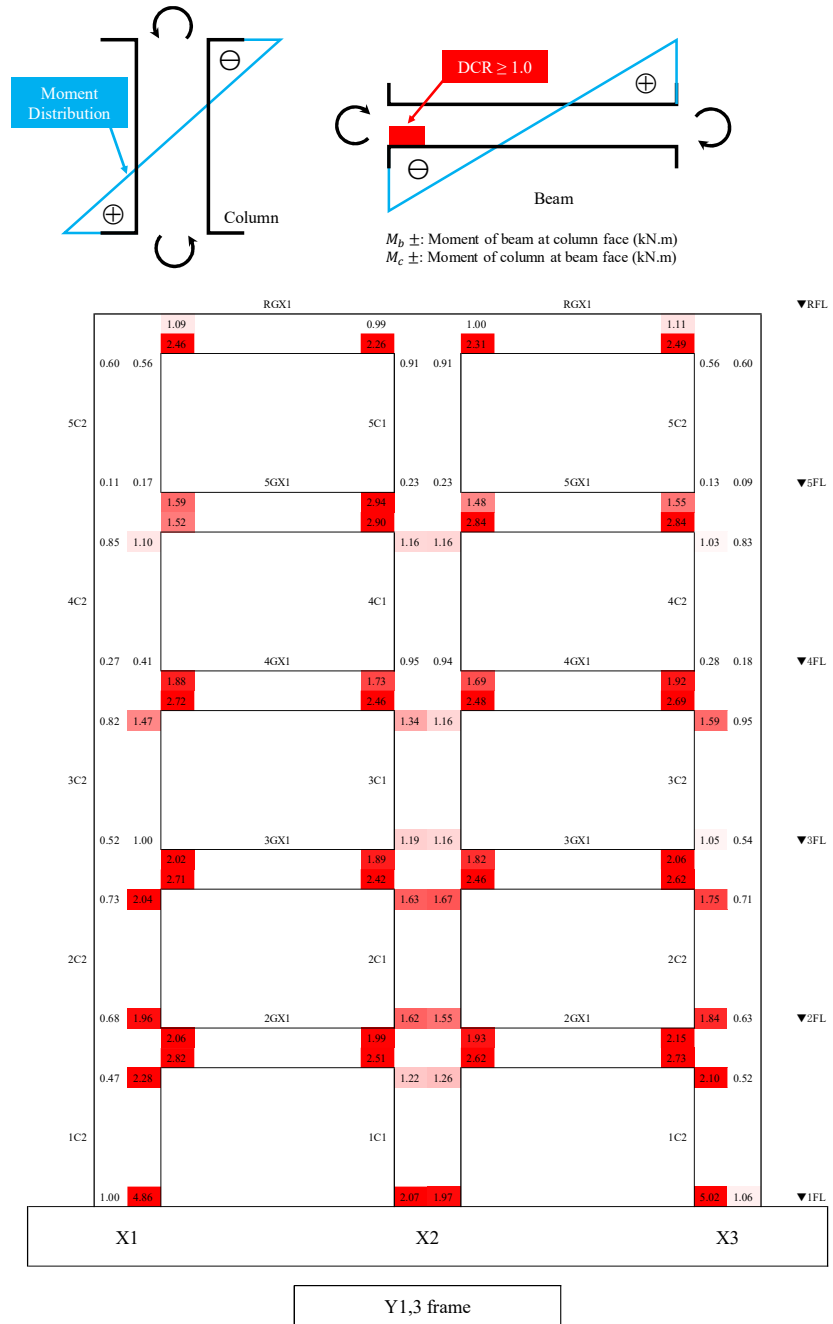


Figure G-2 DCRs with the modified linear model in Run 3.

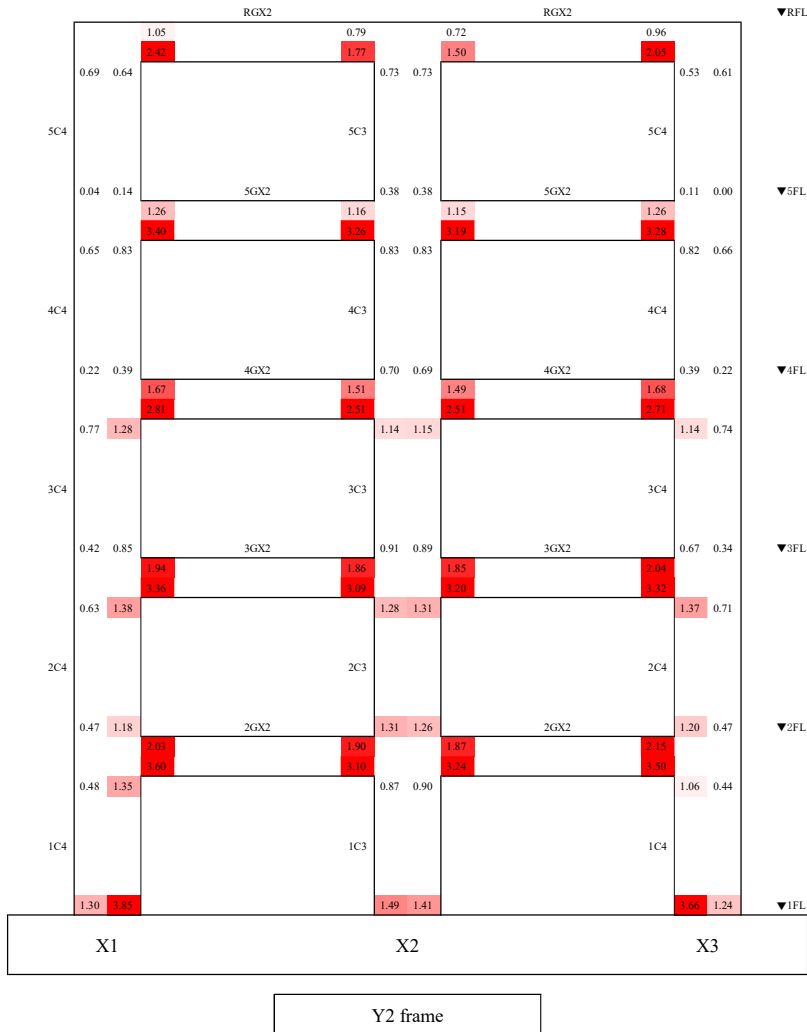


Figure G-2(cont.)DCRs with the modified linear model in Run 3.

Ductility Demand and m-factors

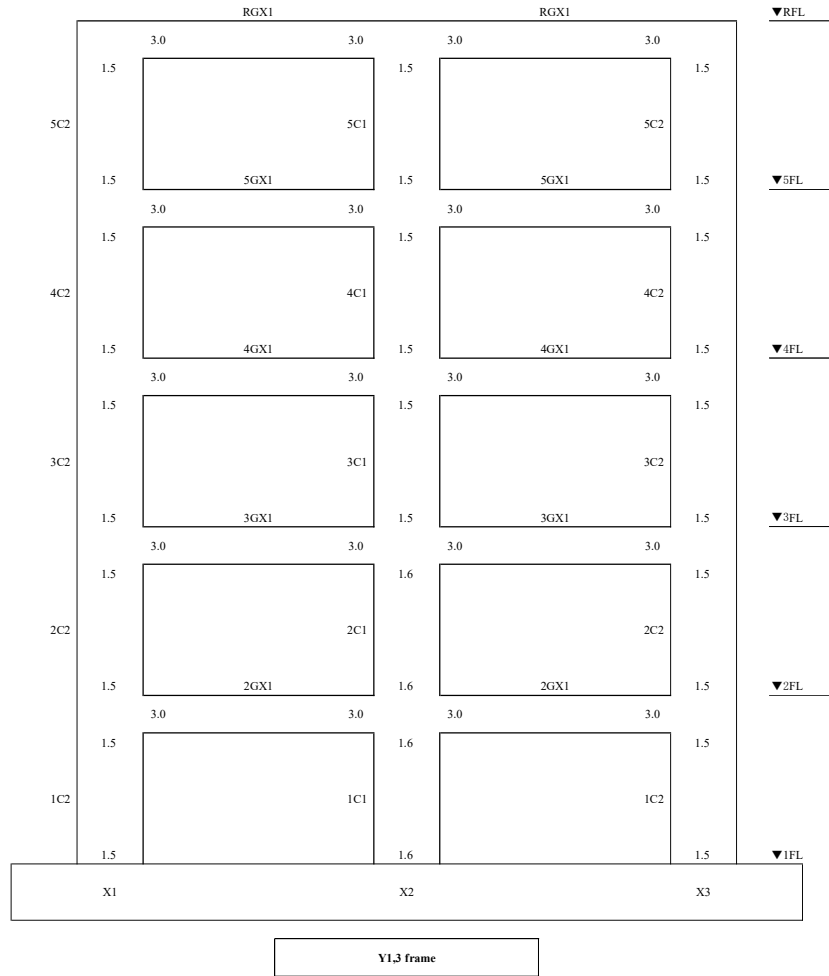
In this appendix, m-factors of beams and columns on each elevation and ductility demand with the linear model and the modified linear model are provided. Also, ductility demand estimated with the linear model and the modified linear model are compared.

H.1 Linear Model

Figure H-1 shows m-factors of Immediate Occupancy (IO) on each elevation.

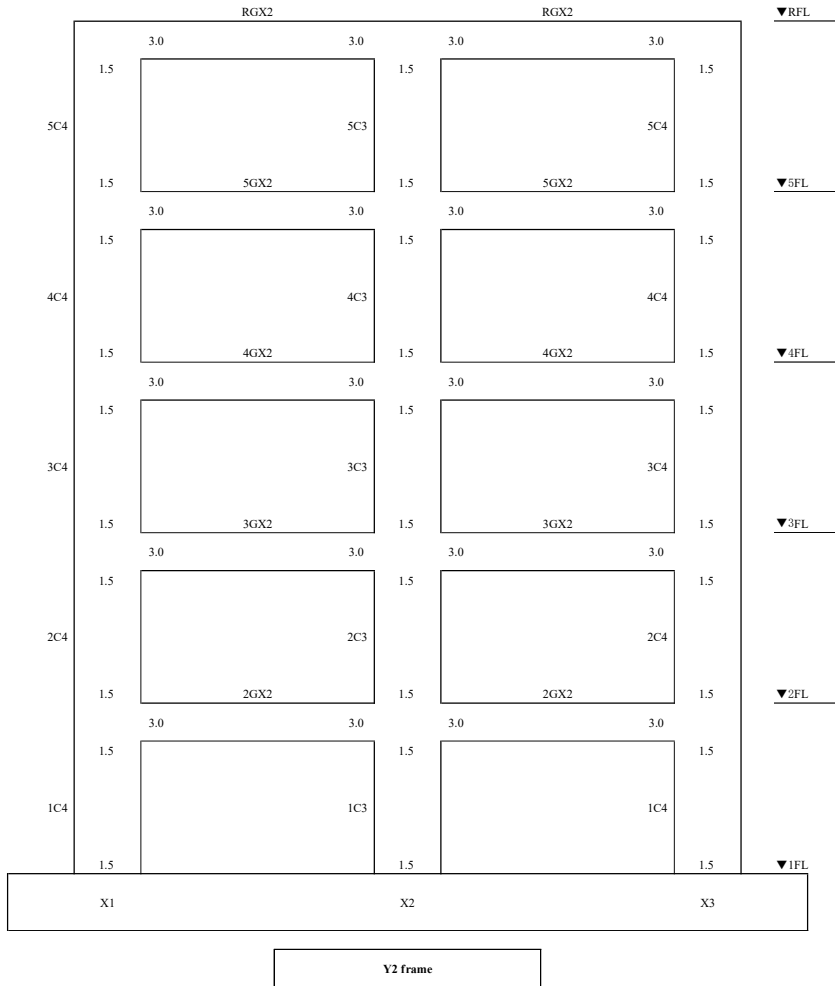
Figure H-2 shows m-factors of Collapse Prevention (CP) on each elevation.

Figure H-3 shows the ratio of ductility demand to m-factors of IO.



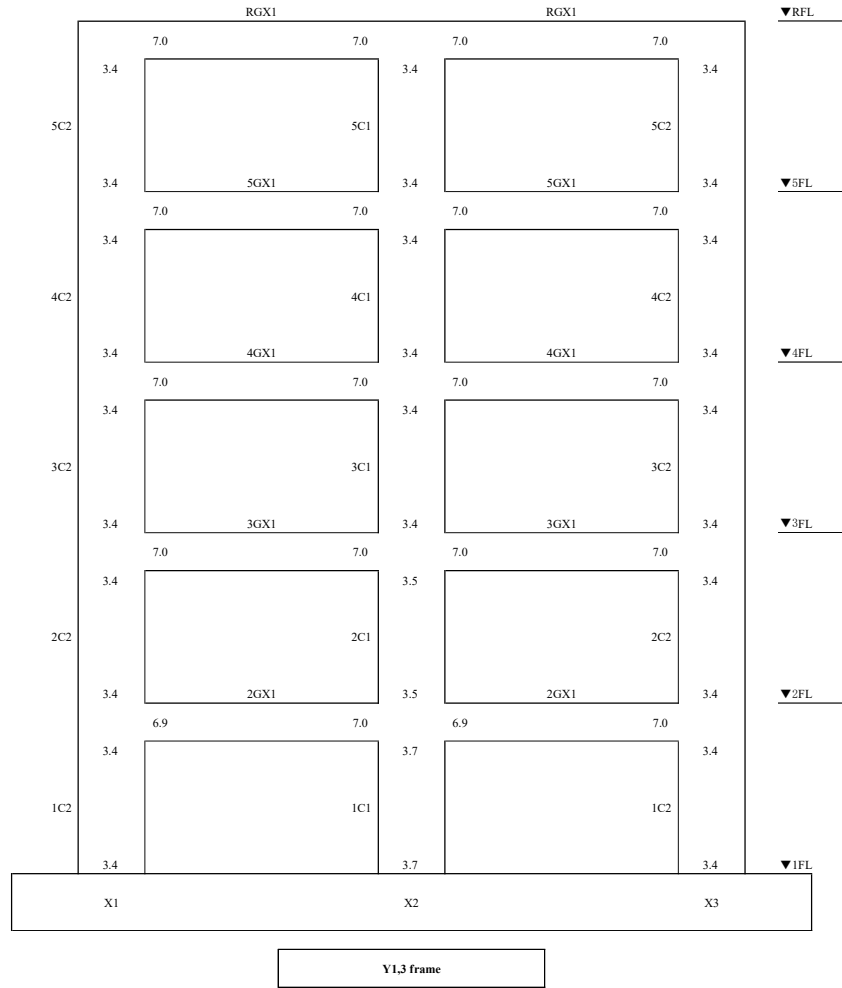
(a) Y1,3 frame

Figure H-1 m-factors of IO with the linear model.



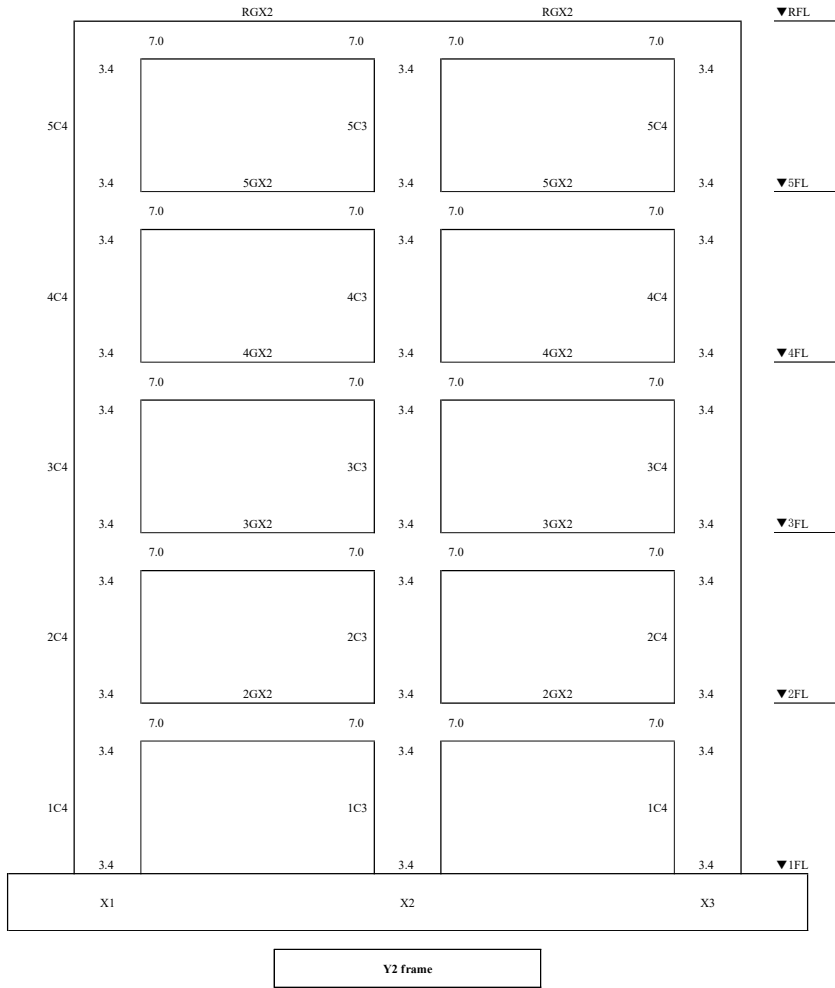
(b) Y2 frame

Figure H-1(cont) m-factors of IO with the linear model.



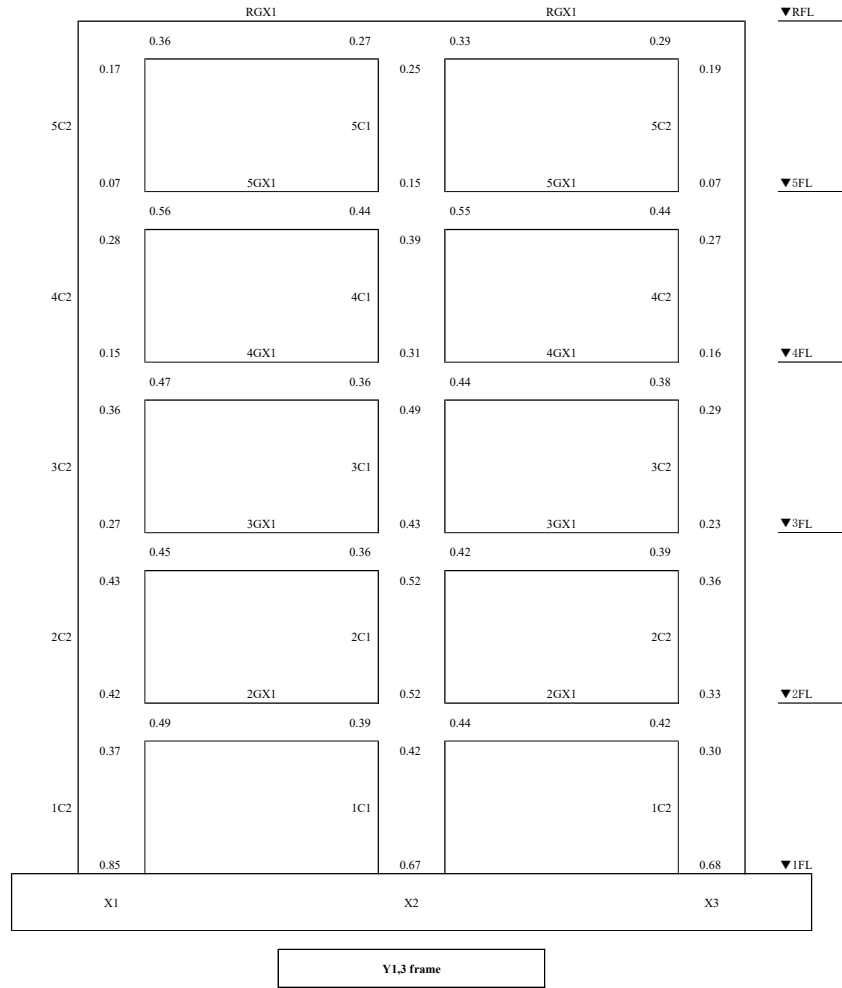
(a) Y1, Y3 frame

Figure H-2 m-factors of CP with the linear model.



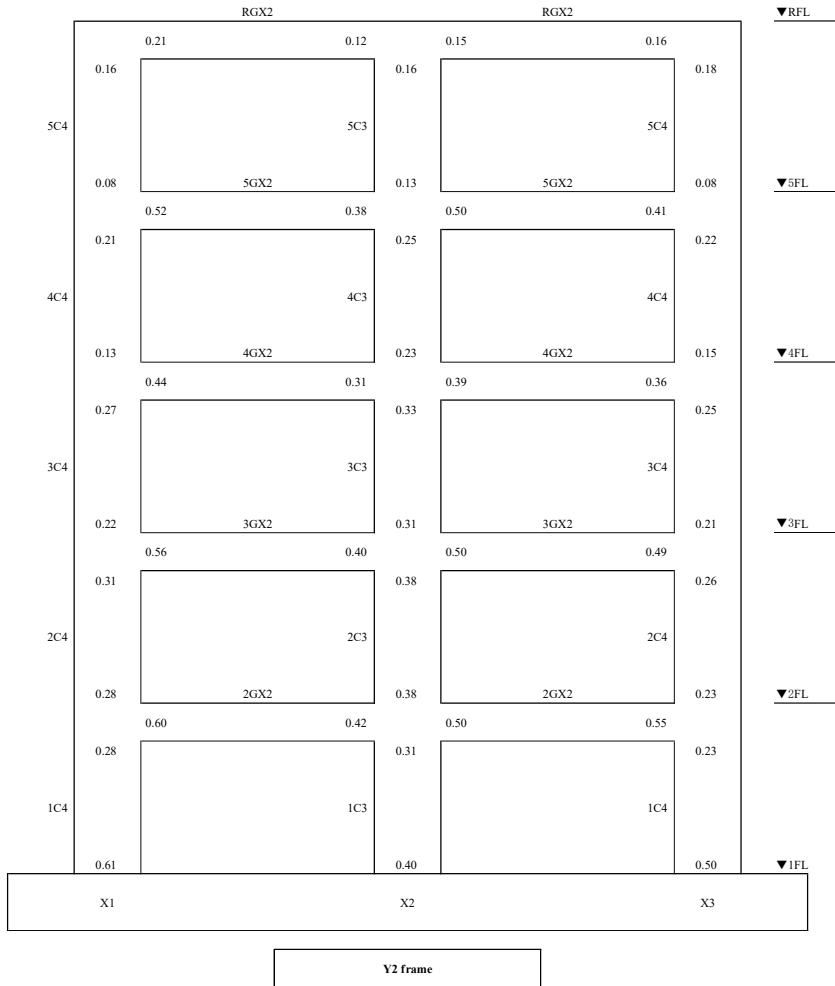
(b) Y2 frame

Figure H-2(cont) m-factors of CP with the linear model.



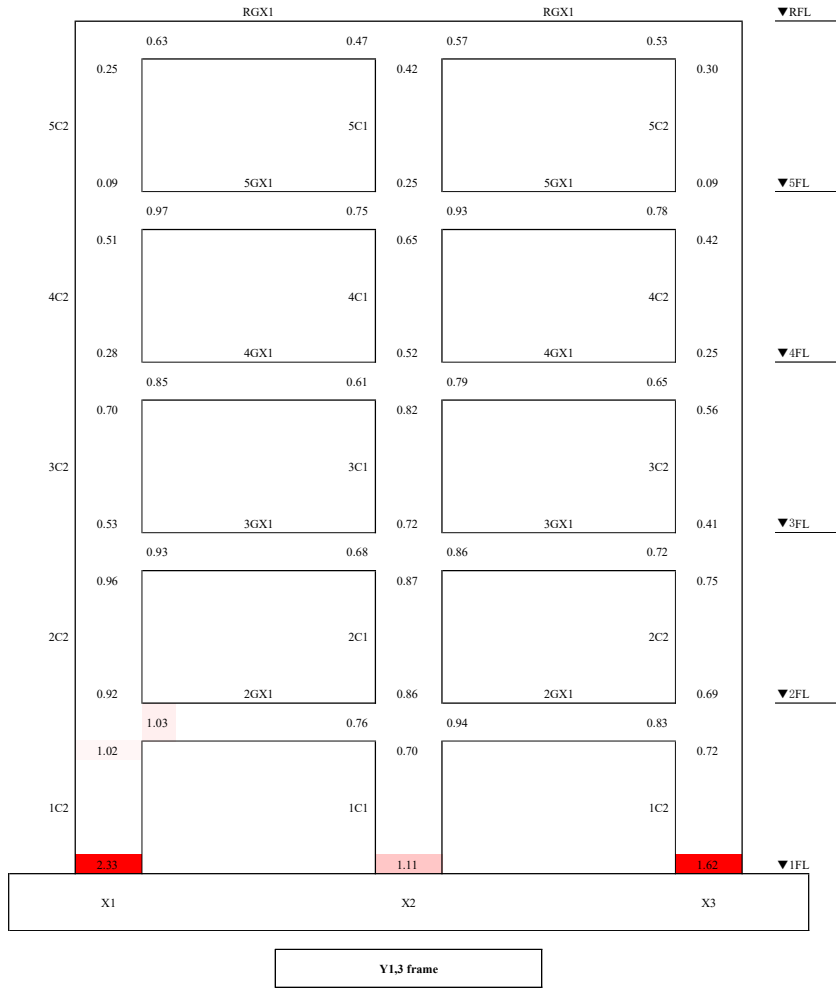
(a-1) IO - Run 1 – Y1,3 frame (Linear model)

Figure H-3 Ratio of ductility demand to m-factors of Primary IO with the linear model.



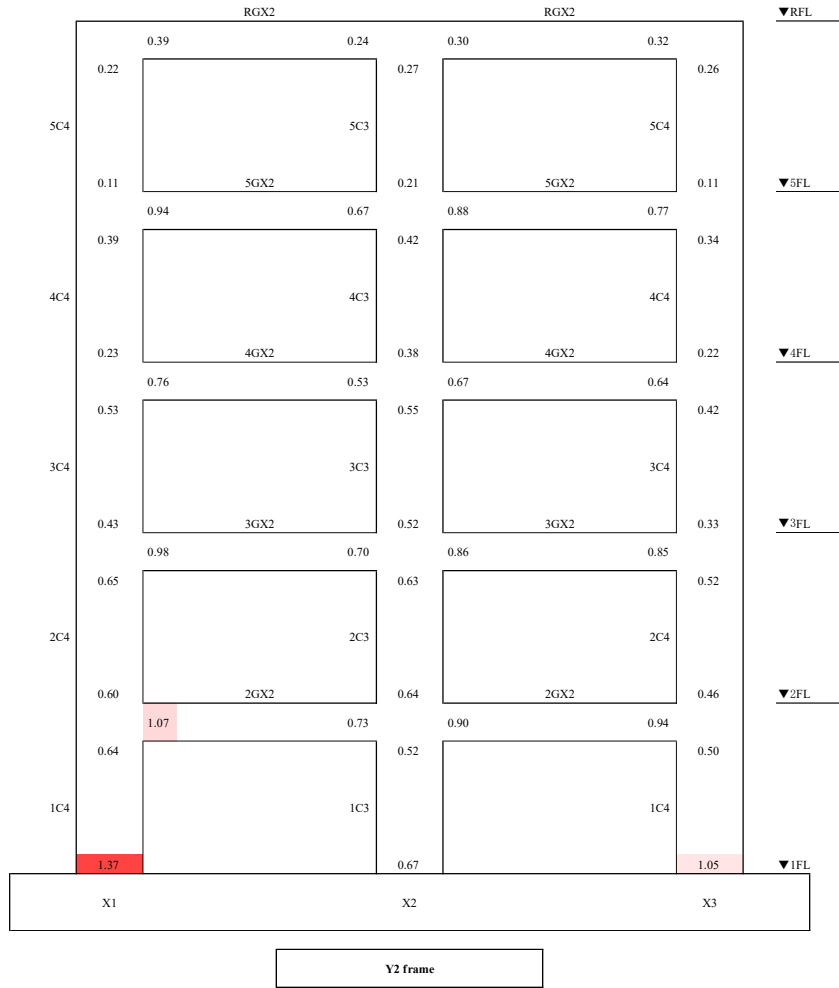
(a-2) IO - Run 1 – Y2 frame (Linear model)

Figure H-3 (cont) Ratio of ductility demand to m-factors of Primary IO with the linear model.



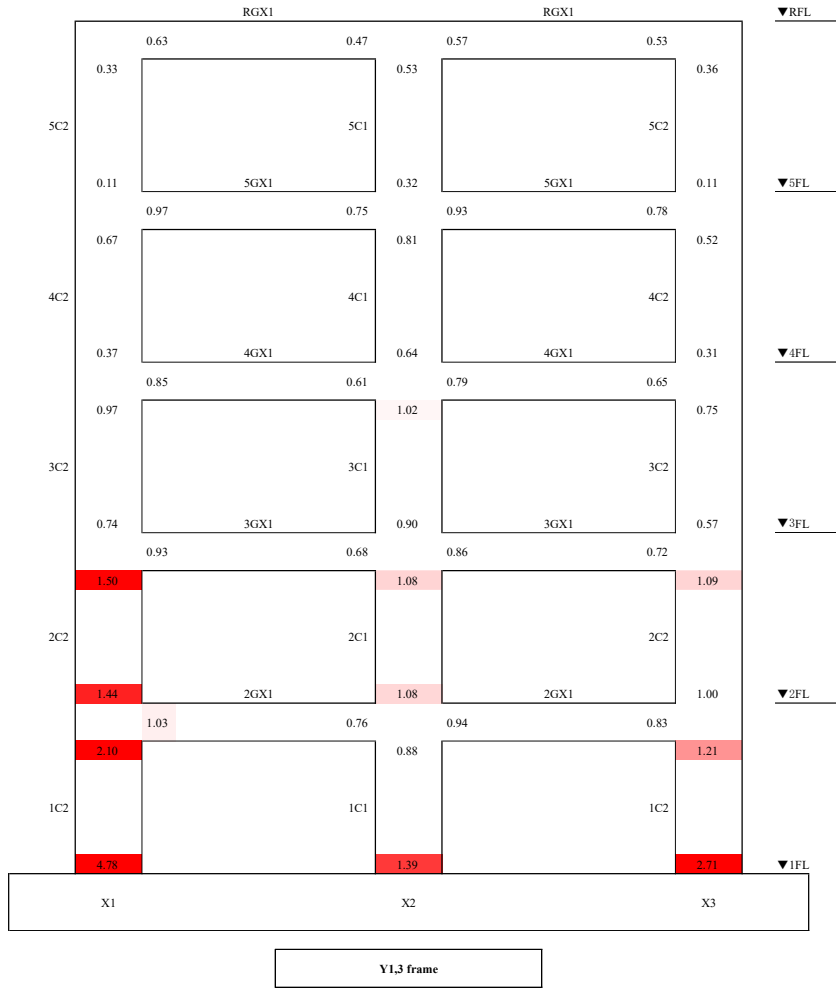
(b-1) IO - Run 2 – Y1,3 frame (Linear model)

Figure H-3 (cont) Ratio of ductility demand to m-factors of Primary IO with the linear model.



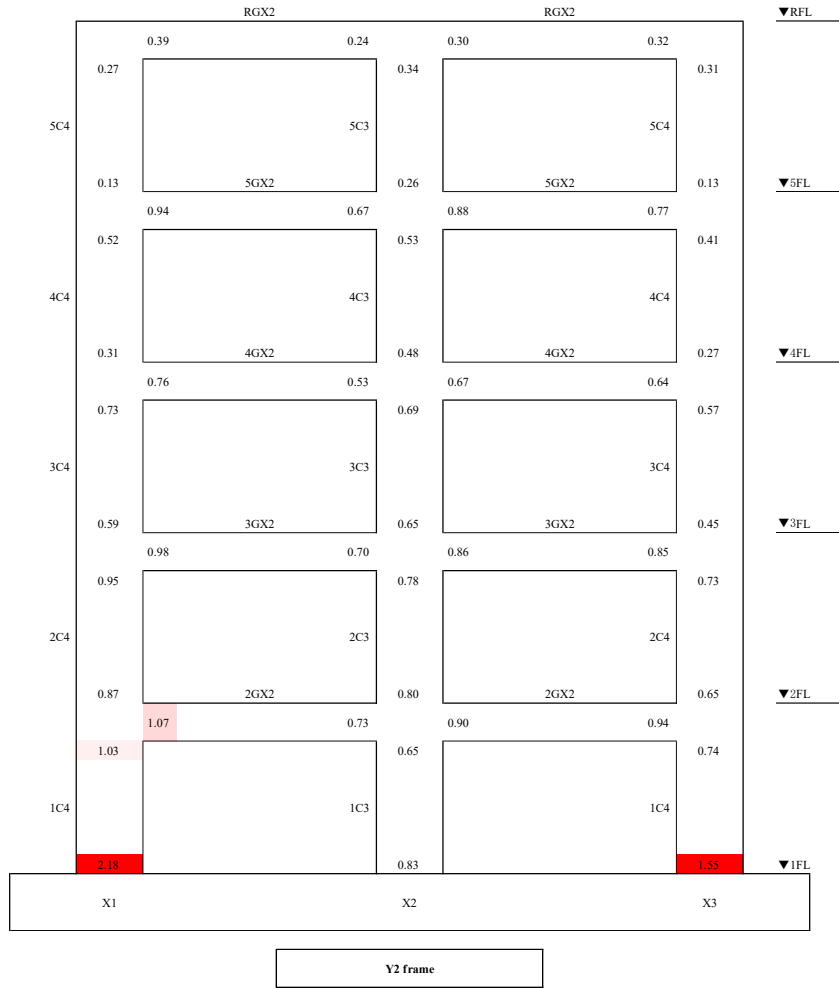
(b-2) IO - Run 2 – Y2 frame (Linear model)

Figure H-3 (cont) Ratio of ductility demand to m-factors of Primary IO with the linear model.



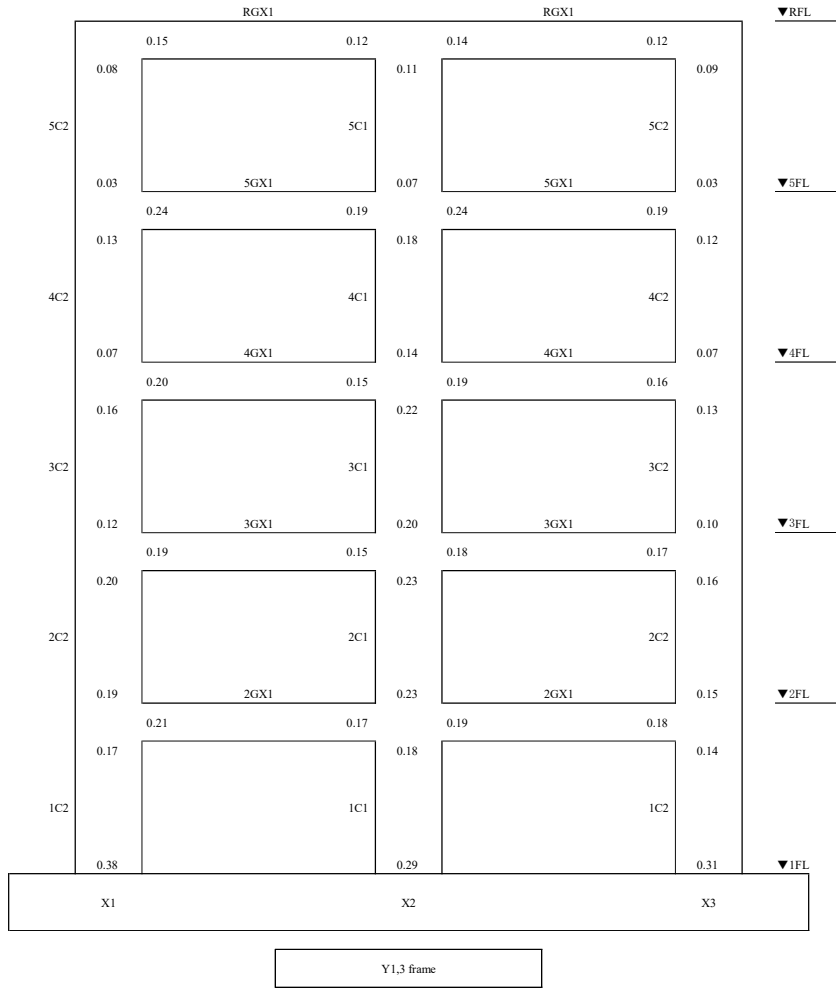
(c-1) IO - Run 3 – Y1,3 frame (Linear model)

Figure H-3 (cont) Ratio of ductility demand to m-factors of Primary IO with the linear model.



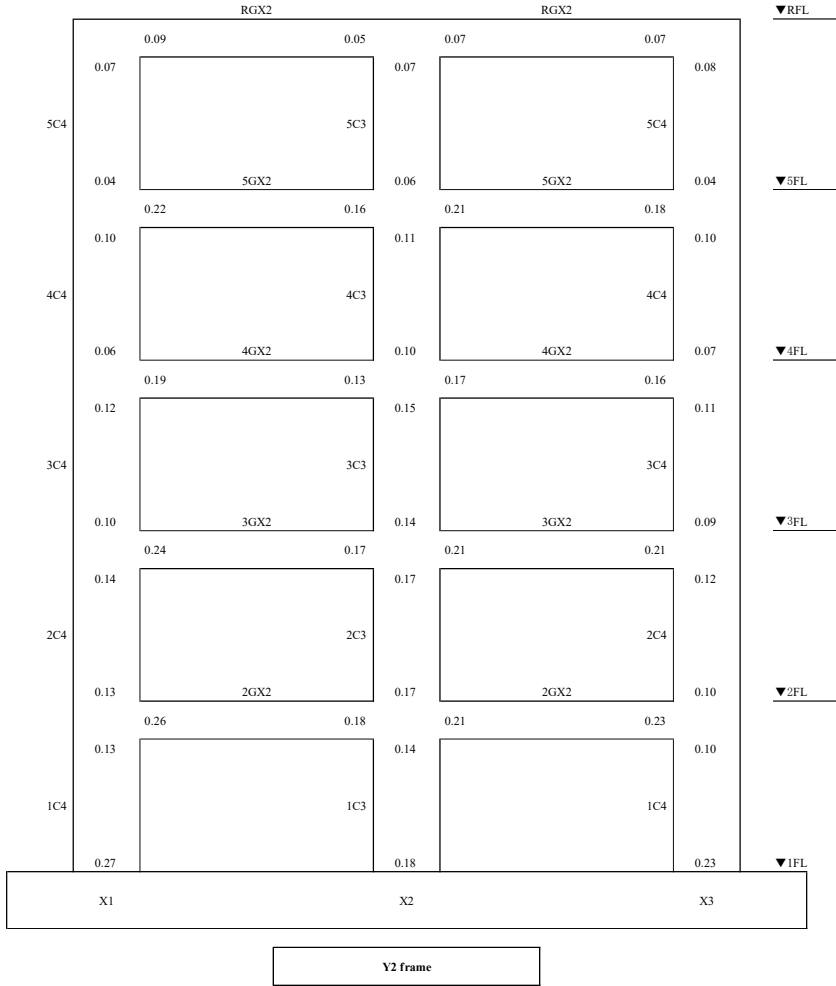
(c-2) IO - Run 3 – Y2 frame (Linear model)

Figure H-3 (cont) Ratio of ductility demand to m-factors of Primary IO with the linear model.



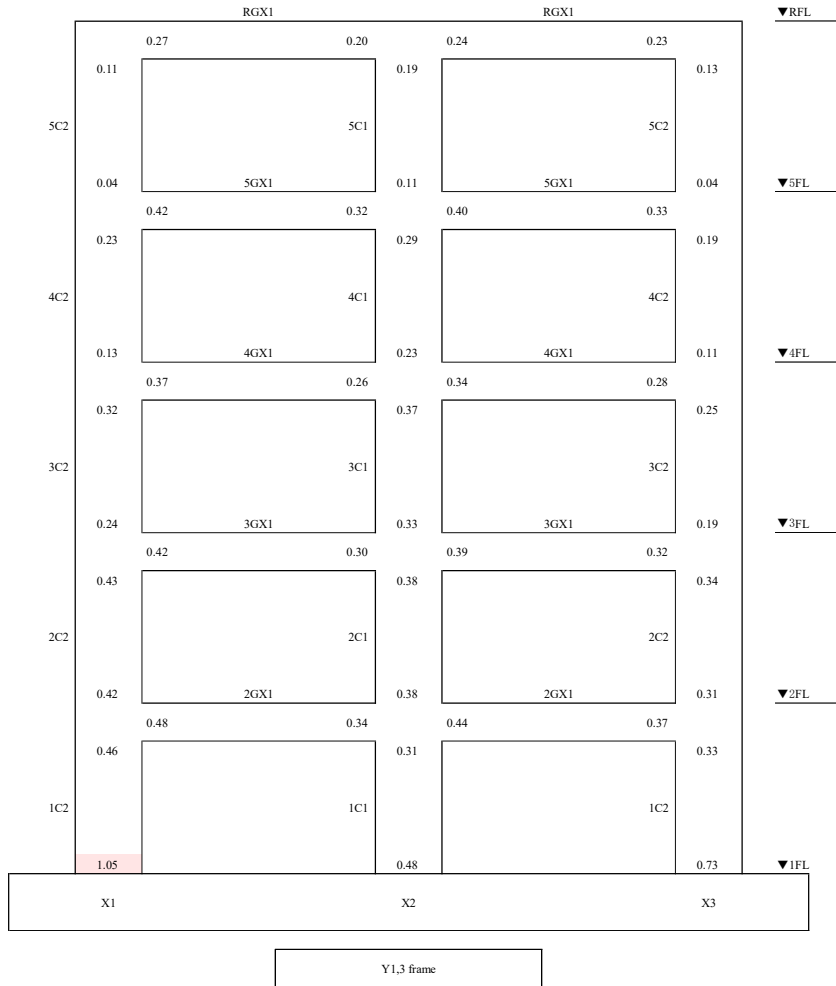
(a-1) CP - Run 1 – Y1,3 frame (Linear model)

Figure H-4 Ratio of ductility demand to m-factors of Primary CP with the linear model.



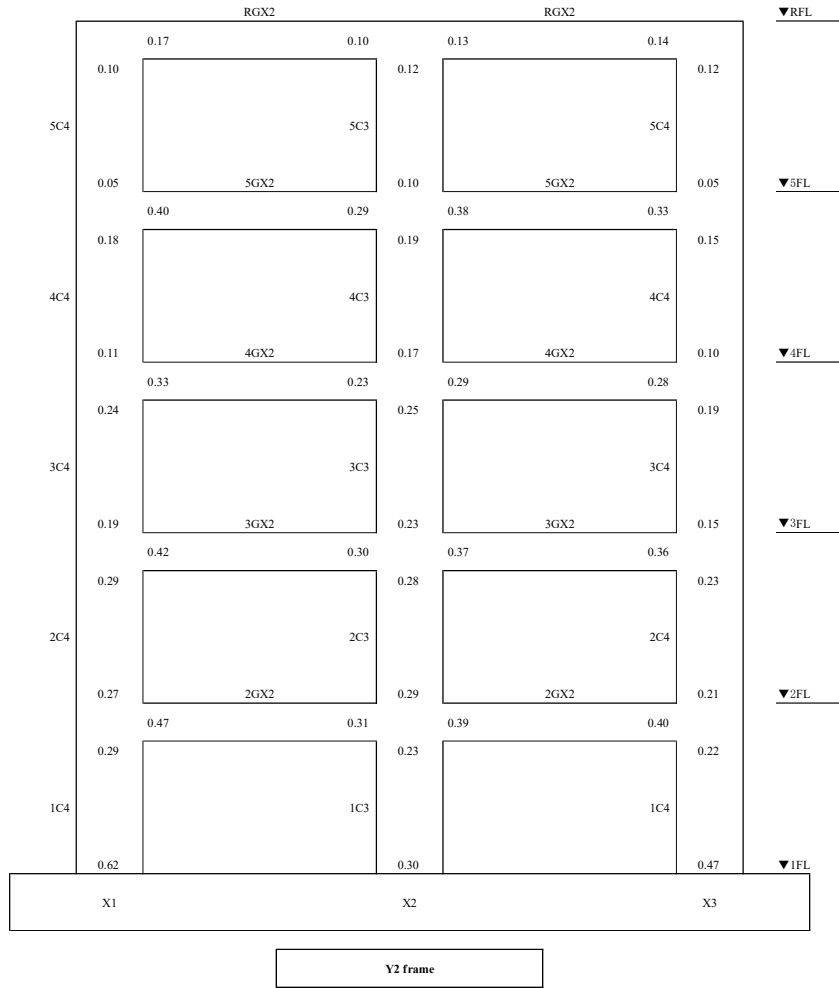
(a-2) CP - Run 1 – Y2 frame (Linear model)

Figure H-4 (cont) Ratio of ductility demand to m-factors of Primary CP with the linear model.



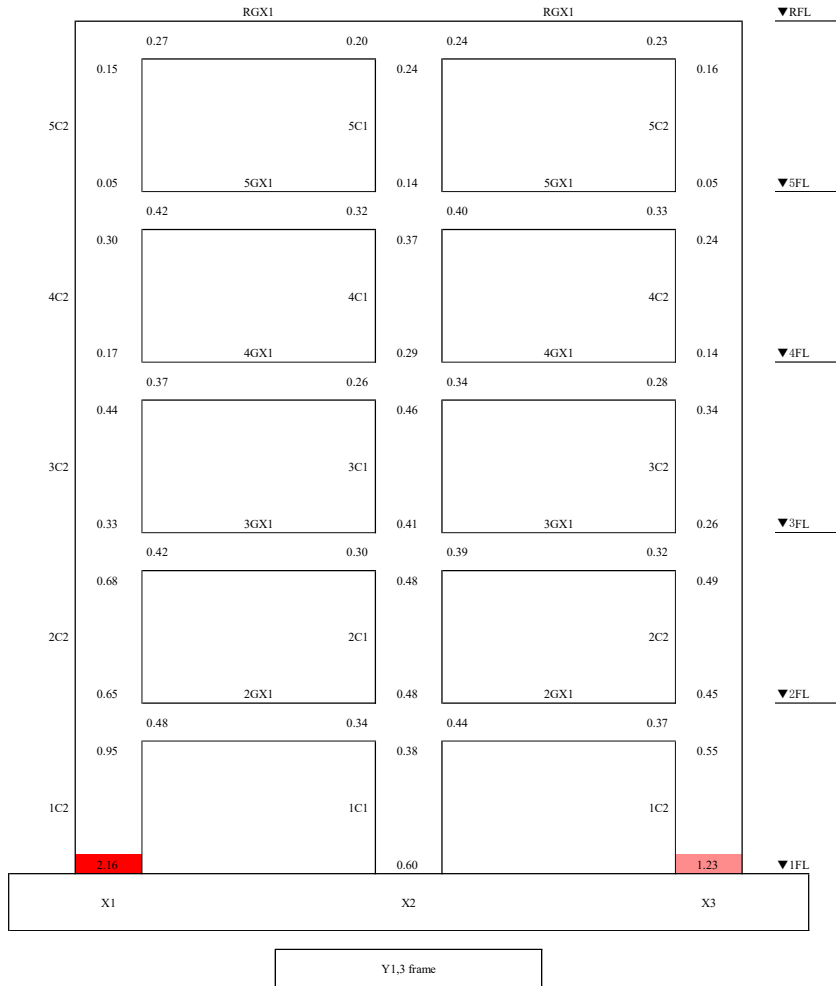
(b-1) CP - Run 2 – Y1,3 frame (Linear model)

Figure H-4 (cont) Ratio of ductility demand to m-factors of Primary CP with the linear model.



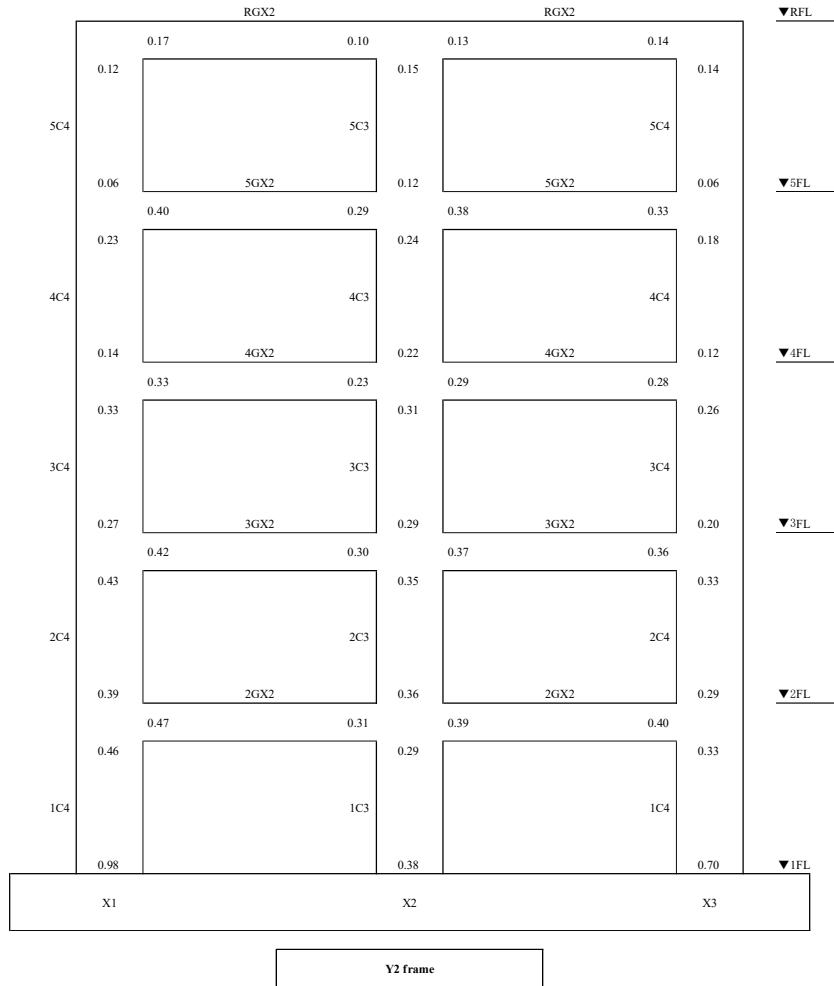
(b-2) CP - Run 2 - Y2 frame (Linear model)

Figure H-4 (cont) Ratio of ductility demand to m-factors of Primary CP with the linear model.



(c-1) CP - Run 3 – Y1,3 frame (Linear model)

Figure H-4 (cont) Ratio of ductility demand to m-factors of Primary CP with the linear model.



(c-2) CP - Run 3 – Y2 frame (Linear model)

Figure H-4 (cont) Ratio of ductility demand to m-factors of Primary CP with the linear model.

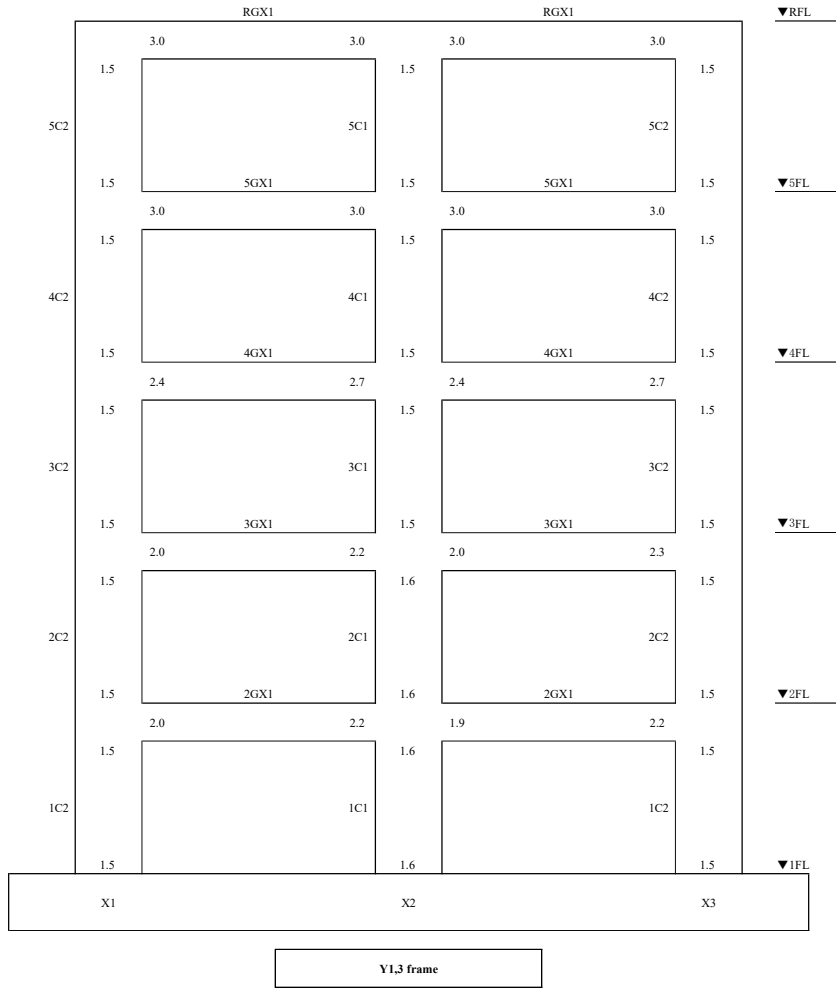
H.2 Modified Linear Model

shows m-factors of IO with the modified linear model

Figure H-1 shows m-factors of Immediate Occupancy (IO) on each elevation.

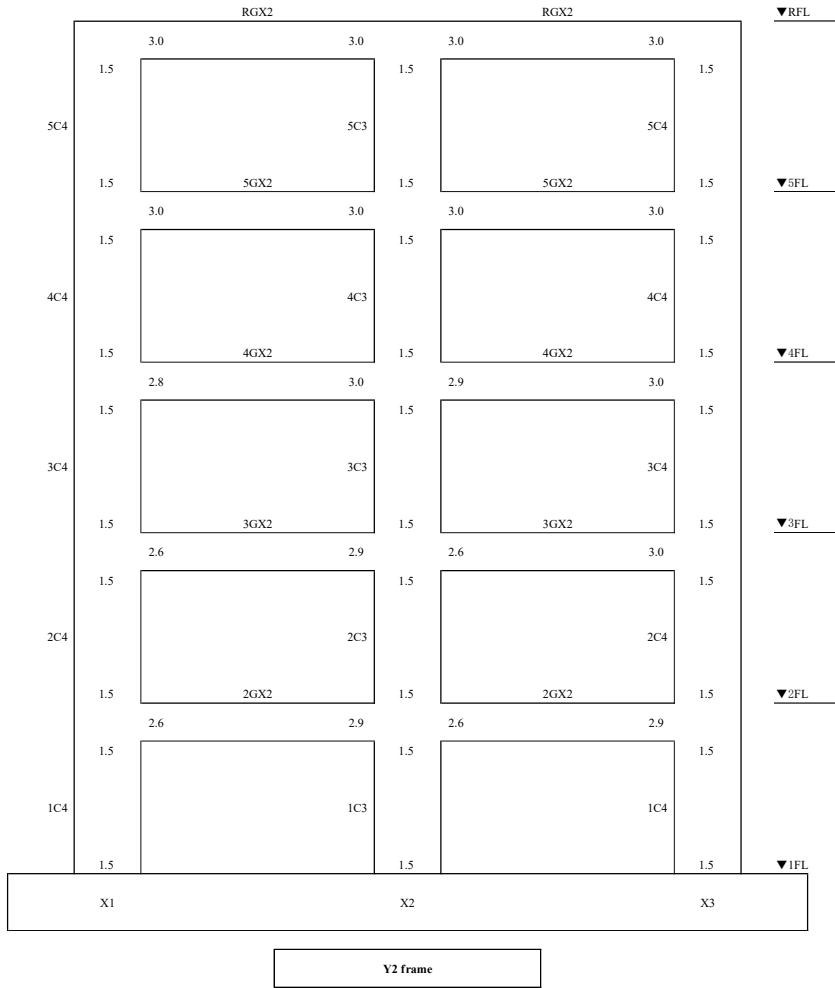
Figure H-2 shows m-factors of Collapse Prevention (CP) on each elevation.

Figure H-3 shows the ratio of ductility demand to m-factors of IO.



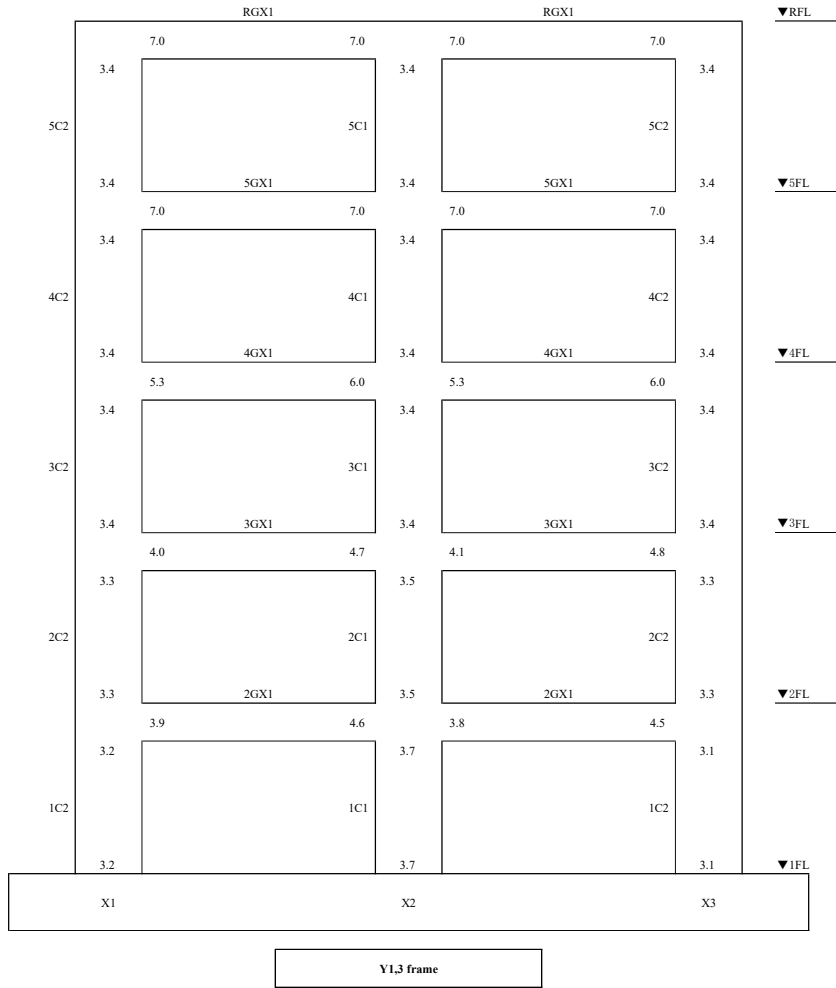
(a) IO - Y1,3 frame

Figure H-1 m-factors of IO with the modified linear model.



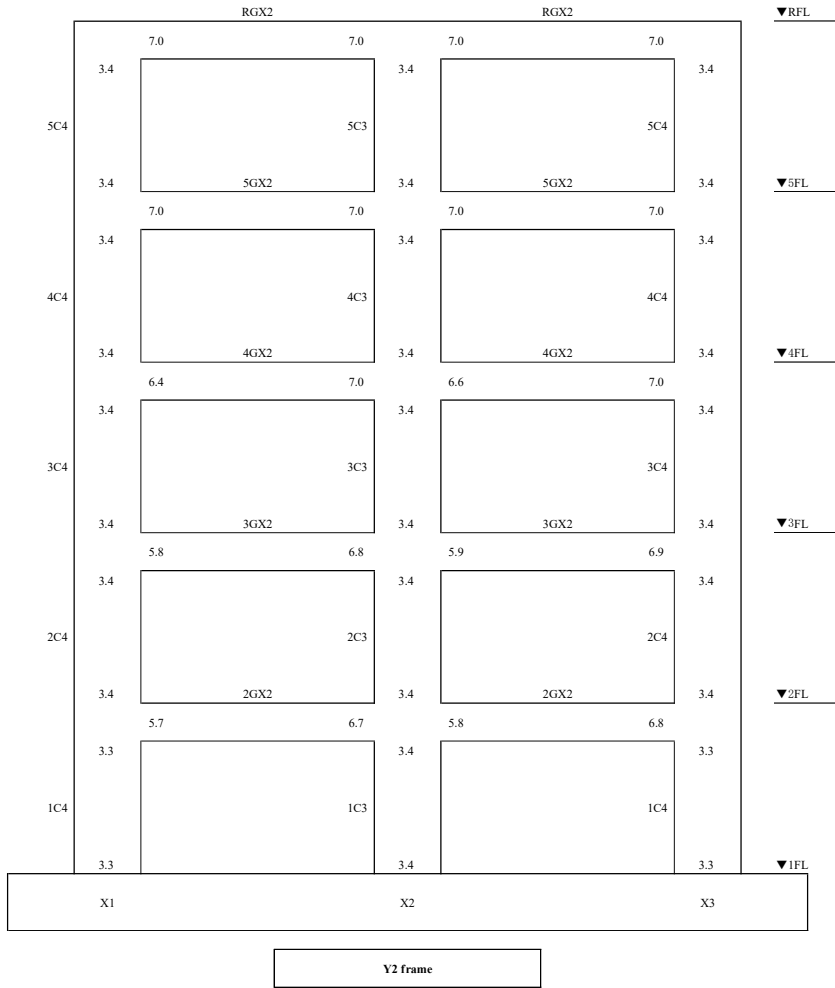
(b) IO – Y2 frame

Figure H-1 (cont)m-factors of IO with the modified linear model.



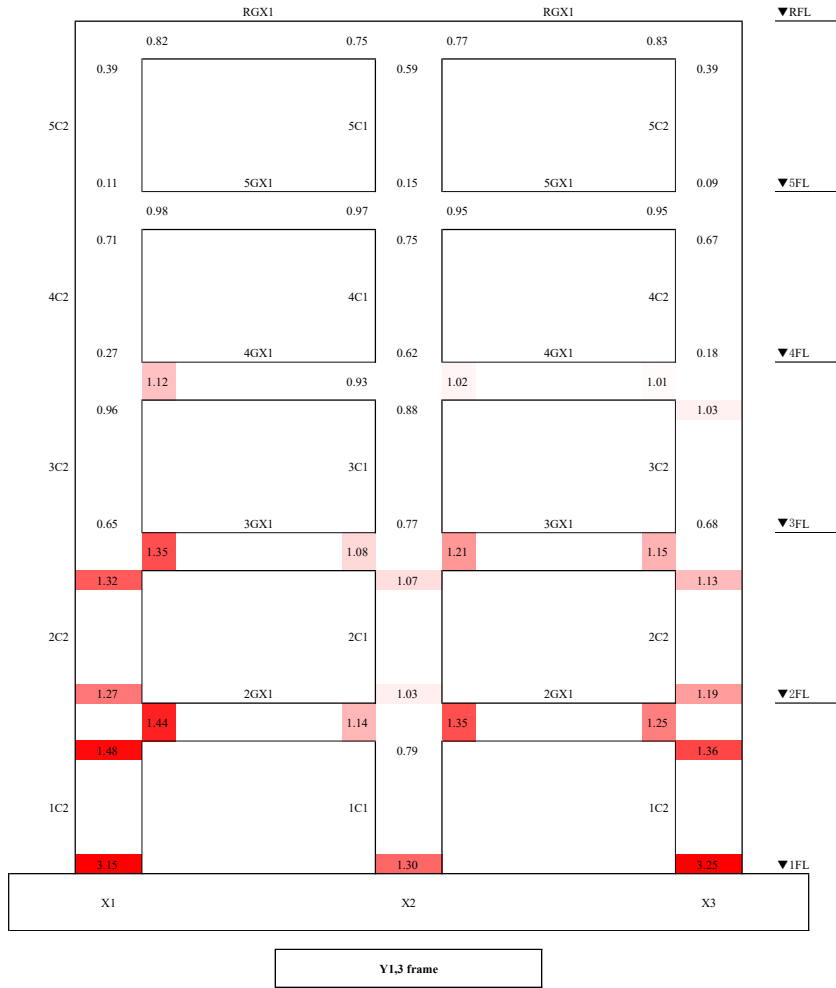
(a) CP - Y1,3 frame

Figure H-2 m-factors of CP with the modified linear model.



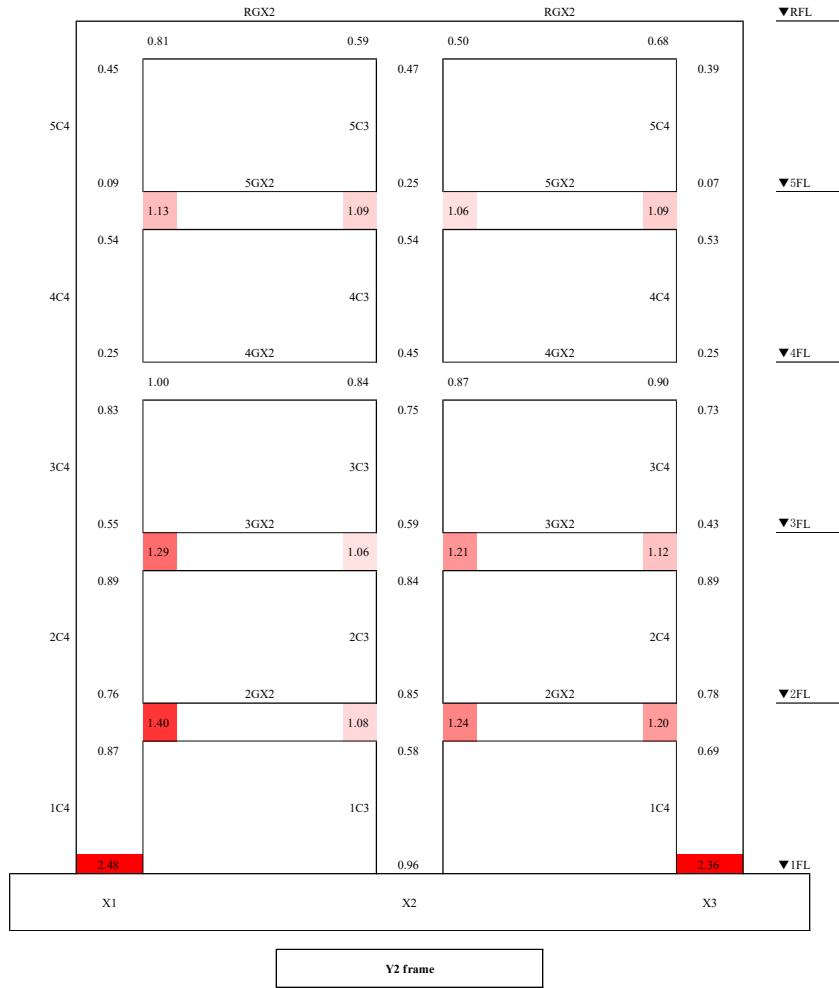
(b) CP – Y2 frame

Figure H-2(cont) m-factors of CP with the modified linear model.



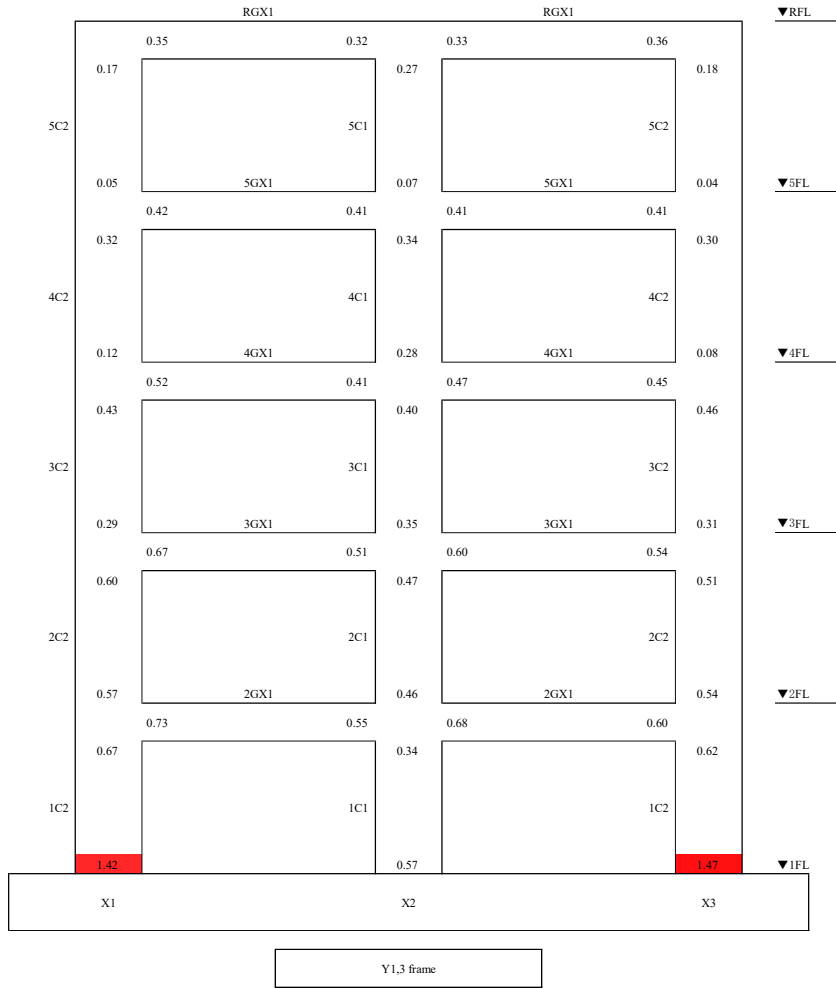
(a-1) IO – Run 3 – Y1,3 frame

Figure H-3 Ratio of ductility demand to m-factors of Primary CP with the modified linear model.



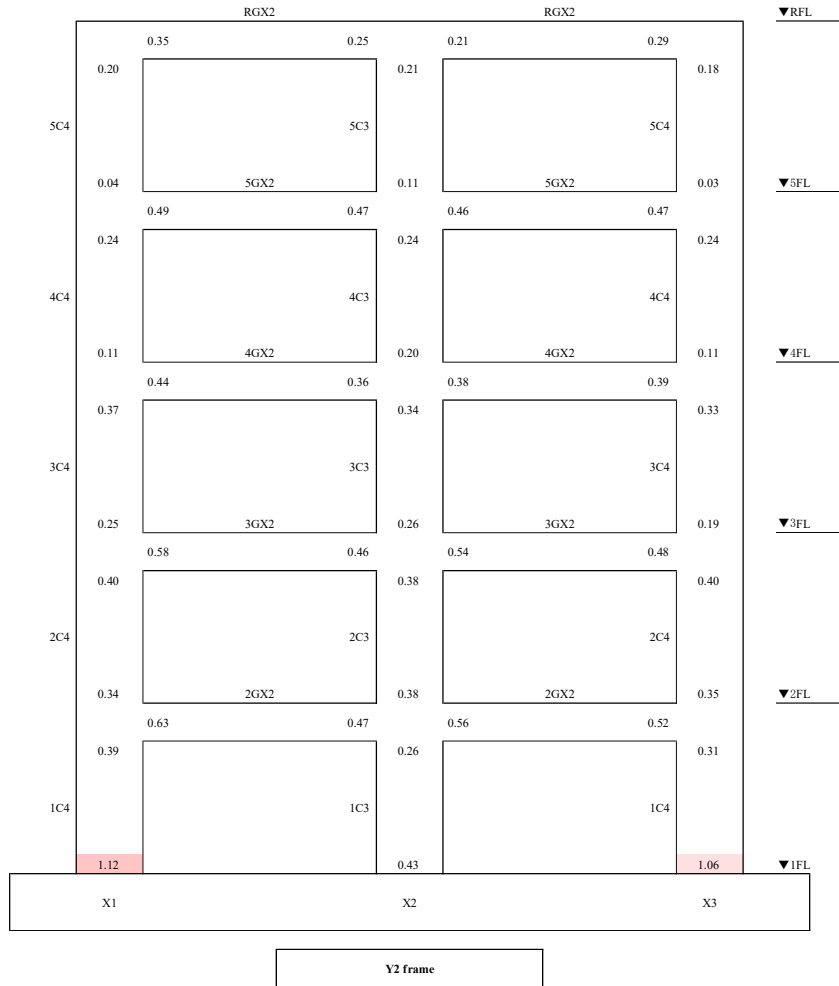
(a-2) IO – Run 3 – Y2 frame

Figure H-3 (cont) Ratio of ductility demand to m-factors of Primary CP with the modified linear model.



(b-1) CP – Run 3 – Y1,3 frame

Figure H-3 Ratio of ductility demand to m-factors of Primary CP with the modified linear model.

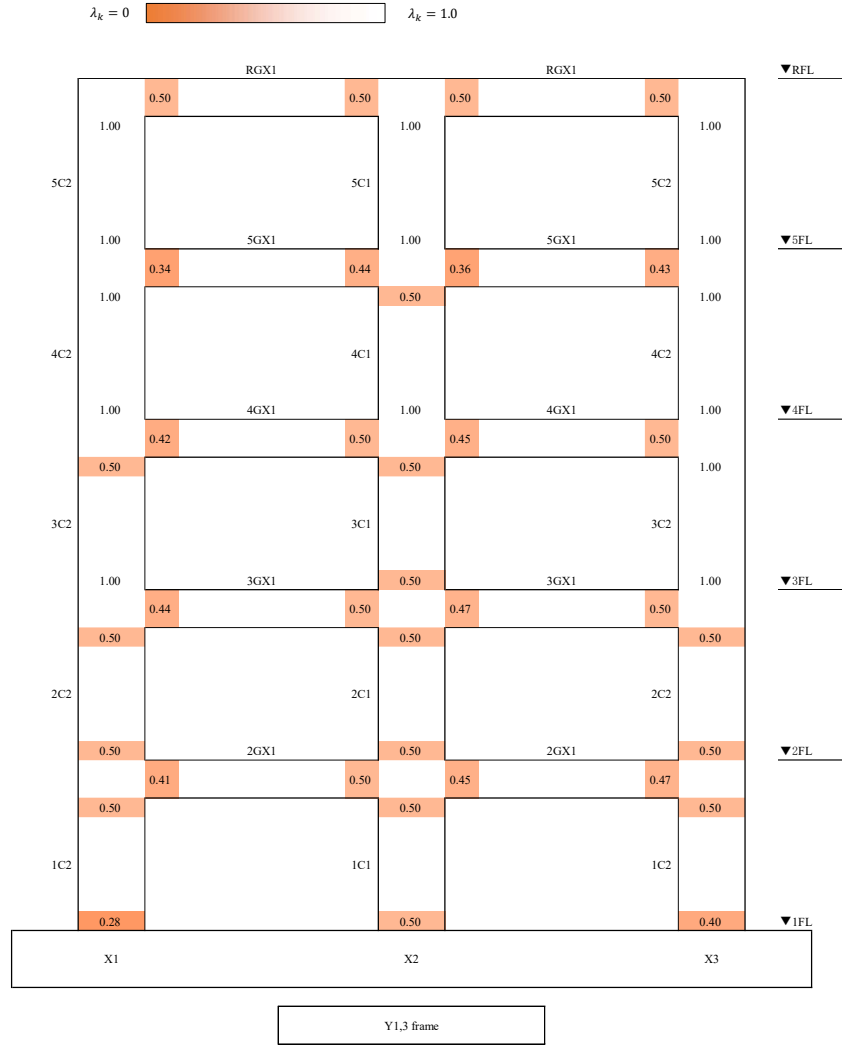


(b-2) CP – Run 3 – Y2 frame

Figure H-3 (cont) Ratio of ductility demand to m-factors of Primary CP with the modified linear model.

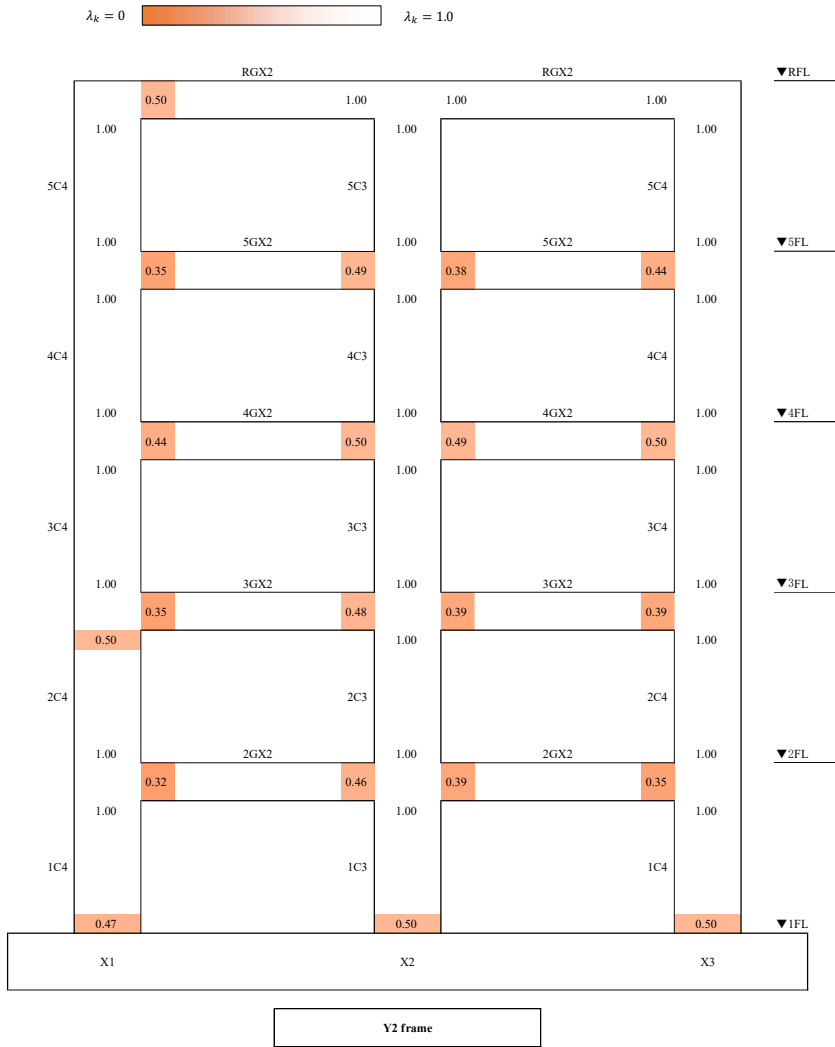
Stiffness Reduction Factors

This appendix indicates stiffness reduction factor for the original linear model in order to generate the modified linear model based on ductility demand in accordance with Figure 3-14. Figure I-1 shows stiffness reduction factors on each plastic hinge based on the ductility demand of Run 2, and these reduction factors were multiplied to the original linear model to obtain the modified linear model for the drift estimation of Run 3. Colored value represents factors less than 1.0.



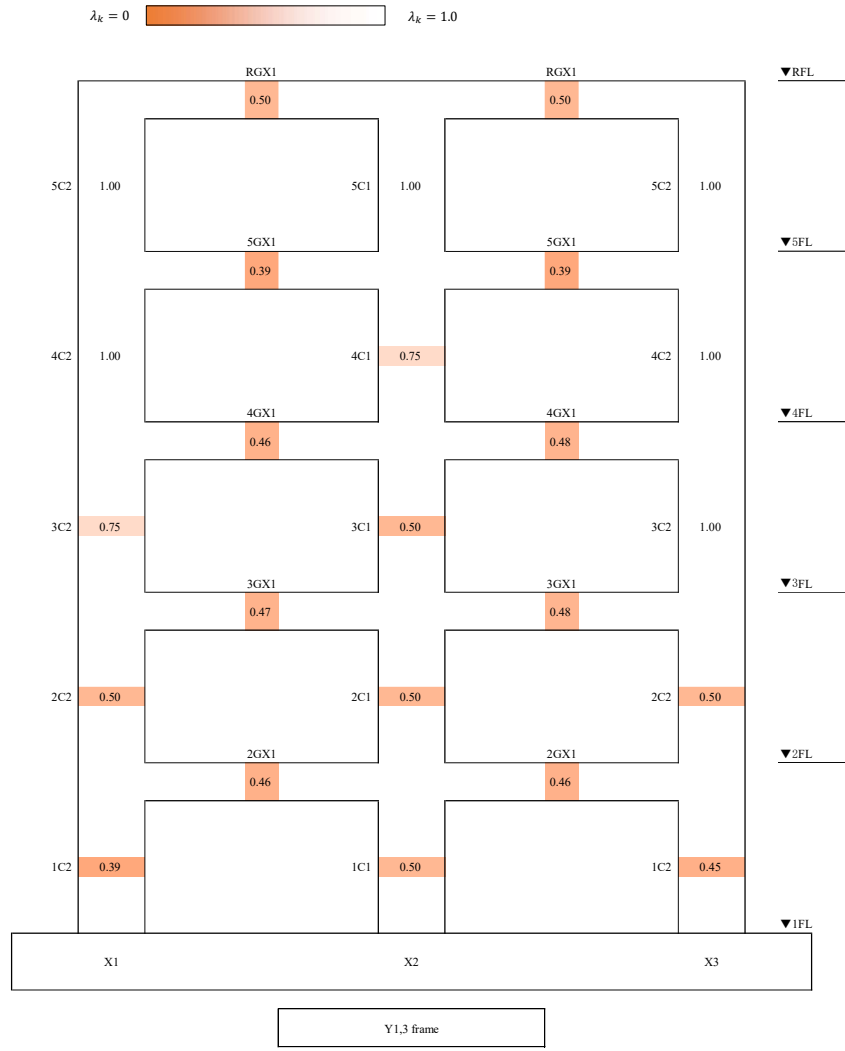
(a) Y1 frame

Figure I-1 Individual stiffness reduction factors on plastic hinges.



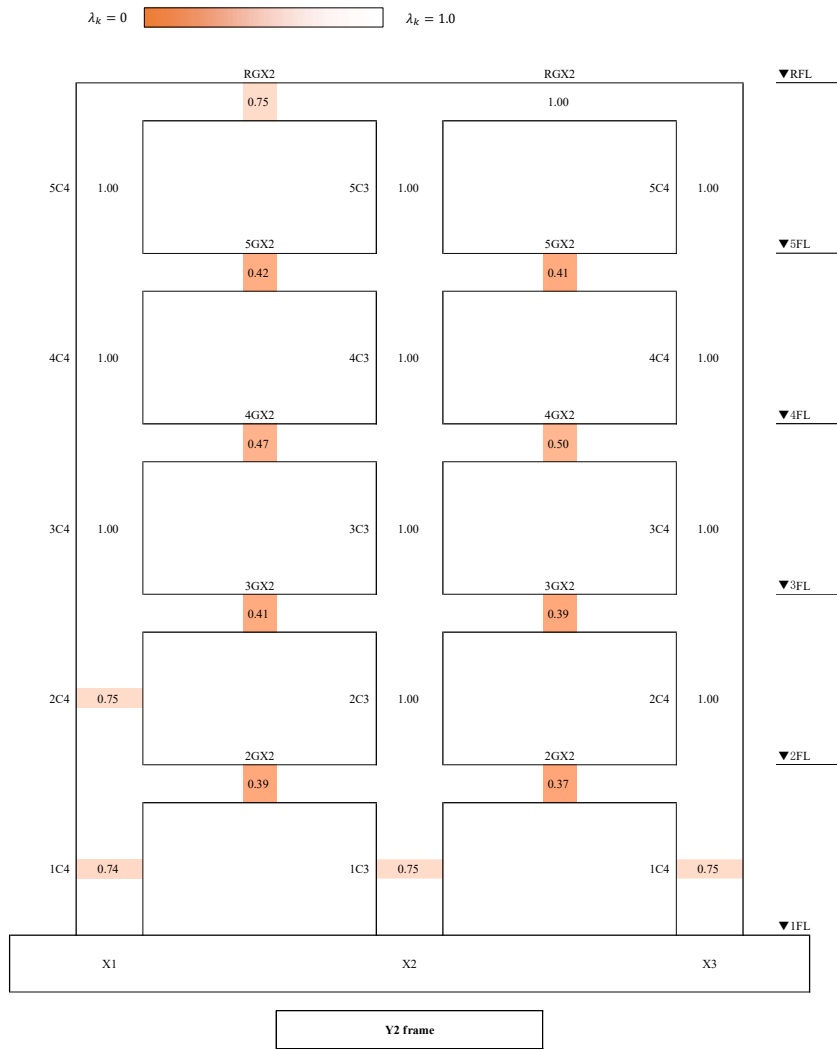
(b) Y2 frame

Figure I-1(cont) Individual stiffness reduction factors on plastic hinges



(a) Y1 frame

Figure I-2 Average stiffness reduction factors.



(b) Y2 frame

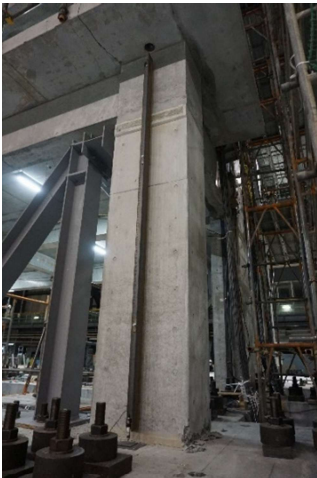
Figure I-2(cont) Average stiffness reduction factors.

Case Study 1

Appendix J

Visual Inspection After Run 4

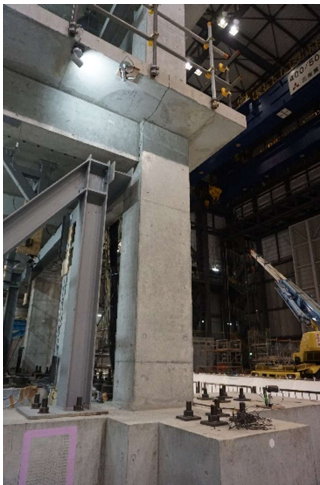
Figure J-1 shows the damage photos after Run 4.



Column 1F X3Y1



Column 1F X3Y1 (zoomed)

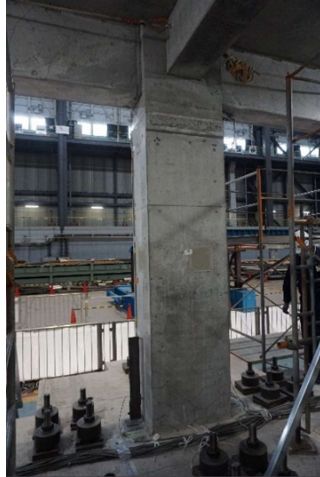


Column 1F X1Y3



Column 1F X1Y3 (zoomed)

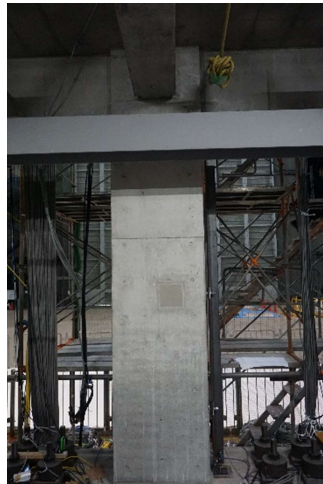
Figure J-1 Damage photos after Run 4.



Column 1F X2Y1



Column 1F X2Y1(zoomed)



Column 1F X3Y2



Column 1F X3Y2 (zoomed)



Column 2F X3Y3



Column 2F X3Y3 (zoomed)

Figure J-1(cont) Damage photos after Run 4.



Column 2F X2Y3



Column 2F X2Y3 (zoomed)



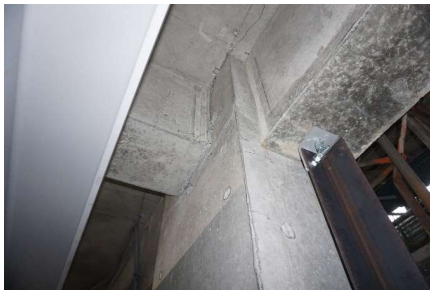
Column 2F X2Y3



Column 2F X2Y3 (zoomed)



Column 2F X3Y2



Column 2F X3Y2 (zoomed)

Figure J-1(cont) Damage photos after Run 4.



Column 2F X2Y2



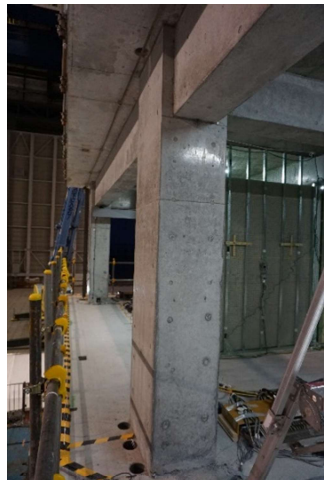
Column 2F X2Y2 (zoomed)



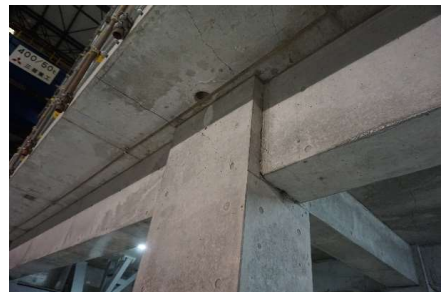
Column 2F X3Y1



Column 2F X3Y1 (zoomed)



Column 2F X2Y1



Column 2F X2Y1 (zoomed)

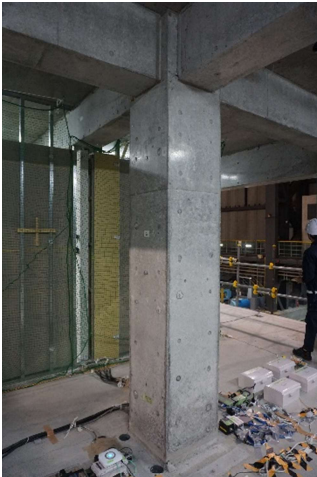
Figure J-1(cont) Damage photos after Run 4.



Column 2F X3Y2



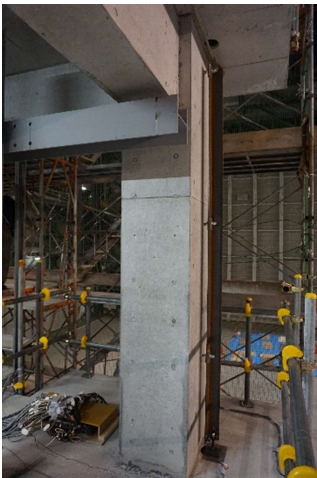
Column 2F X3Y2 (zoomed)



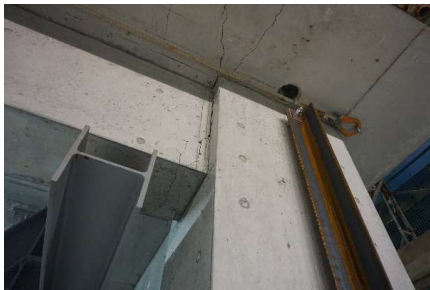
Column 2F X2Y2



Column 2F X2Y2 (zoomed)

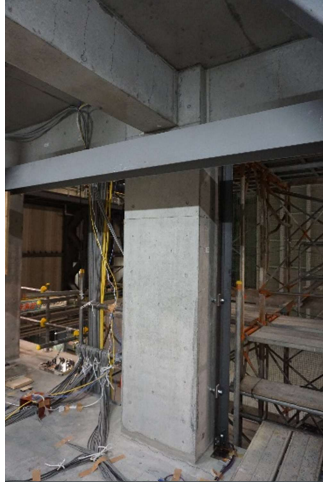


Column 3F X3Y1



Column 3F X3Y1 (zoomed)

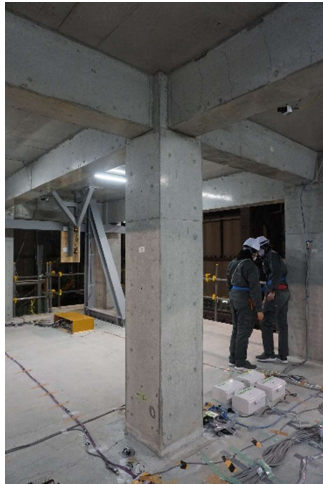
Figure J-1(cont) Damage photos after Run 4.



Column 3F X3Y2



Column 3F X3Y2 (zoomed)



Column 3F X2Y2



Column 3F X2Y2 (zoomed)

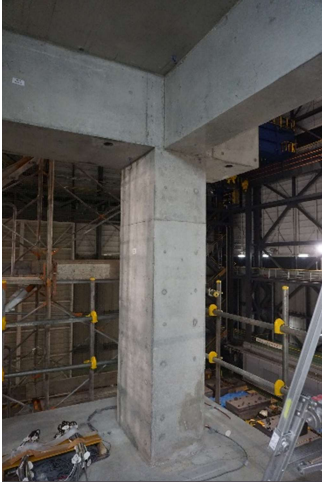


Column 3F X3Y1



Column 3F X3Y1 (zoomed)

Figure J-1(cont) Damage photos after Run 4.



Column 5F X3Y1



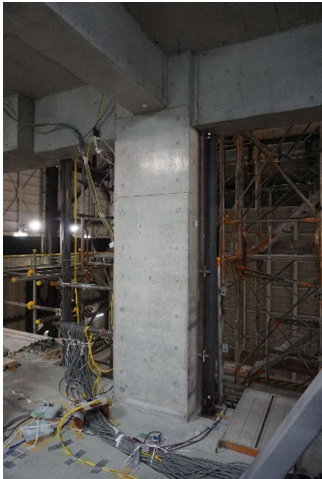
Column 5F X3Y1 (zoomed)



Column 5F X2Y1



Column 5F X2Y1 (zoomed)



Column 5F X2Y2



Column 5F X2Y2 (zoomed)

Figure J-1(cont) Damage photos after Run 4.

Case Study 1

Appendix K

Damping Identification

This section focuses on damping identification using the enhanced frequency domain decomposition (EFDD) method (Brincker et al., 2001). Viscous damping ratio was estimated with EFDD from the response of white noise excitation applied in between each Run (Figure K-1). A detailed procedure and modal estimation are presented the following sections.

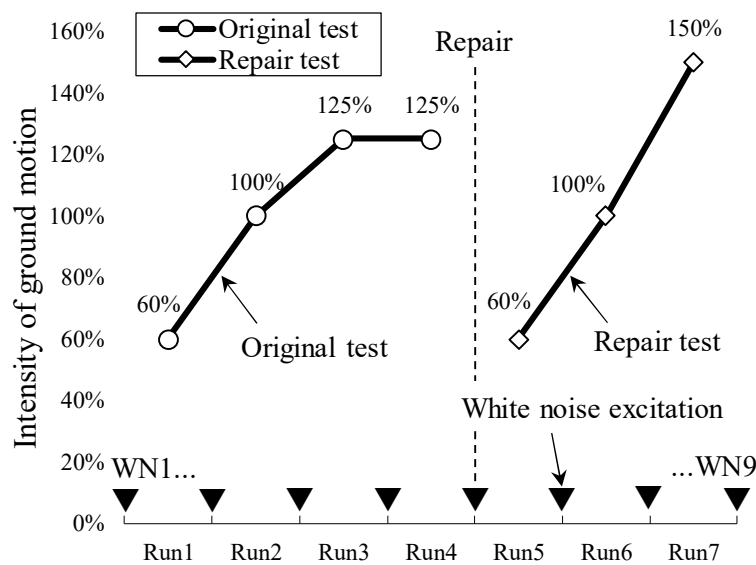


Figure K-1 White noise excitations.

K.1 Singular Value

Figure K-2 shows singular value plots. Singular value can be estimated from power spectrum density (PSD). In order to compute the damping ratio for the first mode, singular values corresponding to the first mode needs to be identified. The corresponding singular values of the first mode can be identified as the singular values around the first peak of the singular value plot. The identified singular value is called SDOF PSD bell function, and details are described in the following section.

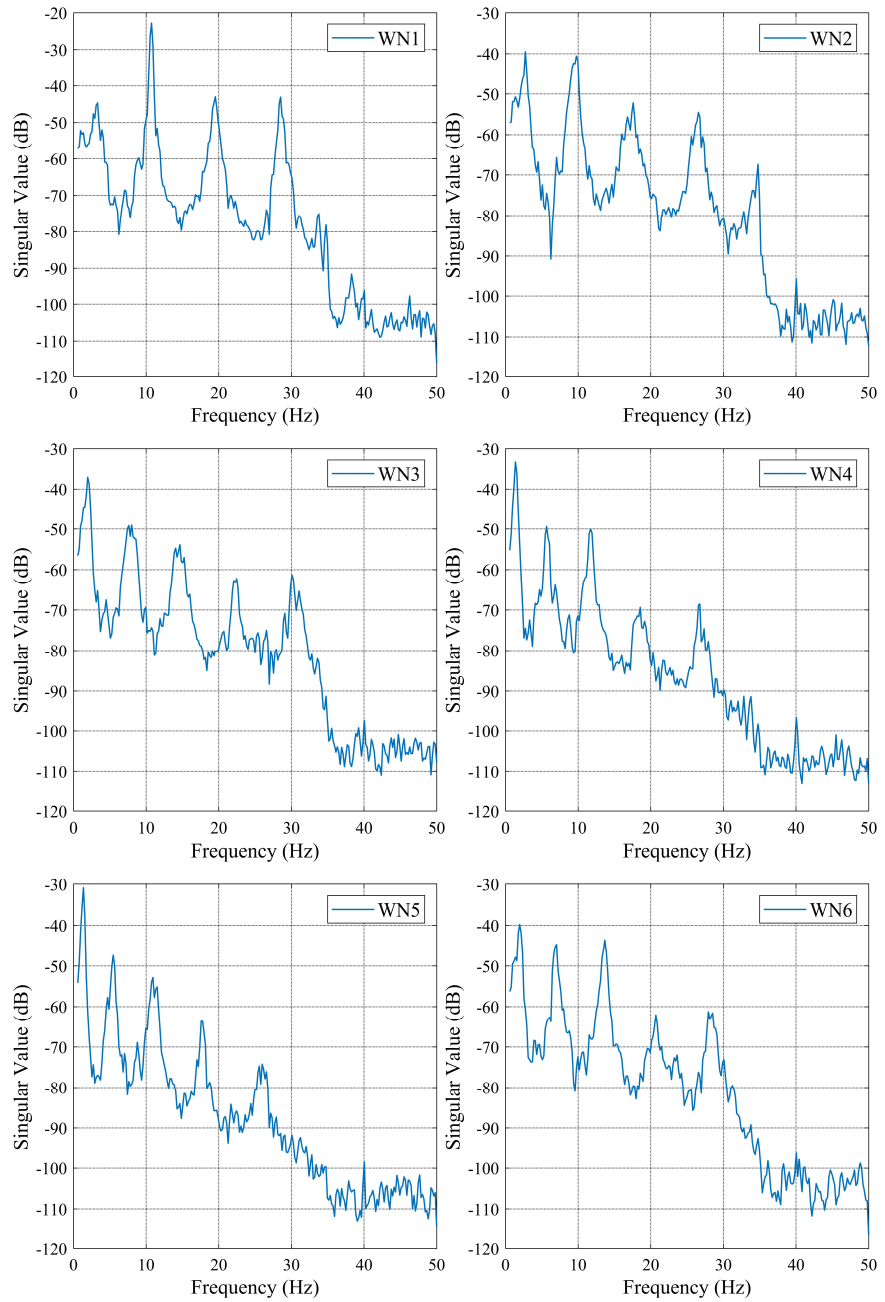


Figure K-2 Singular value plot.

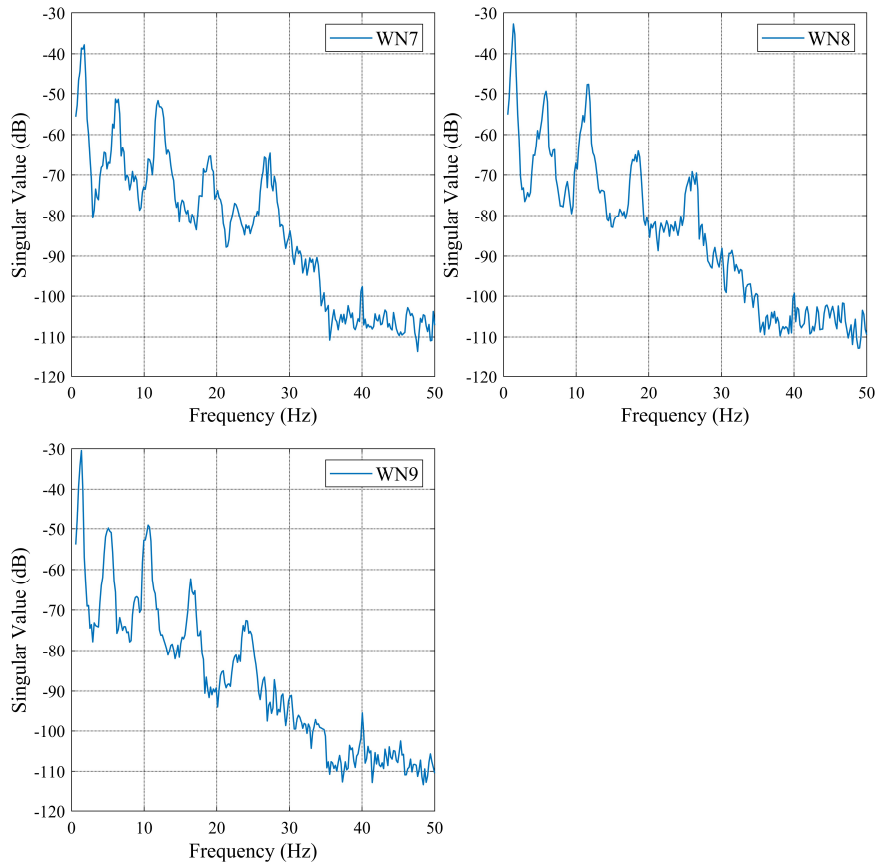


Figure K-2(cont) Singular value plot.

K.2 SDOF PSD Bell Function

The SDOF bell can be identified as a part of singular value plot using modal assurance criterion (MAC). MAC provides a similarity of two mode vectors so, singular values around the peak can be identified as SDOF PSD bell function. Figure K-3 shows SDOF PSD bell function on each white noise excitation. MAC is set as 0.8 herein.

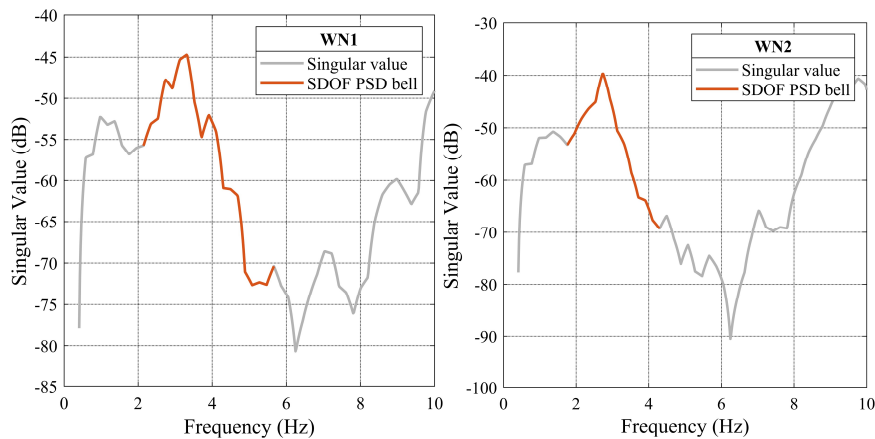


Figure K-3 SDOF PSD bell function.

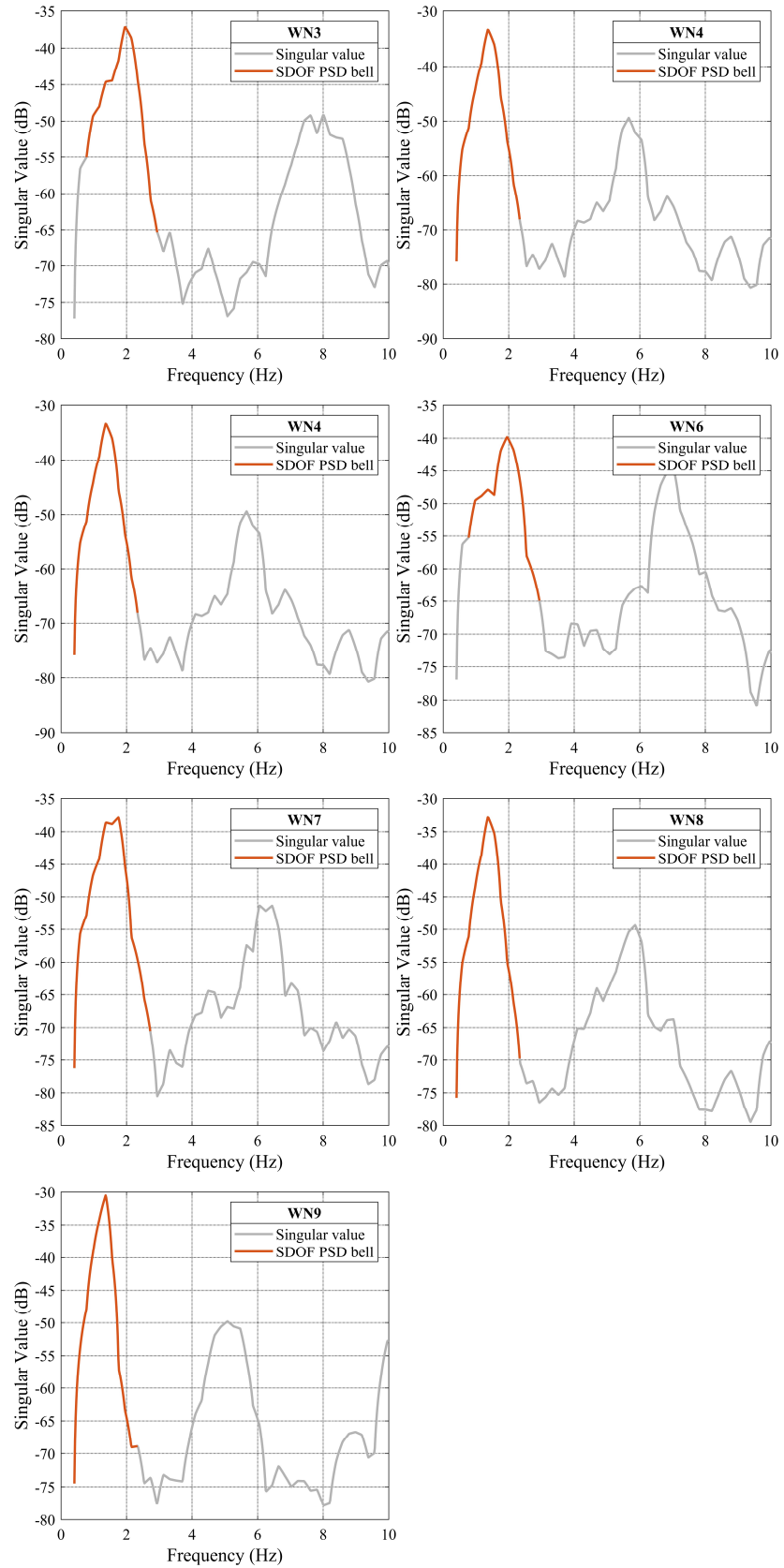


Figure K-3(cont) SDOF PSD bell function.

K.3 Correlation Function

The correlation function can be determined by taking back the SDOF PSD bell function to the time domain with inverse Fast Fourier Transform (IFFT). The correlation function is then normalized by the value at the first peak. The damping ratio can be identified by performing a logarithmic decrement technique to the correlation function. To obtain a logarithmic decrement ratio, linear regression was conducted on the relationship between peak number and $\ln(r_0/r_k)$.

$$\ln(r_0/r_k) = \delta \cdot k$$

Where r_0 : The first peak value, r_k : Correlation function at k th peak, k : Peak number, δ : Logarithmic decrement ratio.

Figure K-4 shows the result of the linear regression. Not only peaks are plotted in the figure, but also are troughs. Figure K-5 presents the normalized correlation function and estimated logarithmic decrement curve.

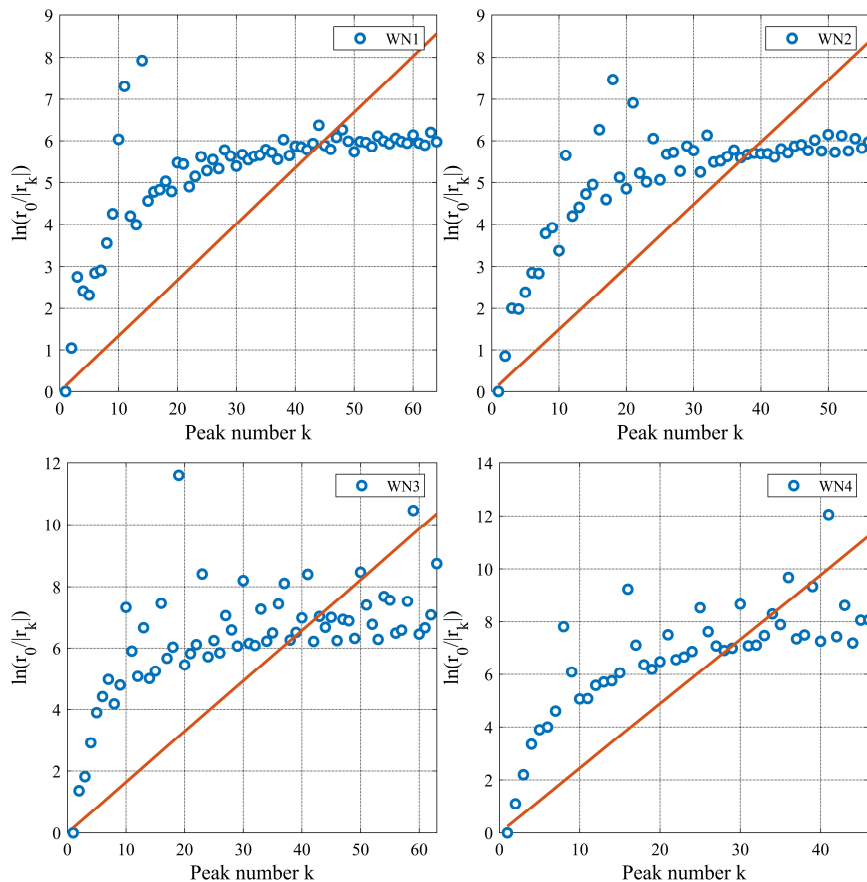


Figure K-4 Linear regression.

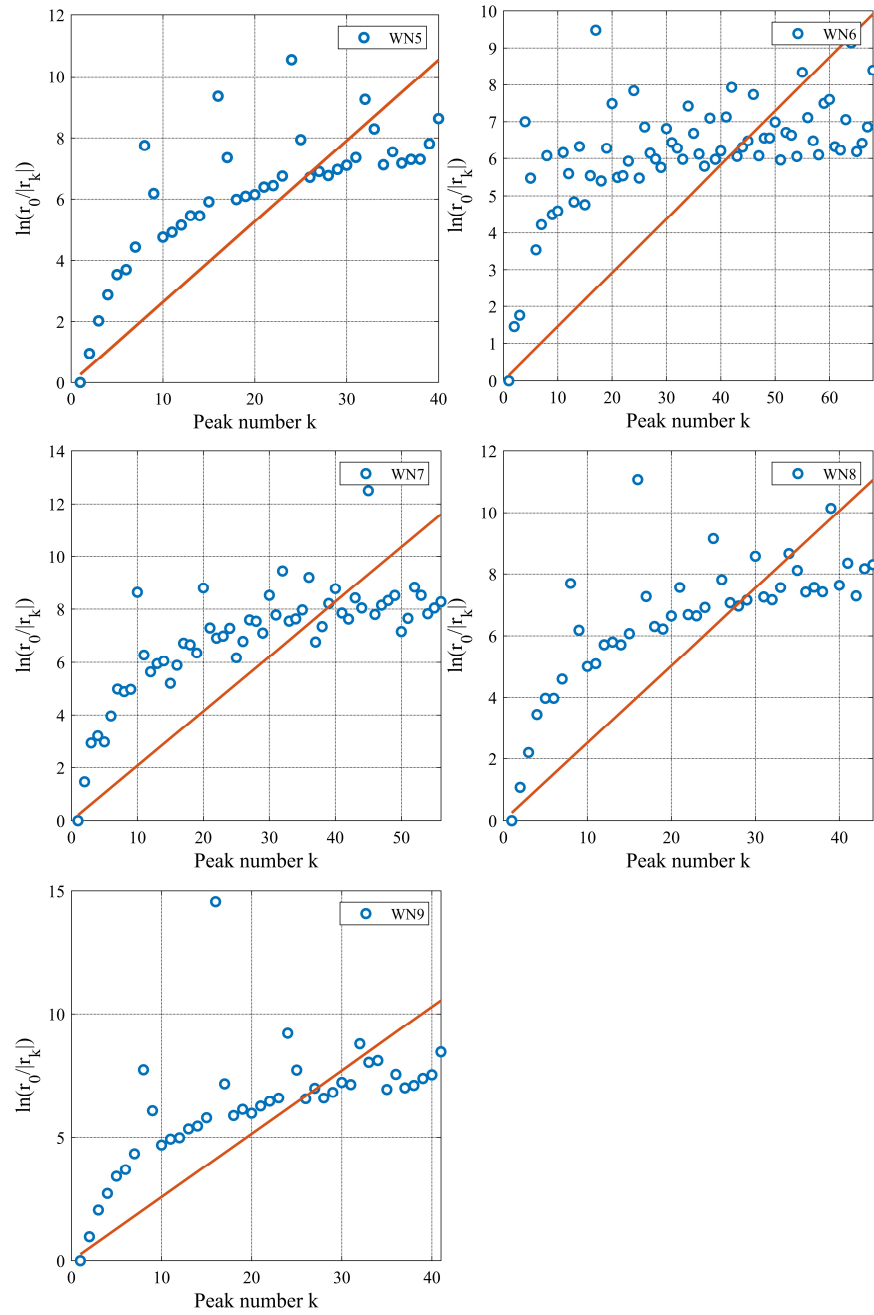


Figure K-4(cont) Linear regression.

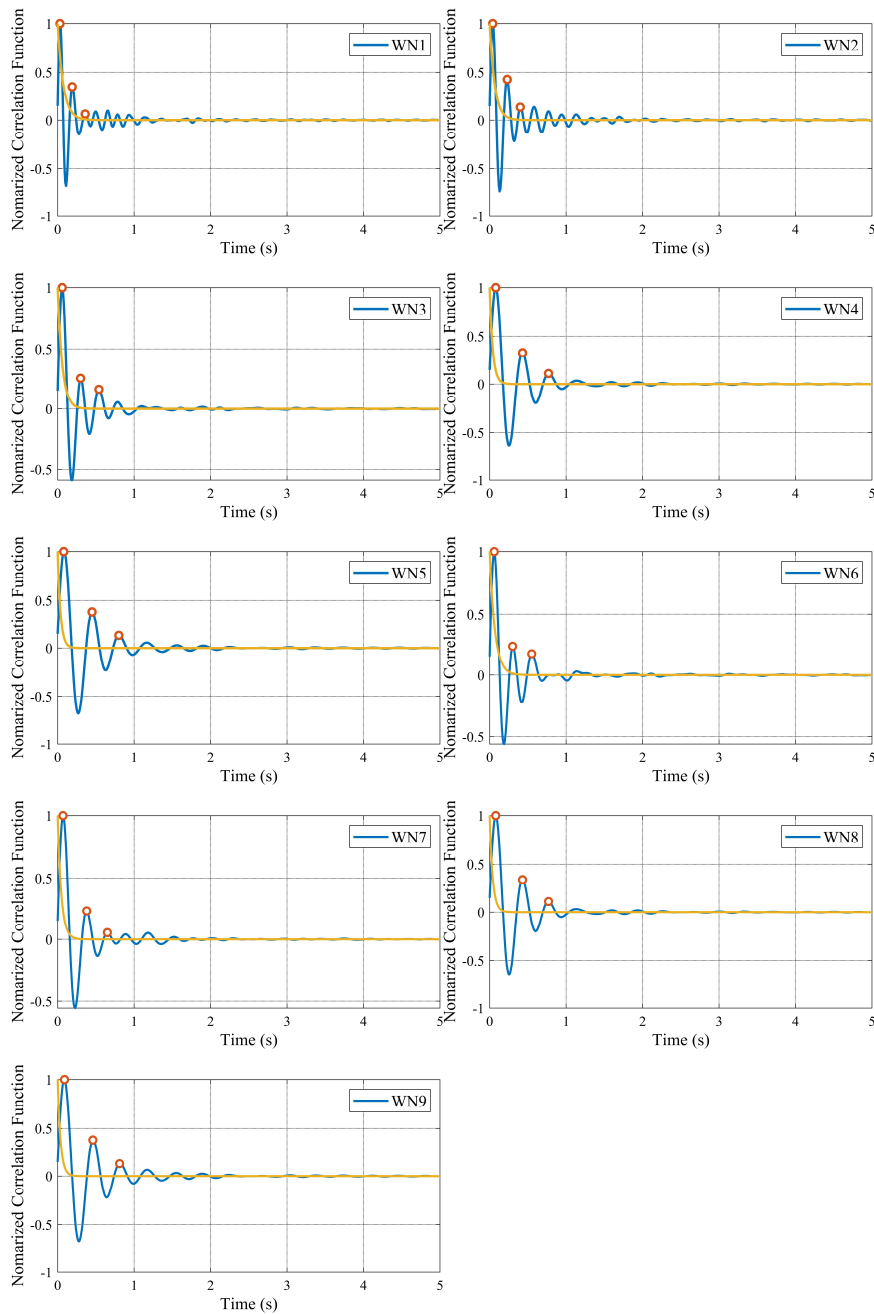


Figure K-5 Normalized correlation.

K.4 Damping Ratio

The relationship between the logarithmic decrement ratio and damping ratio is expressed as follows.

$$\zeta = \frac{\delta}{\sqrt{\delta^2 + (2\pi)^2}}$$

Figure K-7 shows a transition of the damping ratio with excitations and Figure K-7 shows damping ratio versus peak roof drift demand. The damping ratio of the intact structure was 2.0%, which is consistent with the recommendation in the ASCE/SEI 41 (ASCE, 2017) for a linear model. Damping ratio increased following the drift demand and reached 4% with Run 3 and Run 4. This result implies that a damping ratio of a structure damaged by design-level shaking is likely to be about 4%. Moreover, damping ratio after the repair was close to 2%, which indicates the damping ratio of a repaired structure was the same degree as that of an undamaged structure. In the repaired structure, damping ratio increased up to 4% again. Damping ratio increased more steeply than the original specimen as it was imposed higher drift demand at the same scaling of ground motion. In conclusion, damping ratio of undamaged structure can be assumed 2.0%, which is consistent with ASCE/SEI 41 (ASCE, 2017) recommendation. After repair, damping ratio of the repaired structure can be assumed 2.0% as well.

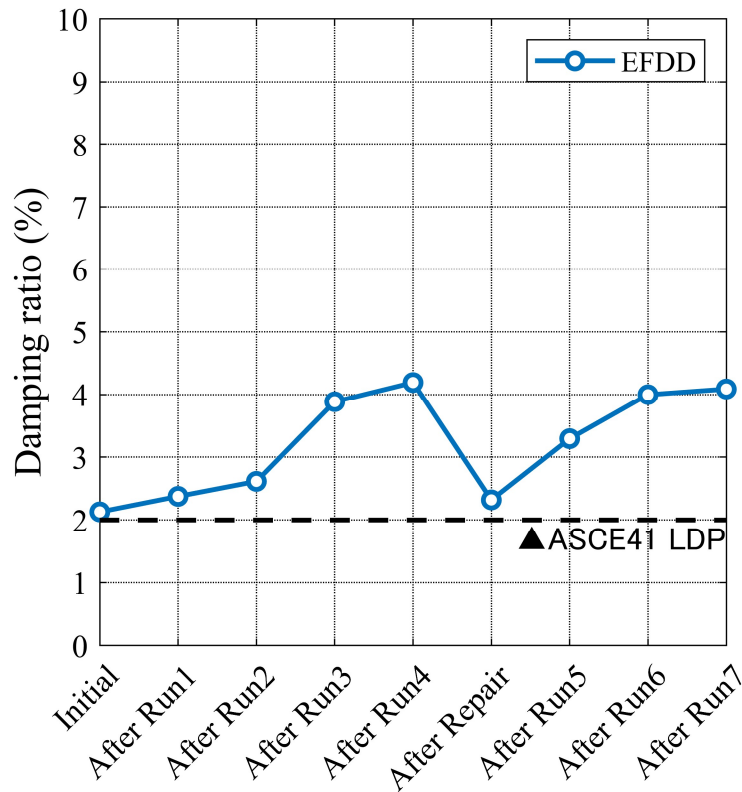


Figure K-6 Transition of damping ratio.

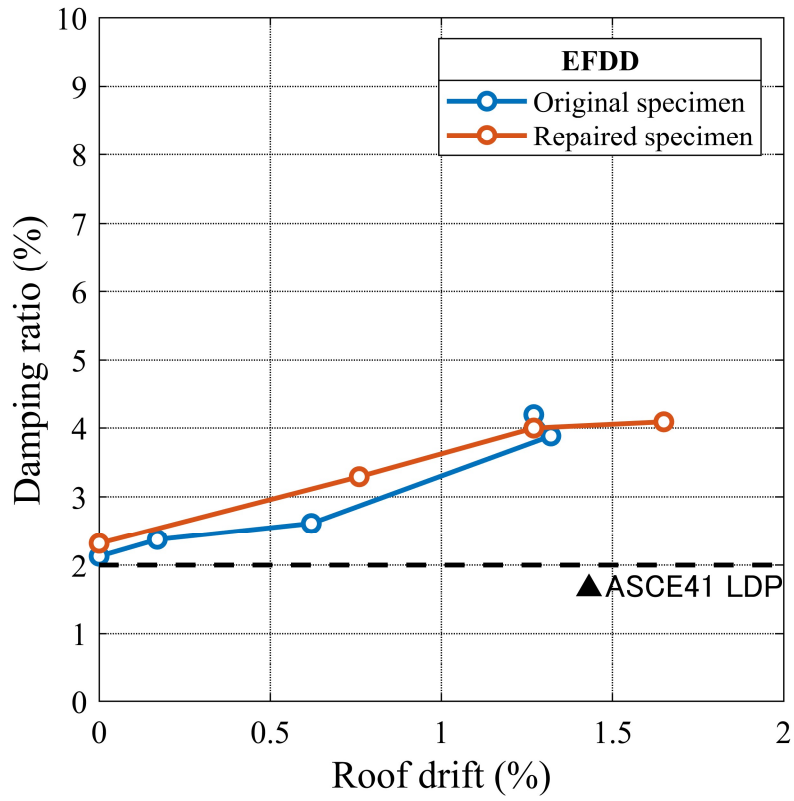


Figure K-7 Damping ratio and peak roof drift.

Alternative Approach of Inspection Locations

As shown in 3.2.1.3, a significant number of plastic hinges were flagged as ILs with a criterion of $DCR > 1.0$ in accordance with ATC-145-1 (ATC, 2020) recommendation. In this section, a new improved approach was proposed and investigated to find the reasonable number of damage locations using analysis.

A new Inspection Location approach proposed in this section sets two criteria below in addition to original approach of ATC-145-1 (ATC, 2020).

- $DCR > 1.0$ and $\delta_{EQ} > 1.0\%$
- $\mu/m_{IO} > 1.0$

Where: δ_{EQ} : Peak story drift, μ : Ductility demand, m_{IO} : m-factor at Immediate Occupancy.

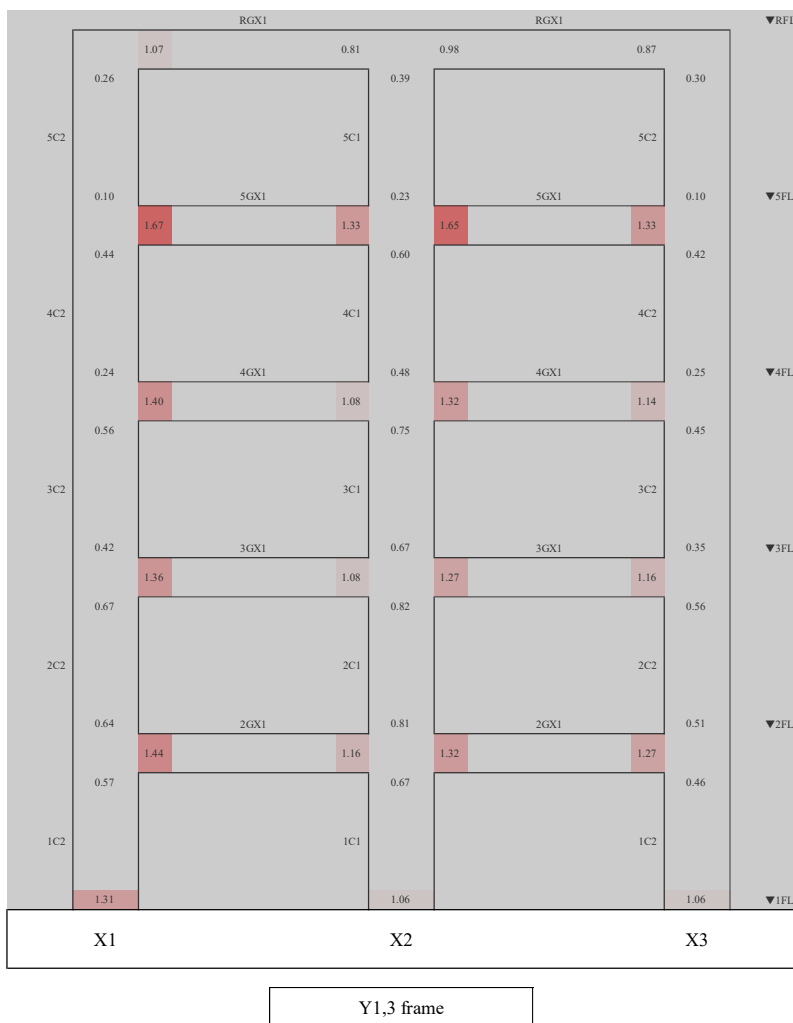
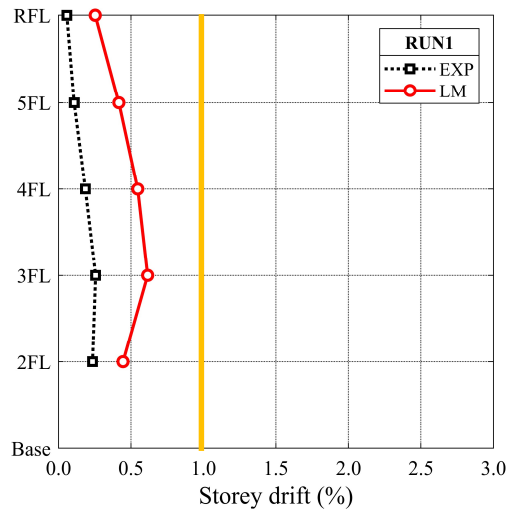
The first criterion is the combination of capacity check and deformation check. It is aimed to exclude beams and columns with low drift demands from ILs, as these ductile components are unlikely to be significantly damaged with the drift demand of lower than 1.0%.

The second criterion is based on ductility demand and expected ductility of selected performance objectives. As ductility demand less than ductility limit of IO can be considered not to associate any severe damages, m_{IO} is set as an IL trigger.

Figure L-1 shows DCRs of each component and exclusion by drift check of 1.0%. DCRs shown in the figure are estimated with the linear model for Run 1 and Run 2, and with the modified linear model for Run 3. Peak story drift plots also correspond to these cases and the analysis models. Shadowed areas in the figure represent the story drift estimated with analysis of less than 1.0% drift.

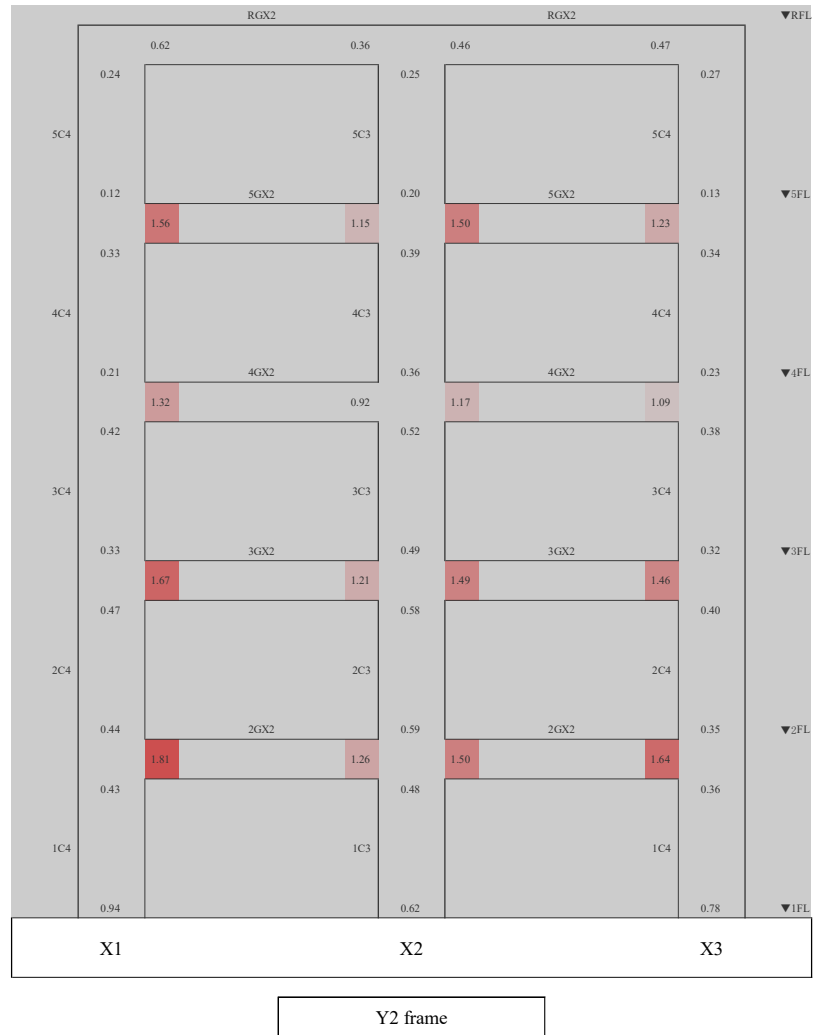
The ratio of ductility demand to the m-factors of IO of each member is shown in Figure H-6. Colored values represent the ratio of greater than 1.0.

As this diagram shows, it is obvious that columns are more likely to exceed the m-factors rather than beams.



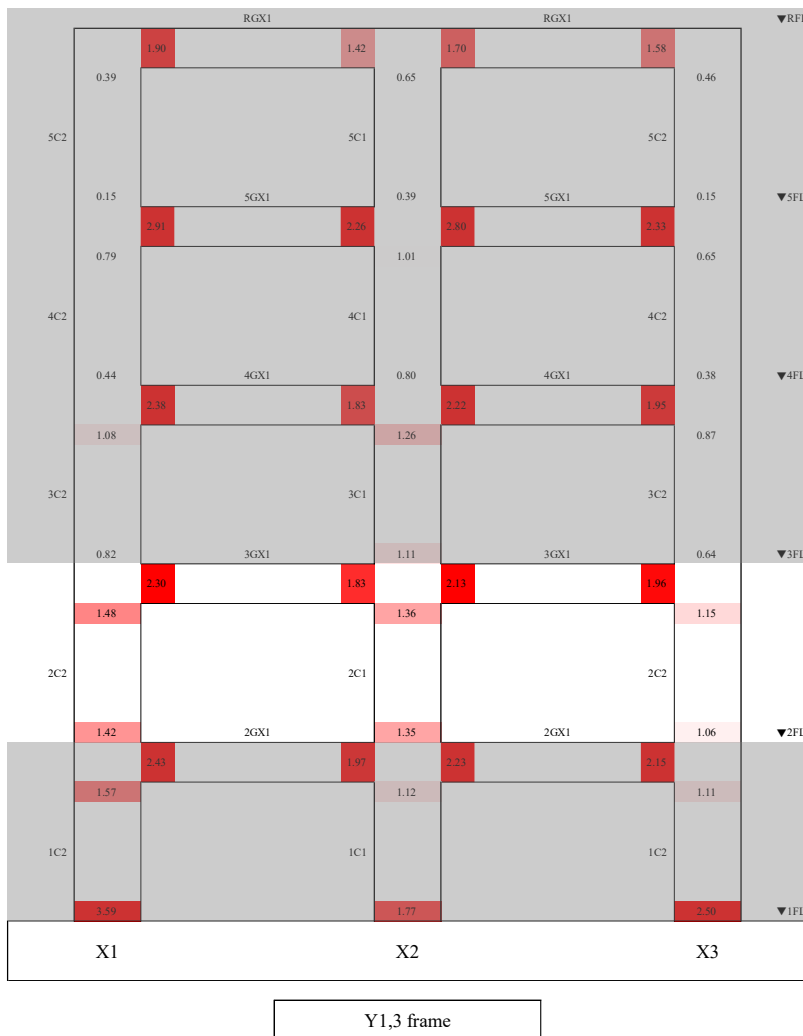
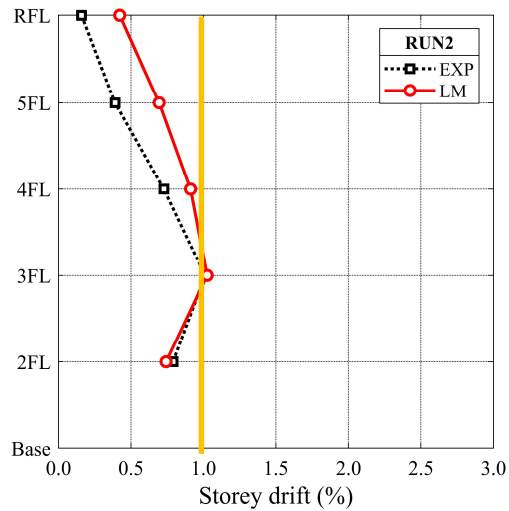
(a) Run 1 (LM)

Figure L-1 IL with drift criteria of 1.0%. Drift estimate with the linear model is shown for Run 1 and Run 2, and with the modified linear model for Run 3.



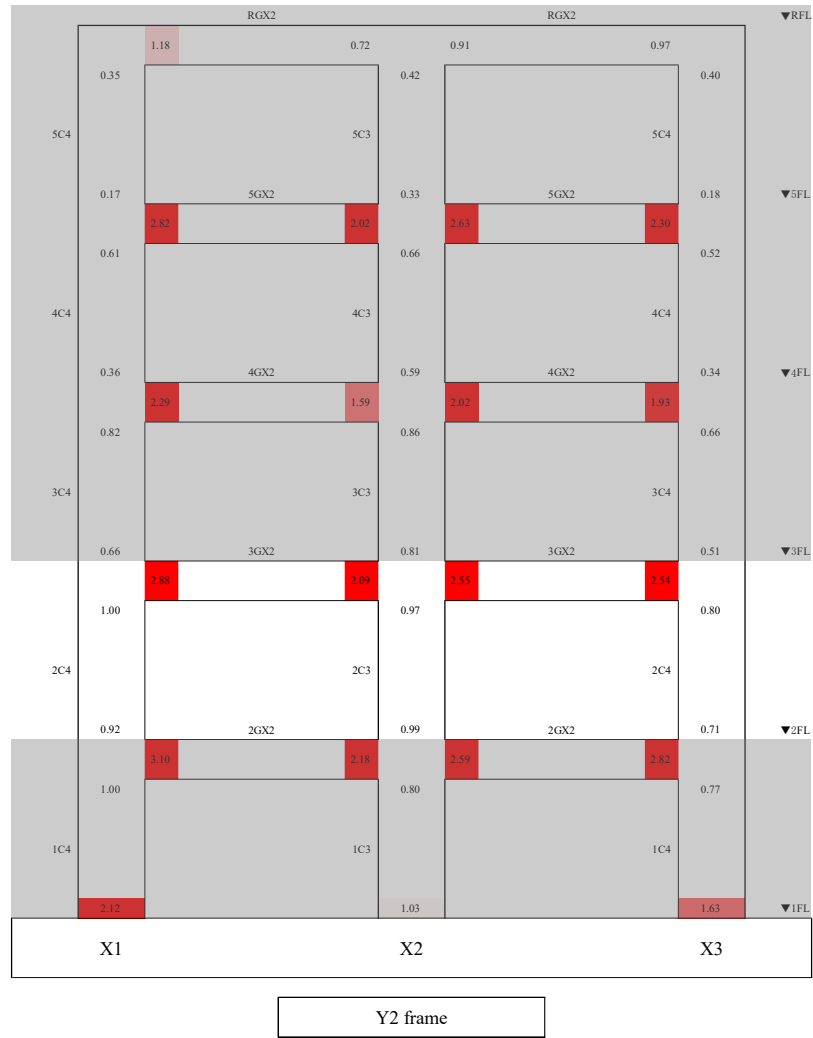
(a) Run 1 (LM)

Figure L-1(cont) IL with drift criteria of 1.0%. Drift estimate with the linear model is shown for Run 1 and Run 2, and with the modified linear model for Run 3.



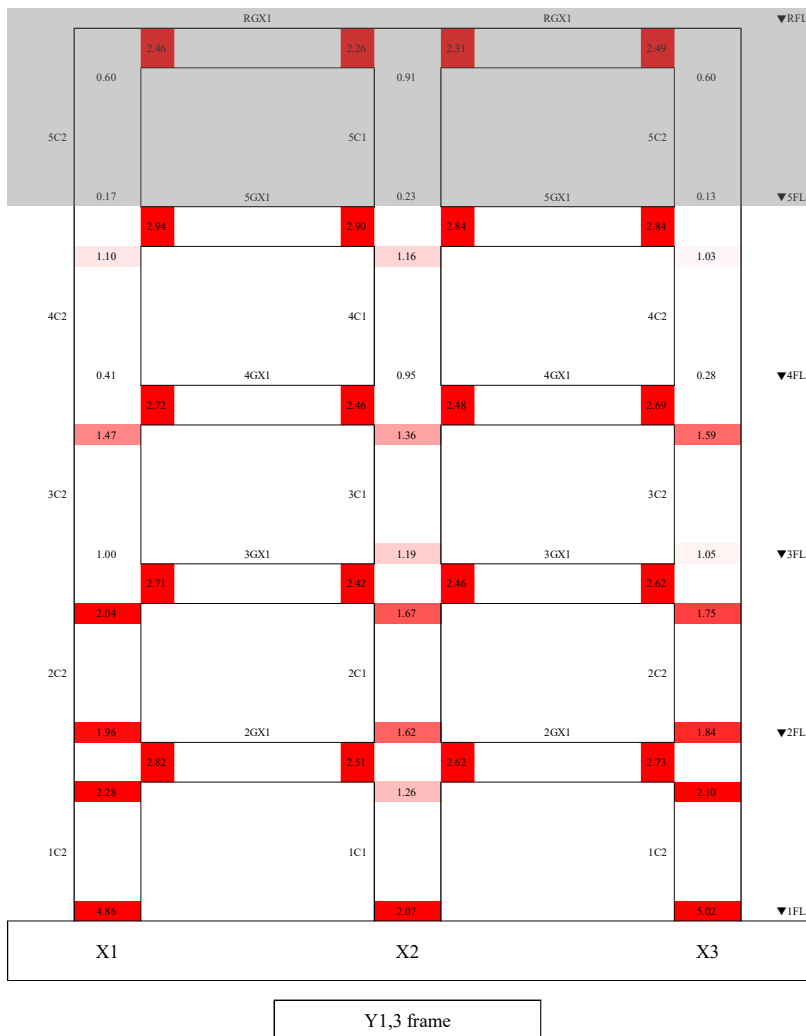
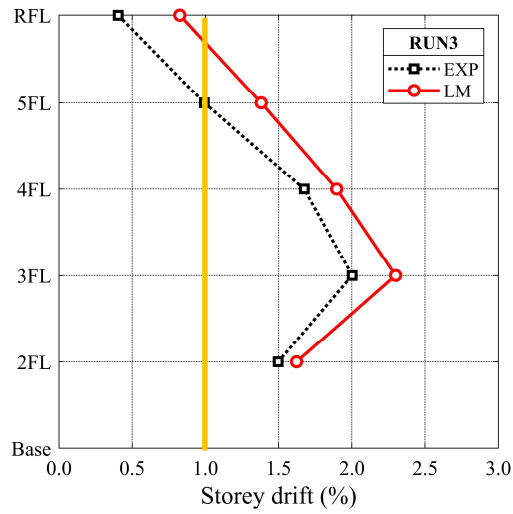
(b) Run 2 (LM)

Figure L-1(cont) IL with drift criteria of 1.0%. Drift estimate with the linear model is shown for Run 1 and Run 2, and with the modified linear model for Run 3.



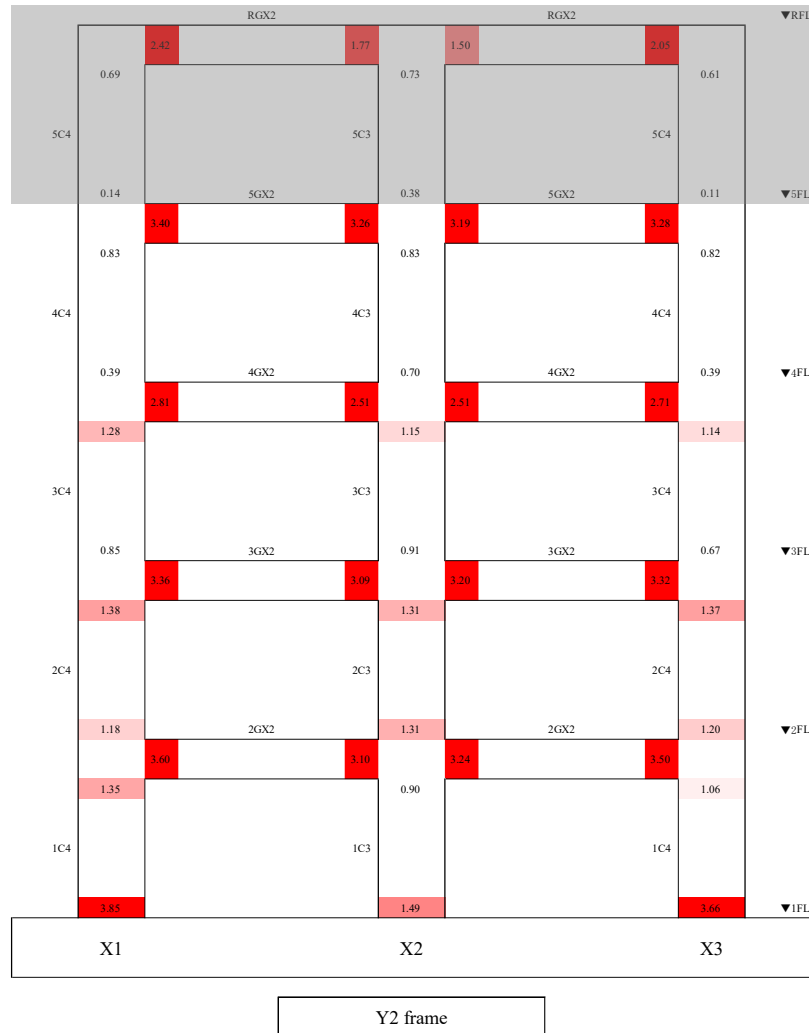
(b) Run 2 (LM)

Figure L-1(cont) IL with drift criteria of 1.0%. Drift estimate with the linear model is shown for Run 1 and Run 2, and with the modified linear model for Run 3.



(c) Run 3 (MLM)

Figure L-1(cont) IL with drift criteria of 1.0%. Drift estimate with the linear model is shown for Run 1 and Run 2, and with the modified linear model for Run 3.



(c) Run 3 (MLM)

Figure L-1(cont) IL with drift criteria of 1.0%. Drift estimate with the linear model is shown for Run 1 and Run 2, and with the modified linear model for Run 3.

Table L-1 shows the number of Inspection Locations estimated with visual inspection and both the linear and modified linear models. The linear model was used to estimate the Inspection Locations in Run 1 and Run 2, and the modified linear model was used for Run 3, since these models well simulated peak story drift demand of the test. Based on the visual inspection, all the hinges were classified into 3 categories, DS0, DS0.5 and DS1 or greater. DS0 represents essentially no damage, which indicate no cracks was observed in the visual inspection. DS1 and Damage States greater than DS1 were defined in accordance with FEMA P-58 Fragility Specification (FEMA, 2019) as applied in section 3.1.1. DS0.5 was introduced as an intermediate Damage State between DS0 and DS1 to fill the gap since there includes a

wide range of damages between “no damage (median drift = 0%)” and “crack width of 1.5 mm (median drift = 2.0%)”. DS0.5 was applied if a component exhibits crack width of 1.5 mm or less (i.e., a component was damaged but not as much damaged as DS1).

Comparing the number of ILs in Run 1 between ATC-145 original and the alternate approaches, while a significant number of ILs was flagged with the ATC-145 original approach, none of them was flagged using the alternate approach. This result was probably consistent with visual inspection results, as no significant damages were observed even in Run 2 (i.e., Damage State of Run 1 was inferred equal to or less than that of Run 2). In a comparison of Run 2, a large number of locations were excluded from ATC-145 original approach results using the alternate approach. Especially, reduction of beams was noticeable, and columns were hardly excluded with the alternate approach. Comparing these analytical estimations to visual inspection results, both the original ATC-145 approach and the alternate approach showed similar numbers to the number of DS0.5. In this case, the ATC-145 original approach provides a close number to the number of DS0.5. In Run 3, a few beams and columns were excluded with the alternate approach, comparing to ATC-145 original approach. Both the ATC-145 original and the alternate approaches exhibited a similar number to that was classified into DS0.5. These results indicate that the alternate approach are able to exclude reasonable number of Inspection Location with story drift criterion of 1.0% as shown in Run 1 and Run 2, and a few beams and columns were excluded in Run 3 with the alternate approach. Also, the number of Inspection Location of beams can be reduced using ratio of ductility demand to m-factor (IO). Moreover, regardless of these approaches, estimated number of locations were typically close to the number of DS0.5.

Table L-1 Compares the Number ILs with Conventional Criterion per ATC-145-1 (ATC, 2020) and the Alternate Criteria Proposed in this Section. Table L-1 The Number of Inspection Locations with an Alternate Approach.

		Total No. of hinges	Visual Inspection			ATC-145 approach	Proposed alternate approach
Criteria			$DS0^{*2}$	$DS0.5^{*3}$	$\geq DS1$	$DCR > 1.0$	$[DCR > 1.0 \ \& \ \delta_{tQ} > 1.0\%]$ or $[\mu/m_{IO} > 1.0]$
Run 1 (LM)	Beam	60	-*1	-*1	-*1	47 (78%)	0 (0%)
	Column	90	-*1	-*1	-*1	6 (7%)	0 (0%)
	Total	150	-*1	-*1	-*1	53 (35%)	0 (0%)
Run 2 (LM)	Beam	60	8 (13%)	52 (87%)	0 (0%)	57 (95%)	12 (20%)
	Column	90	43 (48%)	47 (52%)	0 (0%)	18 (20%)	19 (21%)
	Total	150	51 (34%)	99 (66%)	0 (0%)	75 (50%)	31 (21%)
Run 3 (MLM)	Beam	60	1 (2%)	48 (80%)	11 (18%)	57 (95%)	48 (80%)
	Column	90	33 (37%)	57 (63%)	0 (0%)	51 (57%)	40 (44%)
	Total	150	34 (23%)	105 (70%)	11 (7%)	108 (72%)	88 (59%)

*1 Visual inspection was not performed in Run 1. m_{IO} : m-factor at Immediate Occupancy (IO)

*2 Damage State 0 (DS0) was defined as no damage, which indicate no cracks was observed.

*3 Damage State 0.5 (DS0.5) was defined by crack width of 1.5 mm or less.

Case Study 1

Appendix M

FEMA P-58 Fragility Database

This appendix provides a source of damage definitions per FEMA P-58 fragility database. Figure M-1 shows fragility specifications of ACI 318-conforming concrete Special Moment Frame (SMF) structures.

FEMA P-58 Fragility Specification

NISTIR Classification	B1041.002a				Line 104
NISTIR Name	ACI 318 SMF , Conc Col & Bm = 24" x 36", Beam one side				
Description	ACI318 Concrete SMF, ductile response. Meets the requirements of ACI318 SMF. Costing is on a per joint basis.				
Construction Quality:	Not Specified				
Seismic Installation Conditions:	Not Specified				
Fragility Unit of Measure:	EA 1				
Demand Parameter (unit):	Story Drift Ratio		Unit less		
Number of Damage States:	4				
Damage State:	DS1	DS2	DS3	DS4	
Type of Damage State:	Sequential	Sequential	Mutually Exclusive	Mutually Exclusive	
DS Hierarchy	Seq(DS1,DS2,MutEx(DS3,DS4))				
Descriptions	Beams or joints exhibit residual crack widths > 0.06 in. No significant spalling. No fracture or buckling of reinforcing.	Beams or joints exhibit residual crack widths > 0.06 in. Spalling of cover concrete exposes beam and joint transverse reinforcement but not longitudinal reinforcement. No fracture or buckling of reinforcing.	Beams or joints exhibit residual crack widths > 0.06 in. Spalling of cover concrete exposes a significant length of beam longitudinal reinforcement. Crushing of core concrete may occur. Fracture or buckling of reinforcing requiring replacement may occur.	Beams or joints exhibit residual crack widths > 0.06 in. Spalling of cover concrete exposes beam and joint transverse reinforcement but not longitudinal reinforcement. No fracture or buckling of reinforcing.	
Illustrations					
Damage State Probability:	1.00	1.00	0.80	0.20	
Fragility Parameters					
Median Demand, θ:	0.02	0.0275	0.05	0.05	
Data dispersion, β_d:	Not Specified	0.28	0.15	0.28	
Uncertainty, β_u:	0.4	0.1	0.25	0.1	
Total Dispersion, β:	0.4	0.3	0.3	0.3	
Correlation (Yes / No)	NO				
Directionality (Yes / No)	YES				
Consequence Functions	Data Quality Average		Documentation Quality Superior		
Repair Description	Data Relevance Average		Rationality Superior		
Repair Description	Remove furnishings, ceilings and mechanical, electrical and plumbing systems (as necessary) 8 feet either side of damaged area. Clean area adjacent to the damaged concrete. Prepare spalled concrete and adjacent cracks, as necessary, to be patched and to receive the epoxy injection. Patch concrete with grout. Replace and repair finishes. Replace furnishings, ceilings and mechanical, electrical and plumbing systems as necessary.	Remove furnishings, ceilings and mechanical, electrical and plumbing systems (as necessary) 15 feet either side of damaged area. Shore damaged member(s) a min one level below (more levels may be required). Remove damaged concrete at least 1 inch beyond the exposed reinforcing steel. Place concrete forms. Place concrete. Remove forms. Remove shores after one week. Replace and repair finishes. Replace furnishings, ceilings and mechanical, electrical and plumbing systems (as necessary).	Remove furnishings, ceilings and mechanical, electrical and plumbing systems (as necessary) 15 feet either side of damaged component. Shore damaged member(s) a minimum of one level below (more levels may be required). Remove damaged component. Place and splice (as necessary) new reinforcing steel to existing, undamaged reinforcing. Place concrete forms. Place concrete. Remove forms. Remove shores after one week. Replace and repair finishes. Replace furnishings, ceilings and mechanical, electrical and plumbing systems (as necessary).	Remove furnishings, ceilings and mechanical, electrical and plumbing systems (as necessary) 15 feet either side of damaged area. Shore damaged member(s) a min one level below (more levels may be required). Remove damaged concrete at least 1 inch beyond the exposed reinforcing steel. Place concrete forms. Place concrete. Remove forms. Remove shores after one week. Replace and repair finishes. Replace furnishings, ceilings and mechanical, electrical and plumbing systems (as necessary).	

Figure M-1 FEMA-P58 Fragility Specification for ACI 318-conforming concrete SMF (ACI, 2014).

Case Study 1

References

- ACI, 2014, *Building Code Requirements for Structural Concrete and Commentary*, ACI 318-14, ACI Committee 318, American Concrete Institute, Farmington Hills, Michigan.
- AIJ, 2010, *AIJ Standard for Structural Calculation of Reinforced Concrete Structures Revised*, Architectural Institute of Japan, Tokyo, Japan.
- ASCE, 2017, *Seismic Evaluation and Retrofit of Existing Buildings*, ASCE/SEI 41-17, American Society of Civil Engineers, Reston, Virginia.
- ATC, 2000, *Database on Performance of Structures near Strong-motion recordings: 1994 Northridge California Earthquake*, ATC-38, Applied Technology Council, Redwood City, California.
- ATC, 2020, *Resilient Repair Guide Source Report*, ATC-145-1, Applied Technology Council, Redwood City, California.
- Brincker, R., Zhang, L., and Andersen P., 2001, “Modal identification of output-only systems using frequency domain decomposition”, *Smart Materials and Structures*, Vol. 10, No. 3, pp. 441–445.
- Brown, J. & Kunnath, S. K., 2000, *Low-Cycle Fatigue Behavior of Longitudinal Reinforcement in Reinforced Concrete Bridge Columns*, Technical Report MCEER-00-0007, p. 126.
- Endo M., Tatsuo, Mitsunaga, Koichi; Takahashi, Kiyohum; Kobayashi, Kakuichi; Matsuishi, 1974, “Damage evaluation of metals for random or varying loading-three aspects of rain flow method”, *Mechanical Behavior of Materials*, Vol. 1, pp. 371–380.
- FEMA, 2007, *Interim Testing Protocols for Determining the Seismic Performance Characteristics of Structural and Nonstructural Components*, FEMA 461, prepared by the Applied Technology Council for the Federal Emergency Management Agency, Washington, D.C.

FEMA, 2019, *Provided Fragility Data: Fragility Specification*, FEMA P-58-3.2, prepared by the Applied Technology Council for the Federal Emergency Management Agency, Washington, D.C.

Marder, K. J., 2018, *Post-Earthquake Residual Capacity of Reinforced Concrete Plastic Hinges*, The University of Auckland, Auckland, New Zealand.

Standards New Zealand, 2004, *2002 Structural Design Actions Part 5: Earthquake Actions*, NZS 1170.5, Standards New Zealand, Wellington, New Zealand.

USGS, *The Modified Mercalli Intensity Scale*, United States Geographical Survey, https://www.usgs.gov/natural-hazards/earthquake-hazards/science/modified-mercalli-intensity-scale?qt-science_center_objects=0#qt-science_center_objects.

As outlined in the ATC-145-1 Source Report (ATC, 2020), a case study for a real-world code-conforming special concrete moment frame building was undertaken to test and refine the proposed assessment process, in particular, refinement of the Inspection and Analysis phase to verify that the level of effort is commensurate with the objective of estimating the peak deformation demands and identifying any severe damage states. This report presents the approach, findings, and recommendations from the case study.

1.1 Summary

An eight-story reinforced concrete moment frame building located in Wellington, New Zealand was subjected to the 2016 Kaikoura earthquake. The building reportedly sustained moderate structural damage. Through linear analysis, the building drift demand estimates due to the 2016 Kaikoura were 1.3% to 2%. The moment frames generally exhibited strong-column/weak-beam response, with typical beam ductility demands in the damaged bays ranging from 3 to 5.5. No ground motion data was available at the building site, and demands were estimated by applying the response spectra from the two nearest strong ground motion recording stations with similar soil classification.

Fragility curves were used to infer drift demands based upon the observed damage at each beam-column joint. As identified by Case Study 1, modification of the FEMA P-58 concrete moment frame fragility curve was recommended. The curve was modified by adding DS 0.5 (See Section 4.1.7) to fill the gap between “no observed damage” (0% drift) and DS 1 (2% drift). This modified approach gave drift estimates that were in reasonable agreement with those estimated by analysis and overall damage patterns observed by inspection.

Similar to Case Study 1, the estimated ductility demands by analysis on individual components (beams and columns) suggested more extensive damage than was observed by inspection, particularly on the longitudinal frames. This resulted in a conservative number of Inspection Locations. The ductility demands indicated that many of the beams were between the

Immediate Occupancy and primary Life Safety acceptance criteria per ASCE/SEI 41.

Further modification of the Inspection Location triggers was developed to ensure that components with relatively high strength DCR's (i.e., ductility demand) but low story drifts (i.e., < 1%) were not missed from the visual inspection scope. However, this led to exclusion of beam elements that had undergone moderate ductility demands in the relatively stiff first floor. To correct this, a check for ductility demand, relative to the ASCE/SEI 41 Immediate Occupancy acceptance criteria was added as an additional criterion for the modified inspection criteria.

The building satisfied the safety-assessment checks, with the exception of the fatigue damage screening detailed in the body of the Source Report. However, using the Appendix C simplified approach to estimate fatigue life reduction, the components were determined to meet the safety criteria.

Serviceability drift demands on the damaged frames increased by 50 to 100%, based on the reduced frame stiffness accounting for estimated ductility demand on each component. This was primarily influenced by the extensive beam hinging. The damaged building did not satisfy the NZS 1170.5 serviceability drift limit of 0.5%; however, it should be noted that the building did not satisfy this limit in the pre-damage condition and it was unlikely to have been a requirement at the time of the building's design and construction.

Epoxy injection was estimated to reduce the maximum serviceability drifts by 25 to 40%, to approximately 0.8% story drift. This was approximately 25% higher than the pre-damage condition. As the undamaged building did not satisfy the 0.5% drift limit prescribed by the current loading standard, epoxy injection alone was insufficient to achieve compliance. Thus, more complex repair or strengthening measures are required if the building is to satisfy the serviceability drift limit.

There was limited opportunity to test the use of non-structural damage to infer drift demand due to the small number of published interior observations. Based on limited documentation of partition damage and FEMA P-58 fragility functions, drifts at the center of building were estimated in the range of 0.7 to 1.0%. This was slightly lower than the drift demands estimated by analysis

Case Study 2

Chapter 2

Building Description

The case study building was an eight-story reinforced concrete structure with hollow core precast floors and approximately three inch thick concrete topping, designed in 2004-2005. The current loading standard at that time was the New Zealand Standard 4203: 1992. The primary lateral system consisted of special concrete moment frames located around the perimeter of the building. An interior line of gravity moment frames also provides support to the precast floors. The building was founded on reinforced concrete belled piles. The building was a stand-alone structure, sufficiently set back from adjacent structures such that pounding was unlikely to be a design consideration.

The building was reportedly designed for a system ductility (μ) of 6 (Aurecon, 2017), as permitted by the New Zealand Concrete Structures Standard, NZS 3101. This typically results in relatively flexible buildings that will undergo significant deformation (2 to 2.5% story drift) during a design basis earthquake. Structural and nonstructural damage may also be evident at lower levels of ground shaking intensity, due to the inherently flexible structural response.

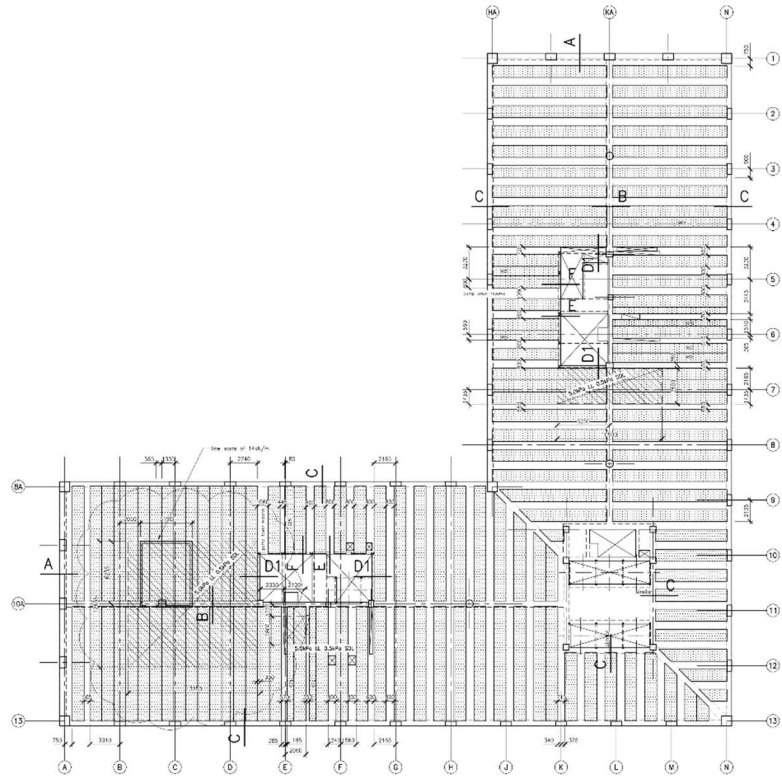


Figure 2-1 Typical floor plan.



Figure 2-2 Isometric View (Google Maps, location details redacted).



(a) Pre-2016 Kaikoura Earthquake



(b) Pre-2016 Kaikoura Earthquake,
during demolition

Figure 2-3 Exterior Elevations (Google Street View).

Case Study 2

Chapter 3

Seismic Event

The 2016 Kaikoura earthquake is the Damaging Earthquake for the case study.

3.1 Ground Motion Recording Sources

Ground motion recordings were taken from local stations, Wellington Thorndon Fire Station (TFSS) and Wellington Victoria University Law School (VUWS), shown in Figure 3-1. These stations were selected based on their proximity to the project site and similarity in soil class. The SRSS response spectra developed from the data recorded at TFSS and VUWS are presented in Figure 3-2. The elastic response spectrum likely used for the original design per NZS 4203: 1992 is also plotted. Per section 4.1.3, the building's fundamental translational periods in each principal direction are both approximately 1.4 seconds.

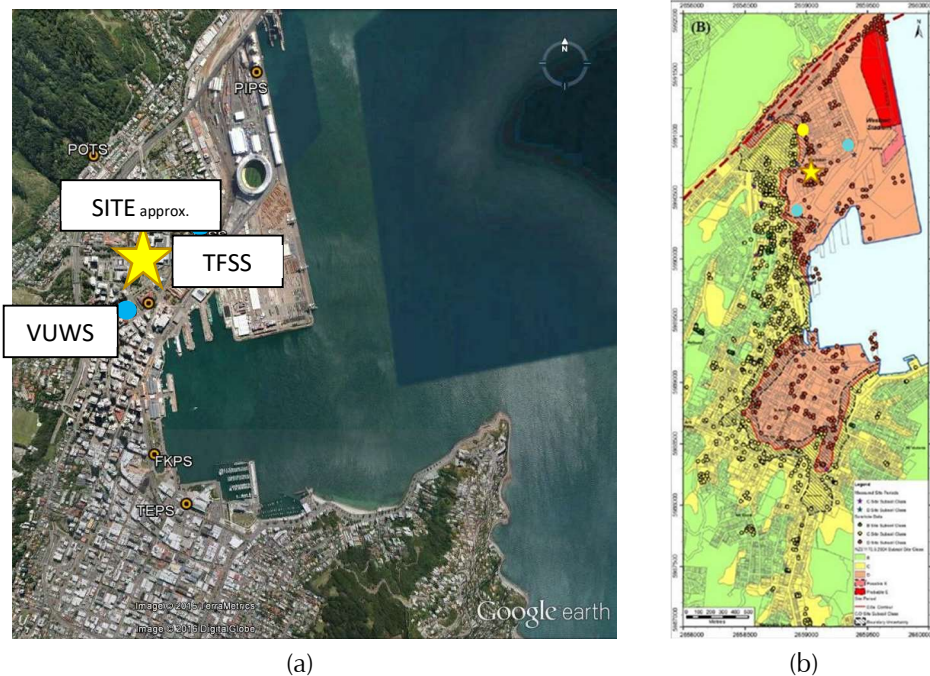


Figure 3-1 (a) Station location map and (b) soil classification map (Semmens, et. al., 2004).

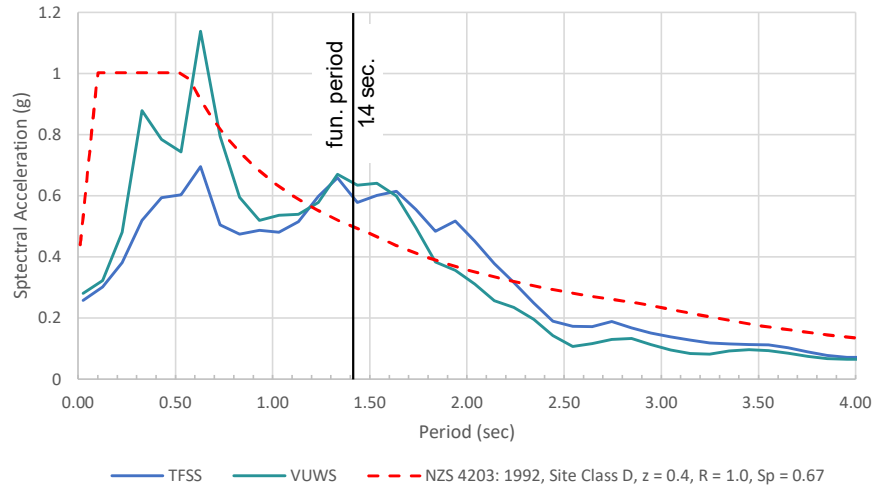


Figure 3-2 Local station spectra (SRSS).

Case Study 2

Chapter 4

Inspection and Analysis Phase

4.1 Preliminary Inspection

A preliminary inspection was conducted by The Inspecting Engineer and documented in the 2017 Damage Report (Aurecon, 2017).

4.1.1 Visual Observation

The Damage Report describes conditions found during a preliminary visual inspection. According to The Inspecting Engineer:

“The structural damage observed in our initial limited visual inspections suggested that the structure of the building had performed as designed and had potentially started to deform. The visible signs of this deformation include the cracking of the concrete which forms the beams and columns. The damage observed was mainly confined to the shorter West and North 4 bay frames. Based on the observations in our limited visual inspection, there is the potential that the reinforcement in the beams at [address redacted] appear to have yielded and further investigations are required...Our inspections have established that damage has occurred on the longer frames at the perimeter of the building away from the damaged end frames. Cracking in the plastic hinge regions of the beams has been noted along Grid 8A and Grid HA and to a lesser extent along Grid 13 and Grid N.”

4.1.2 ATC-38 Form

The ATC-38 form allows an inspecting engineer to evaluate the level of damage experienced after an earthquake. A completed form for the case study building is provided in Appendix A The form is dependent on the ATC-13 (ATC, 1985) methodology which provides a simple approach for determining the level of damage and repair needed after a seismic event given a Modified Mercalli Intensity (MMI). Given an MMI of VI for the site during the Kaikoura earthquake per Dellow, et. al. (Dellow, et al., 2017) and

the Damage Probability Matrix (Table 4-1), the mean damage factor is calculated as follows:

$$MDF_{VI} = \sum_{DS=1}^7 P_{DS}^{VI} * CDF_{DS} = \overline{P}^{VI} \cdot \overline{CDF} = 21.5\% \quad (4-1)$$

where,

MDF_{VI} : mean damage factor given MMI of VI

P_{DS}^{VI} : probability of a single damage state given a MMI of VI per Damage Probability Matrix

CDF_{DS} : central damage factor for a single damage state per Damage Probability Matrix

$$\overline{P}^{VI} = (95, 3, 1.5, 0.4, 0.1, 0, 0)$$

$$\overline{CDF} = (0, 0.5, 5, 20, 45, 80, 100)\%$$

Table 4-1 Damage Probability Matrix (Table 2.1 of ATC-13 (ATC, 1985))

Damage State	Damage Factor Range (%)	Central Damage Factor (%)	Probability of Damage in Percent By MMI and Damage State						
			VI	VII	VIII	IX	X	XI	XII
1 - NONE	0	0	95	49	30	14	3	1	0.4
2 - SLIGHT	0 - 1	0.5	3	38	40	30	10	3	0.6
3 - LIGHT	1 - 10	5	1.5	8	16	24	30	10	1
4 - MODERATE	10 - 30	20	0.4	2	8	16	26	30	3
5 - HEAVY	30 - 60	45	0.1	1.5	3	10	18	30	18
6 - MAJOR	60 - 100	80	-	1	2	4	10	18	39
7 - DESTROYED	100	100	-	0.5	1	2	3	8	38

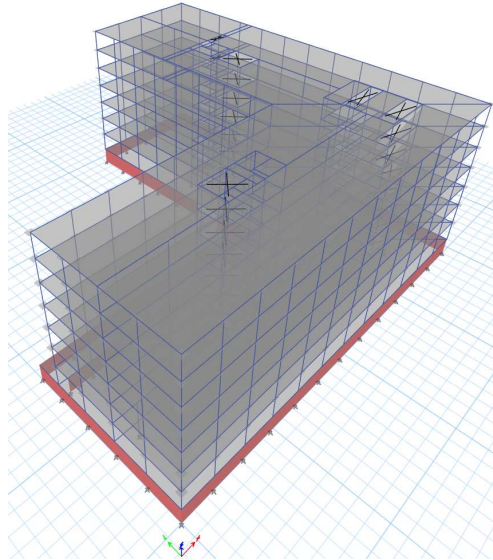
The following definitions can be used as a guideline:

- 1 - NONE: No damage.
- 2 - SLIGHT: Limited localized minor damage not requiring repair.
- 3 - LIGHT: Significant localized damage of some components generally not requiring repair.
- 4 - MODERATE: Significant localized damage of many components warranting repair.
- 5 - HEAVY: Extensive damage requiring major repairs.
- 6 - MAJOR: Major widespread damage that may result in the facility being razed, demolished, or repaired.
- 7 - DESTROYED: Total destruction of the majority of the facility.

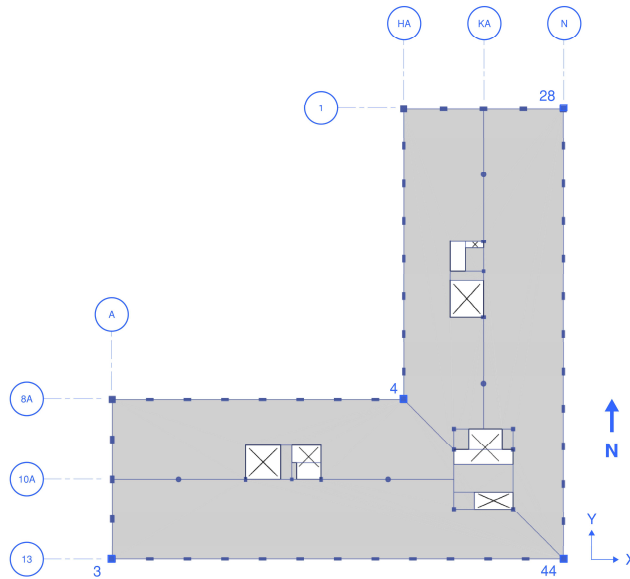
Per Equation 3-1 and the Damage Factor Range shown in Table 4-1, the damage state associated with the given MMI is Moderate. See definition above.

4.1.3 Linear Model

A three-dimensional analysis model was created using ETABS (CSI, 2020) software released by Computers and Structures, Inc. The model was used to run a linear dynamic procedure (LDP) for drift demand estimation during the Damaging Earthquake and identify potential locations where significant damage states may occur. A three-dimensional view and plan are provided in Table 4-1. The first three eigen periods are provided in Table 4-2 below. 5% damping was applied to the model.



(a) 3D ETABS model



(b) model plan view

Figure 4-1 Building model

Table 4-2 Building Eigen Analysis Periods (sec)

Mode	Original	Response
1	1.42	east-west translation
2	1.37	north-south translation
3	1.08	torsional

The analysis completed during the study was based on expected material properties, per the New Zealand Society for Earthquake Engineering

Guidelines, as summarized in Table 4-3 below (units converted from metric to customary US (Standards New Zealand, 2004).

Table 4-3 Expected Material Properties for Moment Frame Elements (ksi)

Element	Story	Steel Yield Strength, F_y	Steel Elastic Modulus, E_s	Concrete Compression Strength, f'_c	Concrete Elastic Modulus, E_c
Beams	all stories	46.4	2,970	3.63	3,430
Columns	L1 – L2	79.0	2,970	4.35	3,760
Columns	L3 – L8	79.0	2,970	3.63	3,430

Furthermore, the effective stiffness values for the moment frame elements, per ASCE/SEI 41 (ASCE, 2017), are provided in Table 4-4.

Table 4-4 Effective Stiffness Values

Element	Action	Effective Stiffness of Original Building
Beams	Axial	$1.0E_cA_g$
	Flexural	$0.3E_cI_g$
Columns	Axial	$1.0E_cA_g$
	Flexural	$(0.2 + \eta_0)E_cI_g$

where, $\eta_0 = \frac{N_{UG}}{A_g f'_c}$, in the range of $0.1 \leq \eta_0 \leq 0.5$.

N_{UG} = are axial forces due to gravity loads

4.1.4 Drift Estimates

Drift estimates at four column lines – identified in Figure 4-1 – around the perimeter of the building are presented in Figure 4-2 and Figure 4-3.

Consistent with the visual observations presented in section 4.1.1, maximum average drifts were estimated to occur in the short moment frame bays at the ends of the L-shaped floor plate (grids A and 1, approaching 2%). This suggests a torsional response, as the average drift demands on the four perimeter moment frames were less than 1.5%.

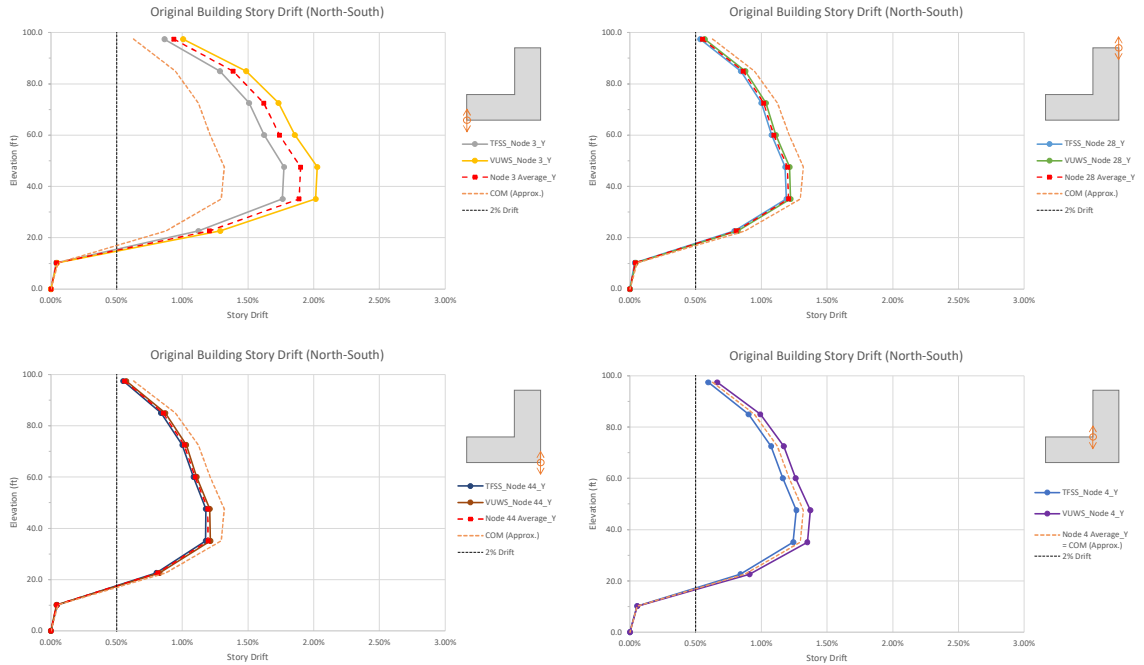


Figure 4-2 Drift estimates in the north-south direction due to the Damaging Earthquake.

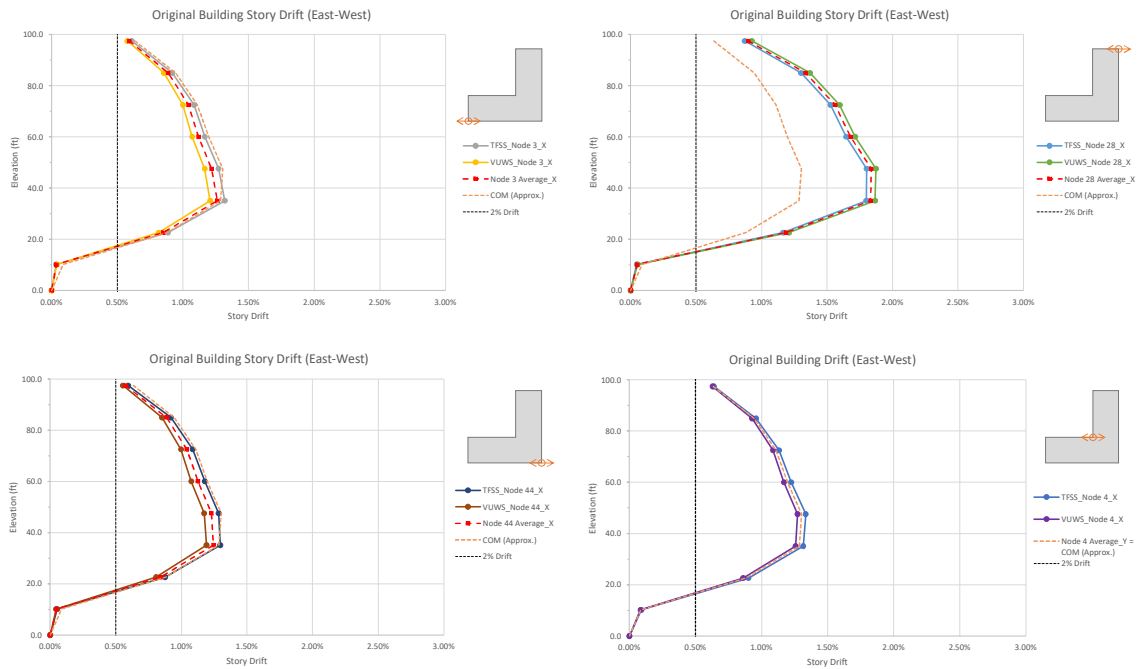


Figure 4-3 Drift estimates in the east-west direction due to Damaging Earthquake.

4.1.5 DCR Estimates

Demand to capacity ratios (DCR) were determined in accordance with ASCE/SEI 41 (ASCE, 2017). For each beam hinge, DCRs were calculated by averaging the maximum flexural demand from the two station spectra

load combinations and comparing it to the beam's flexural capacity. For each column, the DCRs were equated to the ductility factor, m , determined using axial-flexure yield capacity curves. An illustration of a typical column yield curve is provided in Figure 4-4.

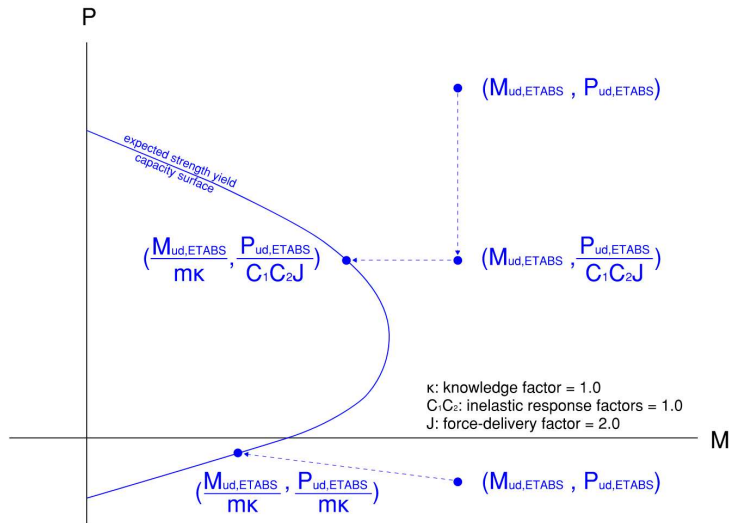


Figure 4-4 Typical column axial-flexure curve used to determine DCRs.

The maximum ductility factor at each beam and column end for each spectral analysis were averaged together and overlaid on moment frame elevations. A detail key for a single frame joint is presented in Figure 4-5. The frame elevation along Gridline 1 is presented in Figure 4-6 with the balance of perimeter moment frame elevations provided in Appendix B. Note that published damage inspection observations were only available for Levels 3, 4 and 5. Additionally, the interior gravity moment frame was found to not significantly contribute to the lateral response of the building. Therefore, the DCR and Inspection Location checks have only been performed at the perimeter moment frames where observations were available. Damage States and inspection findings are further discussed in Section 4.1.7.

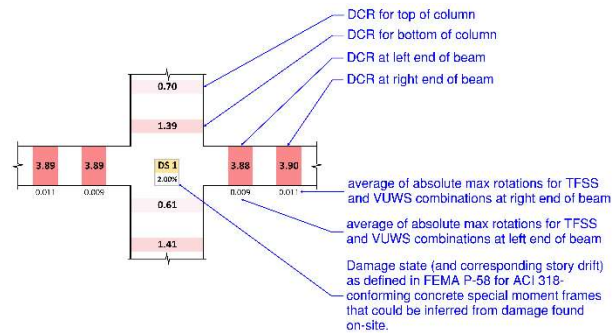


Figure 4-5 Frame damage key.

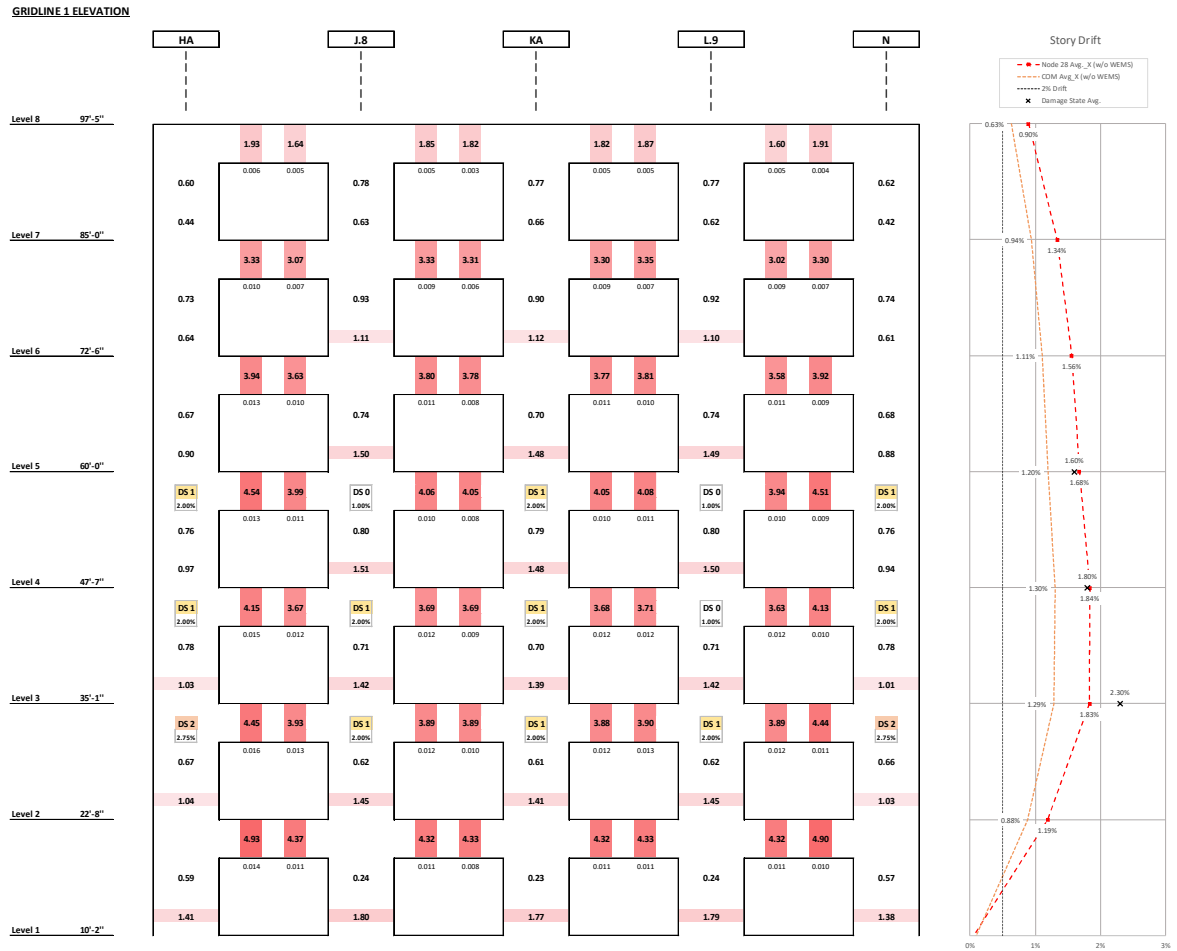


Figure 4-6 Gridline 1 damage elevation.

The analysis reported lower ductility demands than the Primary Life Safety acceptance criteria provided by ASCE/SEI 41. This suggests that significant strength degradation is unlikely to have occurred in the building. Still, at least one round of reconciliation between observation and analysis results is recommended to improve correlation.

4.1.6 Inspection Locations

On the damage elevations, each joint location with a DCR greater than 1.0 was flagged as an Inspection Location (IL). It is clear from the elevations that reported beam DCRs are often significantly greater than 1.0 with a max of 5.5. However, the finding aligns with the ductility factor highlighted in Table 4-5 that is appropriate for the perimeter beam elements. All beam DCRs were found to be less than the ductility factor given for Primary beam components at the Life Safety performance level.

Table 4-5 Numerical Acceptance Criteria for Reinforced Concrete Beams Using Linear Procedures (Table 10-13 of ASCE/SEI41 (ASCE, 2017))

Conditions	<i>m</i> -Factors ^a				
	Performance Level				
	IO	Component Type			
		Primary	Secondary		
	LS	CP	LS	CP	
Condition i. Beams controlled by flexure ^b					
$\rho - \rho'$					
ρ_{bal}	Transverse reinforcement ^c	V^d $b_w d \sqrt{f'_{cE}}$			
≤0.0	C	≤3 (0.25)	3	6	10
≤0.0	C	≥6 (0.5)	2	3	5
≥0.5	C	≤3 (0.25)	2	3	5
≥0.5	C	≥6 (0.5)	2	2	4
≤0.0	NC	≤3 (0.25)	2	3	5
≤0.0	NC	≥6 (0.5)	1.25	2	4
≥0.5	NC	≤3 (0.25)	2	3	4
≥0.5	NC	≥6 (0.5)	1.25	2	3
Condition ii. Beams controlled by shear ^b					
			1.25	1.5	1.75
Stirrup spacing ≤ <i>d</i> /2			1.25	1.5	1.75
Stirrup spacing > <i>d</i> /2				3	4
				2	3
Condition iii. Beams controlled by inadequate development or splicing along the span ^b					
			1.25	1.5	1.75
Stirrup spacing ≤ <i>d</i> /2			1.25	1.5	1.75
Stirrup spacing > <i>d</i> /2				3	4
				2	3
Condition iv. Beams controlled by inadequate embedment into beam-column joint ^b					
			2	2	3
				3	4

Note: f'_{cE} in lb/in.² (MPa) units.

^a Values between those listed in the table shall be determined by linear interpolation.

^b Where more than one of conditions i, ii, iii, and iv occurs for a given component, use the minimum appropriate numerical value from the table.

^c "C" and "NC" are abbreviations for conforming and nonconforming transverse reinforcement. Transverse reinforcement is conforming if, within the flexural plastic hinge region, hoops are spaced at ≤ *d*/3, and if, for components of moderate and high ductility demand, the strength provided by the hoops (V_s) is at least 3/4 of the design shear. Otherwise, the transverse reinforcement is considered nonconforming.

^d *V* is the shear force calculated using limit-state analysis procedures in accordance with Section 10.4.2.4.1.

The Source Report (ATC, 2020) recommends a plastic mechanism check to identify additional inspection locations that may not be captured during the initial analysis. However, based on the damage elevations and regular frame layout, the additional check was not needed to identify additional locations for inspections. The beam DCRs from the analysis being consistently and significantly larger than the column DCRs, indicative of a sway mechanism (e.g., Figure 4-6.)

4.1.7 Analysis and Inspection Reconciliation

Fragility curves were used to infer drift demands based upon the observed damage at each beam-column joint. As identified by Case Study 1, modification of the FEMA P-58 (FEMA, 2018) concrete moment frame fragility curve was recommended. The curve was modified by adding DS 0.5 (See Section 4.1.7) to fill the gap between “no observed damage” (0% drift) and DS 1 (2% drift). The proposed story drift associated with DS 0.5 is 1% and would align with a 50% probability of occurrence. See Figure 4-7. Examples of each Damage State observed in the building inspection are presented in Figure 4-8. This modified approach gave drift estimates that were in reasonable agreement with those estimated by analysis and overall

damage patterns observed by inspection. The agreement can be seen in the story drift plots shown in Figure 4-2, Figure 4-3, and Appendix B.

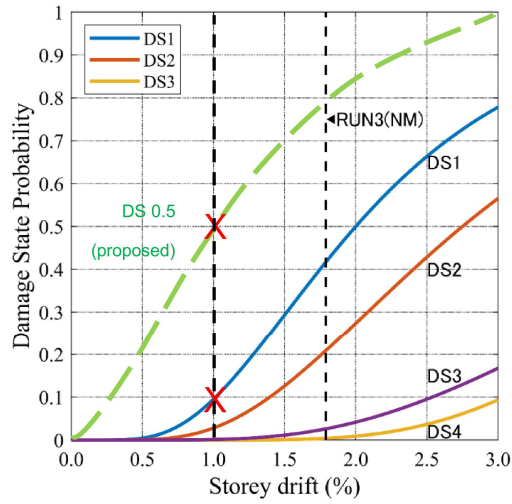


Figure 4-7 Modified FEMA P-58 fragility curve for conforming reinforced concrete moment frame.

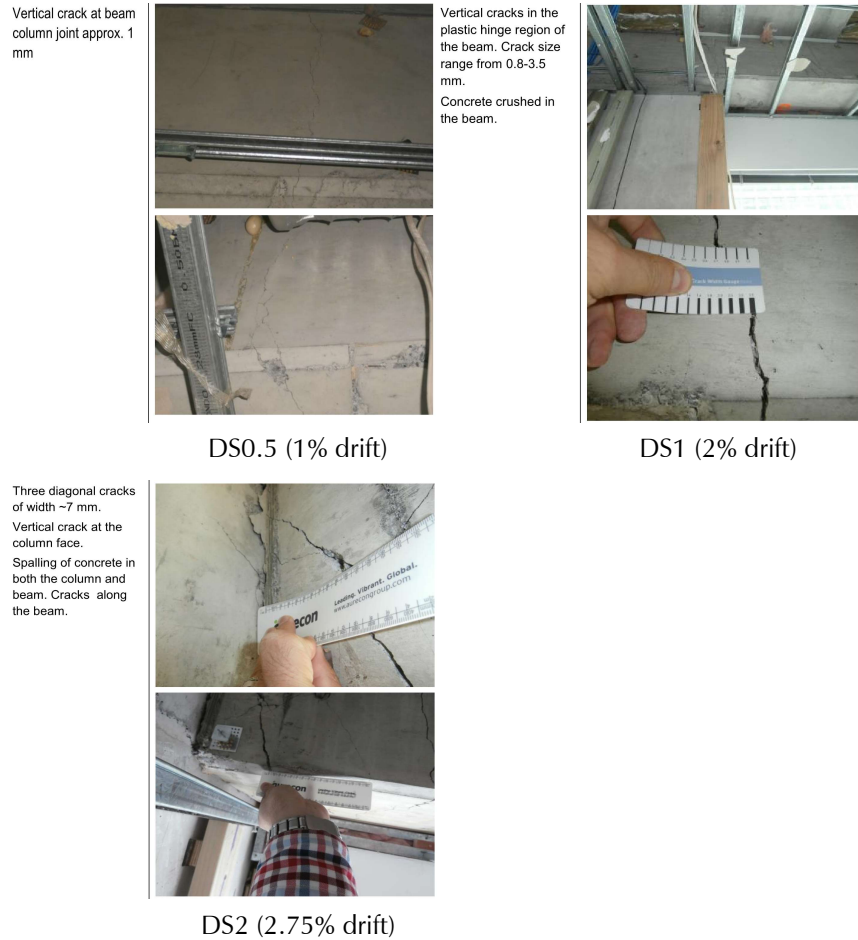


Figure 4-8 Damage state examples.

4.1.8 Test-Modified Inspection Criteria

To reasonably reduce the number of locations flagged for detailed inspection, the working group purposed inspecting joints at levels where beam DCRs exceed 1.0 and story drift exceeds 1%. A total count of inspection locations based on the criteria specified in the Source Report and the test-modified approach is shown in the following table. An additional criterion is shown that adds a trigger for inspection where the element exceeds the ductility limit for Immediate Occupancy (IO) provided in ASCE/SEI 41 (ASCE, 2017).

Table 4-6 Inspection Location Joints Required Based on Analysis Compared to Damage Survey (Levels 3, 4, and 5 Only)

Analysis Triggers:	ATC-145 Standard Approach (Element DCR > 1.0)	Test-Modified Approach (Element DCR > 1.0 & Story Drift > 1.0%)	Patched Approach (Element DCR > 1.0, Story Drift > 1.0%, & m > IO limit)
Total Flagged during Analysis (all floors)	384	252	294
Surveyed and Flagged during Analysis (L3-5)	133	133	133
Total Surveyed (L3-5)	133	133	133
Damage Observed (\geq DS1, L3-5)	79	79	79
Damage Rate (L3-5)	59%	59%	59%
Not Exposed (L3-5)	14	14	14

It is clear from Table 4-6 that a sampling process as outlined in Section 4.2.4 of the Source Report (ATC,2020) would have been ineffective in reducing inspection locations, at the damaged floors inspected (L3-5). However, considering the estimated frame drifts (1.3 to 2.0%) and moderate ductility demands, the almost 60% Damage Rate (ratio of observation to surveyed locations at DS1 or higher) is considered a reasonable level of effort for a visual inspection process. Regardless, in the event that entire floors or frame lines are omitted from inspection per these criteria, it is recommended that at least one location and no less than 5% of all locations be inspected at each excluded floor or frame line to ensure that a significant damage state (i.e., DS1 or higher) is not missed. This also serves to calibrate the analysis model at all floors.

The use of the 1% story drift and IO criteria resulted in all of the top floor (Level 7) frames, and some of the Level 6 frames being excluded from inspection requirements. Additionally, the IO criteria required the Level 1 frames to be inspected, due to the high DCR (i.e., > IO) and despite the low drift (< 1%). Application of these criteria reduce the number of Inspection Locations from the Standard Approach by 23% (384 to 294).

Although published inspection observations were not available for the Level 1 frames, one account from the building inspection suggests that it is unlikely significant damage occurred at the base of the moment frame columns (Brooke, 2021). This is contradictory to the analysis results and frame mechanism analysis, which both indicate that column base hinging should have occurred. It is possible that differing column base fixity and foundation/basement flexibility assumptions contributed to this discrepancy.

Safety Assessment Phase

5.1 System Check

Using the results from the Inspection and Analysis phase, a system-level check is performed to determine if amplification in drift demand during a repeated design-level ground motion is anticipated. The adopted drift demand threshold in the Source Report is 2% story drift. As shown in Figure 4-2 and Figure 4-3, for all perimeter frames, the max drifts, averaged between TFSS and VUWS excitation response, were below 2% story drift, and therefore, meet the system-level safety check.

5.2 Component Checks

The Source Report identifies two component level checks to determine if there has been a significant reduction of the component deformation capacity due to the Damaging Earthquake and indicate if complex repair is likely required to meet building code life-safety objectives. The first check is identifying any locations where frame total chord rotations have exceeded 0.02 radians. Each frame elevation was evaluated under the Damaging Earthquake excitation and found to not exhibit chord rotations exceeding the 0.02 radian threshold. The second check is to evaluate fatigue of longitudinal (flexural) reinforcement.

The fatigue check outlined in the Source Report identifies three conditions given reasonable deformation demands and typical number of cycles and plastic hinge lengths in Section 3.3.3.2 of the Report. (ATC, 2020). The first condition limiting chord rotation to less than 0.02 radians was met and illustrated in Appendix B. The second condition is met as the significant duration of the damaging earthquake was less than 45 seconds as reported by Bradley et al. (Bradley et al., 2017) and repeated in Figure 5-1. However, for all perimeter frame beams, the effective plastic hinge length did not exceed 0.4 times the depth of the member. An example calculation for a relatively shallow beam at the upper levels is provided below.

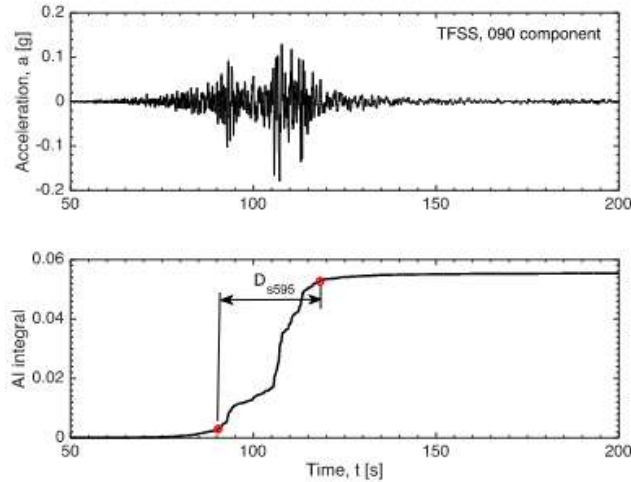


Figure 5-1 TFSS acceleration time series and significant duration, D_{5-95} (from Figure 9 of Ref.)

$$L_p = k_p a + L_{sp} \geq 2L_{sp} \quad (5-1)$$

$$L_p = \left[0.2 \times \left(\frac{f_u}{f_y} - 1 \right) \right] \times a + (0.15 f_y d_b) \geq (0.3 f_y d_b)$$

$$L_p = \left[0.2 \times \left(\frac{65.3 \text{ ksi}}{57.7 \text{ ksi}} - 1 \right) \right] \times 89 \text{ in.} + (0.15 \times 57.7 \text{ ksi} \times 0.79 \text{ in.})$$

$$\geq (0.3 \times 57.7 \text{ ksi} \times 0.79 \text{ in.})$$

$$L_p = 9.66 \text{ in.}$$

where:

a = shear span, i.e., the distance of the critical section from the point of contraflexure (set equal to the distance from column face to midspan for initial check)

L_{sp} = p strain penetration length

f_y = probable yield strength of longitudinal reinforcement

f_u = probable ultimate strength of longitudinal reinforcement

d_b = diameter of longitudinal reinforcement

$$0.4 \times d = 11.8 \text{ in.} > L_p = 9.66 \text{ in.} \quad \text{Condition not met.} \quad (4-2)$$

Thus, further investigation using the simplified approach in Section C.4.1 in Appendix C of the Source Report (ATC, 2020) was undertaken. Critical locations were investigated where beams were deepest and at locations where the analysis indicated max peak chord rotations. The simplified approach resulted in expected fatigue life reductions less than 5%, meeting the 10% threshold specified in the Source Report. Given these results, the perimeter

moment frame beams were deemed sufficient to meet the safety check for component fatigue.

Case Study 2

Chapter 6

Serviceability Assessment

6.1 Drift Check

To check the flexibility of the building in the damaged condition and determine if the non-structural components were vulnerable to damage for future service-level earthquakes, the original building model elements were softened based on the ductility results from the original building analysis. The damaged building model was then analyzed using a linear dynamic procedure for a 25-year return event based on the New Zealand Standard 1170.5 (Standards New Zealand, 2004). NZS 1170.5 is the current loading standard and has superseded NZS 4203. The design serviceability earthquake spectra is presented in Figure 6-1.

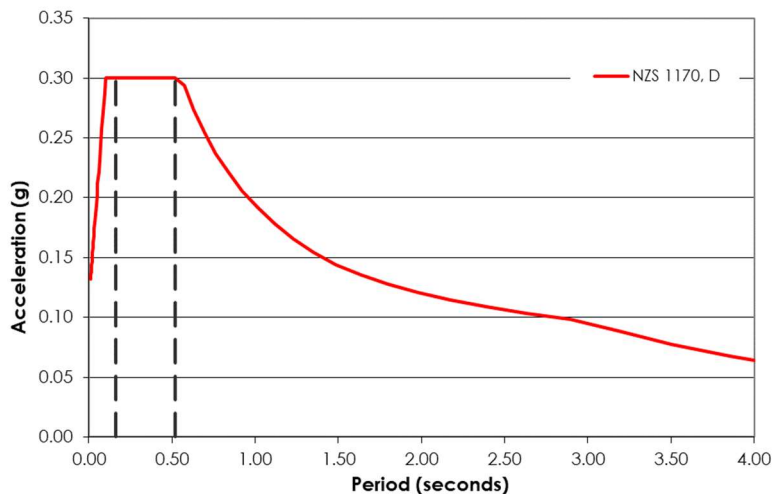


Figure 6-1 Design spectra for a 25-year service-level event.

The moment frame beam and column stiffnesses were reduced as detailed in the Source Report (ATC, 2020) and repeated below.

$$\frac{K_r}{K_y} = \begin{cases} 1.0, & \mu < 1.0 \\ 0.5, & 1.0 \leq \mu \leq 2.0 \\ 1/\mu, & \mu \geq 2.0 \end{cases} \quad (6-1)$$

For comparison, the modal periods and element stiffnesses for the original and damaged building models are shown in Table 6-1 and Table 6-2,

respectively. Values for a repaired condition are provided in the Tables as well where simple epoxy repairs may be applied to the moment frame structure.

Table 6-1 Building Eigen Response Periods (sec)

Mode	Original	Damaged	Repaired	Response
1	1.42	2.25	1.66	east-west translation
2	1.37	2.00	1.58	north-south translation
3	1.08	1.69	1.28	torsional

Table 6-2 Effective Stiffness Values

Element	Action	Effective Stiffness		
		Original	Damaged	Repaired
Beams	Axial	$1.0E_cA_g$	$\frac{K_r}{K_y}E_cA_g$	$\frac{K_r}{K_y}E_cA_g$
	Flexural	$0.3E_cI_g$	$0.3\frac{K_r}{K_y}E_cI_g$	$0.8 \times 0.3E_cI_g$
Columns	Axial	$1.0E_cA_g$	$\frac{K_r}{K_y}E_cA_g$	$\frac{K_r}{K_y}E_cA_g$
	Flexural	$(0.2 + \eta_0)E_cI_g$	$\frac{K_r}{K_y}\eta_0E_cI_g$	$\frac{K_r}{K_y}\eta_0E_cI_g$

where η_0 and N_{UG} are defined in Table 4-4.

Figure 6-2 and Figure 6-3 below show the drift behavior of the damaged model during the service-earthquake. The damaged building did not satisfy the NZS 1170.5 serviceability drift limit of 0.5%; however, it was noted that the building did not satisfy this limit in the original condition (See Figure 6-4 and Figure 6-5) and it was unlikely to have been a requirement at the time of the building's design and construction.

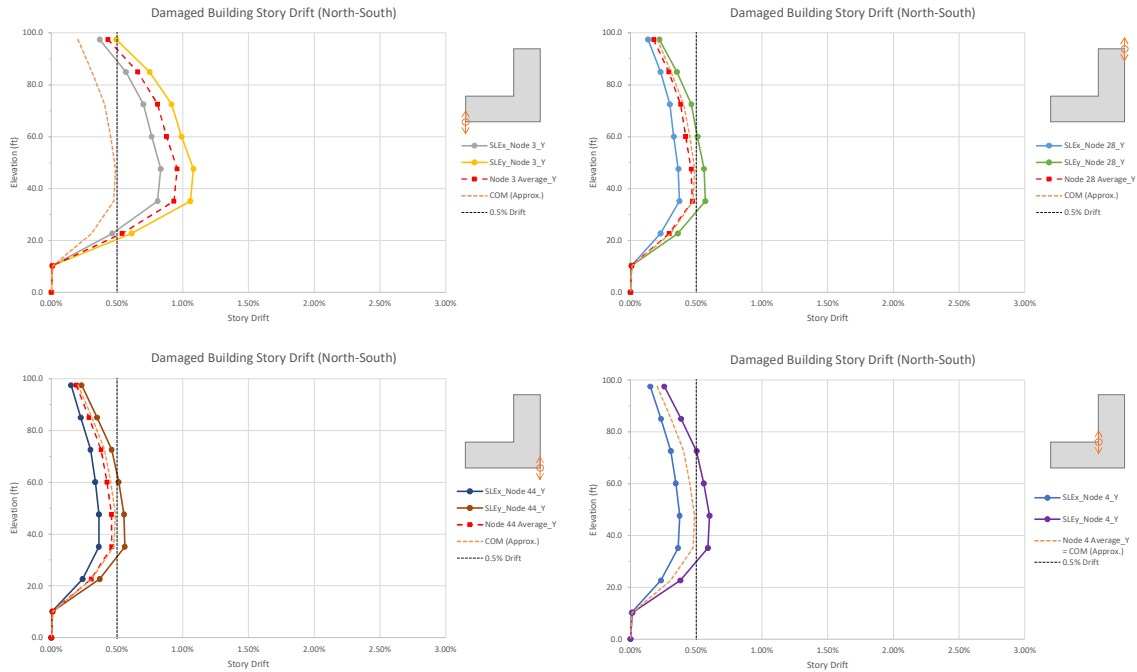


Figure 6-2 Story drift plots of damaged building under service-level earthquake. Drifts measured in north-south direction.

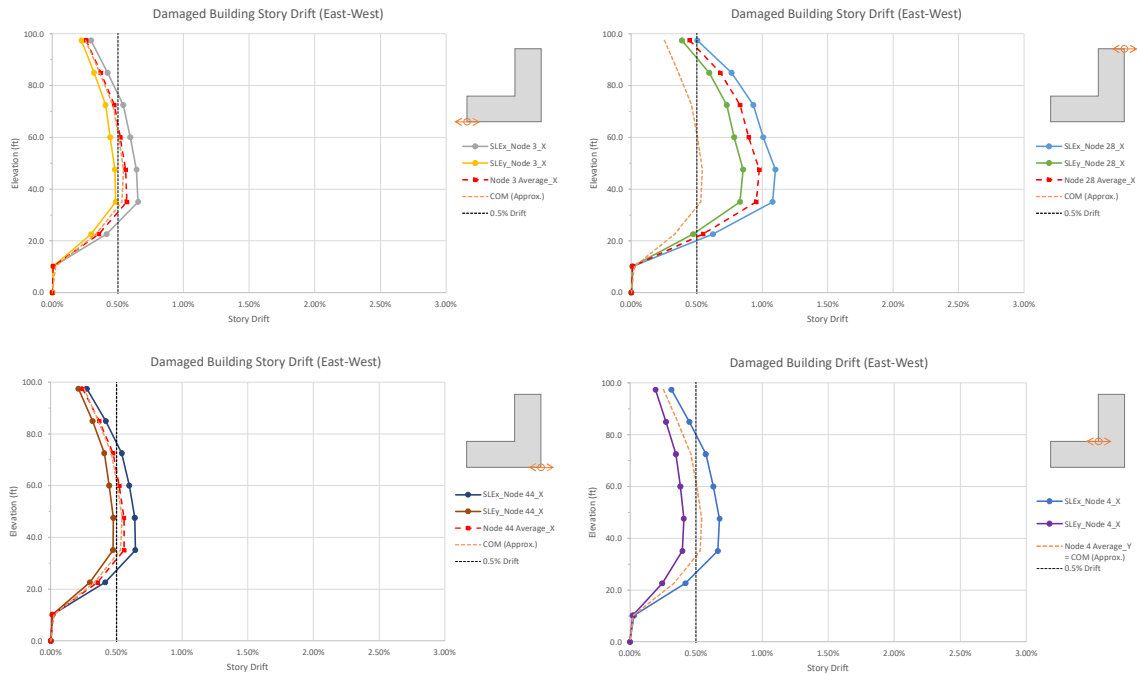


Figure 6-3 Story drift plots of damaged building under service-level earthquake. Drifts measured in east-west direction.

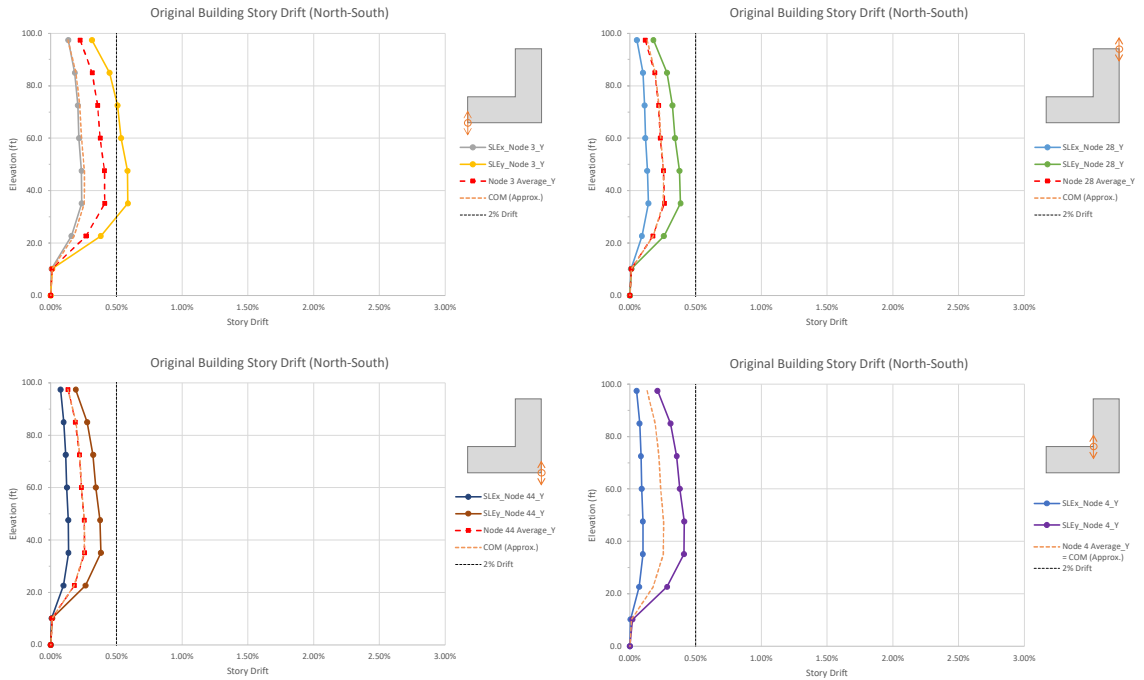


Figure 6-4 Story drift plots of original building under service-level earthquake. Drifts measured in north-south direction.

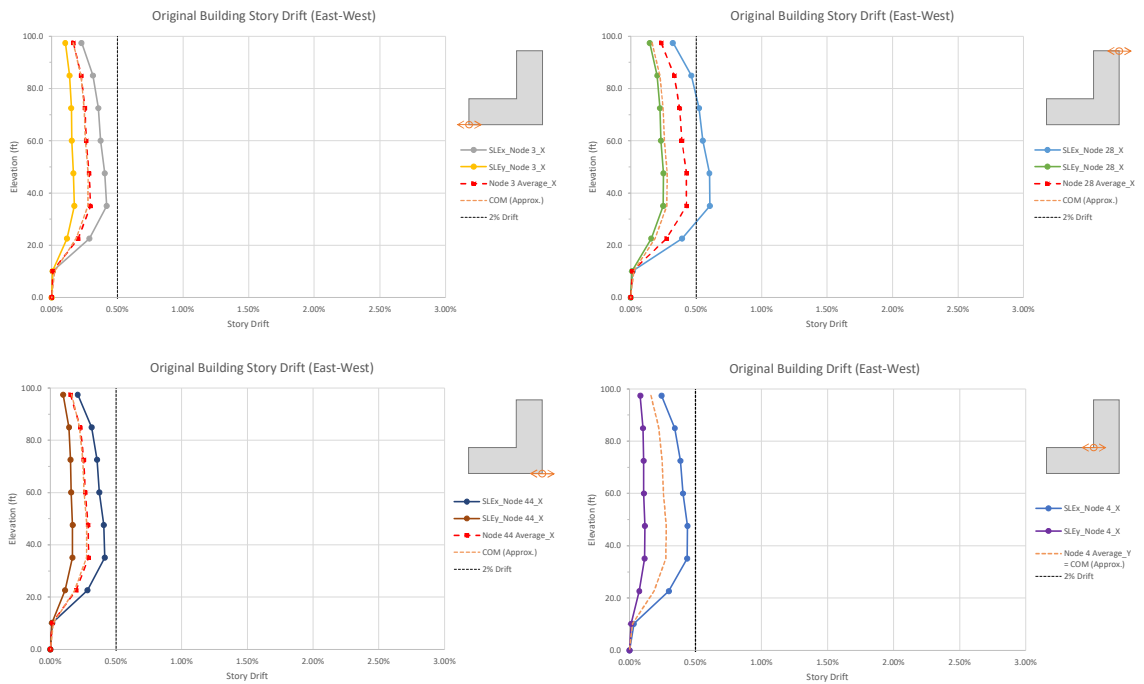


Figure 6-5 Story drift plots of original building under service-level earthquake. Drifts measured in east-west direction.

6.2 Repair Recommendations

Since the story drifts of the damaged building exceed the limit of 0.5%, the building was reanalyzed in the simple repair condition under the same service-level hazard. The repaired building model was generated by starting with the damaged building model and increasing the flexural stiffnesses of the softened perimeter beams to $0.8EI_g$. Damaged columns were not stiffened for the repaired condition, due to the assumed difficulty of effectively epoxy injecting columns with sustained (gravity) axial compression. Story drift plots for the repaired building under NZS1170 are provided in Figure 6-6 and Figure 6-7.

It is clear from the figures that the simple repair would not be sufficient to meet the 0.5% drift limit, predominantly in the transverse direction towards the ends of the L-shaped floor plate. Given the limit has not been met, the Source Report methodology results in triggering Repair Category 2 – Complex Repair, defined by epoxy injection of damaged structural frame members and stiffening of the structure or upgrading nonstructural components to accommodate the anticipated drifts.

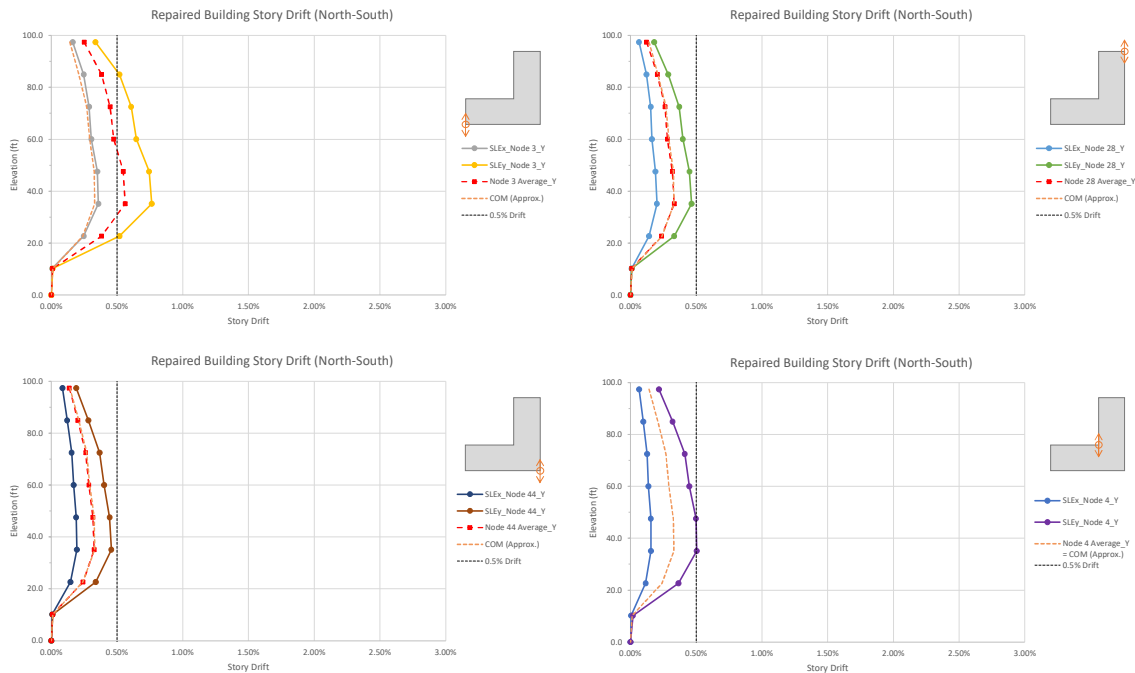


Figure 6-6 Story drift plots of repaired building under service-level earthquake. Drifts measured in north-south direction.

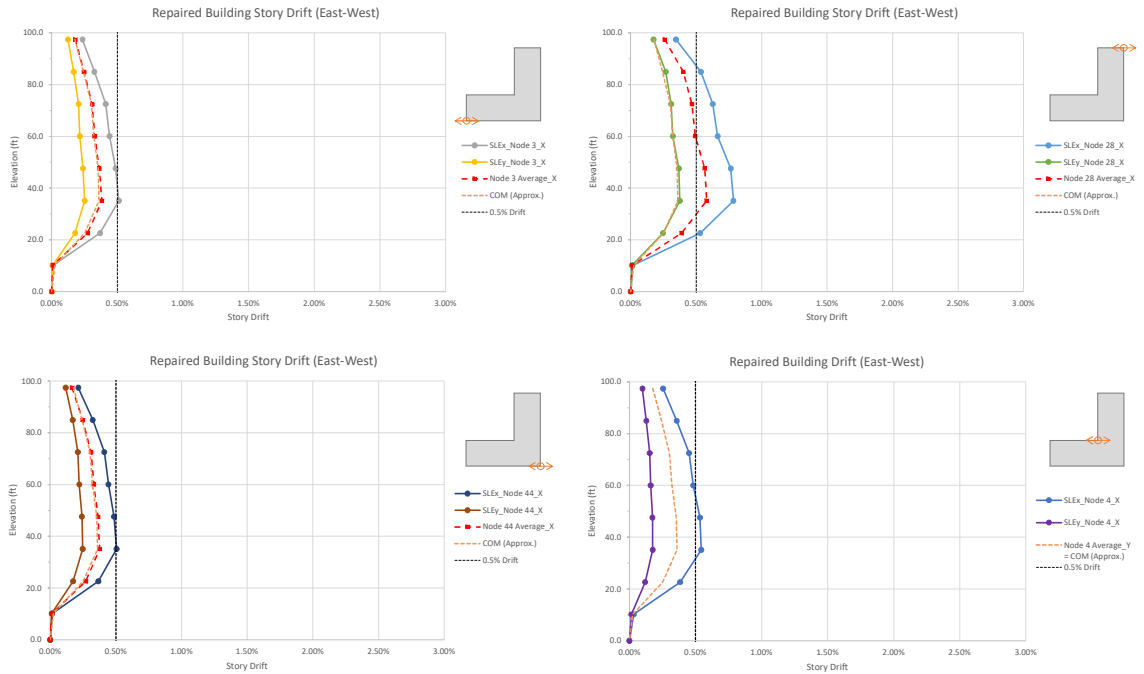
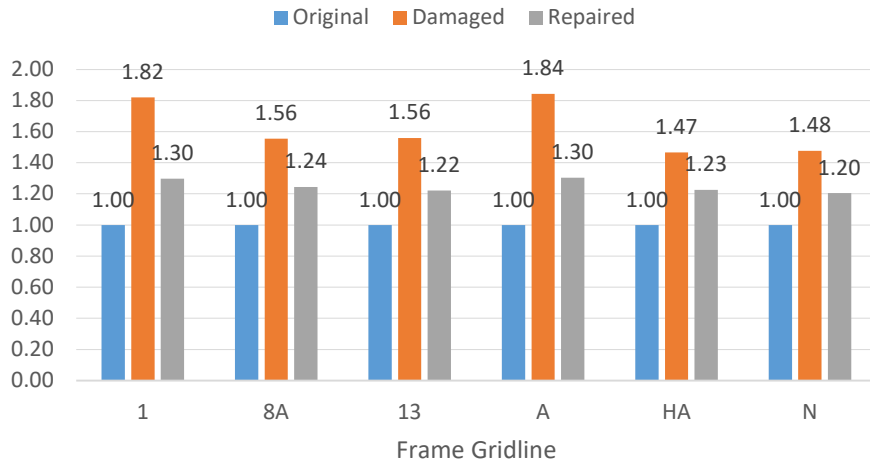
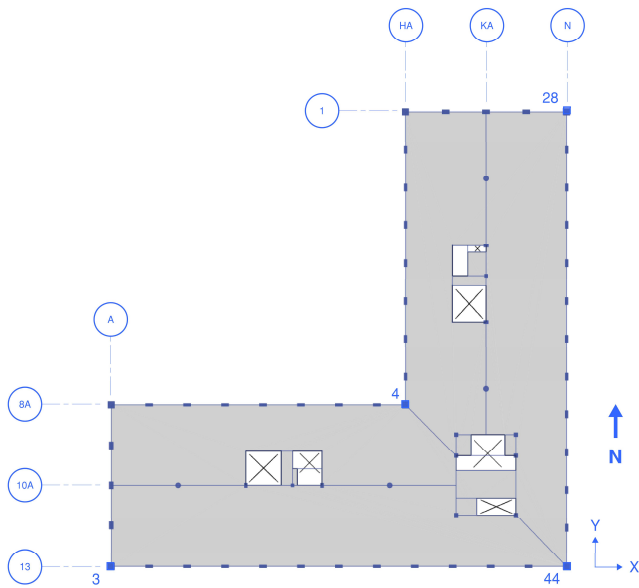


Figure 6-7 Story drift plots of repaired building under service-level earthquake. Drifts measured in east-west direction.

A comparison of the peak story drifts for each model is provided in Figure 6-8.



(a)



(b)

Figure 6-8 (a) Normalized peak story drift for each perimeter frame line (gridline) under the service-level earthquake. (b) Building key plan for gridline reference.

Conclusions and Recommendations

As described previously, application of the Source Report for Case Study 2 yielded the following conclusions and recommendations.

Inspection and analysis using a linear dynamic procedure from local stations with similar soil classification led to good agreement with estimated damage when compared with drifts associated with damage states from FEMA P-58 fragility curves. As identified by Case Study 1, modification of the FEMA P-58 concrete moment frame fragility curve was recommended. The curve was modified by adding DS 0.5 (See Section 4.1.7) to fill the gap between “no observed damage” (0% drift) and DS 1 (2% drift).

ASCE/SEI 41 analysis methods can be used to achieve a reasonable estimate of peak deformation demands and identification of where yielding is likely to have occurred. In Case Study 2, applying ASCE/SEI 41 linear procedures for determination of the element DCRs and ductility led to results well aligned with prescriptive ductility factors. The analysis reported lower ductility demands than the Primary Life Safety acceptance criteria provided by ASCE/SEI 41. This suggests that significant strength degradation is unlikely to have occurred in the building. Still, at least one round of reconciliation between observation and analysis results is recommended to improve correlation.

After comparison of the observation and analysis, it was determined that the analysis identified an over-estimation of detailed inspection locations that would be work intensive in practice. To reasonably reduce the number of inspection locations, the best approach found was to add additional constraints, specifically, to exclude inspection locations at levels that exhibited a story drift less than 1% and to exclude locations where an individual element ductility does not exceed the limit provided in ASCE/SEI 41 for Immediate Occupancy. This approach led to a 23% reduction in inspection locations. In the event that entire floors or frame lines are omitted from inspection per these criteria, but the lower floors are found to be damaged per the inspection process, it is recommended that at-least one

location and no less than 5% of all locations be inspected at each excluded floor or frame line to ensure that a significant damage state (i.e., DS1 or higher) is not missed. This also serves to calibrate the analysis model at all floors.

For the frame locations where published inspection observations were available, the almost 60% Damage Rate (ratio of observation to surveyed locations at DS1 or higher) is considered a reasonable level of effort for a visual inspection process.

For the component fatigue check of the safety assessment phase, further guidance may be warranted in the guidelines to help the end user properly apply the methodologies outlined. This may be done by publishing a spreadsheet tool that takes simple input parameters from the analysis and returns the expected fatigue demand or reduction in fatigue life.

Lastly, structures subject to moderate and extensive ductility demands (i.e., distributed hinging) can be expected to exhibit significantly more flexible response at future service-level earthquakes. Epoxy repair alone may not be sufficient to restore serviceability performance; however, this is highly dependent upon the serviceability criteria, including hazard and drift criteria, specified by the Authority Having Jurisdiction or applicable building regulations. It may be useful to provide direction beyond the scope of ATC 145 where a structure is found in need of a complex repair due to serviceability considerations.

7.1 Recommendations for Future Study

Upon completion of this case study there were a few areas identified that may warrant future study but were not explicitly discussed in the report. A list of these items is provided below.

- Implications and practicality of a linear and/or nonlinear response history analysis
- Sensitivity of inspection criteria to the type of analysis undertaken or level of confidence in the ground motion estimates
- Potential addition of guidance on when additional inspection locations need not be identified, e.g., through a plastic mechanism analysis
- Effects of column base fixity and foundation/basement flexibility

(not applicable to ATC-145 scope)

Candidate for Further Study	FEMA P-58 (PACT): <input type="checkbox"/>	FEMA E-74 (Nonstructural): <input type="checkbox"/>
	FEMA P-154 (RVS): <input type="checkbox"/>	Retrofitted URM: <input type="checkbox"/>

ATC-38 POSTEARTHQUAKE BUILDING PERFORMANCE ASSESSMENT FORM

Incorporating modifications by FEMA P-1024 (ATC 66-5) & ATC-145 Specific Notes (red text)

Note: DO NOT LEAVE ANY BLANK SPACES!

Indicate Unknown (UNK), Not Applicable (NA), or None if necessary.

Building Site Information [1]

Inspector(s) Malcom McGechie	Date: 03/24/2017	Bldg. ID# WG1a Case Study 2	Page 1 of 6
Address: -		Building Name: Confidential Building	
Type of Survey: <input type="checkbox"/> Exterior Only <input checked="" type="checkbox"/> Exterior and Interior	Recording Station ID: TFSS/UWS		
Existing Posting Placard: <input type="checkbox"/> Red <input type="checkbox"/> Yellow <input type="checkbox"/> Green <input type="checkbox"/> None	Photo ID#s:		
Building Owner/Manager Contact – Name:		Phone:	
Civil/Structural Engineer for Repair – Name:		Phone:	
General Damage Classification (Structural): <input type="checkbox"/> None (N) <input type="checkbox"/> Insignificant (I) <input type="checkbox"/> Minor (m) <input checked="" type="checkbox"/> Moderate (M) <input type="checkbox"/> Heavy (H) <input type="checkbox"/> Collapse (C)			
General Damage Classification (Nonstructural): <input type="checkbox"/> None (N) <input type="checkbox"/> Insignificant (I) <input type="checkbox"/> Minor (m) <input checked="" type="checkbox"/> Moderate (M) <input type="checkbox"/> Heavy (H) <input type="checkbox"/> Collapse (C)			

[Note: For “M” or “H” classification, fill out Detailed Damage Description Section on page 5]

Building Construction Data [2]

Construction Date: 2015	Design Date: 2014	Sloped Site: <input type="checkbox"/> Yes <input checked="" type="checkbox"/> No
Number of Stories Above Ground: 7	Number of Basement Levels: 1	
Number of Living Units: -	Foundation Type: Mat + Pile	Soil Type: Class D
Plan Width (ft): 218	Plan Length (ft): 218	Approximate Building Area (sq.ft.): 28200
Occupancy Type (see Glossary): Office	Occupied Prior to Earthquake: <input checked="" type="checkbox"/> Yes <input type="checkbox"/> No <input type="checkbox"/> UNK	
Notes:		

Model Building Type [3]

Predominant Model Building Type (see Glossary): C1	Seismic Retrofit: <input type="checkbox"/> Yes <input checked="" type="checkbox"/> No <input type="checkbox"/> UNK
Describe Building if More Than One Model Building Type Present: N/A	
Describe Retrofit if Present: N/A	
Additions? If yes, describe building type, date of construction: N/A	

Figure A-1 Postearthquake Building Performance Assessment Form (page 1 of 6).

Performance Modifiers [4] (refer to FEMA P-154 for pounding and irregularity criteria)		Bldg. ID#: WG1a Case Study 2	Page 2 of 6
Discontinuous Columns: <input type="checkbox"/> Yes <input checked="" type="checkbox"/> No <input type="checkbox"/> UNK <input type="checkbox"/> NA		Facade Setbacks: <input type="checkbox"/> Yes <input checked="" type="checkbox"/> No <input type="checkbox"/> UNK <input type="checkbox"/> NA	
Pounding Potential: <input type="checkbox"/> Yes <input type="checkbox"/> No <input checked="" type="checkbox"/> UNK <input type="checkbox"/> NA		Seismic Expansion Joints: <input type="checkbox"/> Yes <input checked="" type="checkbox"/> No <input type="checkbox"/> UNK <input type="checkbox"/> NA	
Open Front Plan: <input type="checkbox"/> Yes <input type="checkbox"/> No <input type="checkbox"/> UNK <input checked="" type="checkbox"/> NA		Other Torsional Imbalance: <input checked="" type="checkbox"/> Yes <input type="checkbox"/> No <input type="checkbox"/> UNK <input type="checkbox"/> NA	
Plan Irregularities: <input checked="" type="checkbox"/> Yes <input type="checkbox"/> No <input type="checkbox"/> UNK <input type="checkbox"/> NA		Deterioration of Structure: <input type="checkbox"/> Yes <input checked="" type="checkbox"/> No <input type="checkbox"/> UNK <input type="checkbox"/> NA	
Previous Earthquake Damage: <input type="checkbox"/> Yes <input checked="" type="checkbox"/> No <input type="checkbox"/> UNK <input type="checkbox"/> NA			
Describe Other Vertical Irregularities: N/A			
Describe Other Plan Irregularities: L-shaped building plan with significant re-entrant corner.			
Describe Other Pre-Earthquake Building Conditions: N/A			

Sketch of Building [5]

Plan sketch provided on separate paper: <input checked="" type="checkbox"/> Yes <input type="checkbox"/> No
Elevation sketch provided on separate paper: <input checked="" type="checkbox"/> Yes <input type="checkbox"/> No

Nonstructural Elements [6]

Exterior Cladding/Glazing Code (see Glossary): P
Partitions Code (see Glossary): G
Ceilings Code (see Glossary): H
Fire Protection: <input checked="" type="checkbox"/> Yes <input type="checkbox"/> No <input type="checkbox"/> UNK <input type="checkbox"/> NA
Elevators: <input checked="" type="checkbox"/> Yes <input type="checkbox"/> No <input type="checkbox"/> UNK <input type="checkbox"/> NA
Chimneys: <input type="checkbox"/> Yes <input checked="" type="checkbox"/> No <input type="checkbox"/> UNK <input type="checkbox"/> NA
Parapets: <input type="checkbox"/> Yes <input checked="" type="checkbox"/> No <input type="checkbox"/> UNK <input type="checkbox"/> NA
Major Appendages: <input checked="" type="checkbox"/> Yes <input type="checkbox"/> No <input type="checkbox"/> UNK <input type="checkbox"/> NA
Standard Plumbing, Electrical, Lighting, HVAC: <input checked="" type="checkbox"/> Yes <input type="checkbox"/> No <input type="checkbox"/> UNK <input type="checkbox"/> NA
Describe Major Fixed Equipment: MEP Units and open canopy provided on roof
Describe Unusual Contents: N/A

Figure A-1 Postearthquake Building Performance Assessment Form (page 2 of 6).

General Damage [7]

Bldg. ID#: **WG1a Case Study 2**

Page 3 of 6

General Damage Classification (repeated from Section [1] on page 1):
 None (N) Insignificant (I) Minor (m) Moderate (M) Heavy (H) Collapse (C)

[Note: See Glossary for ATC-13 Damage State Definitions]

ATC-13 Damage State, Structural: M	ATC-13 Damage State, Nonstructural: -
ATC-13 Damage State, Equipment: -	ATC-13 Damage State, Contents: M

Percent of Floor Area Collapsed: 0 % UNK NA

Building off Foundation: <input type="checkbox"/> Yes <input checked="" type="checkbox"/> No <input type="checkbox"/> UNK <input type="checkbox"/> NA	Story out of Plumb: <input type="checkbox"/> Yes <input type="checkbox"/> No <input checked="" type="checkbox"/> UNK <input type="checkbox"/> NA
Damage to Structural Members: <input checked="" type="checkbox"/> Yes <input type="checkbox"/> No <input type="checkbox"/> UNK <input type="checkbox"/> NA	Hazmat: <input type="checkbox"/> Yes <input type="checkbox"/> No <input checked="" type="checkbox"/> UNK <input type="checkbox"/> NA
Parapet Damage: <input type="checkbox"/> Yes <input checked="" type="checkbox"/> No <input type="checkbox"/> UNK <input type="checkbox"/> NA	Chimney Damage: <input type="checkbox"/> Yes <input checked="" type="checkbox"/> No <input type="checkbox"/> UNK <input type="checkbox"/> NA
Exterior Non-building Damage: <input checked="" type="checkbox"/> Yes <input type="checkbox"/> No <input type="checkbox"/> UNK <input type="checkbox"/> NA	Pounding Damage: <input type="checkbox"/> Yes <input checked="" type="checkbox"/> No <input type="checkbox"/> UNK <input type="checkbox"/> NA

Comments about General Damage:

Nonstructural Damage [8] (only complete to extent that this is useful to estimate peak demands on structure)

Cladding Separation or Damage: _____% of wall area UNK NA

Partitions Damage: None (N) Insignificant (I) Minor (m) Moderate (M) Heavy (H) UNK NA

Windows Damage: _____% of windows UNK NA

Lights and Ceilings Damage: None (N) Insignificant (I) Minor (m) Moderate (M) Heavy (H) UNK NA

Buildings Contents Damage: None (N) Insignificant (I) Minor (m) Moderate (M) Heavy (H) UNK NA

Comments about Nonstructural Damage:

(not applicable to ATC-145 scope)

Injuries or Fatalities [9]

No. of Minor Injuries: _____ <input type="checkbox"/> UNK	No. of Major Injuries: _____ <input type="checkbox"/> UNK	No. of Fatalities: _____ <input type="checkbox"/> UNK
Comments about Injuries or Fatalities:		

Figure A-1 Postearthquake Building Performance Assessment Form (page 3 of 6).

(not applicable to ATC-145 scope)

Functionality [10]		Bldg. ID#:	Page <u>4</u> of <u>6</u>
Percent Usable Space Immediately: ___% <input type="checkbox"/> UNK	Percent Usable Space in 1-3 Days: ___% <input type="checkbox"/> UNK		
Percent Usable Space within 1 Week: ___% <input type="checkbox"/> UNK	Percent Usable Space within 1 Mo.: ___% <input type="checkbox"/> UNK		
Percent Usable Space in 1-6 Months: ___% <input type="checkbox"/> UNK	Time Until Full Occupancy: ___ <input type="checkbox"/> UNK <input type="checkbox"/> NA		
Comments about Functionality:			

Geotechnical Failures [11]

Lateral Ground Movement: <input type="checkbox"/> Yes <input type="checkbox"/> No <input checked="" type="checkbox"/> UNK <input type="checkbox"/> NA	Buckled Sidewalks: <input checked="" type="checkbox"/> Yes <input type="checkbox"/> No <input type="checkbox"/> UNK <input type="checkbox"/> NA
Ground Settlement: <input type="checkbox"/> Yes <input type="checkbox"/> No <input checked="" type="checkbox"/> UNK <input type="checkbox"/> NA	Liquefaction Indicators: <input type="checkbox"/> Yes <input type="checkbox"/> No <input checked="" type="checkbox"/> UNK <input type="checkbox"/> NA
Separation Between Building and Ground: <input type="checkbox"/> Yes <input type="checkbox"/> No <input checked="" type="checkbox"/> UNK <input type="checkbox"/> NA	
Landslide: <input type="checkbox"/> Yes <input checked="" type="checkbox"/> No <input type="checkbox"/> UNK <input type="checkbox"/> NA	
Comments about Geotechnical Features:	

Additional Comments

Additional Comments Pertaining to Any Section of Survey Form (use additional pages if necessary):

Figure A-1 Postearthquake Building Performance Assessment Form (page 4 of 6).

DETAILED DAMAGE DESCRIPTION

Bldg. ID#: [WG1a Case Study 2](#)

Page 5 of 6

Vertical Elements

Racking of Main Walls: <input type="checkbox"/> None (N) <input type="checkbox"/> Insignificant (I) <input type="checkbox"/> Moderate (M) <input type="checkbox"/> Heavy (H) <input type="checkbox"/> UNK <input checked="" type="checkbox"/> NA
Racking of Cripple Walls: <input type="checkbox"/> None (N) <input type="checkbox"/> Insignificant (I) <input type="checkbox"/> Moderate (M) <input type="checkbox"/> Heavy (H) <input type="checkbox"/> UNK <input checked="" type="checkbox"/> NA
Buckling, Crippling, Tearing of Steel Beams, Columns, or Braces: <input type="checkbox"/> None (N) <input type="checkbox"/> Insignificant (I) <input type="checkbox"/> Moderate (M) <input type="checkbox"/> Heavy (H) <input checked="" type="checkbox"/> UNK <input type="checkbox"/> NA
Spalling or Cracking of Concrete Columns or Beams: <input type="checkbox"/> None (N) <input type="checkbox"/> Insignificant (I) <input checked="" type="checkbox"/> Moderate (M) <input type="checkbox"/> Heavy (H) <input type="checkbox"/> UNK <input type="checkbox"/> NA
Column Crushing Due to Overturning or Discontinuous Lateral Resisting Elements: <input checked="" type="checkbox"/> None (N) <input type="checkbox"/> Insignificant (I) <input type="checkbox"/> Moderate (M) <input type="checkbox"/> Heavy (H) <input type="checkbox"/> UNK <input type="checkbox"/> NA
Shear Cracking in Columns: <input type="checkbox"/> None (N) <input type="checkbox"/> Insignificant (I) <input type="checkbox"/> Moderate (M) <input type="checkbox"/> Heavy (H) <input checked="" type="checkbox"/> UNK <input type="checkbox"/> NA
Cracked Shear Walls: <input type="checkbox"/> None (N) <input type="checkbox"/> Insignificant (I) <input type="checkbox"/> Moderate (M) <input type="checkbox"/> Heavy (H) <input type="checkbox"/> UNK <input checked="" type="checkbox"/> NA
Percentage of Shear Walls with Cracks: _____% <input type="checkbox"/> UNK <input checked="" type="checkbox"/> NA
Rocking of Shear Walls: <input type="checkbox"/> None (N) <input type="checkbox"/> Insignificant (I) <input type="checkbox"/> Moderate (M) <input type="checkbox"/> Heavy (H) <input type="checkbox"/> UNK <input checked="" type="checkbox"/> NA
Damage to Shear Wall Boundary Elements: <input type="checkbox"/> None (N) <input type="checkbox"/> Insignificant (I) <input type="checkbox"/> Moderate (M) <input type="checkbox"/> Heavy (H) <input type="checkbox"/> UNK <input checked="" type="checkbox"/> NA
Damage to Shear Wall Coupling Beams: <input type="checkbox"/> None (N) <input type="checkbox"/> Insignificant (I) <input type="checkbox"/> Moderate (M) <input type="checkbox"/> Heavy (H) <input type="checkbox"/> UNK <input checked="" type="checkbox"/> NA
/ % of Tiltup Wall Panels Leaning or Fallen Out: _____ / _____% <input type="checkbox"/> UNK <input checked="" type="checkbox"/> NA
Infill Walls Damaged or Fallen Out: <input type="checkbox"/> None (N) <input type="checkbox"/> Insignificant (I) <input type="checkbox"/> Moderate (M) <input type="checkbox"/> Heavy (H) <input type="checkbox"/> UNK <input checked="" type="checkbox"/> NA

Horizontal Elements

Roof Collapse: _____ % of Diaphragm <input checked="" type="checkbox"/> UNK <input type="checkbox"/> NA	Floor Collapse: <u><5%</u> % of Diaphragm <input type="checkbox"/> UNK <input type="checkbox"/> NA
Loss of Vertical Roof Support: _____ % of Roof Area Affected <input type="checkbox"/> UNK <input checked="" type="checkbox"/> NA	
Tearing of Diaphragms at Other Points of High Stress: <u><10%</u> % of Diaphragm <input type="checkbox"/> UNK <input type="checkbox"/> NA	
Damage at Re-entrant Corners: <input type="checkbox"/> None (N) <input type="checkbox"/> Insignificant (I) <input type="checkbox"/> Moderate (M) <input checked="" type="checkbox"/> Heavy (H) <input type="checkbox"/> UNK <input type="checkbox"/> NA	
Damage to Collectors at Walls: <input type="checkbox"/> None (N) <input type="checkbox"/> Insignificant (I) <input type="checkbox"/> Moderate (M) <input type="checkbox"/> Heavy (H) <input type="checkbox"/> UNK <input checked="" type="checkbox"/> NA	
Cross Grain Bending Damage at Roof-to-Wall Connections: _____ % of Connection Length <input type="checkbox"/> UNK <input checked="" type="checkbox"/> NA	

Figure A-1 Postearthquake Building Performance Assessment Form (page 5 of 6).

DETAILED DAMAGE DESCRIPTION (Continued)

Bldg. ID#: **WG1a Case Study 2**

Page 6 of 6

Connections

Girder-Column Connection Damage Including Panel Zones: <input type="checkbox"/> None (N) <input type="checkbox"/> Insignificant (I) <input type="checkbox"/> Moderate (M) <input type="checkbox"/> Heavy (H) <input type="checkbox"/> UNK <input checked="" type="checkbox"/> NA
Column Splice Damage: <input type="checkbox"/> None (N) <input type="checkbox"/> Insignificant (I) <input type="checkbox"/> Moderate (M) <input type="checkbox"/> Heavy (H) <input type="checkbox"/> UNK <input checked="" type="checkbox"/> NA
Damage to Brace Connections: <input type="checkbox"/> None (N) <input type="checkbox"/> Insignificant (I) <input type="checkbox"/> Moderate (M) <input type="checkbox"/> Heavy (H) <input type="checkbox"/> UNK <input checked="" type="checkbox"/> NA
Damage to Column-to-Foundation Connections: <input type="checkbox"/> None (N) <input type="checkbox"/> Insignificant (I) <input type="checkbox"/> Moderate (M) <input type="checkbox"/> Heavy (H) <input checked="" type="checkbox"/> UNK <input type="checkbox"/> NA
Damage to Connections of Precast Elements that are Part of the Lateral Force Resisting System: <input type="checkbox"/> None (N) <input type="checkbox"/> Insignificant (I) <input type="checkbox"/> Moderate (M) <input checked="" type="checkbox"/> Heavy (H) <input type="checkbox"/> UNK <input type="checkbox"/> NA

Foundations

Foundations Cracked or Otherwise Damaged: <input type="checkbox"/> None (N) <input type="checkbox"/> Insignificant (I) <input type="checkbox"/> Moderate (M) <input type="checkbox"/> Heavy (H) <input checked="" type="checkbox"/> UNK <input type="checkbox"/> NA
Slabs-on-Grade Cracked or Otherwise Damaged: <input type="checkbox"/> None (N) <input type="checkbox"/> Insignificant (I) <input type="checkbox"/> Moderate (M) <input type="checkbox"/> Heavy (H) <input checked="" type="checkbox"/> UNK <input type="checkbox"/> NA

Equipment and Systems (only complete to extent that this is useful to estimate peak demands on structure)

Electrical Equipment Damage Including Backup Generators: <input type="checkbox"/> None (N) <input type="checkbox"/> Insignificant (I) <input type="checkbox"/> Moderate (M) <input type="checkbox"/> Heavy (H) <input checked="" type="checkbox"/> UNK <input type="checkbox"/> NA
Damage to Boilers, Chillers, Tanks, etc.: <input type="checkbox"/> None (N) <input type="checkbox"/> Insignificant (I) <input type="checkbox"/> Moderate (M) <input type="checkbox"/> Heavy (H) <input checked="" type="checkbox"/> UNK <input type="checkbox"/> NA
HVAC Damage (Fans, Ducts) : <input type="checkbox"/> None (N) <input type="checkbox"/> Insignificant (I) <input type="checkbox"/> Moderate (M) <input type="checkbox"/> Heavy (H) <input checked="" type="checkbox"/> UNK <input type="checkbox"/> NA
Damage to Water and Sprinkler Lines and Fire Pumps: <input type="checkbox"/> None (N) <input type="checkbox"/> Insignificant (I) <input type="checkbox"/> Moderate (M) <input type="checkbox"/> Heavy (H) <input checked="" type="checkbox"/> UNK <input type="checkbox"/> NA
Elevator Equipment Damage (Car and Counterweight Rails, Cars, Penthouse Equipment): <input type="checkbox"/> None (N) <input type="checkbox"/> Insignificant (I) <input type="checkbox"/> Moderate (M) <input type="checkbox"/> Heavy (H) <input checked="" type="checkbox"/> UNK <input type="checkbox"/> NA

Additional Comments (use additional pages if necessary):
--

Figure A-1 Postearthquake Building Performance Assessment Form (page 6 of 6).

ATC-38 POSTEARTHQUAKE BUILDING PERFORMANCE ASSESSMENT FORM

SURVEYOR INSTRUCTIONS

This form should be filled out as completely as possible by the surveyor(s). Do not leave blank spaces; use "UNK" for "Unknown", "NA" for "Not Applicable", or "None" when appropriate. Talk with the owner to obtain as much information as possible. Assure him/her that detailed name and address information will not be released to the public. Photos should be taken of each exterior building elevation, and of any locations where significant damage is visible. For each strong motion site, obtain or sketch a map of the block or blocks surveyed to identify the locations of each building relative to the strong motion instrument. Distances from the buildings to the instrument should be determined wherever possible.

The ATC-38 Postearthquake Building Assessment Form includes 11 sections as listed below. Refer to the *Glossary of Terms and Codes* for classifications and codes that should be used on the form. The form is intended to be self-explanatory; however, some clarifying comments are included here for each of the 11 sections. In all cases, write down as much information as possible, and state any assumptions you need to make about the building and/or its performance. Too much or repeated information is always better than incomplete information.

1. **Building Site Information.** For Building ID#, use the following notation: station owner, last 3 digits of station number, initials of surveyor, and sequential number. (For example: CDMG386-ER-01.) Be sure to include the Building ID number on each page and indicate the number of pages. For Photo ID#, make sure to note the number(s) on the film roll that were taken of the given building. When the film is developed, write the same numbers on the back of each photo so they will be matched to the proper building.
2. **Building Construction Data.** If possible, indicate design date and construction date by year, not decade.
3. **Model Building Type.** If the building has different model building types in different directions or on different floors, describe in the space provided.
4. **Performance Modifiers.** In this section, describe any other vertical or plan irregularities that are not listed on the form, including unusual pre-earthquake building conditions.
5. **Plan Sketch of Building.** Provide a sketch of the building footprint. Annotate the sketch as appropriate. Note on the sketch the assumed east-west and north-south directions if they are used in other sections of the form, and include a north arrow. Surveyors should carry a compass.
6. **Nonstructural Elements.** Refer to the *Glossary* for codes to be used for cladding and partition types.
7. **General Damage.** This section should be descriptive as well as quantitative. Indicate the General Damage Classification that corresponds to the worst damage to any specific element. (This should be the same General Damage Classification as that checked in Section 1.) Estimate the ATC-13 damage state as defined in the *Glossary* for each building area as shown (for residences, consider chimneys and veneer to be nonstructural and water heaters to be equipment). In the space provided for comments, include possible reasons for damage if appropriate. For buildings with General Damage Classification of "M" or "H", fill out the 2-page *Detailed Damage Description* as described below.

Figure A-2 Surveyor instructions (page 1 of 4).

8. **Nonstructural Damage.** Indicate damage to partitions, lights, ceilings, and contents in terms of General Damage Classification as defined in the *Glossary*.
9. **Injuries or Fatalities.** Include comments where appropriate, such as unusual reasons for casualties.
10. **Functionality.** Indicate percentage of space that can be used for the building's original pre-earthquake function for the various time periods listed, as well as the amount of time needed to restore the building to its full pre-earthquake functionality. In the comments section, include any reasons for closure and note if the building can only be accessed for clean-up.
11. **Geotechnical Failures.** In this section, describe any other geotechnical failures or unusual features that are not listed on the form.

After the 11 main sections of the form, space is provided for additional comments pertaining to any section of the form. Attach additional sheets if necessary, making sure to label each sheet with the Building ID number. For buildings with General Damage Classification of "M" or "H", fill out the 2-page *Detailed Damage Description* as briefly described below.

Detailed Damage Description. This part of the form should be filled out as completely as possible for any buildings with General Damage Classification of "M" or "H". It includes sections for Vertical Elements, Horizontal Elements, Connections, Foundations, and Equipment and Systems. In each case the damage should be described in terms of the General Damage Classification defined in the *Glossary*. Make sure to use "NA" or "UNK" as appropriate. Use the notes section to include additional information about the building and the damage, such as differences by direction or floor level in damage or model building type. The notes section may also be used to indicate the location (i.e., ground floor or top story) of extensive damage to equipment and systems. Add extra pages if necessary, making sure to label each one with the Building ID number.

Figure A-2 Surveyor instructions (page 2 of 4).

ATC-38 GLOSSARY OF TERMS AND CODES

General Damage Classification:

Code	Description
N	No damage is visible, either structural or nonstructural.
I	Damage requires no more than cosmetic repair. No structural repairs are necessary. For nonstructural elements this would include spackling partition cracks, picking up spilled contents, putting back fallen ceiling tiles, and repositioning equipment and furnishings.
m	Minor repairable structural or nonstructural damage has occurred. Repairs can be made without significant disruption to occupants. This damage state includes cracked or dislodged masonry requiring repair.
M	Repairable structural damage has occurred. The existing elements can be repaired in place, without substantial demolition or replacement of elements. For nonstructural elements this would include minor replacement of damaged partitions, ceilings, contents, or equipment.
H	Damage is so extensive that repair of elements is either not feasible or requires major demolition or replacement. Includes URM buildings that require partial or complete reconstruction of damaged masonry walls. For nonstructural elements this would include major or complete replacement of damaged partitions, ceilings, contents, or equipment.
C	Partial or complete loss of gravity support with collapse.

Occupancy Type:

Occupancy Type	Code
Apartment	A
Auto Repair	AR
Church	C
Dwelling	D
Data Center	DC
Garage	G

Gas Station	GS
Government	GV
Hospital	H
Hotel	HL
Manufacturing	M
Office	O
Restaurant	R

Retail	RS
School	S
Theater	T
Utility	U
Warehouse	W
Other	OTH
Unknown	UNK

Model Building Type:

Framing System	Reference Codes and Diaphragm Types
Steel Moment Frame	S1 - Stiff Diaphragms; S1A - Flexible Diaphragms
Steel Braced Frame	S2 - Stiff Diaphragms ; S2A - Flexible Diaphragms
Steel Light Frame	S3
Steel Frame w/ Concrete Shear Walls	S4 - Stiff Diaphragms; S4A - Flexible Diaphragms
Steel Frame w/ Infill Masonry Shear Walls	S5 - Stiff Diaphragms; S5A - Flexible Diaphragms
Concrete Moment Frame	C1 - Stiff Diaphragms; C1A - Flexible Diaphragms
Concrete Shear Wall Building	C2 - Stiff Diaphragms; C2A - Flexible Diaphragms
Concrete Frame w/ Infill Masonry Shear Walls	C3 - Stiff Diaphragms ; C3A - Flexible Diaphragms
Reinforced Masonry Bearing Wall	RM1 - Flexible Diaphragms; RM2 - Stiff Diaphragms
Unreinforced Masonry Bearing Wall	URM - Flexible Diaphragm; URMA - Stiff Diaphragm
Precast/Tiltup Concrete Shear Walls	PC1 - Flexible Diaphragms; PC1A - Stiff Diaphragms
Precast Concrete Frame w/ Conc. Shear Walls	PC2
Wood Light Frame	W1
Commercial or Long-Span Wood Frame	W2
Mobile Home/School Portable	MH
Multi-unit, multi-story residential	W1A

Figure A-2 Surveyor instructions (page 3 of 4).

ATC-38 GLOSSARY OF TERMS AND CODES (continued)

Exterior Cladding/Glazing Codes:

Cladding/Glazing Type	Code
Stucco	S
Wood Product	W
Curtain Wall	C
Brick	B
Glass	G
Concrete	O
Metal	M
Exposed Structure	E
Window Wall	I
Pre-cast Panels	P
PC Fascia	F
Stone	N
Marble	R
URM	U
Masonry	Y
Ceramic Tiles	T

Partitions Codes:

Partition Type	Code
Gypsum Board	G
Plaster	P
Wood Lath	W
URM	U
Metal	M
Concrete	C
Brick	B
Marble	R
Masonry	Y

Ceilings Codes:

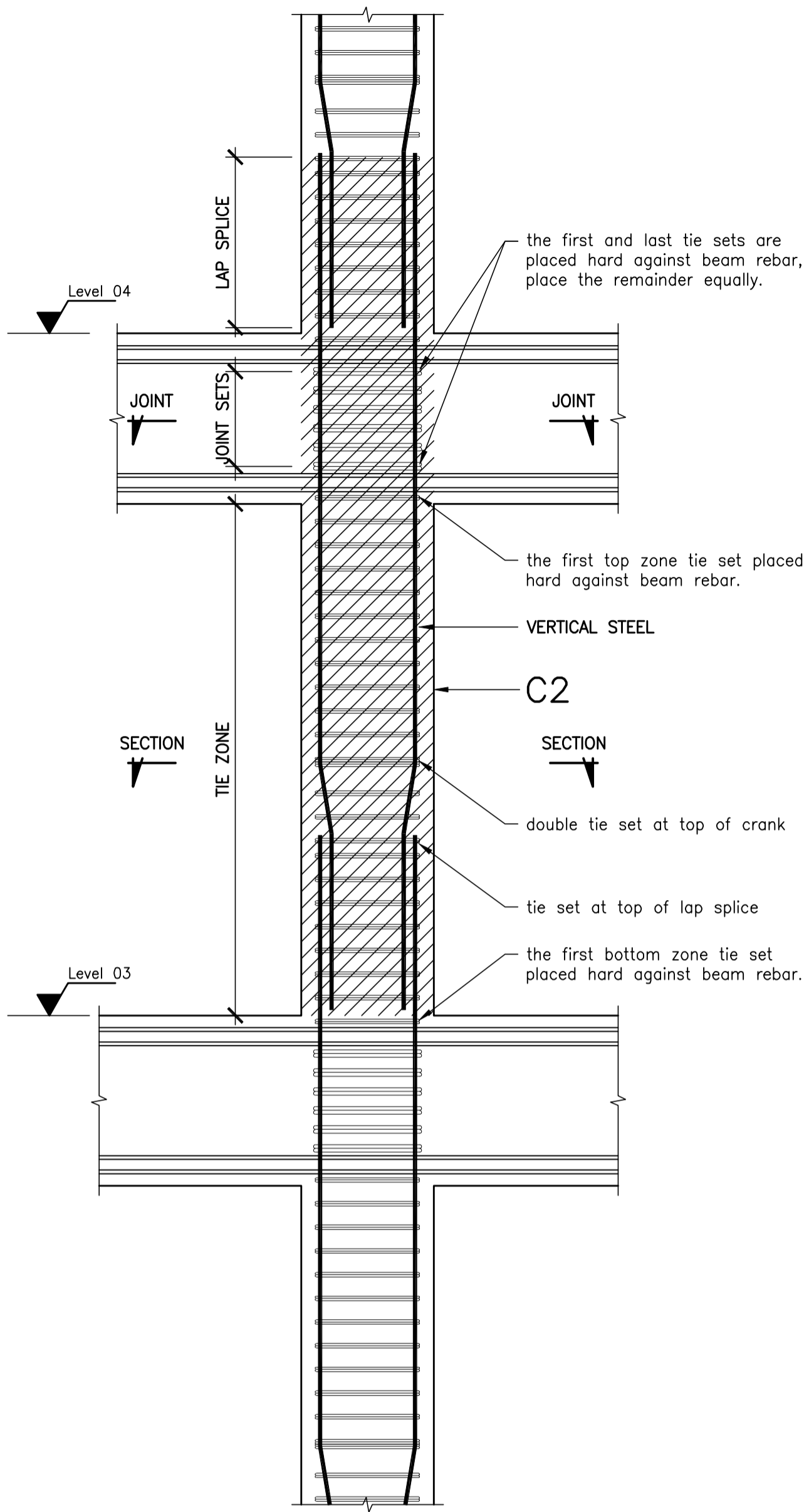
Ceiling Type	Code
Gypsum Board – nailed directly to framing	G
Gypsum Board - suspended	H
Suspended Tile	S
Lath and plaster – attached directly to framing	L
Lath and plaster - suspended	P
Exposed Slab	E
Metal	M
Wood	W
Glued Tiles	T
Suspended acoustic T-Bar	A

ATC-13 Damage State Definitions:

Damage State	Percent Damage (damaged value ÷ replacement value)
0 Unknown	Unknown
1 None	0%
2 Slight	0% - 1%
3 Light	1% - 10%
4 Moderate	10% - 30%
5 Heavy	30% - 60%
6 Major	60% - 100%
7 Destroyed	100%

Figure A-2 Surveyor instructions (page 4 of 4).

Frame Damage Elevations



typical column elevation

refer to schedule for details

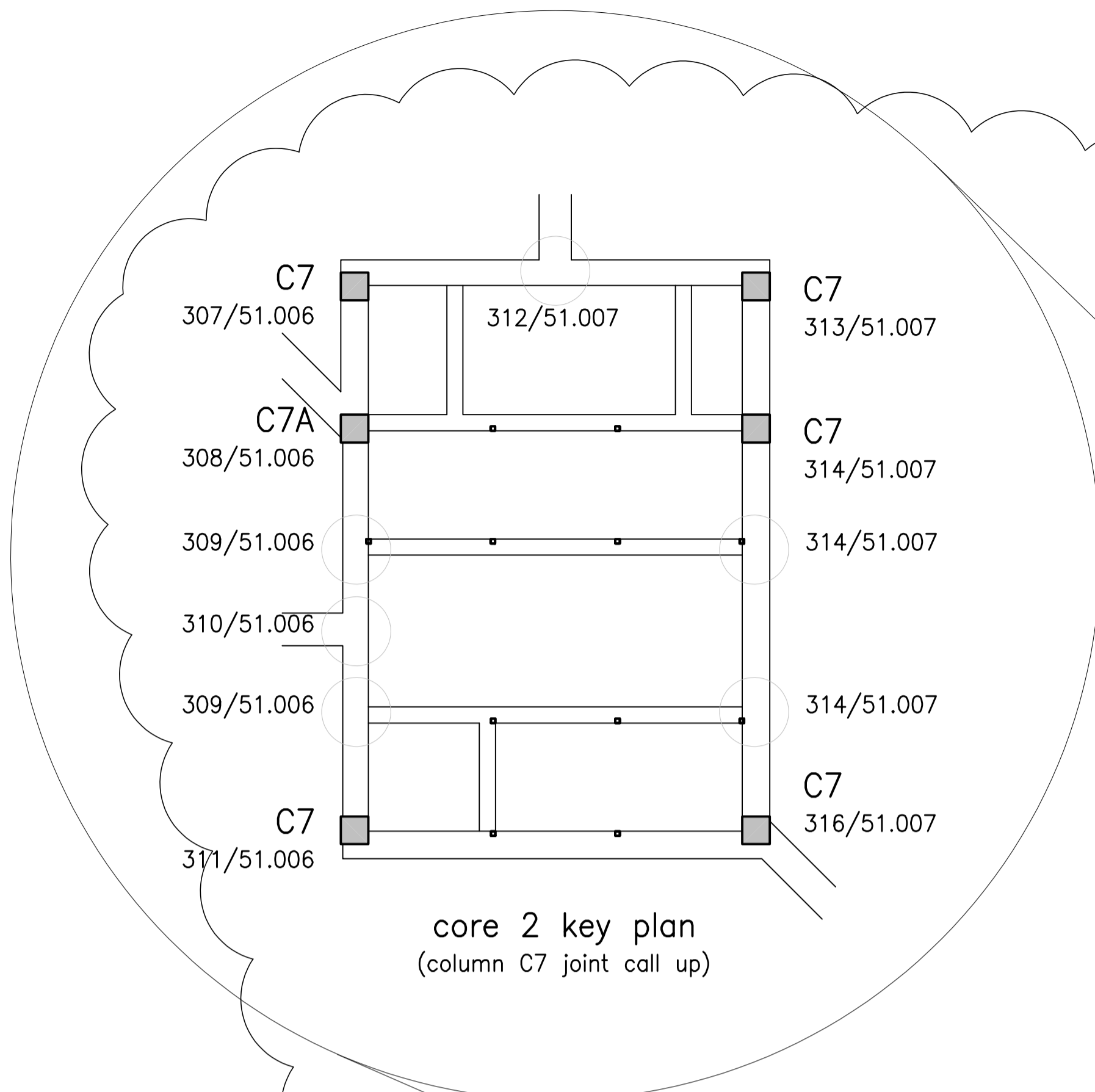
DEFORMED GRADE 500	
Bar size	Lap length
YD32	1350
YD25	900
YD20	600
YD16	500

to lap bars of unequal size use lap length for larger bar

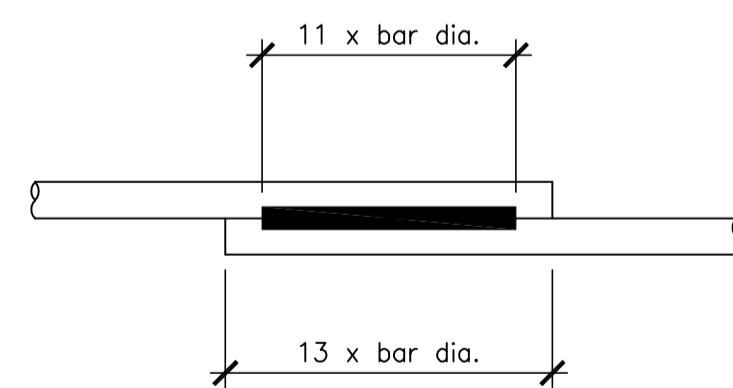
lap schedule for columns

Notes:

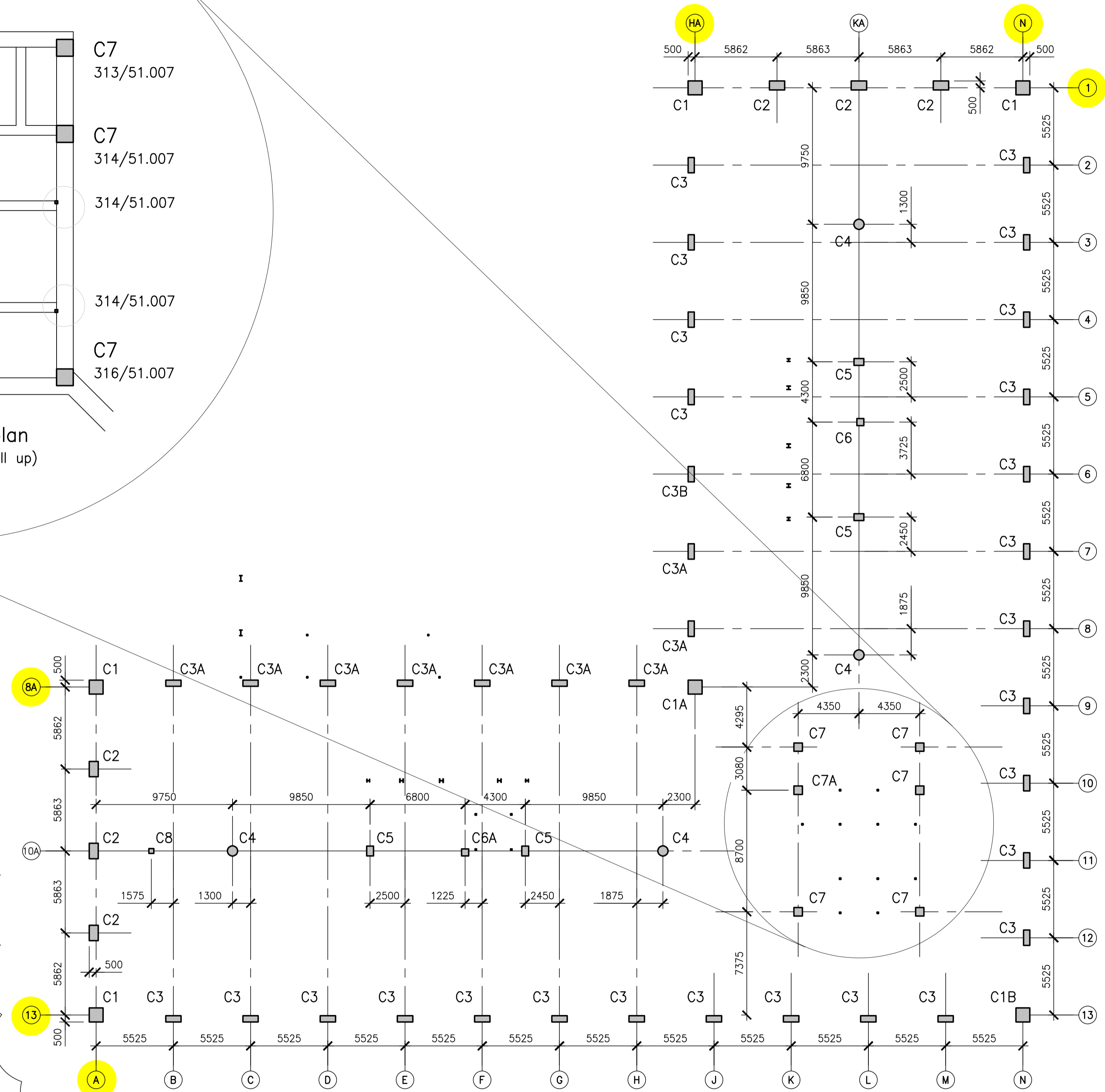
- All column reinforcement is to be grade 500E - YD.
- All perimeter column starter bars are to be grade 300E - D.
- Concrete strength varies, refer to the individual cells of the column schedule for MPa rating. It is acceptable to use a strength higher than that stated.
- Spiral ties may be substituted by welded hoops in beam/column joints, refer to lap welding detail for requirements.
- Spiral ties shall be lapped either by lap welding or a 135° termination. Lap splicing without either is not permitted.



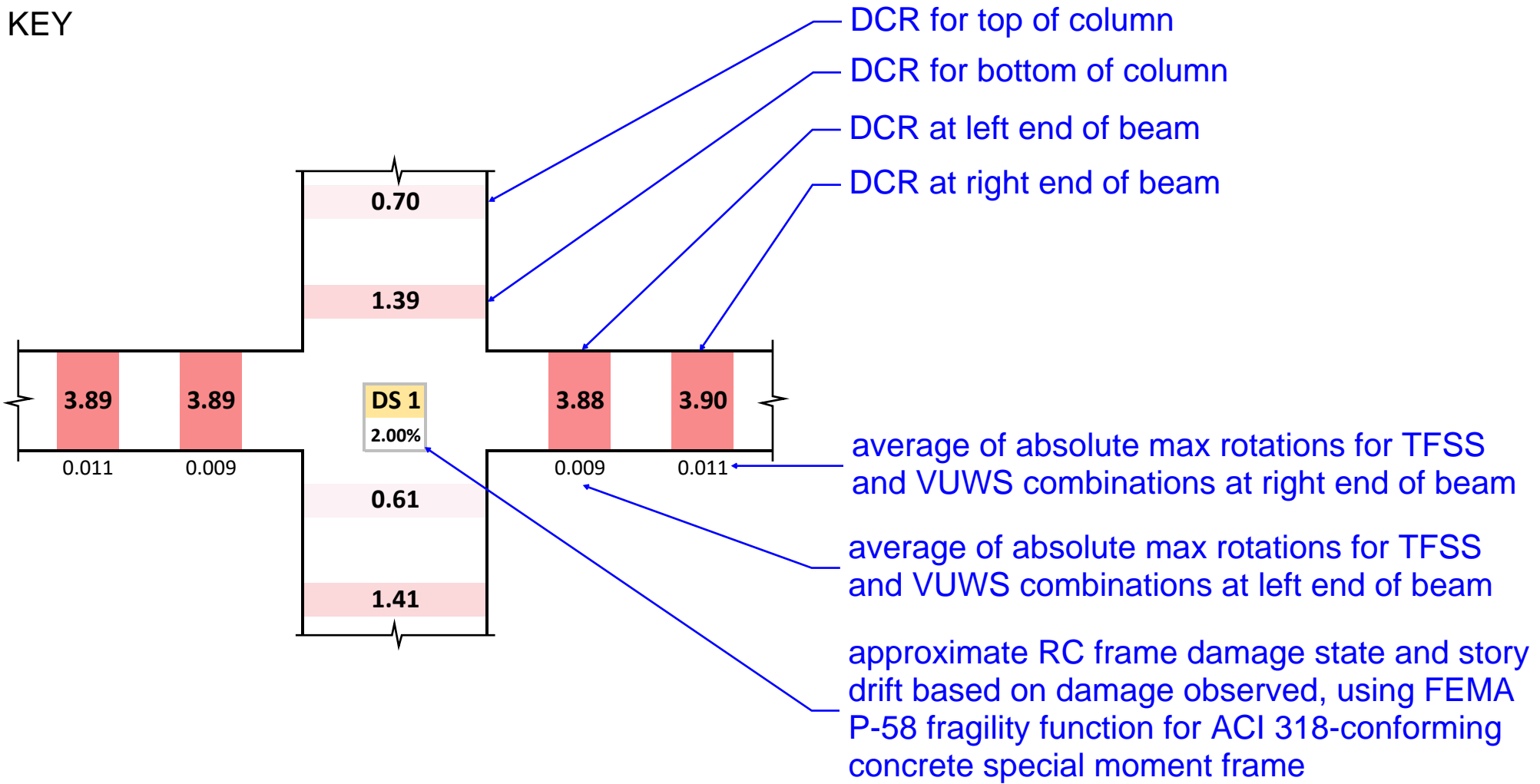
core 2 key plan
(column C7 joint call up)



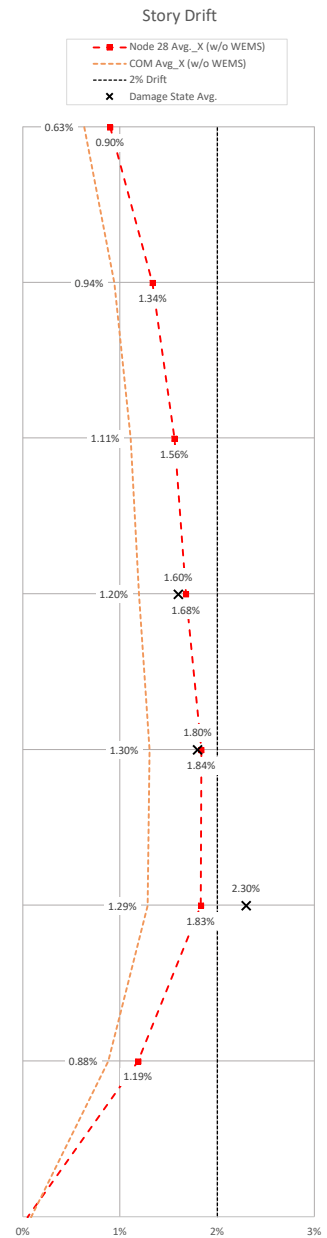
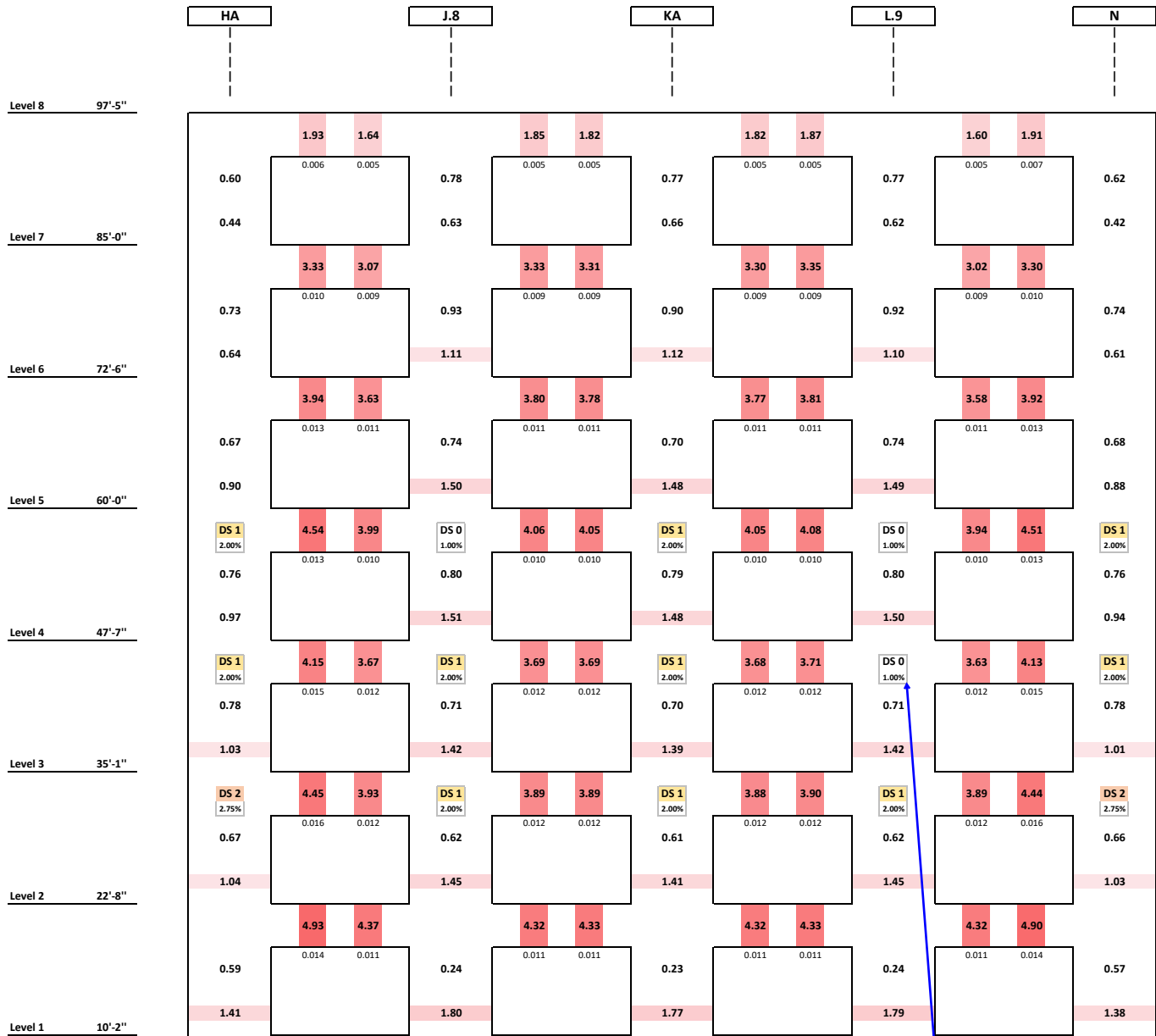
single lap weld detail
see NZS 4702



KEY

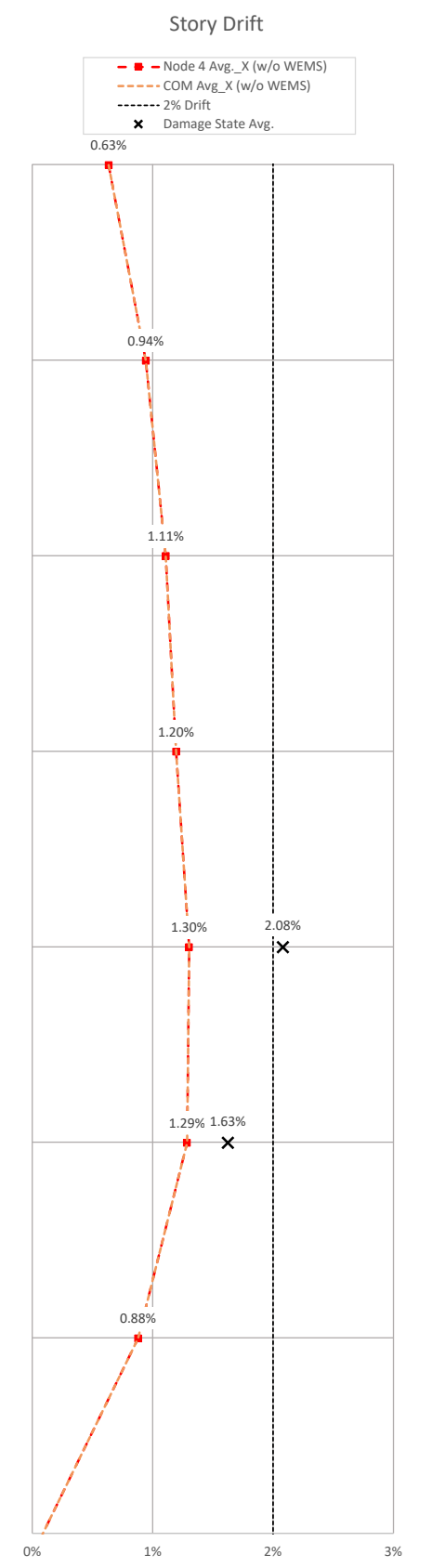
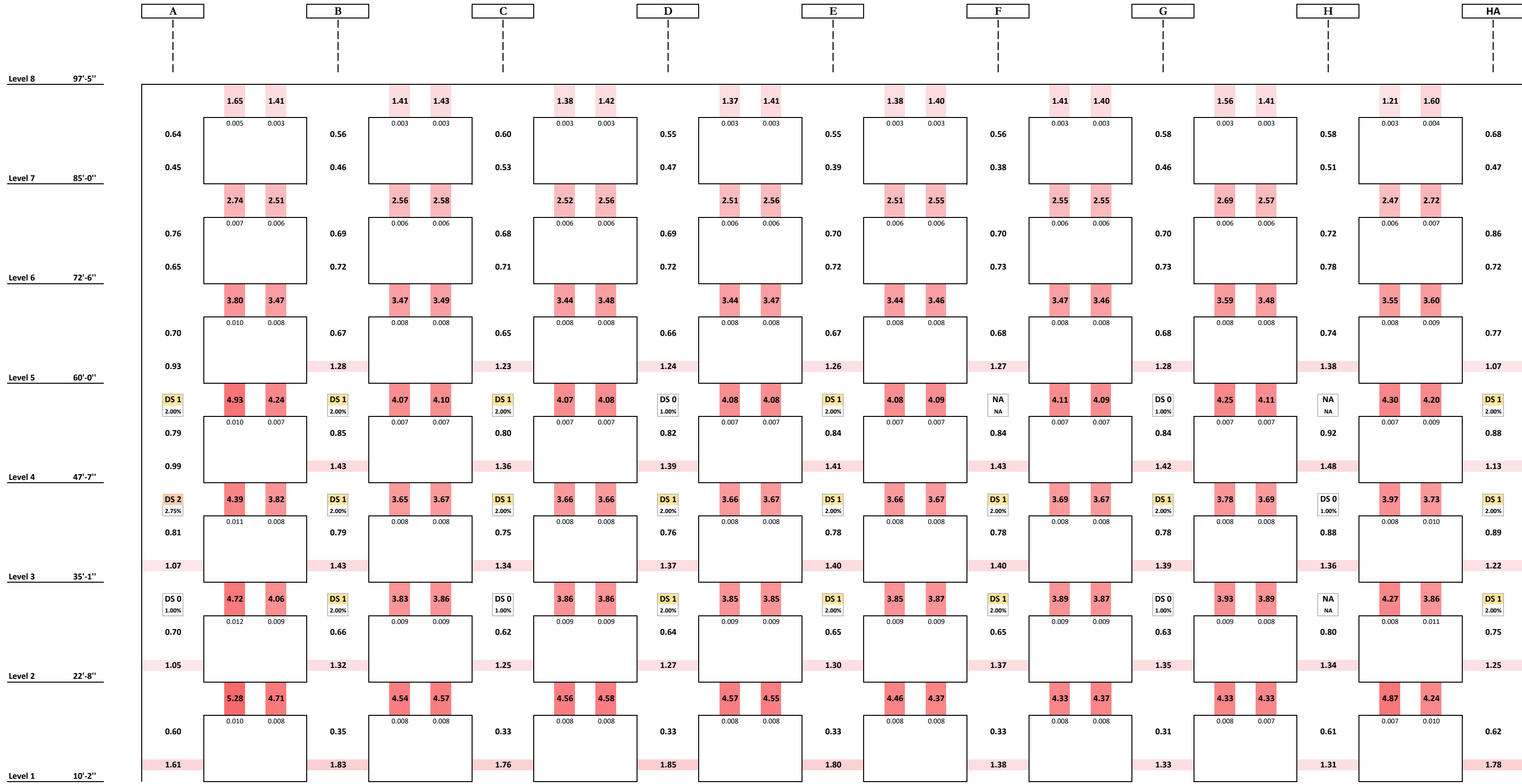


GRIDLINE 1 ELEVATION

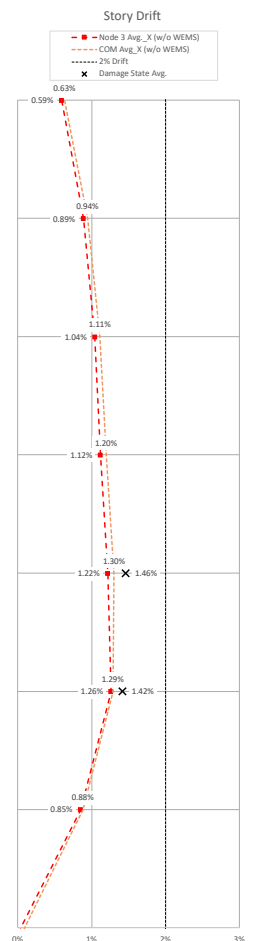
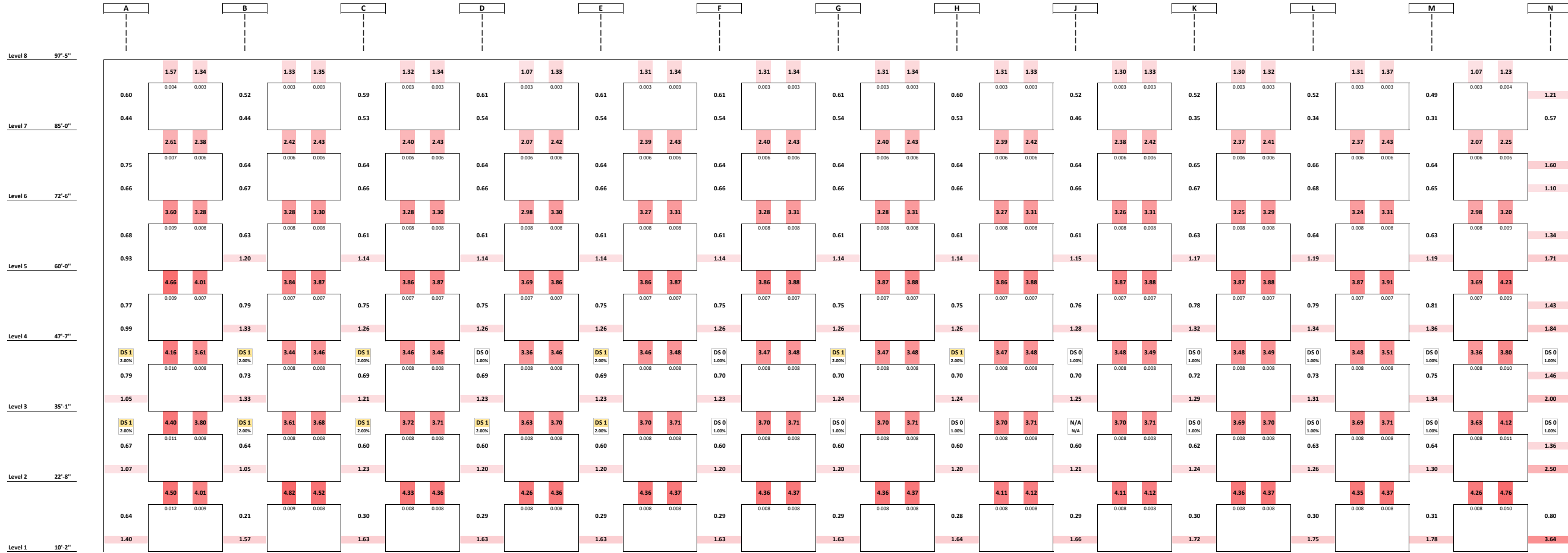


Note: DS0 = DS0.5 through App. B, as defined in the body of the report (1.0% median drift)

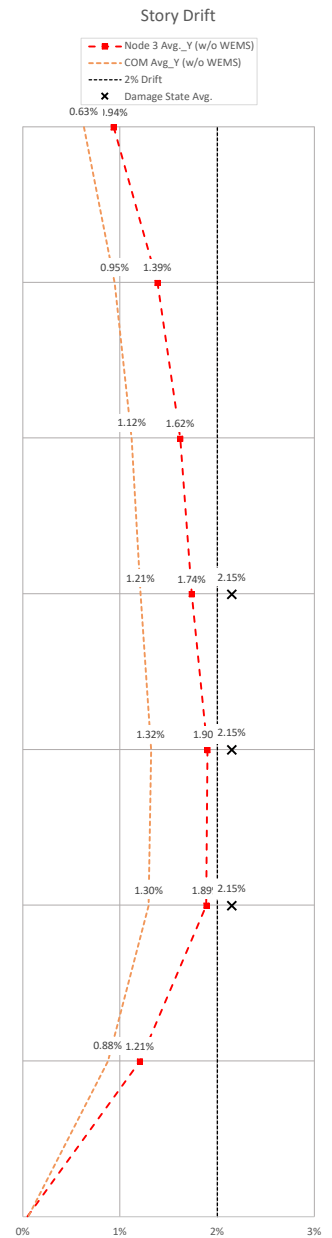
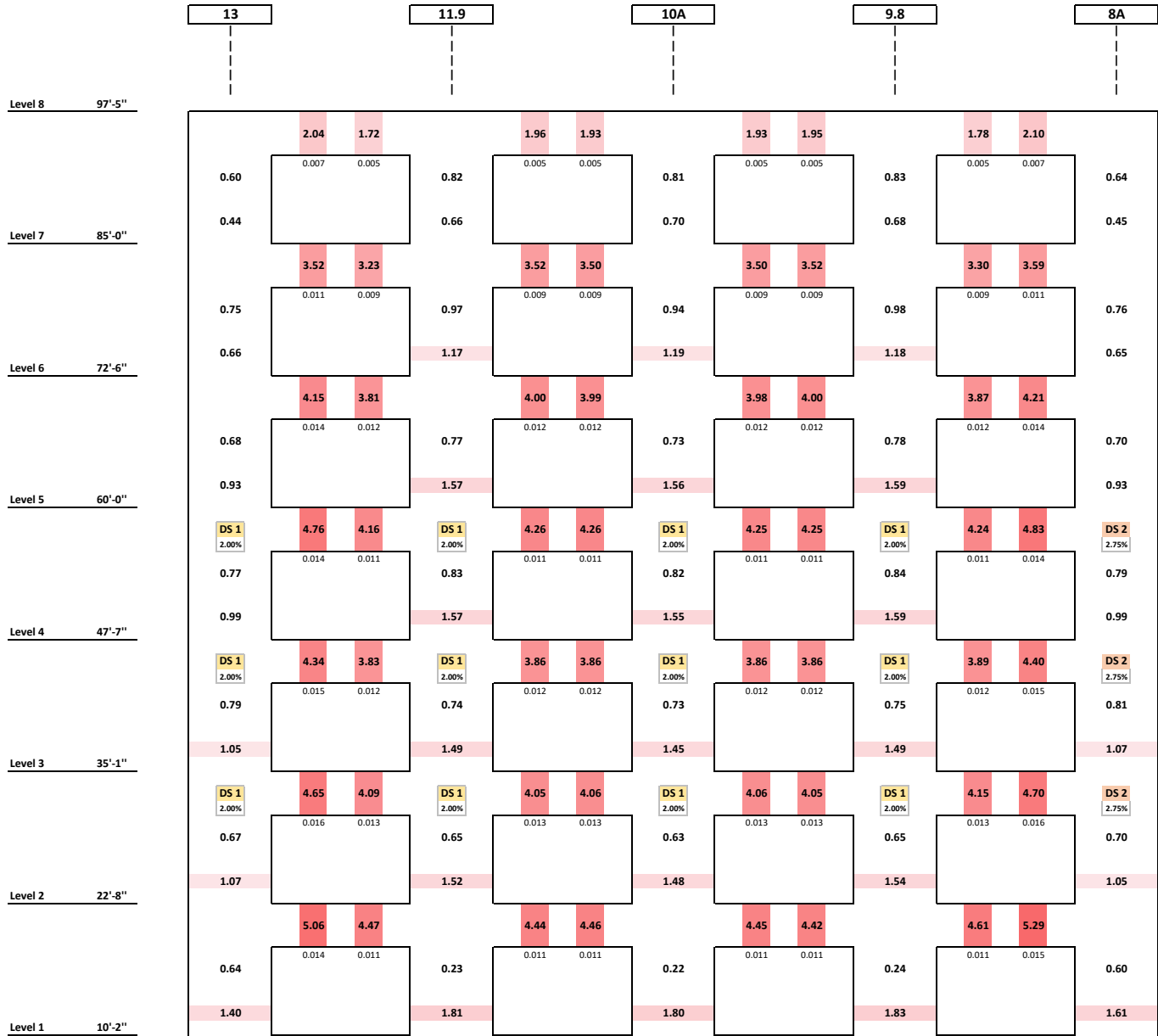
GRIDLINE 8A ELEVATION



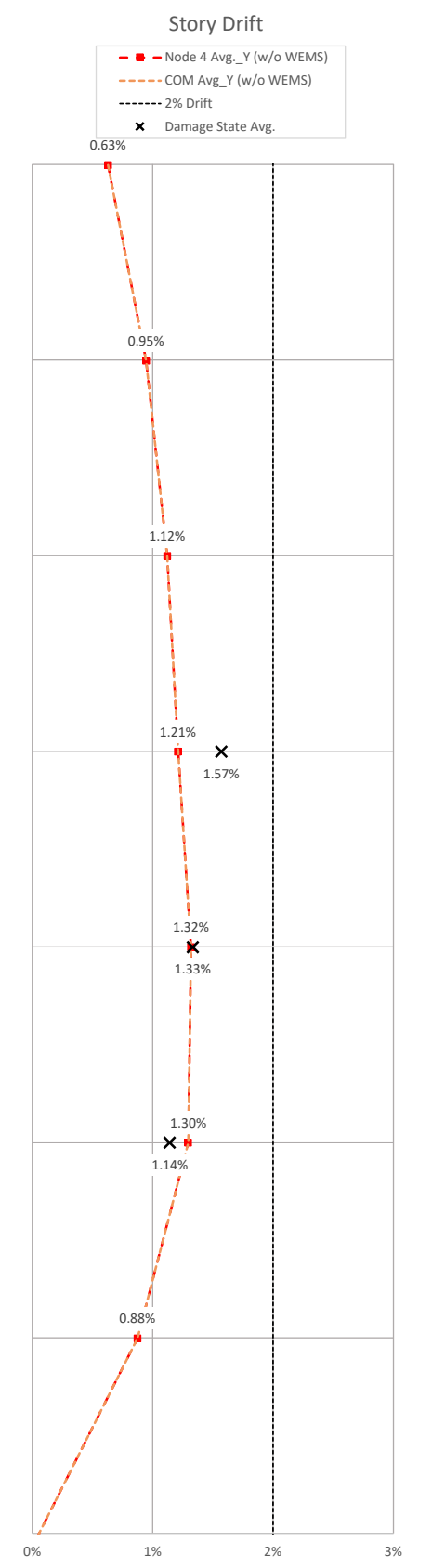
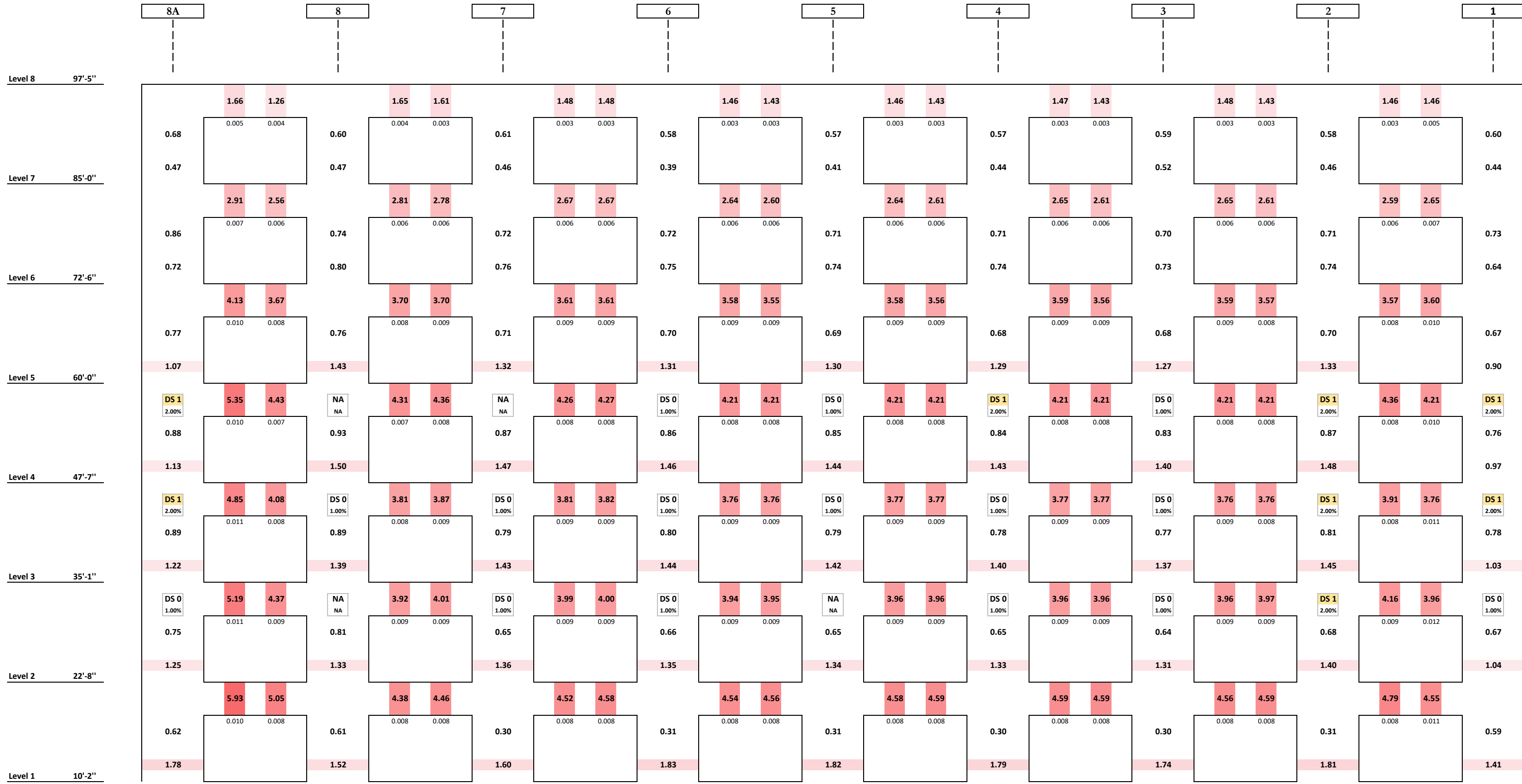
GRIDLINE 13 ELEVATION



GRIDLINE A ELEVATION

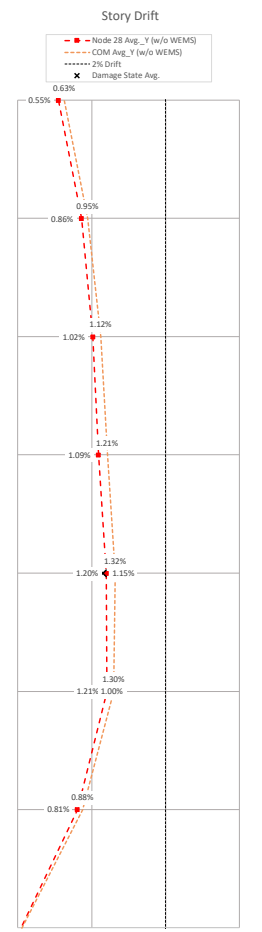


GRIDLINE HA ELEVATION

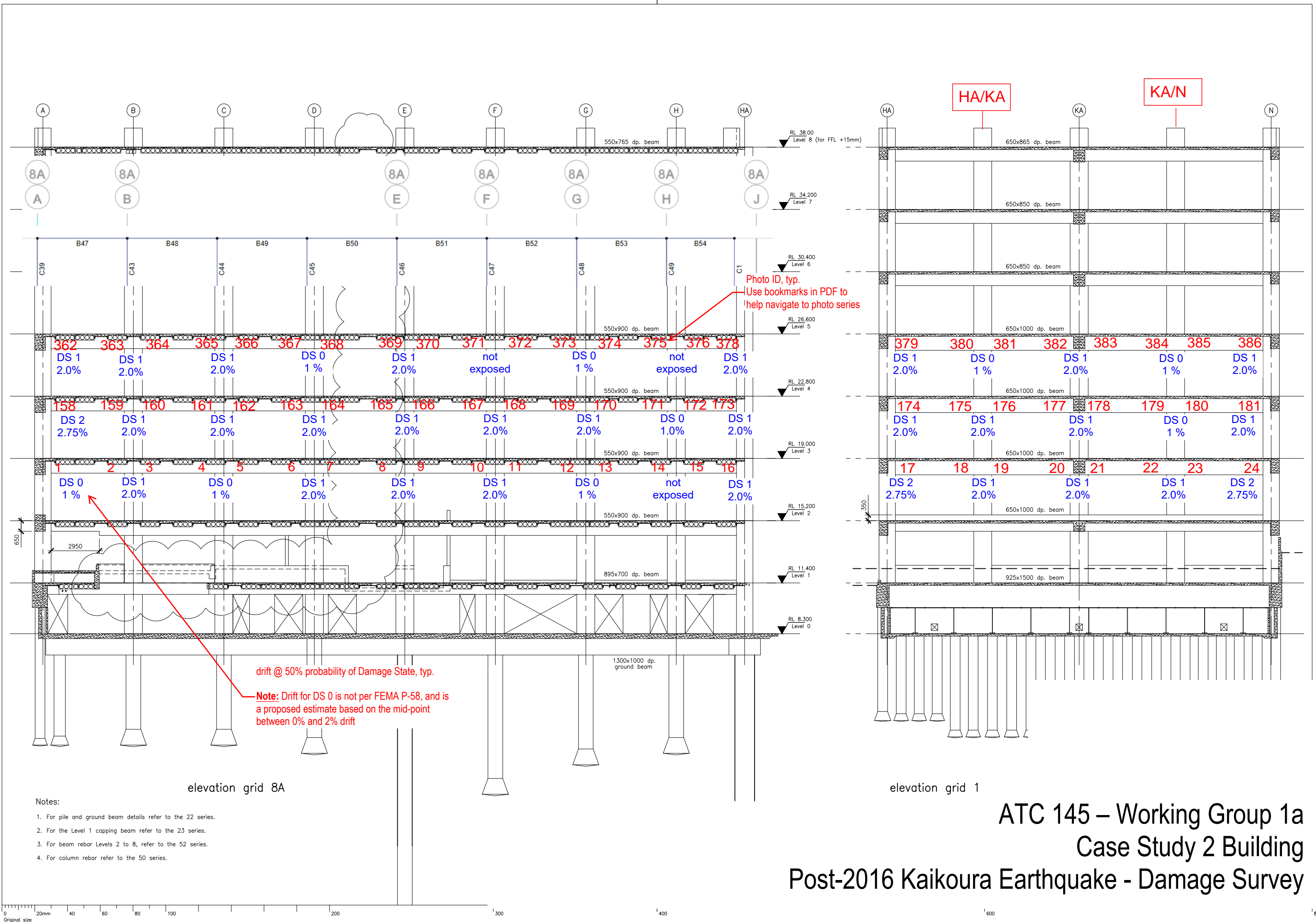


GRIDLINE N ELEVATION

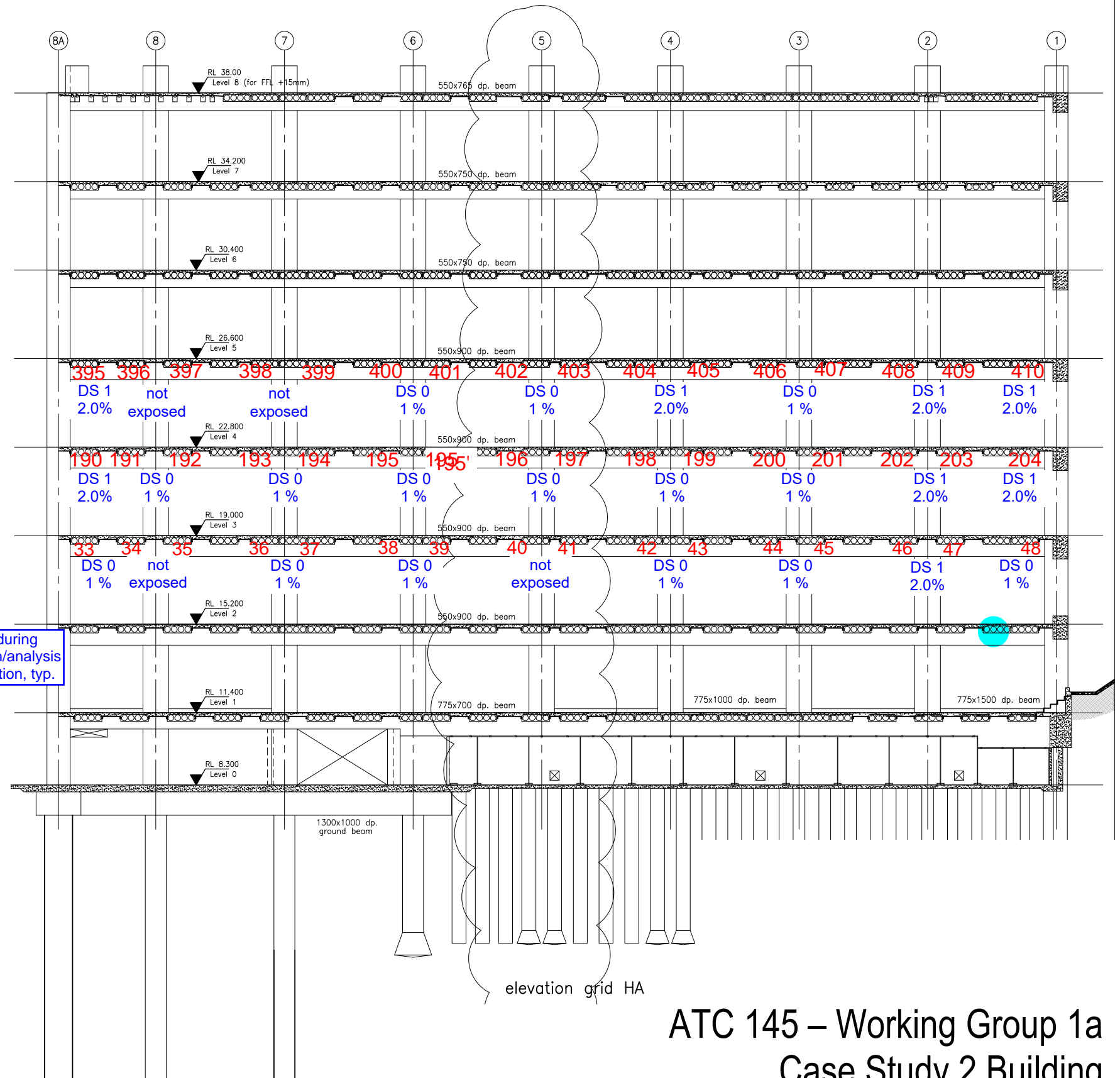
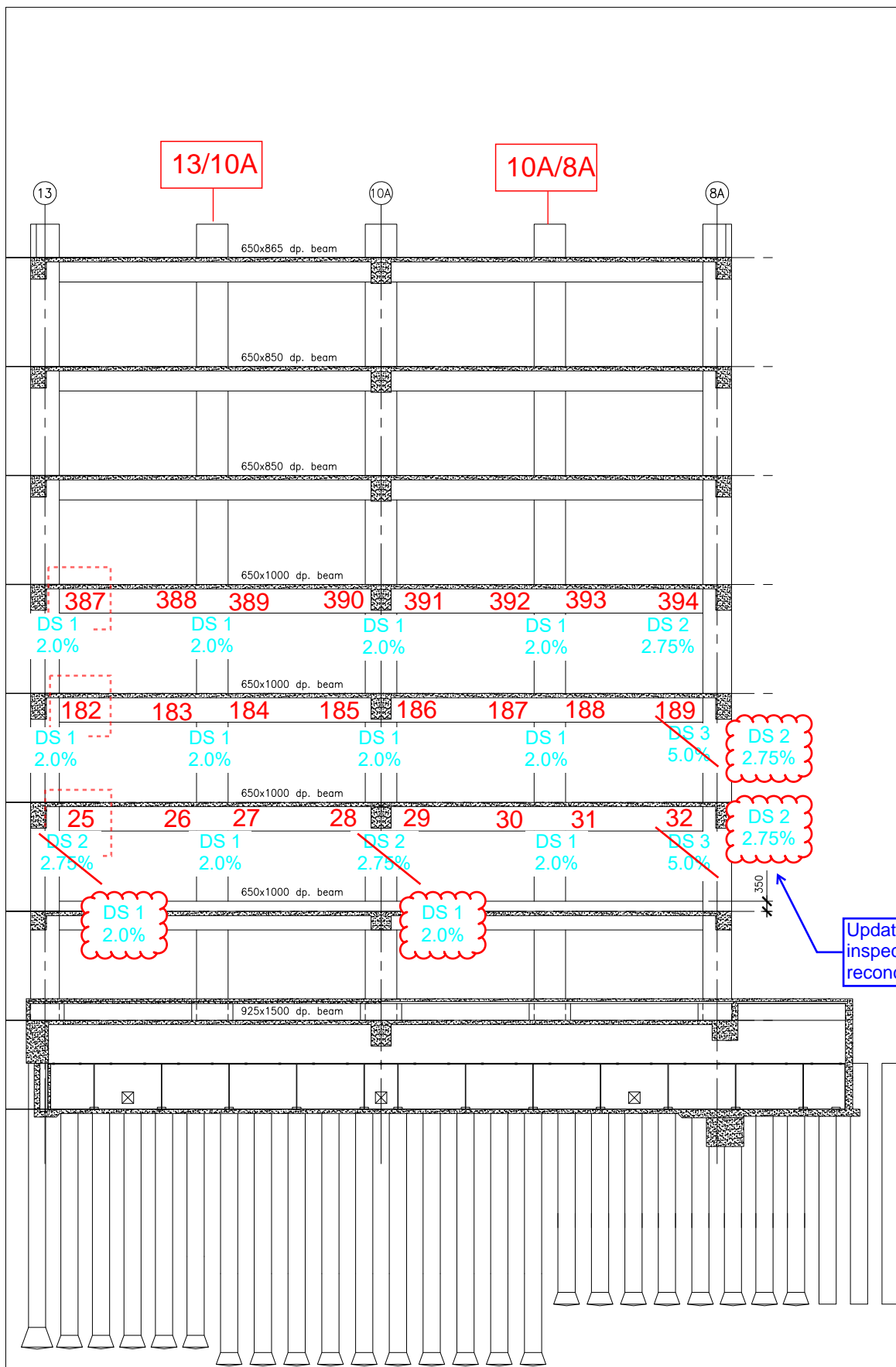
	13	12	11	10	9	8	7	6	5	4	3	2	1	
Level 8 97'-5"	1.24 0.004 0.003	1.08 0.003 0.003	1.36 0.003 0.003	1.32 0.003 0.003	1.31 0.003 0.003	1.31 0.003 0.003	1.30 0.003 0.003	1.31 0.003 0.003	1.32 0.003 0.003	1.34 0.003 0.003	1.33 0.003 0.003	1.33 0.003 0.003	1.34 0.003 0.003	1.33 0.003 0.003
Level 7 85'-0"	1.21 0.57	0.49 0.31	0.52 0.35	0.52 0.34	0.51 0.41	0.57 0.51	0.61 0.54	0.61 0.54	0.61 0.54	0.61 0.54	0.59 0.53	0.52 0.43	0.62 0.42	
Level 6 72'-6"	1.60 1.10	0.64 0.65	0.65 0.67	0.65 0.67	0.64 0.66	0.64 0.66	0.64 0.66	0.64 0.66	0.64 0.66	0.64 0.66	0.64 0.66	0.64 0.66	0.64 0.66	
Level 5 60'-0"	1.34 1.71	0.63 1.19	0.64 1.19	0.63 1.19	0.62 1.17	0.61 1.15	0.61 1.14	0.61 1.14	0.61 1.14	0.61 1.14	0.61 1.14	0.61 1.14	0.62 1.19	
Level 4 47'-7"	1.43 1.84	0.80 1.35	0.79 1.33	0.78 1.32	0.76 1.29	0.74 1.26	0.74 1.25	0.74 1.25	0.74 1.25	0.74 1.25	0.74 1.25	0.74 1.26	0.78 1.32	
Level 3 35'-1"	DS 1 2.00 1.46	3.76 0.010 0.008 0.74	3.33 0.008 0.008 0.72	DS 0 1.00% 3.46 0.008 0.008 0.72	3.45 0.008 0.008 0.72	DS 0 1.00% 3.43 0.008 0.008 0.70	3.44 0.008 0.008 0.69	DS 0 1.00% 3.53 0.008 0.008 0.70	3.44 0.008 0.008 0.69	DS 0 1.00% 3.43 0.008 0.008 0.69	3.45 0.008 0.008 0.69	DS 0 1.00% 3.44 0.008 0.008 0.69	3.45 0.008 0.008 0.69	DS 0 1.00% 3.44 0.008 0.008 0.69
Level 2 22'-8"	1.36 2.50	0.62 1.26	0.60 1.23	0.60 1.22	0.59 1.20	0.57 1.17	0.57 1.17	0.57 1.17	0.57 1.17	0.57 1.17	0.57 1.17	0.57 1.17	0.61 1.25	
Level 1 10'-2"	0.80 3.64	0.29 1.69	0.29 1.66	0.29 1.65	0.28 1.61	0.27 1.56	0.27 1.55	0.27 1.55	0.27 1.55	0.27 1.55	0.27 1.54	0.28 1.60	0.57 1.38	



Frame Visual Inspection



ATC 145 – Working Group 1a
 Case Study 2 Building
 Post-2016 Kaikoura Earthquake - Damage Survey



Notes:

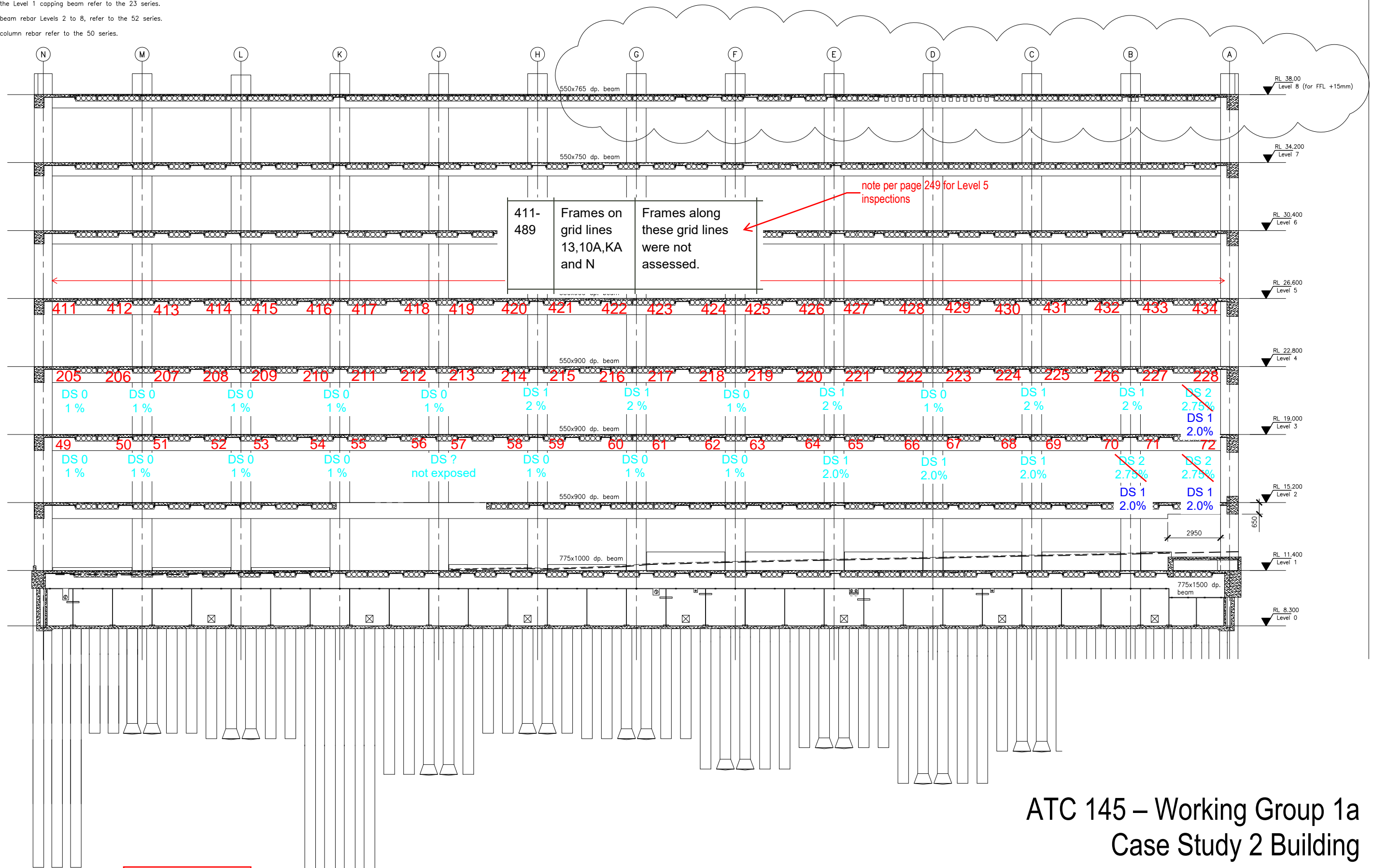
1. For pile and ground beam details refer to the 22 series.
2. For the Level 1 capping beam refer to the 23 series.
3. For beam rebar Levels 2 to 8, refer to the 52 series.
4. For column rebar refer to the 50 series.



ATC 145 – Working Group 1a
Case Study 2 Building
Post-2016 Kaikoura Earthquake - Damage Survey

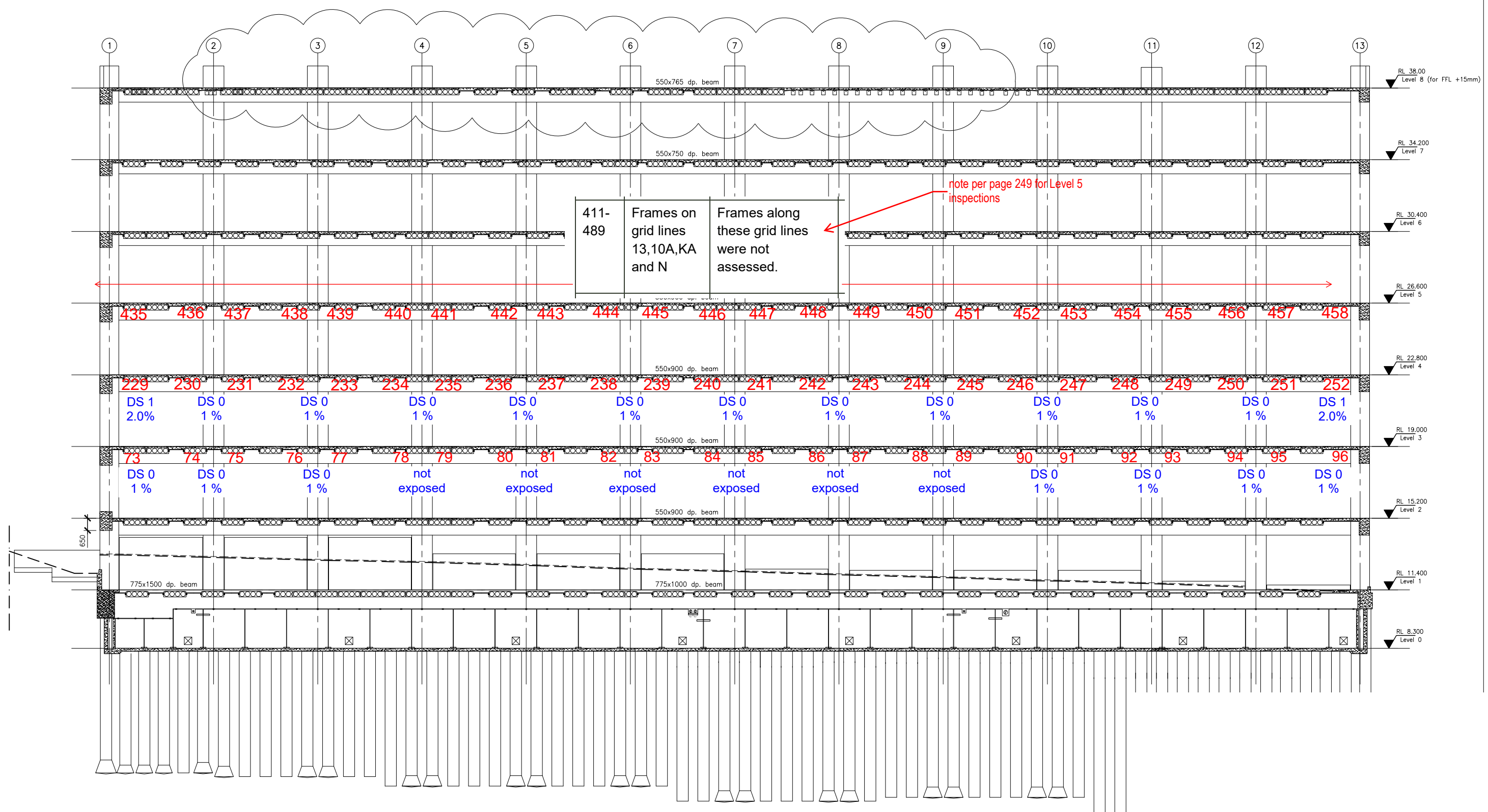
Notes:

1. For pile and ground beam details refer to the 22 series.
2. For the Level 1 capping beam refer to the 23 series.
3. For beam rebar Levels 2 to 8, refer to the 52 series.
4. For column rebar refer to the 50 series.



elevation grid 13

ATC 145 – Working Group 1a
Case Study 2 Building
Post-2016 Kaikoura Earthquake - Damage Survey


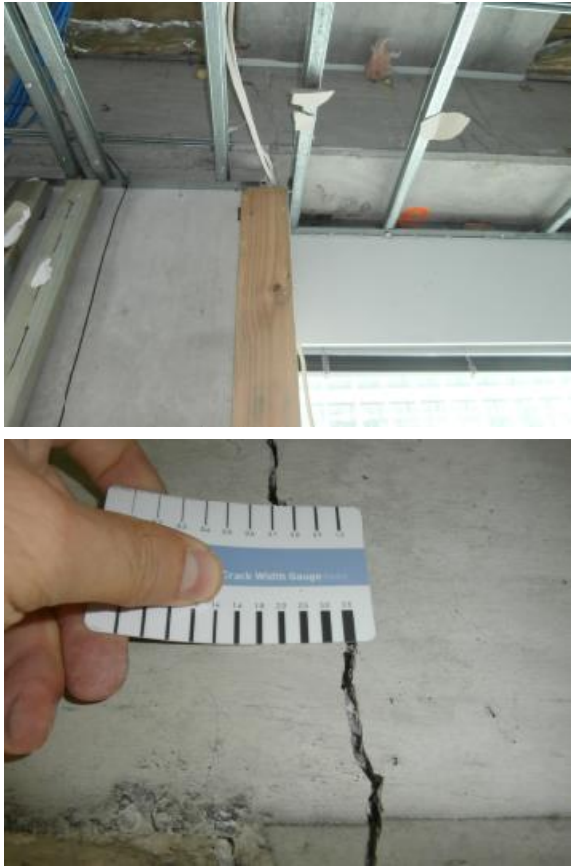



elevation grid N



- Notes:
1. For pile and ground beam details refer to the 22 series.
 2. For the Level 1 capping beam refer to the 23 series.
 3. For beam rebar Levels 2 to 8, refer to the 52 series.
 4. For column rebar refer to the 50 series.



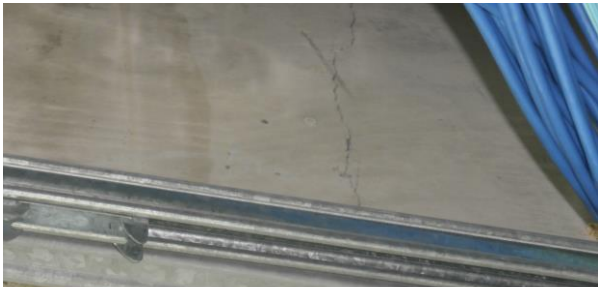
ATC 145 – Working Group 1a
 Case Study 2 Building
 Post-2016 Kaikoura Earthquake - Damage Survey




transverse drift (floor unit rotation)

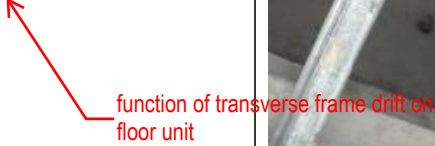

ID.	Location	Comment	Photographs
1	Elevation 8A-Grid A. Beam column joint underside of level 3 DS 0 1 %	Loss of concrete in the beam. Loss of support to Dycore units, seating is exposed. Approximately 11 hairline cracks along the beam	
2/3	Elevation 8A-Grid B. Beam column joint underside of level 3 DS 1 2.0%	Vertical cracks in the plastic hinge region of the beam. Crack size range from 0.8-3.5 mm. Concrete crushed in the beam.	
4/5	Elevation 8A-Grid C. Beam column joint underside of level 3 DS 0 1 %	Vertical cracks at beam column joint 0.8-1.5 mm Diagonal cracks in beam approx. 0.3 mm	


DS 1



			
6/7	Elevation 8A- Grid D. Beam column joint underside of level 3 DS 1 2.0%	Vertical cracking at beam column joint 0.8-1.5 mm Spalling of concrete in beam column joint	

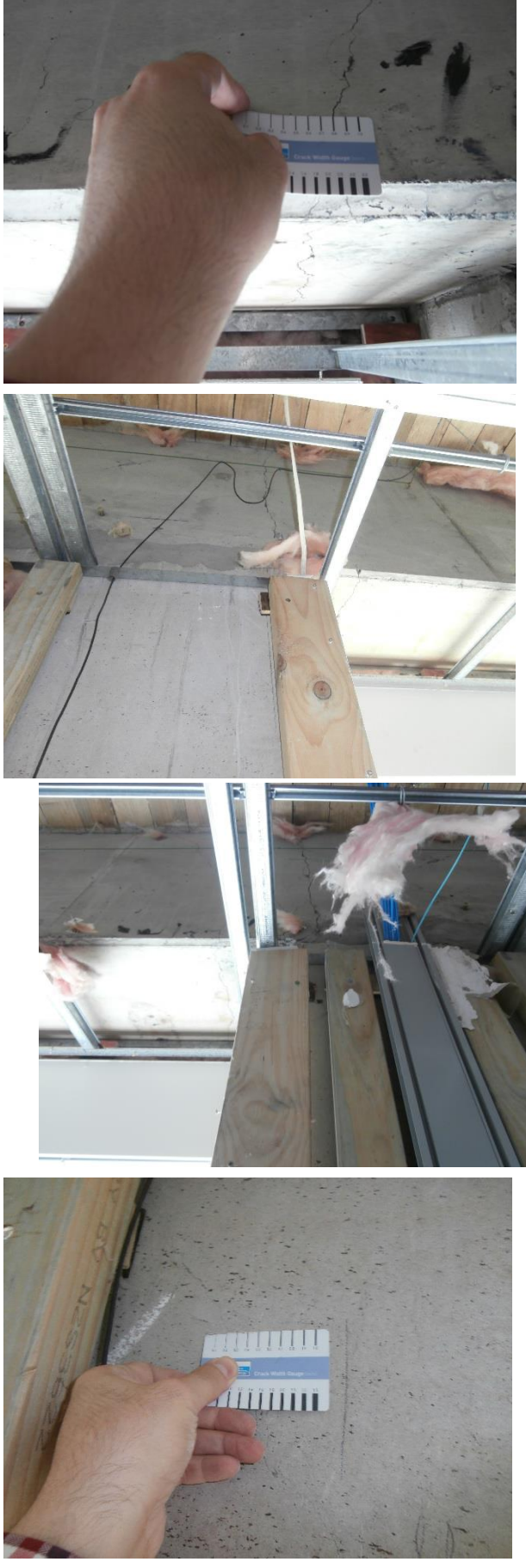
			
<p>8/9</p>	<p>Elevation 8A- Grid E. Beam column joint underside of level 3</p> <p>DS 1 2.0%</p>	<p>Spalling of concrete on right hand side of beam column joint Vertical crack at beam column joint 0.8 mm</p>	
<p>10/11</p>	<p>Elevation 8A- Grid F. Beam column joint underside of level 3</p>	<p>Vertical cracking at beam column joint approx. 1-1.5 mm Spalling in beam</p>	

			
<p>12/13</p>	<p>Elevation 8A- Grid G. Beam column joint underside of level 3</p> <p>DS 0 1 %</p>	<p>Vertical crack at beam column joint approx. 1 mm</p>	
<p>14/15</p>	<p>Elevation 8A- Grid H. Beam column joint underside of level 3</p> <p>not exposed</p>	<p>Column lining was still in place, as per photo. Beam column joint was exposed but we could not inspect for cracking.</p>	

16	Elevation 8A- Grid HA. Beam column joint underside of level 3 DS 2 2.75% DS 1 2.0%	Approximately 2.5 mm wide vertical crack on the face of the beam column joint. Diagonal crack underside of the Dycore unit. Concrete crushed and loss of support. 	
----	--	---	---


17	Elevation 1- Grid HA. Beam Column joint underside of level 3 DS 2 2.75%	Three diagonal cracks of width ~7 mm. Vertical crack at the column face. Spalling of concrete in both the column and beam. Cracks along the beam.	
----	---	--	---

			
<p>18/19.</p>	<p>Elevation 1- Grid HA/KA. Beam Column joint underside of level 3 DS 1 2.0%</p>	<p>Width of the diagonal cracks in the beam column joint range from 0.2-2 mm. Width of verical cracks range from 2-4 mm in the beam column joint. Diagonal hairline cracks in the column. 10 hairline cracks along the beam between HA/KA and KA.</p>	



			
--	--	--	---

<p>20/21</p>	<p>Elevation 1- Grid KA. Beam Column joint underside of level 3.</p> <p>DS 1 2.0%</p>	<p>Width of diagonal cracks on both sides of the beam column joint range from 0.7-0.9 mm.</p> <p>Width of verical cracks approximately 3 mm and 3.5 mm.</p> <p>Spalling of concrete at the beam joint.</p> <p>Several cracks along the beam between KA and KA/N. Width of the cracks vary from 0.7 mm to 0.1 mm.</p>	
--------------	---	--	---

<p>22/23</p>	<p>Elevation 1- Grid KA/N. Beam Column joint underside of level 3.</p> <p>DS 1 2.0%</p>	<p>Width of diagonal cracks in the beam column joint range from 1-1.6 mm.</p> <p>Width of verical cracks range from 2.5-3 mm.</p> <p>Loss/spalling of concrete in the beam.</p>	
--------------	---	---	---


<p>24</p>	<p>Elevation 1- Grid N. Beam Column joint underside of level 3.</p> <p>DS 2 2.75%</p>	<p>Width of diagonal cracks approximately 1 mm.</p> <p>Width of verical cracks range from 3-5 mm.</p> <p>Loss of concrete in the beam, and concrete crushed in the column</p>	
-----------	---	---	---

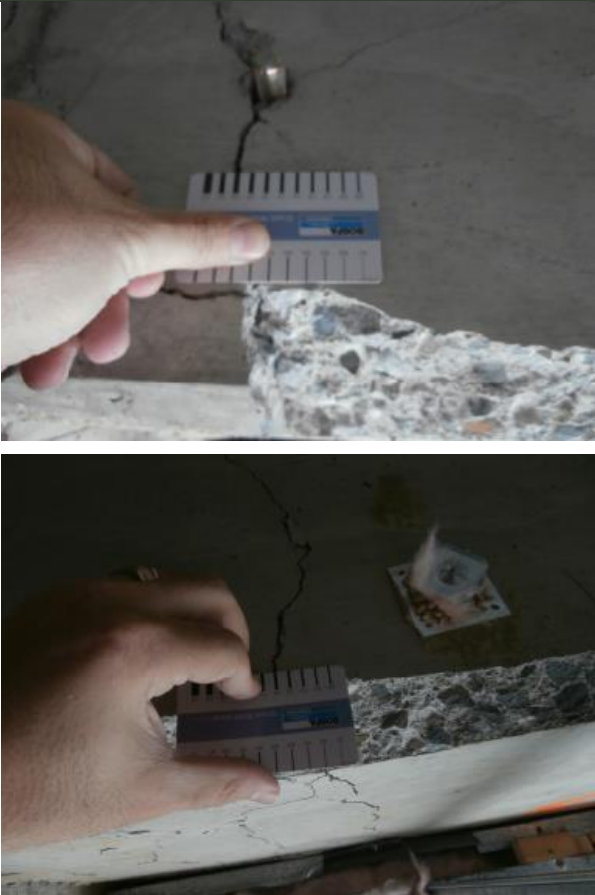

no photo, but assume this is a true
observation; pushes from DS1 to 2

<p>25</p>	<p>Elevation A-Grid 13. Beam Column joint underside of level 3.</p> <p>DS 2 2.75%</p> <p>DS 1 2.0%</p>	<p>Width of vertical cracks range from 1-3 mm. Approximately 6 cracks at the B/C (beam/column) joint.</p> <p>Spalling/ loss of concrete in several locations around the joint. Loss of support at the joint.</p>	
<p>26/27</p>	<p>Elevation A-Grid 13/10A. Beam Column joint underside of level 3.</p> <p>DS 1 2.0%</p>	<p>Three vertical cracks of 3 mm wide on the right and 4 vertical cracks of 3.5 mm wide on the left side of the joint.</p> <p>Cracks around the joint including diagonal cracks in the column. Width of these cracks range from 0.4-0.7 mm.</p>	

--	--	--






<p>28/29</p>	<p>Elevation A-Grid 10A. Beam Column joint underside of level 3.</p> <p>DS 2 2.75%</p> <p>DS 1 2.0%</p>	<p>Width of the vertical cracks range from 2-2.5 mm on both sides of the joint.</p> <p>Several smaller cracks of width range from 0.6-1.4 mm.</p> <p>Diagonal cracks on the in the joint and in the column.</p> <p>Several hairline cracks along the beam.</p> <p>Loss of concrete, spalling and concrete crush in the joint.</p>	
--------------	--	--	---




			
<p>30/31</p>	<p>Elevation A-Grid 10A/8A. Beam Column joint underside of level 3.</p> <p>DS 1 2.0%</p>	<p>Three diagonal cracks of width range from 0.5-2 mm on the left side of the joint.</p> <p>Two cracks of width 2 mm and 3 mm on the right side of the joint.</p> <p>Honeycomb in the concrete beam.</p> <p>Several hairline cracks around the joint and along the beam.</p>	


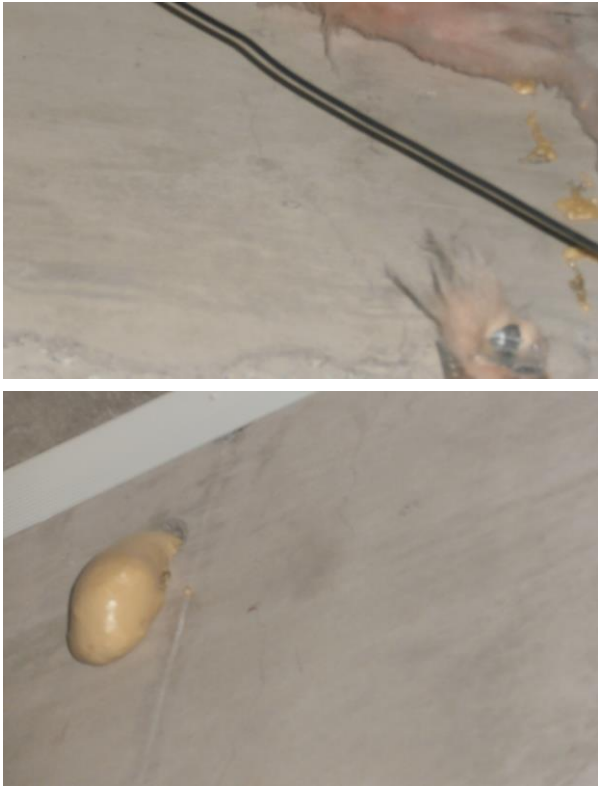

--	--	--



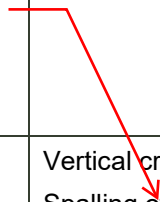
<p>32</p>	<p>Elevation A-Grid 8A. Beam Column joint underside of level 3.</p> <p>DS 3 5.0%</p> <p>DS 2 2.75%</p>	<p>Combination of diagonal and vertical cracks in the joint. The width of the cracks range from 1-3 mm.</p> <p>Loss of concrete in the column, reinforcement is exposed.</p> <p>Concrete crushed in the joint.</p>	
-----------	---	--	---



<p>33</p>	<p>Elevation HA-Grid 8A. Beam column joint underside level 3. DS 0 1 %</p>	<p>Vertical crack in the beam column joint.</p>	
<p>34/35</p>	<p>Elevation HA-Grid 8. Beam column joint underside of level 3</p>	<p>No access to the frame.</p>	



36/37	Elevation HA-Grid 7. Beam column joint underside of level 3. DS 0 1 %	Vertical crack at beam column joint.	
38/39	Elevation HA-Grid 6. Beam column joint underside of level 3. DS 0 1 %	Vertical cracking either side of beam column joint.	 




40/41	Elevation HA-Grid 5. Beam column joint underside of level 3.	We could not get access to assess damage.	
42/43	Elevation HA-Grid 4. Beam column joint underside of level 3. DS 0 1 %	Hairline diagonal cracks in beam.	
44/45	Elevation HA-Grid 3. Beam column joint underside of level 3. DS 0 1 %	Vertical crack 0.7 mm Spalling of concrete in beam and beam column joint.	

appears to be due to floor unit rotation due to drift in perpendicular direction towards the end frame




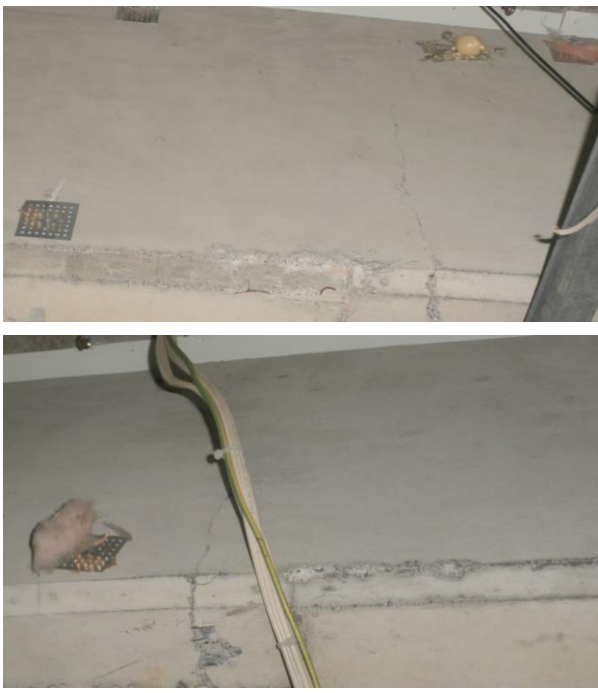

			
46/47	Elevation HA-Grid 2. Beam column joint underside of level 3. DS 1 2.0%	Vertical cracks range from 0.3-2 mm wide. Few hairline cracks in the beam.	




48	Elevation HA-Grid 1. Beam column joint underside of level 3. DS 0 1 %		 <p>crack at joint?</p>
49	Elevation 13-Grid N. Beam column joint underside of level 3. DS 0 < 2.0%	Crack underside of the B/C joint. Width of the crack is approximately 0.3-0.5 mm.	



50/51	Elevation 13-Grid M. Beam column joint underside of level 3. DS 0 < 2.0%	Hairline vertical cracks.	
52/53	Elevation 13-Grid L. Beam column joint underside of level 3. DS 0 < 2.0%	Vertical cracks approx. 0.5 mm.	
54/55	Elevation 13-Grid K. Beam column joint underside of level 3. DS 0 < 2.0%	Hairline vertical cracks.	
56/57	Elevation 13-Grid J. Beam column joint underside of level 3. DS ?	Area not exposed at time of inspection.	






DS ?




-



<p>58/59</p>	<p>Elevation 13-Grid H. Beam column joint underside of level 3.</p> <p>DS 0 < 2.0%</p>	<p>Vertical cracks in beam column joint 0.7 mm.</p>	
<p>60/61</p>	<p>Elevation 13-Grid G. Beam column joint underside of level 3.</p> <p>DS 0 < 2.0%</p>	<p>Vertical cracks in beam column joint 0.5-1.2 mm.</p>	
<p>62/63</p>	<p>Elevation 13-Grid F. Beam column joint underside of level 3.</p> <p>DS 0 < 2.0%</p>	<p>Hairline vertical cracks in beam column joint.</p>	



			
<p>64/65</p>	<p>Elevation 13-Grid E. Beam column joint underside of level 3.</p> <p>DS 1 2.0%</p>	<p>Vertical cracks in beam column joint approx 0.8 mm.</p> <p>Spalling of concrete in beam column joint.</p>	
<p>66/67</p>	<p>Elevation 13-Grid D. Beam column joint underside of level 3.</p> <p>DS 1 2.0%</p>	<p>Vertical cracks in beam column joint 0.5-1 mm</p> <p>Significant spalling of concrete in plastic hinge region of beam.</p>	




			
<p>68/69</p>	<p>Elevation 13- Grid C. Beam column joint underside of level 3.</p> <p>DS 1 2.0%</p>	<p>Hairline diagonal cracks in beam Spalling of concrete in plastic hinge region of beam.</p>	




			
70/71	<p>Elevation 13-Grid B. Beam column joint underside of level 3.</p> <p>DS 2 2.73%</p> <p>DS 1 2.0%</p>	<p>Width of the vertical cracks are 1.8 mm and 2 mm.</p> <p>Spalling/loss of concrete in the beam.</p> <p>Loss of support to the Dycore units.</p> <p>function of transverse drift</p>	  
72	<p>Elevation 13-Grid A. Beam column joint underside of level 3.</p> <p>DS 2 2.73%</p> <p>DS 1 2.0%</p>	<p>Vertical crack in the B/C joint. Loss of concrete in the centre of the beam.</p> <p>Loss of support to the Dycore units.</p>	




<p>73</p>	<p>Elevation N-Grid 1. Beam column joint underside of level 3</p> <p>DS 0 1 %</p>	<p>Loss of concrete cover in the column.</p>	
<p><u>74/75</u></p>	<p>Elevation N-Grid 2. Beam column joint underside of level 3</p> <p>DS 0 1 %</p>	<p>Three cracks in the B/C joint. The width of the cracks less than 0.3mm.</p>	
<p><u>76/77</u></p>	<p>Elevation N-Grid 3. Beam column joint underside of level 3</p> <p>DS 0 1 %</p>	<p>Loss of concrete in the beam around the B/C joint.</p> <p>A hairline crack along the beam.</p> <p>floor unit rotation</p>	


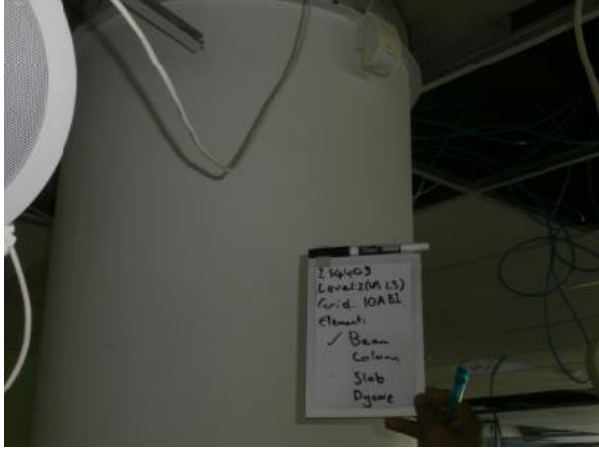


78/79	Elevation N-Grid 4. Beam column joint underside of level 3	This area has since been exposed however, we have not been back to inspect.	 A photograph showing a white wall in an interior space. A large orange number '4' is hand-painted on the wall, enclosed in a circle. The wall is part of a beam-column joint. Through a window to the left, a white car is visible outside. The ceiling above has some exposed pipes and a light fixture.
80/81	Elevation N-Grid 5. Beam column joint underside of level 3	This area has since been exposed however, we have not been back to inspect.	 A photograph of a room with large windows. The ceiling is dark with a grid pattern. A white wall is visible, and a beam-column joint is partially visible. The room appears to be empty and somewhat dimly lit.



82/83	Elevation N-Grid 6. Beam column joint underside of level 3	This area has since been exposed however, we have not been back to inspect.	
84/85	Elevation N-Grid 7. Beam column joint underside of level 3	This area has since been exposed however, we have not been back to inspect.	


<p>86/87</p>	<p>Elevation N-Grid 8. Beam column joint underside of level 3</p>	<p>This area has since been exposed however, we have not been back to inspect.</p>	
<p>88/89</p>	<p>Elevation N-Grid 9. Beam column joint underside of level 3</p>	<p>This area has since been exposed however, we have not been back to inspect.</p>	
<p>90/91</p>	<p>Elevation N-Grid 10. Beam column joint underside of level 3</p> <p>DS 0 1 %</p>	<p>A crack less than 0.3 mm wide on one side. Several hairline cracks along the beam.</p>	


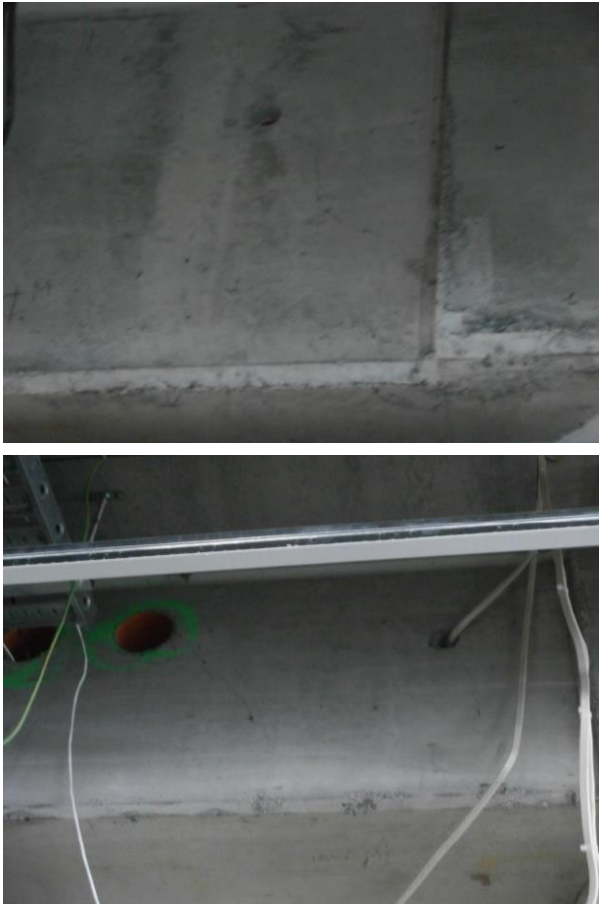
			
<p>92/93</p>	<p>Elevation N-Grid 11. Beam column joint underside of level 3</p> <p>DS 0 1 %</p>	<p>Two cracks in the B/C joint. The width of the cracks approximately less than 0.3 mm.</p> <p>Five hairline cracks along the beam.</p>	
<p>94/95</p>	<p>Elevation N-Grid 12. Beam column joint underside of level 3</p> <p>DS 0 1 %</p>	<p>Two cracks in the B/C joint. The width of the cracks approximately less than 0.3 mm.</p>	


			
<p>96</p>	<p>Elevation N-Grid 13. Beam column joint underside of level 3</p> <p>DS 0 1 %</p>	<p>Vertical crack in the beam column joint. Hairline cracks along the beam.</p>	
<p>97</p>	<p>Elevation 10A-Grid A. Beam column joint underside of level 3</p>	<p>Vertical crack in the beam column joint. Width of diagonal cracks in the beam range from 0.7-1 mm.</p>	


			
98/99	Elevation 10A-Grid B'. Beam column joint underside of level 3	<p>Width of diagonal crack in the B/C joint is less than 1 mm.</p> <p>Loss of concrete in the beam at the joint.</p> <p>Loss of Dycore support.</p> <p>Concrete column toe crushed.</p>	  




			
100/101	Elevation 10A-Grid D'. Beam column joint underside of level 3	This area has since been exposed however, we have not been back to inspect.	
102/103	Elevation 10A-Grid E'. Beam column joint underside of level 3	This area has since been exposed however, we have not been back to inspect.	
104/105	Elevation 10A-Grid F'. Beam column joint underside of level 3	This area has since been exposed however, we have not been back to inspect.	
106/107	Elevation 10A-Grid H'. Beam column joint underside of level 3	This area has since been exposed however, we have not been back to inspect.	
108	Elevation KA-Grid 1. Beam column joint underside of level 3	Width of vertical crack in the joint is 1.5 mm. Diagonal cracks in the beam on both the sides. The width of the diagonal cracks range from 0.7-1 mm. Four cracks along the beam.	


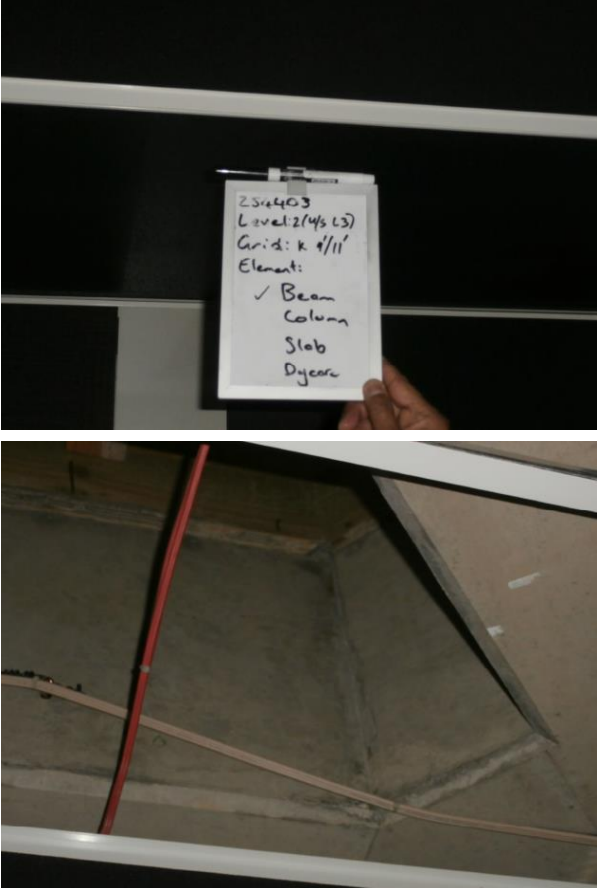
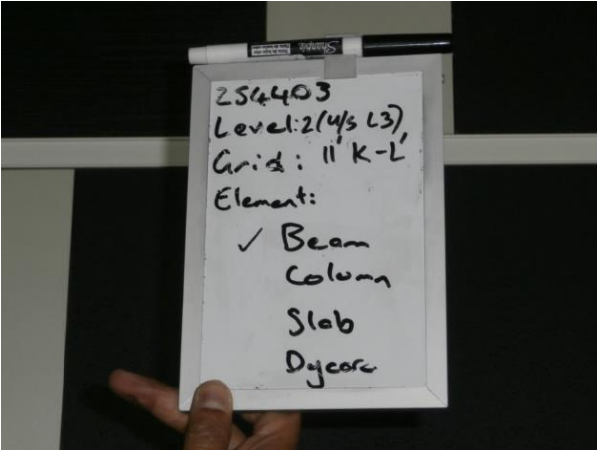
			 <p>The table contains four photographs of wall damage. The top photo shows a vertical crack in a grey wall with a hand holding a ruler for scale. The second photo shows a similar crack with a ruler. The third photo shows a wider view of the wall with a hole and a crack. The bottom photo shows a corner of a room with a large hole in the wall and a crack.</p>
--	--	--	---

			
109/110	Elevation KA-Grid 2'. Beam column joint underside of level 3	Width of vertical cracks in the B/C joint is less than 0.5 mm. A width of 0.2 mm crack in the mid height of the column.	



			
111/112	Elevation KA-Grid 4'. Beam column joint underside of level 3	This area has since been exposed however, we have not been back to inspect	
113/114	Elevation KA-Grid 5'. Beam column joint underside of level 3	This area has since been exposed however, we have not been back to inspect	
115/116	Elevation KA-Grid 6'. Beam column joint underside of level 3	This area has since been exposed however, we have not been back to inspect	



117/118	Elevation KA-Grid 8'. Beam column joint underside of level 3	Diagonal hairline cracks of width less than 0.3 mm. Concrete crushed at the edge in the beam column joint.	
---------	--	---	---



			
<p>119</p>	<p>Elevation KA-Grid 9/10. Beam joint underside of level 3</p>	<p>A crack of width less than 0.3 mm. The crack is on the underside of the beam to beam joint.</p>	
<p>120, 121/122 and 123</p>	<p>Elevation L'-Grids between 11' to 9'. Beam on the underside of level 3</p>	<p>Combined vertical and diagonal cracks along the beam. The width of the cracks range from 0.8-1.2 mm. Several hairline cracks along the beam.</p>	


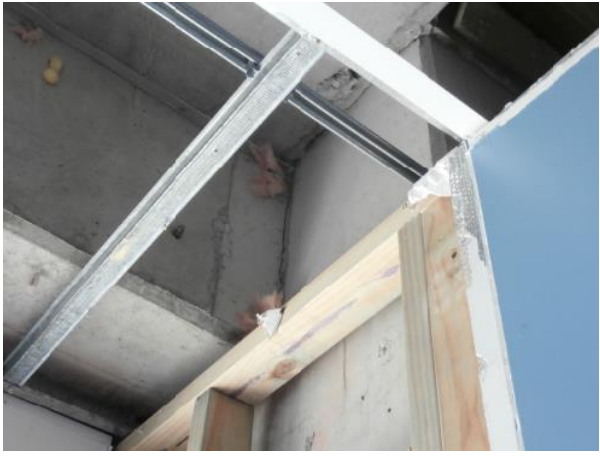
			
<p>124, 125/126 and 127</p>	<p>Elevation K- Grids between 11' to 9'. B/C joints and beams underside of level 3</p>	<p>Approximately four cracks along the beam. The width of the cracks are less than 0.5 mm.</p>	
<p>127(a)</p>	<p>Elevation 11'- Grids between K to L'. B/C joints and beams underside of level 3 (Refer to Dycore plan for the reference)</p>	<p>Width of cracks along the beam range from 0.8-1.2 mm. Approximately three hairline cracks along the beam.</p>	



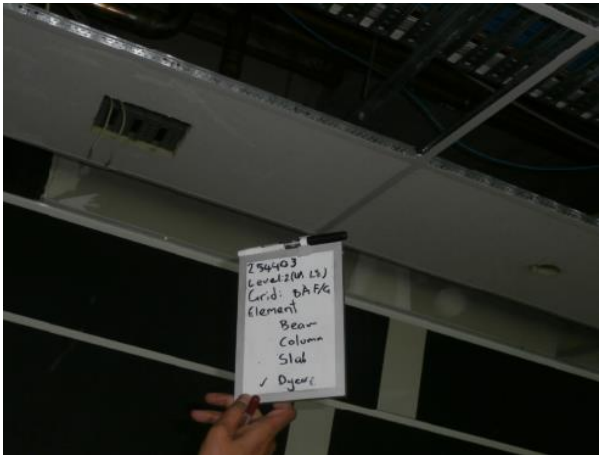
			
127 (b&c)	Elevation 13'- Grids between N to J. B/C joints and beams underside of level 3. (Refer to Dycore plan for the reference)	Width of 1.2 mm crack in the B/C joint. Approximately 10 hairline cracks along the beam.	

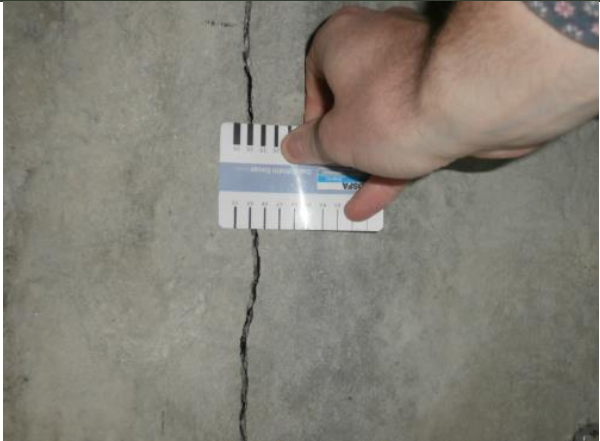

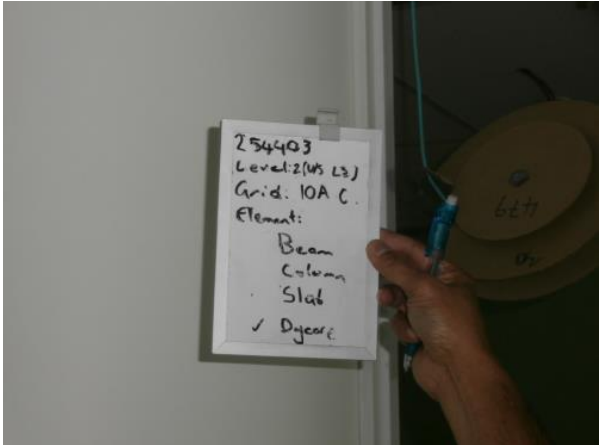

			
<p>127(d)</p>	<p>Elevation 9'- Grids between K to L'. B/C joints and beams underside of level 3 (Refer to Dycore plan for the reference)</p>	<p>A vertical crack, width of 1.4 mm in the beam. 1 mm wide crack underside of the Dycore at the beam-to- beam joint.</p>	



<p>128</p>	<p>Dycore units Underside of level 3. Grid numbers between HA- KA and 1-2.</p>	<p>More than 5 mm wide diagonal crack, underside of the Dycore unit at location 1/HA. This crack is vertically dislocated. A diagonal hairline crack at location 1/KA.</p>	
<p>129</p>	<p>Dycore units Underside of level 3. Grid numbers between KA-N and 1-2.</p>	<p>A width of 2 mm diagonal crack, underside of the Dycore unit at location 1/N.</p>	



			
130	Dycore units Underside of level 3. Grid numbers between HA-KA and 2-3.	No visible crack observed	
131	Dycore units Underside of level 3. Grid numbers between KA-N and 2-3.	No visible crack observed	
132	Dycore units Underside of level 3. Grid numbers between HA-KA and 3-8.	A 3.5 mm wide longitudinal crack, underside of the Dycore unit at location HA/6-7	


			
133	Dycore units Underside of level 3. Grid numbers between KA-N and 3-8.	No visible crack observed	
134	Dycore units Underside of level 3. Grid numbers between 8-11 and H-KA.	A 2 mm wide diagonal crack, underside of the Dycore unit at location HA/8A. Loss of concrete and crushed at the corner.	



			
135	Dycore units Underside of level 3. Grid numbers between KA-N and 8-13.	A width of 1 mm diagonal crack, underside of the Dycore unit at location KA/9'.	
136	Dycore units Underside of level 3. Grid numbers between H-N and 11-13.	No visible crack observed	
137	Dycore units Underside of level 3. Grid numbers between 8A-10A and C-H.	A 2mm wide longitudinal crack, underside of the Dycore unit at location 8A/G. A longitudinal crack less than 0.5 mm wide, underside of the Dycore unit at location 8A/F.	 


			 
138	Dycore units Underside of level 3. Grid numbers between 13- 10A and C-H.	A longitudinal crack less than 0.5 mm wide, underside of the Dycore unit at location 13/C-H.	 

139	Dycore units Underside of level 3. Grid numbers between 8A- 10A and B-C.	No visible crack observed	
140	Dycore units Underside of level 3. Grid numbers between 10A- 13 and B-C.	A longitudinal crack underside of the Dycore unit, at location 13/D A diagonal crack underside of the Dycore unit, at location 10A/C.	
141	Dycore units Underside of level 3. Grid numbers between 8A- 10A and A-B.	A width of 5 mm diagonal crack underside of the Dycore units, at location 8A/A. A transverse crack underside of the Dycore units end. Loss of Dycore unit support. Spalling of concrete in the beam.	
142	Dycore units Underside of level 3. Grid numbers between 10A- 13 and A-B.	A transverse crack. Loss of Dycore unit support. Spalling of cover concrete on beam.	


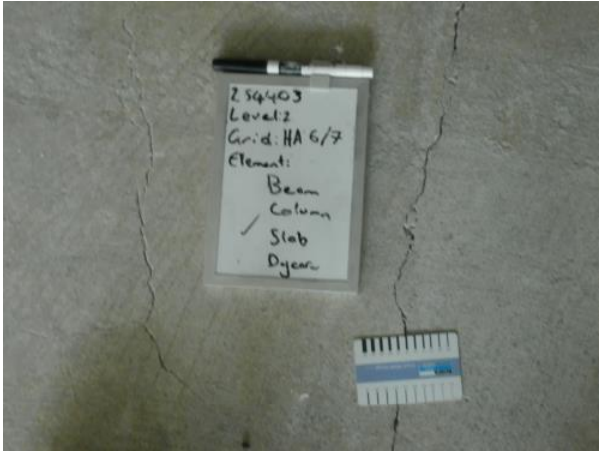
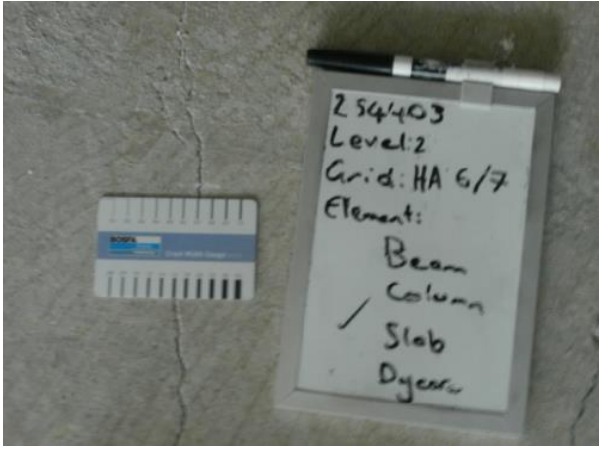
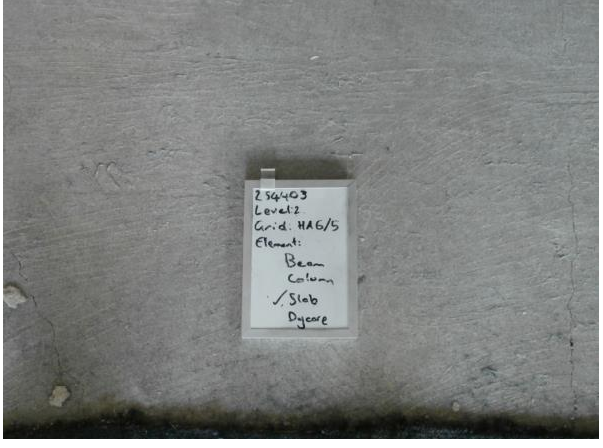
			
<p>143</p>	<p>Floor slab level 2. Grid numbers between HA-KA and 1-2.</p>	<p>Diagonal cracks on the floor range from 0.8-7 mm wide.</p> <p>Diagonal cracks spread over grid HA/(HA-KA) and 1/2. More cracks around the corner column on grid 1/HA</p> <p>Some of the cracks vertically dislocated.</p> <p>A longitudinal crack 1.8 mm wide along the grid line 2 and between HA to KA.</p> <p>A transverse crack of 7mm wide along the grid line KA and between 1 to 2.</p>	



			 <p>The table contains four photographs documenting concrete damage. The first photo shows a crack in a concrete surface with a white scale placed across it. The second photo shows a red spirit level placed on a crack in a concrete floor. The third photo shows a crack in a concrete surface with a small white label placed on it. The fourth photo shows a crack in a concrete surface with a white ruler placed across it.</p>
--	--	--	--

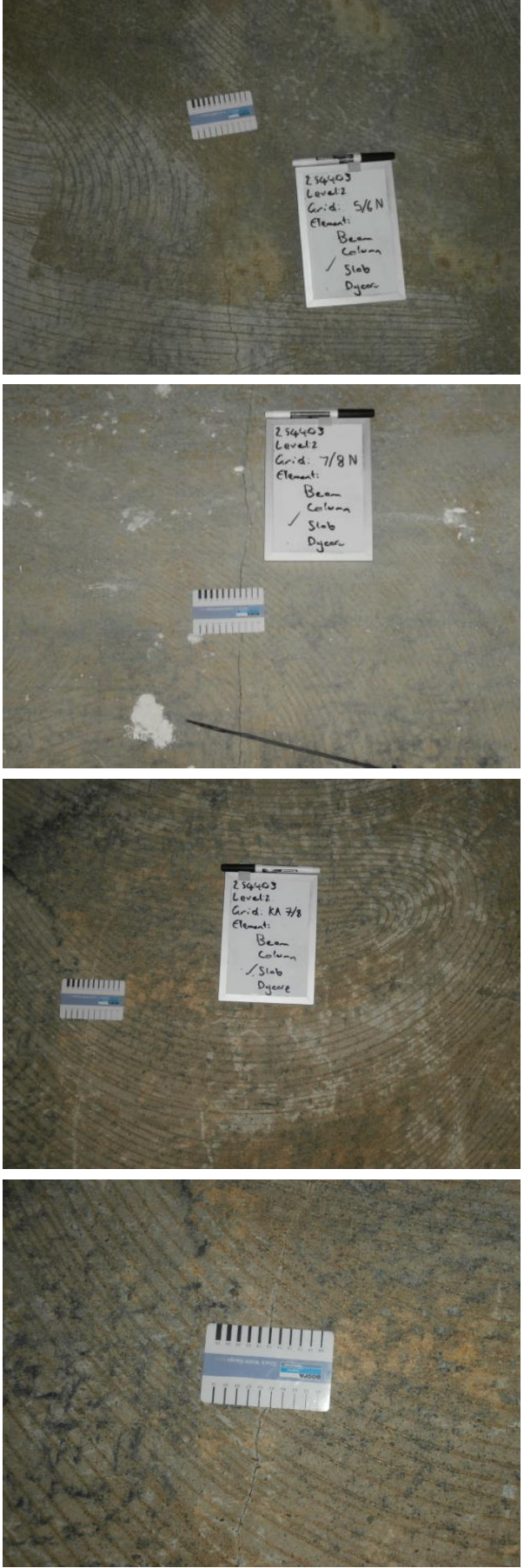
			
<p>144</p>	<p>Floor slab level 2. Grid numbers between KA-N and 1-2.</p>	<p>Diagonal cracks on the floor range from 1 mm to 1.4 mm wide. More cracks close to the corner column.</p> <p>Cracked concrete topping slab removed to inspect reinforcement. One bar of the mesh was fractured while another mesh bar and one saddle bar were</p>	

		<p>Some of the cracks vertically dislocated.</p> <p>A longitudinal crack of 5 mm wide along the grid line between KA/N and 2.</p> <p>A transverse crack width of 1.8 mm along the grid KA and between 1 to 2.</p>	 <p>The top two photographs are close-up views of a crack in a concrete floor slab. A ruler is placed across the crack to provide a scale. The crack is longitudinal and appears to be vertically dislocated. The bottom photograph shows a wider view of the floor slab, with a red level placed on the surface to indicate the floor's level. The floor shows signs of damage, including a diagonal crack and transverse cracks around a column.</p>
145	<p>Floor slab level 2. Grid numbers between HA-KA and 2-3.</p>	<p>A diagonal crack of width 1.4 mm on the floor located at grid 3/HA-KA.</p> <p>Transverse cracks range from 1.2 mm to 2.5mm wide around the column located at 3/KA.</p>	

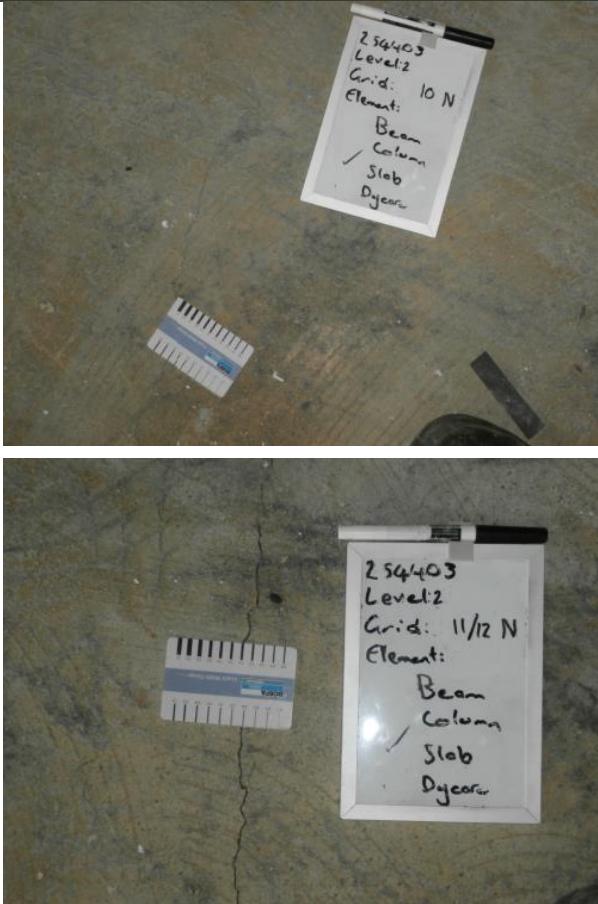
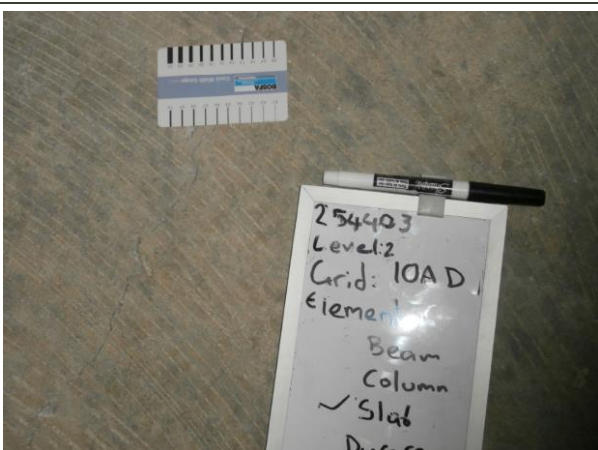
<p>146</p>	<p>Floor slab level 2. Grid numbers between KA-N and 2-3.</p>	<p>Transverse cracks range from 1.2 mm to 2.5 mm wide around the column.</p> <p>A longitudinal crack of 1.4mm wide on the floor along the grid KA/N and between 2/3</p>	
------------	---	---	---

			
147	Floor slab level 2. Grid numbers between HA-KA and 3-8.	Longitudinal cracks range from 0.7 mm 1.6 mm wide over the grid area between HA/KA and 3/8.	 <p>254403 Level:2 Grid: HA 6/7 Element: Beam Column ✓ Slab Dyear</p>  <p>254403 Level:2 Grid: HA 6/7 Element: Beam Column ✓ Slab Dyear</p>  <p>254403 Level:2 Grid: HA 6/5 Element: Beam Column ✓ Slab Dyear</p>

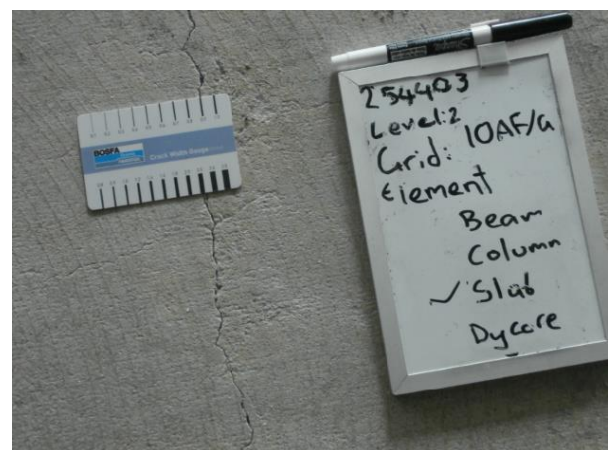
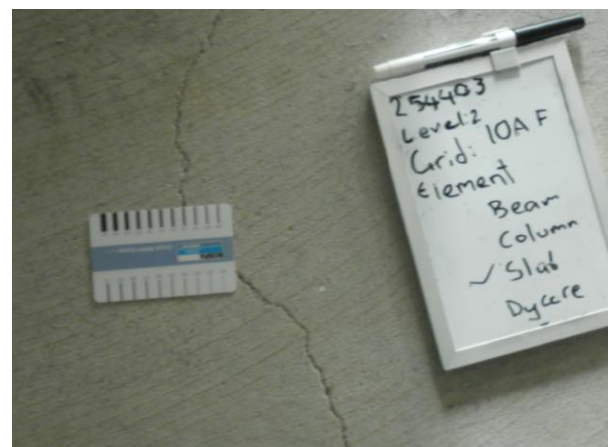
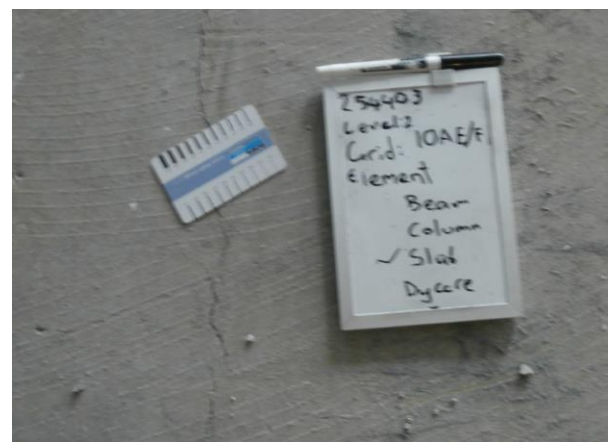
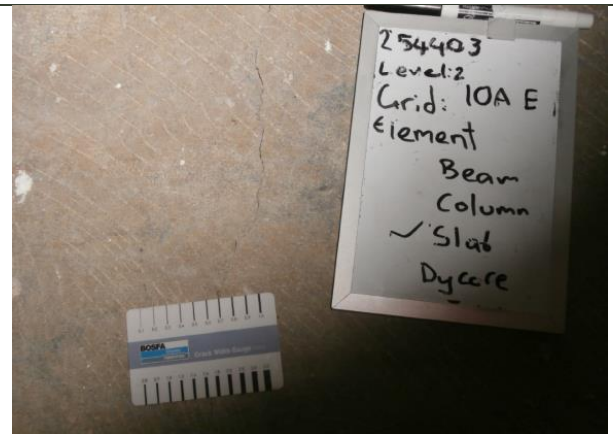
			
<p>148</p>	<p>Floor slab level 2. Grid numbers between KA-N and 3-8.</p>	<p>Longitudinal cracks range from 0.9 mm 1.6 mm wide over the grid area between KA/N and 3-8.</p>	

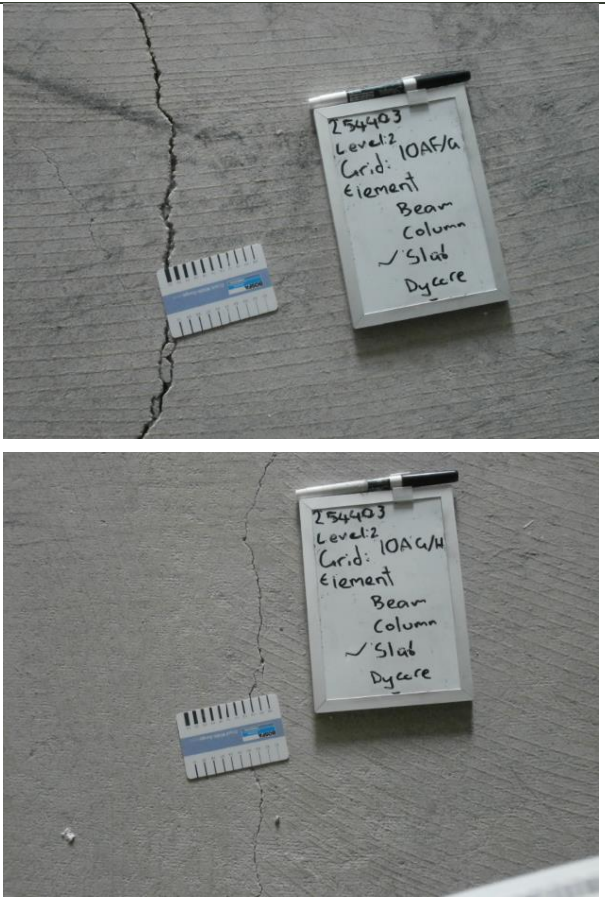
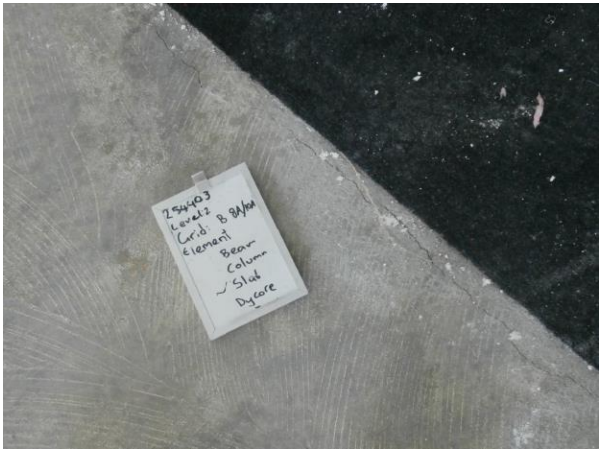
			 <p>The rightmost column of the table contains four photographs of concrete surfaces, likely from a building's interior or exterior. Each photograph shows a close-up of a concrete surface with a visible rebar pattern. A white scale bar is placed on the surface for reference. A handwritten label is attached to each photograph, providing specific location information. The labels are as follows:</p> <ul style="list-style-type: none">Top photo: 25q403, Level 2, Grid: 5/6 N, Element: Beam, Column, Slab, Dygar.Second photo: 25q403, Level 2, Grid: 7/8 N, Element: Beam, Column, Slab, Dygar.Third photo: 25q403, Level 2, Grid: RA 7/8, Element: Beam, Column, Slab, Dygar.Bottom photo: No label.
--	--	--	---


<p>149</p>	<p>Floor slab level 2. Grid numbers between HA-KA and 8-11.</p>	<p>Two longitudinal cracks 3.5 mm and 1.8 mm wide over the grid area between HA/KA and 8-11.</p>	
<p>150</p>	<p>Floor slab level 2. Grid numbers between KA-N and 8-13.</p>	<p>Longitudinal cracks range from 1.2 mm and 1.4 mm wide over the grid area between HA/N and 8/13.</p>	

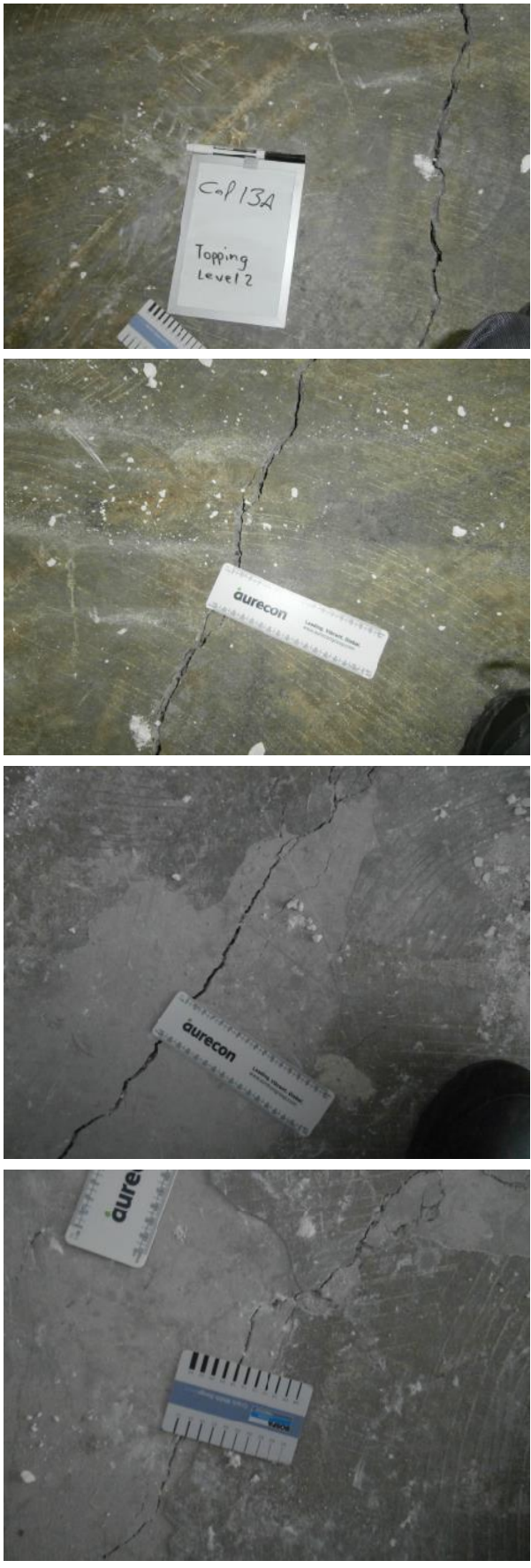
			
151	Floor slab level 2. Grid numbers between 10A-13 and H-N.	Carpet had not been removed at the time of our inspection.	
152	Floor slab level 2. Grid numbers between 10A-8A and C-H.	Longitudinal cracks range from 1 mm and 3.5 mm wide over the grid area between 10A/8A and C/H.	


--	--	--




			
153	Floor slab level 2. Grid numbers between 10A-13 and C-H.	Carpet had not been removed at the time of our inspection.	
154	Floor slab level 2. Grid numbers between 10A-8A and B-C.		
155	Floor slab level 2. Grid numbers between 10A-13 and B-C.	Carpet had not been removed at the time of our inspection.	

156	Floor slab level 2. Grid numbers between 10A-8A and A-B.	<p>Diagonal cracks on the floor range from 1.2 mm to 3.5 mm wide.</p> <p>More cracks around the corner column on grid 8A/A.</p> <p>Some of the cracks vertically dislocated.</p> <p>Longitudinal cracks 3.5 mm wide along the grid B between 8A and 10A.</p> <p>A transverse crack of 10 mm wide along the grid 10A between A and B</p>	 <p>The first photograph shows a corner of a room where a diagonal crack runs across the floor slab. A wooden board is leaning against the wall. The second photograph shows a longitudinal crack in the floor slab, with a ruler placed across it to measure its width. The third photograph shows a crack in the floor slab with a red spirit level placed over it to check for vertical displacement. The fourth photograph shows a transverse crack in the floor slab, with a ruler placed across it to measure its width.</p>
-----	--	---	---


157	Floor slab level 2. Grid numbers between 10A-13 and A-B.	<p>Diagonal cracks on the floor range from 1.8 mm to 5 mm wide.</p> <p>More cracks around the corner column on grid 13/A.</p> <p>Some of the cracks vertically dislocated.</p> <p>A longitudinal crack 10mm wide along the grid B between 13 and 10A.</p> <p>A wide crack along the grid 10A between A and B. Concrete has been removed to inspect the slab reinforcement. Slab reinforcement fractured.</p>	
-----	--	--	---



			
--	--	--	---

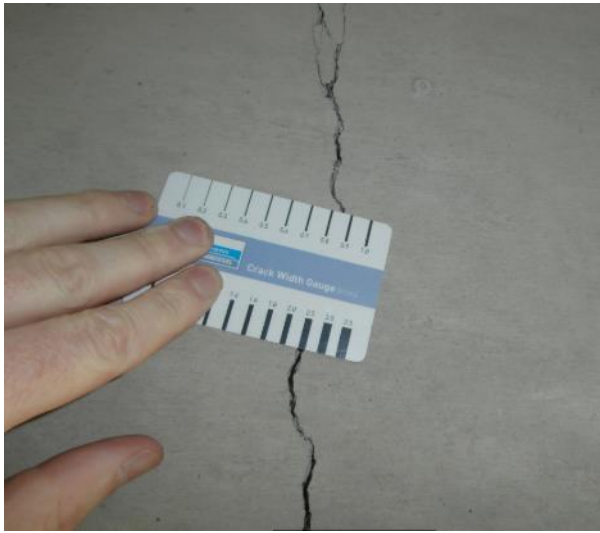



ID.	Location	Comment	Photographs
158	Elevation 8A- Grid A. Beam column joint underside of level 4	<p>Width of vertical crack in the beam column joint is approximately 10 mm.</p> <p>Diagonal cracks on beam continuing to underside of the beam.</p> <p>Loss of concrete in the beam and in the column.</p> <p>Vertical cracks along the beam length. Width of the cracks range from 0.1-0.7 mm</p>	






			The rightmost column of the table contains three vertically stacked photographs documenting structural damage. The top photograph shows a concrete wall with several prominent, jagged horizontal and diagonal cracks. Below the wall, there is a metal bracket or support structure. The middle photograph shows a concrete ceiling with a large, irregular area of spalling or missing material, revealing the internal aggregate. A vertical wooden post is visible on the right side of the frame. The bottom photograph shows a corner of the room with a concrete wall and ceiling. There is significant damage, including a large piece of peeling white material (possibly plaster or insulation) and exposed wooden framing. A metal bracket is also visible in the bottom right corner of this photo.
--	--	--	---



<p>159/160</p>	<p>Elevation 8A-Grid B. Beam column joint underside of level 4</p> <p>DS 1 2.0%</p>	<p>Combination of vertical and diagonal cracks in the plastic hinge region of the beam. Width of the vertical cracks are 2.5 mm. Diagonal cracks are approximately 0.5 mm wide.</p> <p>Beam damage, and loss of cover concrete.</p>	
<p>161/162</p>	<p>Elevation 8A-Grid C. Beam column joint underside of level 4</p> <p>DS 1 2.0%</p>	<p>Vertical cracks in the beam column joint are 2.5 mm wide.</p> <p>Damage around the joint and spalling of concrete.</p>	



			
<p>163/164</p>	<p>Elevation 8A- Grid D. Beam column joint underside of level 4</p> <p>DS 1 2.0%</p>	<p>Combination of vertical and diagonal cracks in the beam column joint. Width of the cracks are approximately 2 mm.</p> <p>Diagonal crack in the column.</p> <p>Spalling of concrete in the beam column joint.</p> <p>Vertical cracks along the beam length.</p>	

<p>165/166</p>	<p>Elevation 8A-Grid E. Beam column joint underside of level 4 DS 1 2.0%</p>	<p>Width of vertical cracks in the plastic hinge region of the beam range from 2-2.5 mm. Spalling of concrete in the beam column joint. Three vertical cracks along the beam length.</p>	
<p>167/168</p>	<p>Elevation 8A-Grid F. Beam column joint underside of level 4 DS 1 2.0%</p>	<p>Vertical cracks at the beam column joint are 2 mm wide. Approximately two vertical cracks along the beam length.</p>	
<p>169/170</p>	<p>Elevation 8A-Grid G. Beam column joint underside of level 4 DS 1 2.0%</p>	<p>Vertical cracks at the beam column joint are 2 mm wide. A diagonal crack in the beam column joint. Loss of cover concrete in the beam. Hairline vertical cracks along the beam length.</p>	
<p>171/172</p>	<p>Elevation 8A-Grid H. Beam column joint underside of level 4 DS 0 1.0%</p>	<p>Vertical cracks at the beam column joint range from 1.4-1.6 mm. A diagonal hairline crack in the column. Spalling of cover concrete in the joint.</p>	

			
173	Elevation 8A- Grid HA. Beam column joint underside of level 4 DS 1 2.0%	A 2 mm wide vertical crack in the beam column joint.	


			
<p>174</p>	<p>Elevation 1- Grid HA. Beam column joint underside of level 4</p> <p>DS 1 2.0%</p>	<p>Combination of vertical and diagonal cracks around the beam column joint. Width of the cracks range from 1-5 mm.</p> <p>Loss of cover concrete in the joint and concrete crushed.</p> <p>Column toe had honey combed concrete.</p> <p>Rusty longitudinal column bars were visible.</p> <p>Combination of diagonal and vertical cracks along the beam length.</p>	

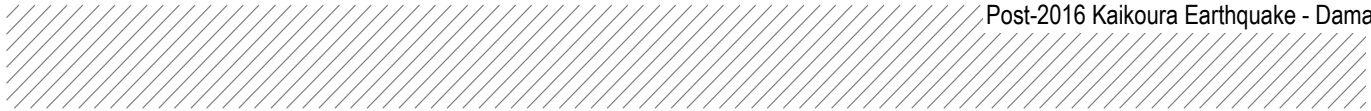
			
<p>175/176</p>	<p>Elevation 1- Grid HA/KA. Beam column joint underside of level 4</p> <p>DS 1 2.0%</p>	<p>Combination of diagonal and vertical cracks around the beam column joint. Width of the cracks range from 0.6-1.4 mm.</p> <p>Concrete crushed around the joint. Diagonal hairline cracks in the column.</p> <p>Approximately 7 hairline cracks along the beam length.</p>	



			
<p>177/178</p>	<p>Elevation 1- Grid KA. Beam column joint underside of level 4</p> <p>DS 1 2.0%</p>	<p>Combination of diagonal and vertical cracks around the B/C joint.</p> <p>Width of the cracks range from 0.6-3 mm.</p> <p>Spalling of concrete around the beam column joint.</p> <p>Diagonal hairline cracks in the column.</p> <p>Approximately 6 hairline cracks along the beam length.</p>	





			<p>The rightmost column of the table contains four vertically stacked photographs documenting structural damage. The top photo shows a corner where a wall meets a ceiling, with a large area of missing plaster and exposed aggregate. The second photo shows a hand holding a blue and white ruler against a horizontal crack in a grey concrete or plaster surface. The third photo shows a ceiling with a vertical crack, a small circular hole, and some peeling material. The bottom photo shows a ceiling with a vertical crack and two electrical wires with red caps protruding from the surface.</p>
--	--	--	--

179/180	Elevation 1- Grid KA/N. Beam column joint underside of level 4 DS 0 1 %	Combination of diagonal and vertical cracks around the beam column joint. Width of the cracks range from 0.5-1.2 mm. Diagonal hairline cracks in the column. Approximately 8 hairline cracks along the beam length.	
---------	---	--	---





			
181	Elevation 1- Grid N. Beam column joint underside of level 4 DS 1 2.0%	Combination of diagonal and vertical cracks around the beam column joint. Width of the cracks range from 1.4-3.5 mm. Diagonal hairline cracks in the column. Concrete spalled off in the beam.	



			
182	Elevation A-Grid 13. Beam column joint underside of level 4 DS 1 2.0%	Combination of diagonal and vertical cracks around the beam column joint. Width of the cracks range from 0.9-3 mm. Diagonal cracks less than 0.5 mm wide along the beam.	



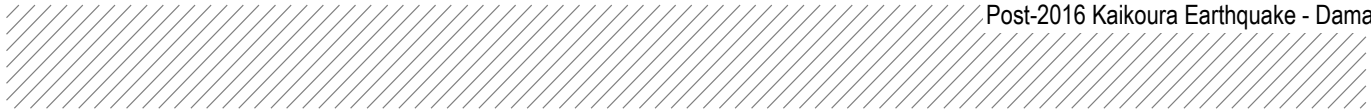
			The table contains three photographs documenting structural damage. The top photograph shows a close-up of a grey concrete ceiling with several irregular cracks and two small circular holes. The middle photograph shows a hand holding a white crack gauge against a crack in the concrete, with a white ruler placed below it for scale. The ruler has the 'aurecon' logo and the text 'Leading. Vib' and 'www.aurecon' visible. The bottom photograph shows a corner of a room where the ceiling is cracked and the wooden framing of a window or door is visible.
--	--	--	---

			
<p>183/184</p>	<p>Elevation A-Grid 13/10A. Beam column joint underside of level 4</p> <p>DS 2 2.75%</p>	<p>Combination of diagonal and vertical cracks around the beam column joint. Width of the cracks range from 1.2-5 mm. Diagonal hairline cracks in the column. Loss of concrete, crushed and spalled off in the beam column joint. Diagonal hairline cracks along the beam length.</p>	




			The rightmost column of the table contains three vertically stacked photographs documenting concrete damage. The top photograph shows a hand holding a white ruler with the 'aurecon' logo and 'Leading - Vibrant. Global. www.aurecongroup.com' printed on it. The ruler is placed over a crack in a grey concrete surface. Handwritten text 'L3 GA10A/13' is visible above the crack. A circular hole is present in the upper right corner of the photo. The middle photograph shows a white, curved object, possibly a piece of tape or a probe, positioned over a crack in the concrete. The bottom photograph shows a network of multiple cracks in the concrete, with the handwritten number '121' visible in the upper right area.
--	--	--	---

<p>185/186</p>	<p>Elevation A- Grid 10A. Beam column joint underside of level 4</p> <p>DS 1 2.0%</p>	<p>Combination of diagonal and vertical cracks around the beam column joint. Width of the cracks range from 1.4-3 mm. Loss of concrete in the beam column joint. Diagonal hairline cracks in the column.</p>	
----------------	---	--	---



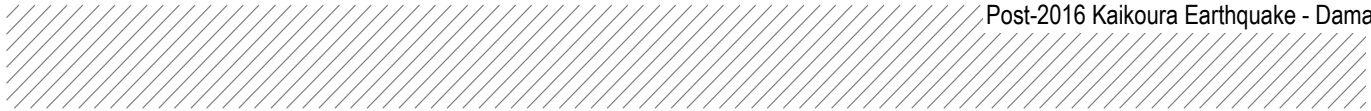
--	--	--





187/188	Elevation A-Grid 10A/8A. Beam column joint underside of level 4	Combination of diagonal and vertical cracks around the beam column joint. Width of the cracks range from 0.6 - 7 mm. Diagonal hairline cracks in the column.	
---------	--	--	---




			The rightmost column of the table contains two photographs. The top photograph shows a close-up of a light-colored concrete surface with several irregular, thin cracks. A black cable runs vertically on the right side of the frame. The bottom photograph shows a corner or edge of a concrete structure with significant cracking. A metal channel is visible, and there is a piece of white material, possibly insulation or a repair patch, attached to the surface.
--	--	--	--





			
<p>189</p>	<p>Elevation A-Grid 8A. Beam column joint underside of level 4</p> <p>DS 3 5.0%</p> <p>DS 2 2.75%</p>	<p>Combination of diagonal and vertical cracks around the beam column joint. Width of the cracks is approximately 3 mm.</p> <p>Loss of concrete in the beam and the reinforcement is exposed.</p> <p>No fracture in the stirrups observed.</p> <p>Loss of concrete in the column.</p> <p>Conceret crushed in the beam column joint.</p>	







			
--	--	--	---






			
190	Elevation HA-Grid 8A. Beam column joint underside of level 4 DS 1 2.0%	Approximately 5 mm wide vertical crack in the joint.	









191/192	Elevation HA-Grid 8. Beam column joint underside of level 4 DS 0 1 %	Minor vertical cracks in the beam column joint. Cracks width approximately 0.5 mm. Underside of the beam is patched with concrete.	
193/194	Elevation HA-Grid 7. Beam column joint underside of level 4 DS 0 1 %	Width of vertical cracks in the beam column are less than 1 mm. Concrete spalled off around the joint. Minor vertical cracks along the beam length.	




<p>195/195'</p>	<p>Elevation HA-Grid 6. Beam column joint underside of level 4</p> <p>DS 0 1 %</p>	<p>Width of vertical cracks in the beam column are less 1 mm.</p> <p>A minor diagonal crack in the column.</p> <p>Approximately 2 hairline cracks along the beam width.</p>	
<p>196/197</p>	<p>Elevation HA-Grid 5. Beam column joint underside of level 4</p> <p>DS 0 1 %</p>	<p>Width of vertical cracks in the beam column are less than 1 mm.</p> <p>A minor diagonal crack in the column.</p> <p>A hairline crack in the beam.</p>	



<p>198/199</p>	<p>Elevation HA-Grid 4. Beam column joint underside of level 4</p> <p>DS 0 1 %</p>	<p>Crack width of 0.2 mm under side of the beam in the joint.</p> <p>Underside of the beam is patched with concrete.</p> <p>A minor diagonal crack in the column.</p> <p>Minor cracks along the beam length</p>	
<p>200/201</p>	<p>Elevation HA-Grid 3. Beam column joint underside of level 4</p> <p>DS 0 1 %</p>	<p>Width of vertical crack in the beam column are less than 1 mm.</p> <p>A minor diagonal crack in the column.</p> <p>Underside of the beam is patched with concrete.</p> <p>Minor cracks along the beam length.</p>	
<p>202/203</p>	<p>Elevation HA-Grid 2. Beam column joint underside of level 4</p> <p>DS 1 2.0%</p>	<p>Vertical cracks in the beam column are 2.5 mm wide.</p> <p>Minor cracks along the beam length range from 0.2 - 0.5 mm.</p>	

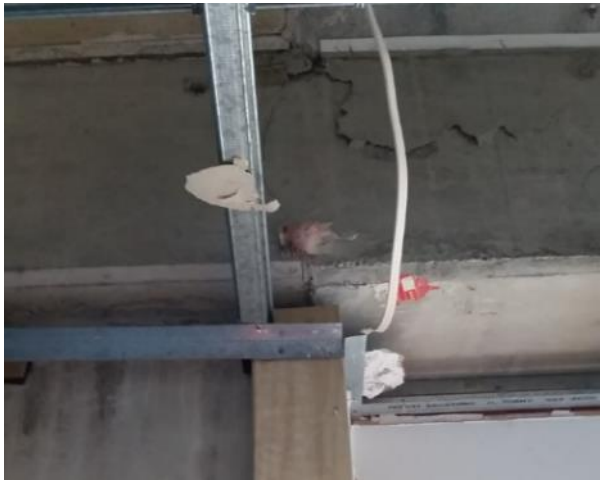




			
204	Elevation HA-Grid 1. Beam column joint underside of level 4 DS 1 2.0%	A vertical crack in the beam column joint approximately 4 mm wide.	


			
205	<p>Elevation 13-Grid N. Beam column joint underside of level 4</p> <p>DS 0 1 %</p>	<p>A vertical crack in the beam column joint less than 1 mm wide.</p> <p>Approximately 4 vertical hairline cracks along the beam length.</p>	
206/207	<p>Elevation 13-Grid M. Beam column joint underside of level 4</p> <p>DS 0 1 %</p>	<p>Vertical cracks in the beam column joint 0.6 wide.</p> <p>Approximately 4 vertical hairline cracks along the beam length.</p>	
208/209	<p>Elevation 13-Grid L. Beam column joint underside of level 4</p> <p>DS 0 1 %</p>	<p>A vertical crack in the beam column joint less than 1 mm wide.</p> <p>Approximately 4 vertical hairline cracks along the beam length.</p>	


<p>210/211</p>	<p>Elevation 13-Grid K. Beam column joint underside of level 4</p> <p>DS 0 1 %</p>	<p>A vertical crack in the beam column joint less than 1 mm wide.</p> <p>Approximately 4 vertical hairline cracks along the beam length.</p>	
<p>212/213</p>	<p>Elevation 13-Grid J. Beam column joint underside of level 4</p> <p>DS 0 1 %</p>	<p>A vertical crack in the beam column joint less than 0.5 mm wide.</p> <p>Approximately 3 vertical hairline cracks along the beam length.</p>	
<p>214/215</p>	<p>Elevation 13-Grid H. Beam column joint underside of level 4</p> <p>DS 1 2 %</p>	<p>A vertical crack in the beam column joint approximately 0.3 mm wide.</p> <p>Approximately 2 vertical hairline cracks along the beam length.</p> <p>Loss of concrete in two locations along the beam length.</p>	




<p>216/217</p>	<p>Elevation 13- Grid G. Beam column joint underside of level 4</p> <p>DS 1 2 %</p>	<p>Combination of diagonal and vertical cracks in the beam column joint approximately 0.6 mm wide.</p> <p>Loss of concrete in the joint.</p> <p>Approximately 5 vertical hairline cracks along the beam length.</p>	
<p>218/219</p>	<p>Elevation 13- Grid F. Beam column joint underside of level 4</p> <p>DS 0 1 %</p>	<p>Vertical cracks in the beam column joint approximately 0.6 mm wide.</p> <p>Approximately 5 vertical hairline cracks along the beam length.</p>	

<p>220/221</p>	<p>Elevation 13-Grid E. Beam column joint underside of level 4</p> <p>DS 1 2 %</p>	<p>Vertical cracks in the beam column joint approximately 1 mm wide.</p> <p>Loss of concrete and concrete spalled off in the beam.</p> <p>Approximately 2 vertical hairline cracks along the beam length.</p>	
<p>222/223</p>	<p>Elevation 13-Grid D. Beam column joint underside of level 4</p> <p>DS 0 1 %</p>	<p>Vertical cracks in the beam column joint less than 0.5 mm wide.</p> <p>Approximately 5 vertical hairline cracks along the beam length.</p>	
<p>224/225</p>	<p>Elevation 13-Grid C. Beam column joint underside of level 4</p> <p>DS 1 2 %</p>	<p>Vertical cracks in the beam column joint less than 0.5 mm wide.</p> <p>Approximately 8 vertical hairline cracks along the beam length.</p> <p>Concrete crushed close to the beam column joint and spalling of concrete in the beam.</p>	






226/227	Elevation 13- Grid B. Beam column joint underside of level 4 DS 1 2 %	Vertical cracks in the beam column joint approximately 1 mm wide. A hairline crack in the column. Approximately 11 vertical cracks along the length of the beam range from 0.1 - 0.4 mm wide. Concrete spalled off.	
---------	---	---	---




228	Elevation 13- Grid A. Beam column joint underside of level 4 DS 2 2.75% DS 1 2.0%	<p>A vertical crack of 10 mm wide in the beam column joint.</p> <p>Loss of concrete in the beam.</p> <p>transverse frame drift</p>	<p>opening up of pin connection to column (likely)</p> 
-----	---	--	--





			
229	Elevation N-Grid 1. Beam column joint underside of level 4 DS 1 2.0%	Combination of diagonal and vertical cracks in the beam column joint. Width of the cracks range from 1.4 - 3.5 mm. Concrete spalling off in the joint. Approximately 3 vertical hairline cracks along the beam length.	
230/231	Elevation N-Grid 2. Beam column joint underside of level 4 DS 0 1 %	Vertical cracks in the beam column joint approximately 1 mm wide. Concrete spalling in the beam. Approximately 3 vertical hairline cracks along the beam length.	









<p>232/233</p>	<p>Elevation N-Grid 3. Beam column joint underside of level 4 DS 0 1 %</p>	<p>Vertical cracks in the beam column joint less than 0.3 mm wide. Approximately 5 vertical hairline cracks along the beam length.</p>	




<p>234/235</p>	<p>Elevation N-Grid 4. Beam column joint underside of level 4</p> <p>DS 0 1 %</p>	<p>Vertical cracks in the beam column joint less than 0.3 mm wide.</p> <p>Approximately 7 vertical hairline cracks along the beam length.</p>	
<p>236/237</p>	<p>Elevation N-Grid 5. Beam column joint underside of level 4</p> <p>DS 0 1 %</p>	<p>Vertical cracks in the Bbeam column joint less than 0.3 mm wide.</p> <p>Approximately 5 vertical hairline cracks along the beam length.</p>	
<p>238/239</p>	<p>Elevation N-Grid 6. Beam column joint underside of level 4</p> <p>DS 0 1 %</p>	<p>Vertical cracks in the beam column joint less than 0.5 mm wide.</p> <p>Vertical cracks along the beam length.</p> <p>Width of the cracks range from 0.1 - 0.5 mm.</p>	




<p>240/241</p>	<p>Elevation N-Grid 7. Beam column joint underside of level 4</p> <p>DS 0 1 %</p>	<p>Vertical cracks in the beam column joint less than 0.3 mm wide.</p> <p>Approximately 6 vertical cracks along the beam length.</p>	
<p>242/243</p>	<p>Elevation N-Grid 8. Beam column joint underside of level 4</p> <p>DS 0 1 %</p>	<p>A vertical crack in the beam column joint less than 0.2 mm wide.</p> <p>Approximately 5 vertical cracks along the beam length.</p>	
<p>244/245</p>	<p>Elevation N-Grid 9. Beam column joint underside of level 4</p> <p>DS 0 1 %</p>	<p>Vertical cracks in the beam column joint approximately 0.3 mm wide.</p> <p>Approximately 8 vertical cracks along the beam length.</p>	


<p>246/247</p>	<p>Elevation N-Grid 10. Beam column joint underside of level 4</p> <p>DS 0 1 %</p>	<p>Vertical cracks in the beam column joint approximately 0.2 mm wide.</p> <p>Approximately 10 vertical cracks along the beam length.</p>	
<p>248/249</p>	<p>Elevation N-Grid 11. Beam column joint underside of level 4</p> <p>DS 0 1 %</p>	<p>Vertical cracks in the beam column joint approximately 0.2 mm wide.</p> <p>Approximately 5 vertical cracks along the beam length.</p>	
<p>250/251</p>	<p>Elevation N-Grid 12. Beam column joint underside of level 4</p> <p>DS 0 1 %</p>	<p>Vertical cracks in the beam column joint approximately 0.3 mm wide.</p> <p>Approximately 3 vertical hairline cracks and a 1 mm wide crack along the beam length.</p>	
<p>252</p>	<p>Elevation N-Grid 13. Beam column joint underside of level 4</p> <p>DS 1 2.0%</p>	<p>No crack observed in the joint.</p> <p>Spalling of concrete close to the beam column joint.</p>	

			
253	Elevation 10A-Grid A. Beam column joint underside of level 4	Combination of vertical and diagonal cracks in the beam column joint range from 1.5 - 5 mm wide. Approximately 4 minor cracks along the beam length.	  


254/255	Elevation 10A-Grid B'. Beam column joint underside of level 4	<p>Cracks each side of the beam column joint. Width of cracks less than 2 mm.</p> <p>Approximately 5 vertical cracks including a 0.3 mm wide crack along the beam length.</p> <p>Concrete spalled off in the beam.</p>	
256/257	Elevation 10A-Grid D'. Beam column joint underside of level 4		


258/259	Elevation 10A-Grid E'. Beam column joint underside of level 4	No photos taken/ No access at the time of inspection	
260/261	Elevation 10A-Grid F'. Beam column joint underside of level 4		
262/263	Elevation 10A-Grid H'. Beam column joint underside of level 4	A diagonal crack width of 0.3 mm on the beam face and underside of the beam. Minor hairline cracks along the beam length.	
264	Elevation KA-Grid 1. Beam column joint underside of level 4	Minor vertical crack less than 1 mm in the beam column joint. Approximately 8 vertical cracks less than 0.5 mm wide along the beam length.	



			
265/266	Elevation KA-Grid 2'. Beam column joint underside of level 4	Combination of vertical and diagonal cracks less than 1 mm wide in the beam column joint. Concrete spalling in the beam.	 
267/268	Elevation KA-Grid 4'. Beam column joint underside of level 4	This area has since been exposed however, we have not been back to inspect	
269/270	Elevation KA-Grid 5'. Beam column joint underside of level 4	This area has since been exposed however, we have not been back to inspect	



271/272	Elevation KA-Grid 6'. Beam column joint underside of level 4	This area has since been exposed however, we have not been back to inspect	
273/274	Elevation KA-Grid 8'. Beam column joint underside of level 4	Cracks less than 0.5 mm wide in the beam column joint.	
275	Elevation KA-Grid 9/10. Beam column joint underside of level 4	This area has since been exposed however, we have not been back to inspect	
276	Elevation L'-Grid 11'. Beam column joint underside of level 4	This area has since been exposed however, we have not been back to inspect	




277/278	Elevation L'- Grid 10. Beam column joint underside of level 4	This area has since been exposed however, we have not been back to inspect	
279	Elevation L'- Grid 9'. Beam column joint underside of level 4	This area has since been exposed however, we have not been back to inspect	
280	Elevation K- Grid 11'. Beam column joint underside of level 4	This area has since been exposed however, we have not been back to inspect	
281/282	Elevation K- Grid 10. Beam column joint underside of level 4	This area has since been exposed however, we have not been back to inspect	
283	Elevation K- Grid 9'. Beam column joint underside of level 4	This area has since been exposed however, we have not been back to inspect	
283 (a)	Elevation 11'- Grids between K to L'. B/C joints and beams underside of level 4 (Refer to Dycore plan for the reference)	This area has since been exposed however, we have not been back to inspect	

<p>283 (b&c)</p>	<p>Elevation 13'- Grids between N to J'. B/C joints and beams underside of level 4. (Refer to Dycore plan for the reference)</p>	<p>This area has since been exposed however, we have not been back to inspect</p>	
<p>284</p>	<p>Dycore units Underside of level 4. Grid numbers between HA- KA and 1-2.</p>	<p>Minor diagonal crack, underside of the Dycore unit at location 1/HA. Spalling of concrete around the crack. Minor longitudinal crack close to the perimeter beam.</p>	 <p>The photographs show three different views of the damage. The top photo shows a diagonal crack in a concrete slab above a metal beam. The middle photo shows a longitudinal crack in a concrete slab next to a metal beam, with some spalling of concrete. The bottom photo shows a similar view from a different angle, highlighting the crack and the surrounding concrete structure.</p>

285	Dycore units Underside of level 4. Grid numbers between KA-N and 1-2.	<p>Minor diagonal crack, underside of the Dycore unit at location 1/KA. Width of the cracks less than 0.5 mm.</p> <p>A combination of diagonal and longitudinal cracks underside of the Dycore unit at location 1/N.</p> <p>Loss of concrete and crushed at the corner.</p>	
286	Dycore units Underside of level 4. Grid numbers between HA- KA and 2-3.	No visible crack observed	



287	Dycore units Underside of level 4. Grid numbers between KA-N and 2-3.	A longitudinal crack underside of the Dycore unit close to the grid location 2/N.	
288	Dycore units Underside of level 4. Grid numbers between HA- KA and 3-8.	A crack underside of the Dycore unit close to the grid location 5/HA. Concrete spalled off (suspected at the time of installation) on grid location 3/HA.	


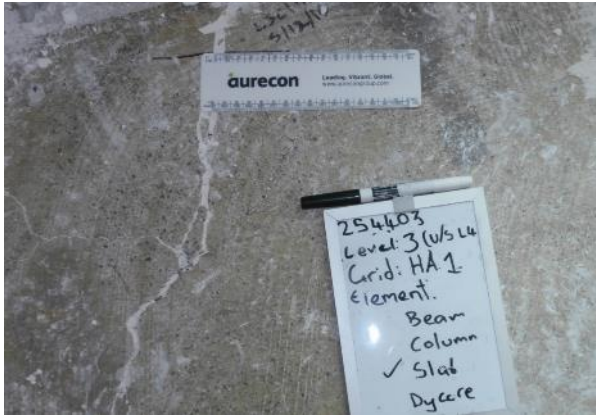
289	Dycore units Underside of level 4. Grid numbers between KA-N and 3-8.	Concrete spalled off in the Dycore units close to the grid location 4/N, suspected at the time of installation.	
290	Dycore units Underside of level 4. Grid numbers between 8-11 and H-KA.	Combination of diagonal and longitudinal cracks underside of the Dycore units around the corner column located on grid HA/8A. Diagonal cracks range from minor to 2 mm wide.	
292	Dycore units Underside of level 4. Grid numbers between H-N and 11-13.	A longitudinal crack with loss of concrete and tendon exposed close to the grid 13/J. A minor crack with concrete spalled off.	

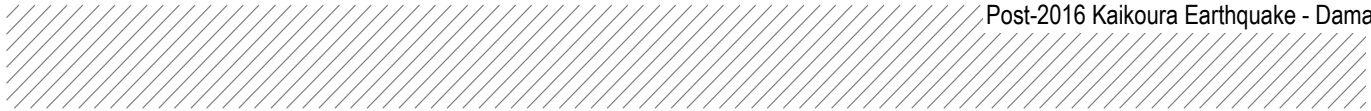
			
<p>293</p>	<p>Dycore units Underside of level 4. Grid numbers between 13- 10A and C-H.</p>	<p>Minor damage to corner of Dycore</p>	
<p>294</p>	<p>Dycore units Underside of level 4. Grid numbers between 8A- 10A and C-H</p>	<p>Diagonal corner cracking in 4 slabs, Grids D, E and F. Longitudinal crack in member at Grid E</p>	



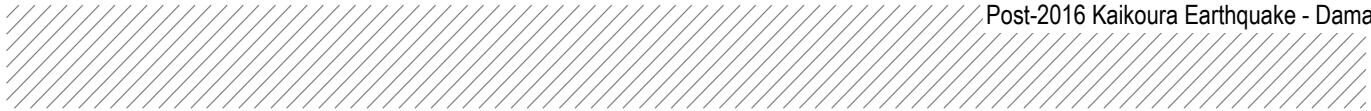
			<p>The rightmost column of the table contains three vertically stacked photographs documenting damage to a building's interior. The top photograph shows a ceiling with a silver, reflective light fixture and a white horizontal trim piece. A small, dark mark is visible on the concrete ceiling surface. The middle photograph shows a close-up of a concrete wall with a vertical crack and some surface discoloration. The bottom photograph shows a metal rod with a hook and a nut, secured to a concrete wall, with a wooden beam or pipe running parallel to it.</p>
--	--	--	--

295	Dycore units Underside of level 4. Grid numbers between 8A-10A and B-C	Minor damage to corner of Dycore unit	
296	Dycore units Underside of level 4. Grid numbers between 10A-13 and A-B	Minor damage to corner of Dycore unit	
297	Dycore units Underside of level 4. Grid numbers between 10A - 13 and A-B	Diagonal crack of Dycore unit, crack width approx 1.8 mm. Loss of concrete at end of Dycore unit.	

			
298	Dycore units Underside of level 4. Grid numbers between 8A-10A and A-B.	Minor cracking, less than 0.3 mm	
299	Floor slab level 3. Grid numbers between HA-KA and 1-2.	<p>Diagonal cracking spreading from corner column on grid 1HA.</p> <p>Crack at column 1HA 7 mm wide with vertical dislocation.</p> <p>Cracking spreading out from column range between 2 - 0.8 mm</p> <p>Longitudinal crack along gridline 2 approx 4 mm wide.</p>	




		<p>Transverse crack along grid line KA approx 12 mm</p>	
--	--	---	---



			<p>The table contains four photographs documenting concrete damage. The top photograph shows a horizontal crack in a concrete slab, with a ruler and a label '254.03 Level 3 Corid HA/RM Element Beam Column Slab Dyere'. The middle photograph is a close-up of a crack with a ruler. The bottom photograph shows a vertical crack with a ruler and a label. The bottom-most photograph is a close-up of a crack with a ruler.</p>
--	--	--	---





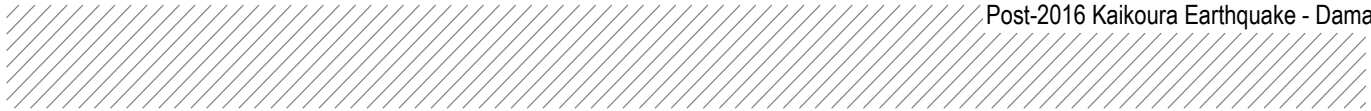
			
--	--	--	---

300	Floor slab level 3. Grid numbers between KA-N and 1-2.	Transverse crack along grid line KA approx 5 mm wide. Longitudinal crack along grid line 2, 2.5 - 5 mm wide. Cracking at base of column 1N approx 7 mm wide.	 <p>The top photograph shows a vertical crack in a concrete floor slab. A white ruler is placed horizontally across the crack to measure its width. A handwritten note on a piece of paper is placed next to the crack. The note reads: '254403 Level: 3 (w/s L4) Grid: KA/N1 element. Beam Column ✓ Slab Dycere'. A blue and white ruler is also visible in the top left corner.</p> <p>The bottom photograph shows a horizontal crack in a concrete floor slab. A white ruler is placed horizontally across the crack. A handwritten note on a piece of paper is placed above the crack. The note reads: '254403 Level: 3 (w/s L4) Grid: KA/N1 element. Beam Column ✓ Slab Dycere'. A blue and white ruler is also visible in the bottom right corner.</p>
-----	--	--	---


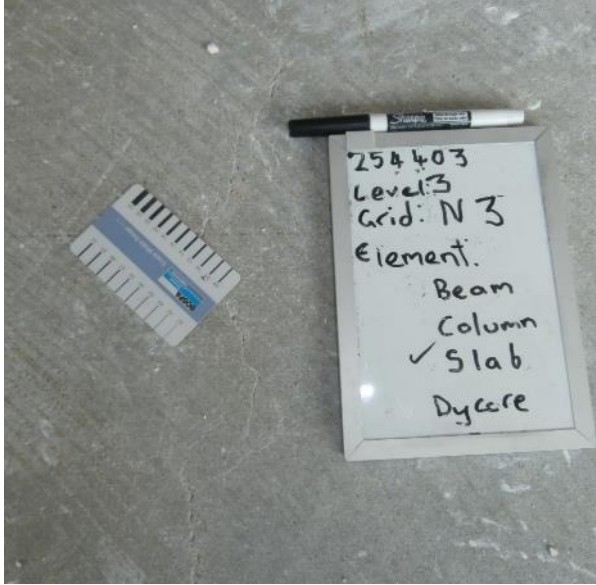



301	Floor slab level 3. Grid numbers between HA-KA and 2-3.	This area has since been exposed however, we have not been back to inspect.	
302	Floor slab level 3. Grid numbers between KA-N and 2-3.	<p>Longitudinal crack near grid line 3 approx 1.4 mm wide.</p> <p>Transverse crack along grid line KA approx 0.6 mm wide.</p>	

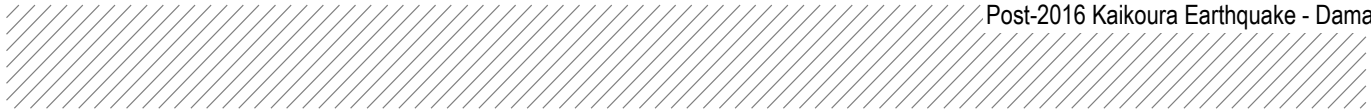
			
303	Floor slab level 3. Grid numbers between HA-KA and 3-8.	Longitudinal crack in between grid lines 5-6 approx 2.5 mm. Transverse cracking along frame KA at grid 7 approx 1.2 mm wide.	



			<p>The table contains three photographs of concrete damage. Each photo shows a crack in the concrete with a small white tag and a blue ruler for scale. The tags contain handwritten notes:</p> <ul style="list-style-type: none">Top photo: Tag text includes "256 103", "Level 3", "Grid KA 2/8", "Element", "Column", "Beam", "Slab", and "Dycore".Middle photo: Tag text includes "256 103", "Level 3", "Grid KA 2/8", "Element", "Column", "Beam", "Slab", and "Dycore".Bottom photo: Tag text includes "256 103", "Level 3", "Grid KA 2/8", "Element", "Column", "Beam", "Slab", and "Dycore".
--	--	--	--

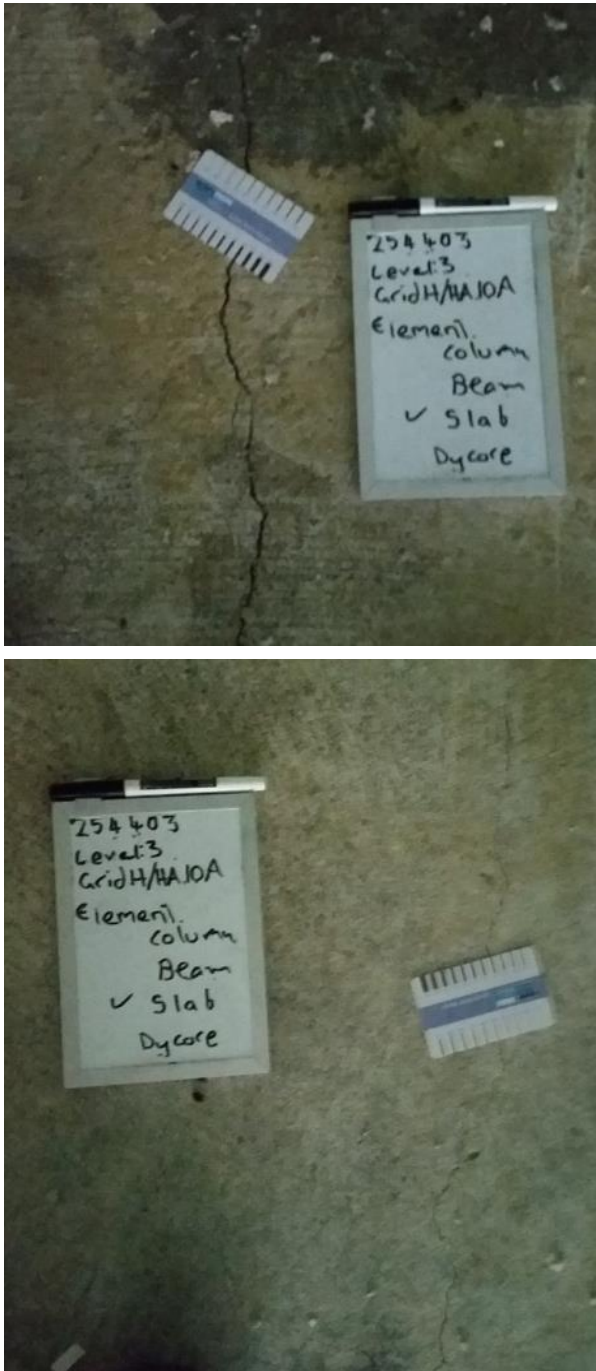
			
<p>304</p>	<p>Floor slab level 3. Grid numbers between KA-N and 3-8.</p>	<p>Minor longitudinal crack near grid 3 approx 1.4 mm wide.</p>	
<p>305</p>	<p>Floor slab level 3. Grid numbers between H-KA and 8-10A.</p>	<p>2.5 mm wide diagonal crack starting at the lift shaft on Grid point 11/K.</p>	

306	Floor slab level 3. Grid numbers between KA-N and 8-13.	Minor longitudinal cracks between grids 8 and 9 approx 1.4 mm wide.	 <p>The image contains two photographs of a concrete floor slab. The top photograph shows a longitudinal crack in the slab. A ruler is placed across the crack to measure its width. A handwritten label is placed next to the crack, containing the following text: '254403', 'Level: 3', 'Grid KA 9/8', 'Element: Column', 'Beam', 'Slab', and 'Dycore'. The bottom photograph shows the same crack from a different angle, with the ruler and label still present.</p>
-----	---	---	--




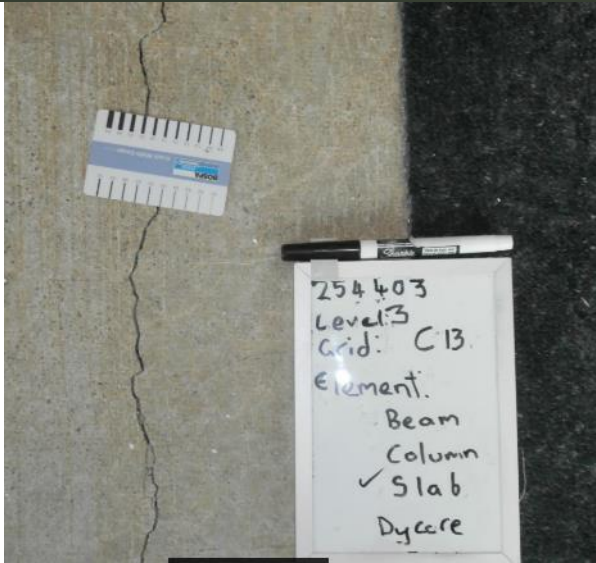
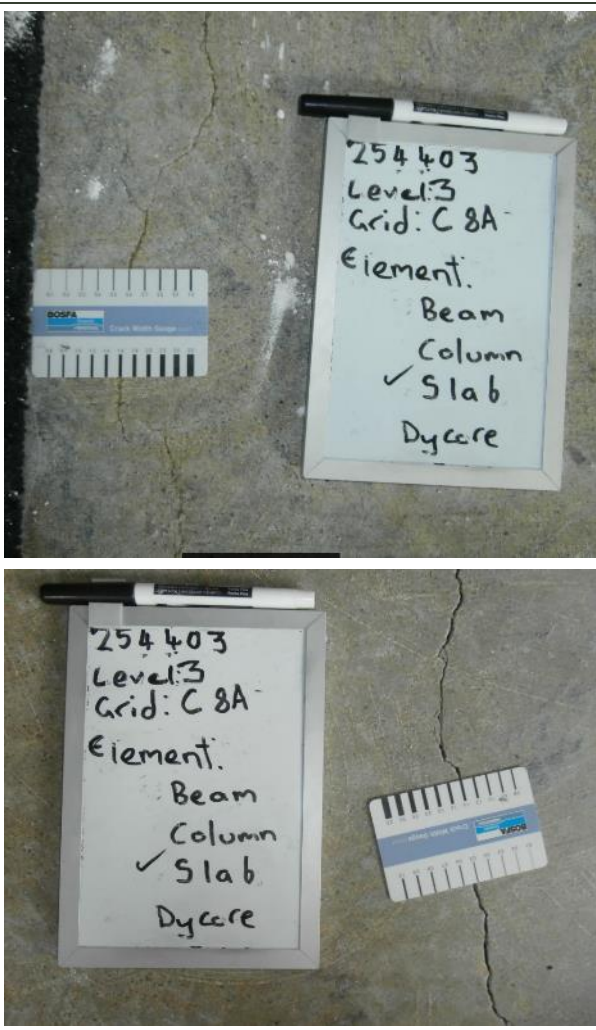
			<p>The top photograph shows a corner of a room with green walls and a dark baseboard. The floor slab is severely damaged, appearing as a large, irregularly shaped, light-colored mass of concrete and debris, partially detached from the walls. The surrounding floor is dark and appears to be a different material or finish.</p> <p>The bottom photograph is a close-up of the damaged concrete slab. A white clipboard with a black pen is placed on the surface. The clipboard has handwritten text: "254 403", "Level: 3", "Grid KA 9/8", "Element: column", "Beam", "Slab", and "Dycore" with a checkmark next to it. A blue and white ruler is placed horizontally below the clipboard for scale. The concrete surface is cracked and shows signs of spalling.</p>
--	--	--	--




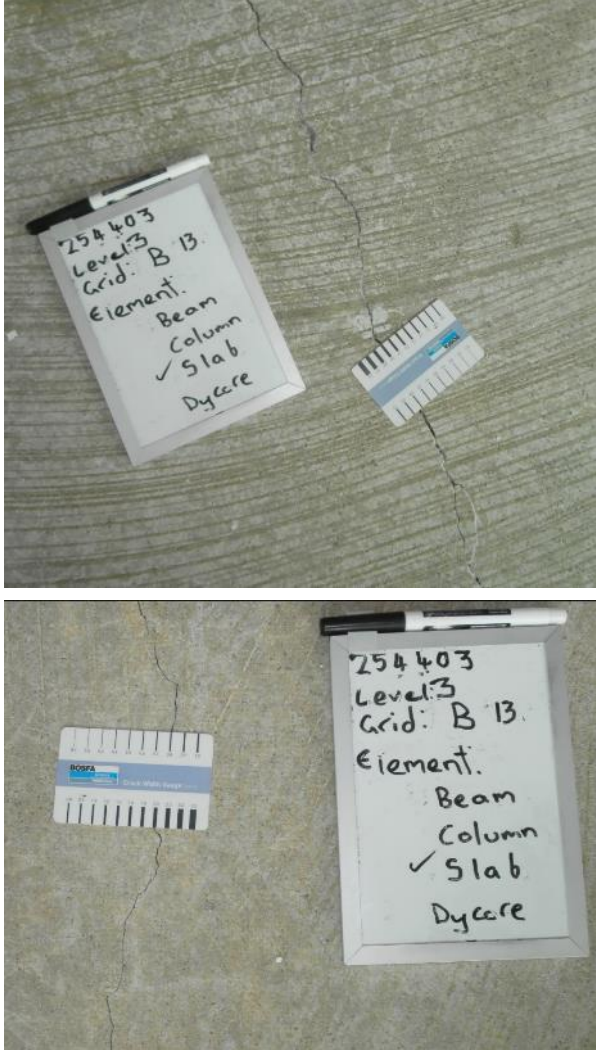
307	Floor slab level 3. Grid numbers between 10A-13 and H-N.	Longitudinal cracks spreading from central column between grids H and J, cracks range from 2 – 0.8 mm wide.	
-----	--	---	---

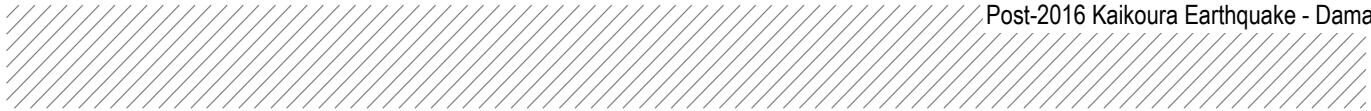
<p>308</p>	<p>Floor slab level 3. Grid numbers between 10A-8A and C-H.</p>	<p>Transverse cracks along inner frame on grid 10A between Grids G-H, E-F and C-D widths ranging 1-1.4 mm.</p> <p>Longitudinal cracks from Grid C-D with widths ranging from 0.6-1 mm.</p>	 <p>The three photographs show different views of a concrete floor slab with a vertical crack. Each image includes a ruler for scale and a handwritten note with the following text: '254403 Level: 3 Grid: D8A Element: Beam Column ✓ Slab Dycere'. The crack is clearly visible in all three images, running vertically through the concrete.</p>
------------	---	--	--

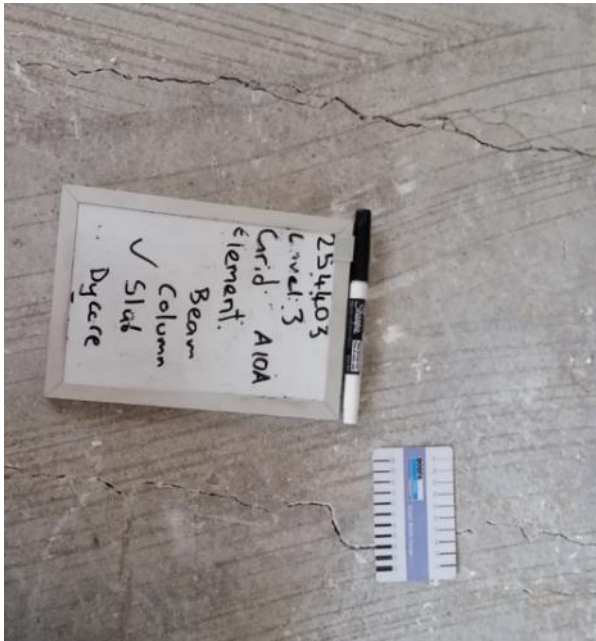

			 <p>The three photographs show a floor slab with a crack. The top photo shows a crack with a ruler and a label. The middle photo shows a crack with a ruler and a label. The bottom photo shows a crack with a ruler and a label.</p>
309	Floor slab level 3. Grid numbers between 10A-13 and C-H.	<p>Longitudinal crack along grid C approx 2 mm wide.</p> <p>Transverse crack along grid line 10A at point D approx 1.2 mm.</p>	

			
<p>310</p>	<p>Floor slab level 3. Grid numbers between 10A-8A and B-C.</p>	<p>Longitudinal cracks along grid line C and B approx 1.4 mm wide. Transverse cracking around column in inner frame width ranging 1.6-2.5 mm.</p>	

			 <p>The top photograph shows a survey tag with handwritten text: '254403', 'Level: 3', 'Grid: B8A', 'Element: Beam', 'Column', '✓ Slab', and 'Dycare'. A scale is placed next to it for reference. The middle and bottom photographs show the same tag and scale from a different angle, with a person's foot visible in the bottom right corner of the lower image.</p>
--	--	--	---

			
<p>311</p>	<p>Floor slab level 3. Grid numbers between 10A-13 and B-C.</p>	<p>Longitudinal cracking between along slab widths ranging 0.8-2 mm.</p>	



312	Floor slab level 3. Grid numbers between 10A-8A and A-B.	<p>Diagonal cracking spreading from corner column A8A width ranges from 4 – 1.2 mm.</p> <p>Cracking at column base at A8A.</p> <p>Longitudinal crack along the span of the floor approx 2 mm width.</p> <p>Transverse crack along gridline 10A approx 8 mm.</p> <p>Longitudinal crack along perimeter frame at grid A approx 4 mm wide.</p>	 
-----	--	---	--

			 <p>The image contains two photographs of a concrete slab. The top photograph shows a wide, irregular crack in the concrete. A white label with handwritten text is placed on the slab. The text on the label reads: "254403", "Level: 3", "Grid A 10A/8A", "Element:", "Beam", "Column", "✓ Slab", and "Dycore". A white ruler with the "aurecon" logo is visible in the upper left corner of the photo. The bottom photograph is a closer view of the same crack and label. The label text is the same as in the top photo. The "aurecon" ruler is also visible in the upper right corner of this photo.</p>
--	--	--	---




			The table contains two photographs documenting structural damage. The top photograph shows a vertical crack in a light-colored concrete wall. A white ruler and a scale with the 'aureco' logo are placed against the wall to measure the crack's width. The bottom photograph shows a large, jagged crack on a concrete floor in a room. Debris is scattered on the floor, and a red marker is visible near the crack. A shadow is cast across the floor, and a metal structure is partially visible on the left.
--	--	--	--



--	--	--	--



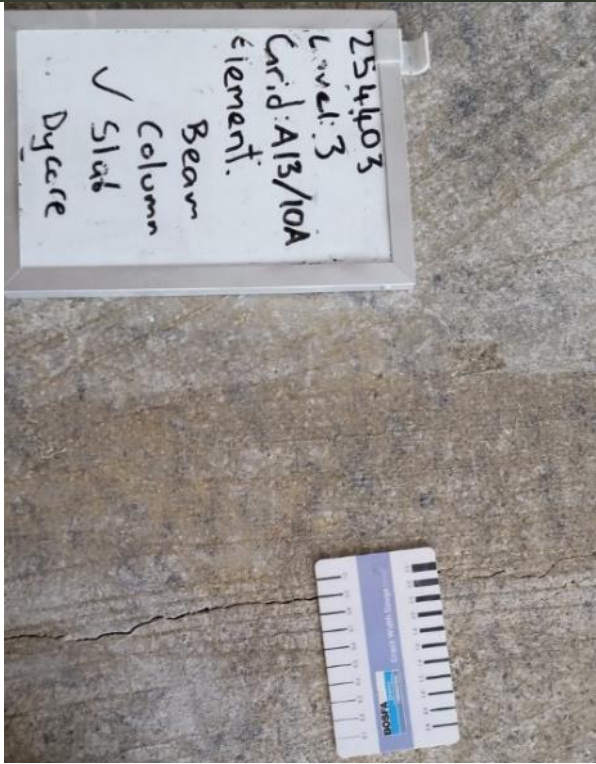
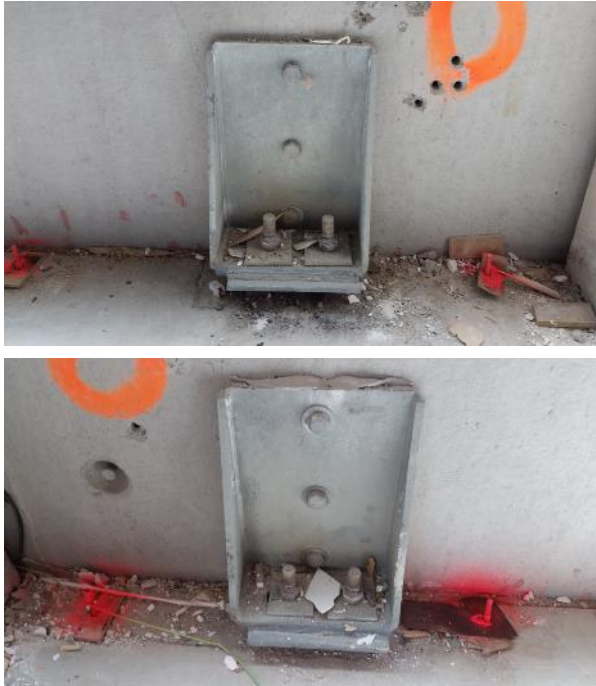
			<p>The top photograph shows a corner of a room with significant damage. A vertical wooden stud is leaning against a wall. The floor is cracked and covered with debris, including a red object. A metal plate is attached to the base of the stud. A red circle is marked on the wall in the background. The bottom photograph shows a close-up of the cracked floor and debris, with a bright light source creating a strong shadow on the ground.</p>
--	--	--	---

<p>313</p>	<p>Floor slab level 3. Grid numbers between 10A-13 and A-B.</p>	<p>Diagonal cracking spreading from corner column at A13 widths ranging 7-1.8 mm. Mesh exposed at places.</p> <p>Loss of concrete at toe of column A13.</p> <p>Longitudinal crack along the span of the floor approx 0.9 mm width.</p> <p>Transverse crack along gridline 10A approx 2.5 mm.</p>	 <p>The top photograph shows a diagonal crack in a concrete floor slab, spreading from a corner column. A handwritten note on a clipboard is visible, with text including '254403', 'Level: 3', 'Grid: A13', 'element', 'Beam', 'Column', and '✓ Slab'. The bottom photograph shows a transverse crack in the concrete floor slab, with a ruler and a handwritten note for scale and location. The ruler is marked in centimeters and millimeters, and the note includes '254403', 'Level: 3', 'Grid: A13', 'element', 'Beam', 'Column', and '✓ Slab'.</p>
------------	---	--	---





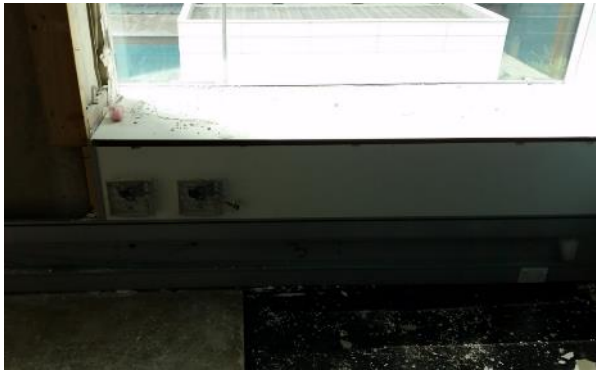


			A vertical column of four photographs documenting structural damage. The top photo shows a close-up of a concrete surface with a ruler for scale and a crack. The second photo shows a corner of a room with significant concrete spalling and debris. The third photo is a similar view of a corner, showing the extent of the damage. The bottom photo shows another corner with debris and damaged concrete.
--	--	--	---






			
314	Elevation 8A, Grids between A-B. Precast façade panels in level 3.	Diagonal cracks approximately 3mm wide around the bottom connection of the precast panel.	






			
315	Elevation 8A, Grids between B-C. Precast façade panels in level 3.	Diagonal cracks approximately 3mm wide around the bottom connection of the precast panel.	



316	Elevation 8A, Grids between C-D. Precast façade panels in level 3.	Bulkhead was not removed at the time of inspection.	
317	Elevation 8A, Grids between D-E. Precast façade panels in level 3.	No crack was observed in the panel at the time of inspection.	
318	Elevation 8A, Grids between E-F. Precast façade panels in level 3.	Panel damaged, likely not related with the earthquake. No crack seen in the panel.	






			
319	Elevation 8A, Grids between F-G. Precast façade panels in level 3.	A 2mm wide vertical crack in the center of the panel. No cracks around the connections.	 

			
320	Elevation 8A, Grids between G-H. Precast façade panels in level 3.	No crack was observed in the panel at the time of inspection.	
321	Elevation 8A, Grids between H-HA. Precast façade panels in level 3.	No crack was observed in the panel at the time of inspection.	

			
322	Elevation 1, Grids between HA-HA/KA. Precast façade panels in level 3.	A vertical harline crack around the bottom connection of the precast panel.	



323	Elevation 1, Grids between HA/KA-KA. Precast façade panels in level 3.	Combination of vertical and diagonal cracks between 0.3mm to 0.2mm wide around the connection and in the precast panel.	 The top photograph shows a close-up of a precast concrete panel's connection to a steel beam. A vertical crack is visible on the left side of the panel, and a diagonal crack runs from the top edge towards the center. The bottom photograph shows a similar view from a slightly different angle, highlighting the diagonal crack more prominently.
324	Elevation 1, Grids between KA-KA/N. Precast façade panels in level 3.	Diagonal cracks in upper pannel approx 0.2 mm wide.	 The top photograph shows a diagonal crack in the upper portion of a precast concrete panel, extending from the top edge towards the center. The bottom photograph shows a similar view from a different angle, showing the crack more clearly against the background of the steel structure.

			
325	Elevation 1, Grids between KA/N-N. Precast façade panels in level 3.	Diagonal cracks between 0.3mm to 0.2mm wide around the connection and in the precast panel. Diagonal cracks approximately 0.2mm wide in the top of the precast panel. Top fixing plates were bent.	

326	Elevation A, Grids between 13-13/10A. Precast façade panels in level 3.	No crack was observed in the bottom of the panel at the time of inspection. A hairline crack in the top of the panel.	
-----	--	--	--





			The rightmost column of the table contains two photographs stacked vertically. The top photograph shows a grey metal cabinet or enclosure, possibly a fire safe, with its door open. The interior is cluttered with debris, including what appears to be a broken metal mesh or grate. The cabinet is supported by wooden framing. The bottom photograph shows a similar view of the same metal cabinet, but from a slightly different angle, showing more of the surrounding wooden structure and the debris on the floor.
--	--	--	---




			
327	Elevation A, Grids between 13/10A-10A. Precast façade panels in level 3.	No crack was observed around the bottom connection. Minor damage/dislocation of concrete around the top connection. Top connection plates are bent.	










328	Elevation A, Grids between 10A-10A/8A. Precast façade panels in level 3.	Diagonal cracks approximately 0.3mm wide close to the bottom connection of the precast panel. Vertical crack in upper pannel approx 0.2 mm.	


			
<p>329</p>	<p>Elevation A, Grids between 10A/8A-8A. Precast façade panels in level 3.</p>	<p>Vertical cracks between 0.5mm to 0.2mm wide in the bottom of the precast panel. Concrete spalling and a width of 0.2mm crack in the top of the panel. Top connection bolts are bent.</p>	

			
330	Elevation HA, Grids between 8A-8. Precast façade panels in level 3.	No crack/damage was observed in the panel at the time of inspection.	
331	Elevation HA, Grids between 8-7. Precast façade panels in level 3.	A diagonal crack 0.2mm wide around the bottom connection of the precast panel.	

			
332	Elevation HA, Grids between 7-6. Precast façade panels in level 3.	No crack/damage was observed in the panel at the time of inspection.	
333	Elevation HA, Grids between 6-5. Precast façade panels in level 3.	No crack/damage was observed in the panel at the time of inspection.	

			
334	Elevation HA, Grids between 5-4. Precast façade panels in level 3.	No crack/damage was observed in the panel at the time of inspection.	
335	Elevation HA, Grids between 4-3. Precast façade panels in level 3.	No crack/damage was observed in the panel at the time of inspection.	
336	Elevation HA, Grids between 3-2. Precast façade panels in level 3.	No crack/damage was observed in the panel at the time of inspection.	

337	Elevation HA, Grids between 2-1. Precast façade panels in level 3.	No crack/damage was observed in the panel at the time of inspection.	
338	Elevation 13, Grids between N-M. Precast façade panels in level 3.	Bulkhead not removed at the time of inspection	
339	Elevation 13, Grids between M-L. Precast façade panels in level 3.	Diagonal cracks approximately 0.3mm wide around the bottom connection of the precast panel. Diagonal crack approx 0.8 mm.	

			
340	Elevation 13, Grids between L-K. Precast façade panels in level 3.	<p>Diagonal cracks between 0.3mm to 0.5mm wide around the bottom connections of the precast panel.</p> <p>Top connection bolts are bent.</p> <p>0.2 mm diagonal crack in upper pannel.</p>	





			<p>The fourth column of the table contains four photographs documenting structural damage. The top photo shows a hand holding a blue and white ruler against a crack in a grey concrete ceiling. The second and third photos are close-up views of a grey metal bracket or anchor bolt that has been crushed and bent, with a wooden block placed against it. The bottom photo shows a circular hole in a concrete floor, with a metal cap or plug partially visible inside the hole.</p>
--	--	--	---



341	Elevation 13, Grids between K-J. Precast façade panels in level 3.	Diagonal cracks between 0.3mm to 0.5mm wide around the bottom connections of the precast panel. 0.4 mm diagonal cracking either side of upper panel.	





<p>342</p>	<p>Elevation 13, Grids between J-H. Precast façade panels in level 3.</p>	<p>Diagonal cracks approximately 0.4mm wide around the bottom connections of the precast panel.</p> <p>Right side plate bent.</p>	



		<p>0.3 mm diagonal cracking on left side of upper panel.</p>	
<p>343</p>	<p>Elevation 13, Grids between H-G. Precast façade panels in level 3.</p>	<p>Diagonal and horizontal cracks between 0.3mm to 0.5mm wide in the precast panel. Bolts and plates of the top connections are bent. 0.2 mm diagonal cracking on left of panel 0.3 mm on right side in upper connection.</p>	



			The rightmost column of the table contains four vertically stacked photographs documenting structural damage. The top photo shows a hand holding a blue and white 'Boof' brand crack gauge against a concrete surface, with a visible crack. The second photo shows a metal bracket or anchor bolt assembly that has become loose and is surrounded by concrete debris. The third photo is a close-up of a metal bracket with several bolts. The bottom photo shows a metal bracket mounted on a concrete surface, with a blue line drawn on the concrete below it.
--	--	--	---




			
<p>344</p>	<p>Elevation 13, Grids between G-F. Precast façade panels in level 3.</p>	<p>Diagonal cracks range between 0.3mm to 0.5mm wide around the bottom connections. 0.2 mm diagonal cracking on left of panel 0.3 mm on right side in upper connection.</p>	





			
345	Elevation 13, Grids between F-E. Precast façade panels in level 3.	Diagonal cracks approximately 0.4mm wide around the bottom connections. 0.5 mm diagonal cracking on left of panel 0.2 mm on right side in upper panel.	




			The table contains three photographs of structural damage. The top photograph shows a close-up of metal reinforcement bars (rebar) protruding from a concrete surface, with some orange material visible. The middle photograph shows a wide view of a concrete floor with several prominent, irregular cracks. A blue horizontal line is drawn across the floor. The bottom photograph shows another view of the cracked concrete floor, featuring a red circular marker and a wooden box or structure in the lower right corner.
--	--	--	--

			
<p>346</p>	<p>Elevation 13, Grids between E-D. Precast façade panels in level 3.</p>	<p>Diagonal cracks 0.4mm wide around the bottom connections and in the panel.</p>	
<p>347</p>	<p>Elevation 13, Grids between D-C. Precast façade panels in level 3.</p>	<p>Diagonal cracks 0.4mm wide around the bottom connections. Right side plate bent.</p>	

			
348	Elevation 13, Grids between C-B. Precast façade panels in level 3.	<p>Diagonal cracks range between 0.2mm to 0.5mm wide around the bottom connections.</p> <p>0.5 mm diagonal cracking on left of panel 0.3 mm on right side in upper connections</p> <p>Both plates bent.</p>	




			The rightmost column of the table contains three vertically stacked photographs documenting structural damage. The top photograph shows a close-up of a galvanized steel anchor bolt assembly embedded in a concrete wall, with a blue pipe visible above it. The middle photograph shows a circular hole in a concrete wall, with a blue horizontal line drawn across the surface below it. The bottom photograph shows a larger area of concrete wall with significant surface spalling and exposed aggregate.
--	--	--	--

349	Elevation 13, Grids between B-A. Precast façade panels in level 3.	<p>Diagonal cracks range between 0.3mm to 0.4mm wide around the bottom connections.</p> <p>Bolts and plates in the top connections are bent.</p> <p>0.2 mm diagonal cracking on left of panel.</p> <p>0.4 mm diagonal cracking on Right of panel.</p>	
-----	--	---	---



			
350	Elevation N, Grids between 1-2. Precast façade panels in level 3.	Bulk head not removed at the time of inspection Left side plates bent.	 
351	Elevation N, Grids between 2-3. Precast façade panels in level 3.	Diagonal cracks 0.4mm wide around the bottom connections. Two diagonal cracks 0.3 mm wide on left side	





			The rightmost column of the table contains four photographs documenting structural damage. The top photo shows a vertical crack in a light-colored concrete slab, with a hand holding a white 10cm scale bar for reference. The second photo is a view looking down into a wooden frame structure, possibly a staircase or a floor joist system. The third photo shows a metal bracket or anchor bolt assembly mounted on a concrete wall. The bottom photo shows a metal plate or bracket mounted on a wall, with some debris and a crack visible nearby.
--	--	--	--

352	Elevation N, Grids between 3-4. Precast façade panels in level 3.	Diagonal cracks approximately 0.6mm wide around the bottom connections. Right side panel bent.	
-----	---	--	---



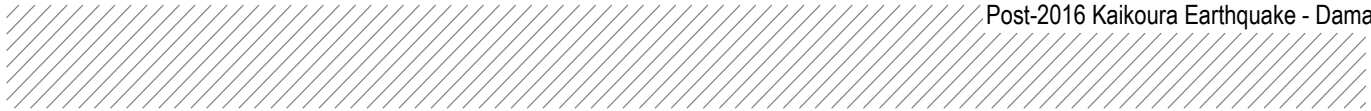
			
353	Elevation N, Grids between 4-5. Precast façade panels in level 3.	Diagonal cracks between 0.3mm to 0.5mm wide around the bottom connections and in the panel.	





			
554	Elevation N, Grids between 5-6. Precast façade panels in level 3.	Diagonal cracks between 0.1mm to 0.4mm wide around the bottom connections and in the panel. Right hand plate bent.	





			
355	Elevation N, Grids between 6-7. Precast façade panels in level 3.	Diagonal cracks between 0.5mm to 0.6mm wide around the bottom connections and in the panel.	



356	Elevation N, Grids between 7-8. Precast façade panels in level 3.	Diagonal cracks between 0.3mm to 0.4mm wide around the bottom connections.	

357	Elevation N, Grids between 8-9. Precast façade panels in level 3.	Diagonal cracks between 0.2mm to 0.4mm wide around the bottom connections.	
358	Elevation N, Grids between 9-10. Precast façade panels in level 3.	Diagonal cracks between 0.3mm to 0.4mm wide around the bottom connections and in the panel.	



			
359	Elevation N, Grids between 10-11. Precast façade panels in level 3.	Diagonal cracks between 0.2mm to 0.3mm wide around the bottom connections and in the panel.	




--	--	--





<p>360</p>	<p>Elevation N, Grids between 11-12. Precast façade panels in level 3.</p>	<p>Diagonal cracks 0.2mm wide around the bottom connections.</p>	
------------	--	--	---




			
361	Elevation N, Grids between 12-13. Precast façade panels in level 3.	Diagonal and vertical cracks 0.2mm wide around the connections and in the panel.	

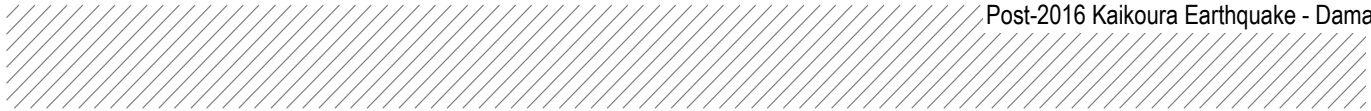



			A vertical column of four photographs documenting the damage to a metal electrical enclosure. The top photo shows the enclosure with a white cable and some debris. The second photo shows the enclosure with its door open, revealing internal components. The third photo shows the enclosure lying on its side on a concrete floor. The bottom photo shows the enclosure lying flat on the floor, with a wooden plank nearby.
--	--	--	--








			The rightmost column of the table contains two photographs of a concrete floor. The top photograph shows a light-colored concrete surface with a wooden door handle on the left and a metal door stop on the right. The bottom photograph shows a similar concrete surface with a circular hole or hole in the center, surrounded by some debris and a metal object on the right.
--	--	--	---




ID.	Location	Comment	Photographs
362	Elevation 8A-Grid A. Beam column joint underside of level 5 DS 1 2.0%	8 mm crack at face of column. 6 vertical cracks along beam approx. 0.2 mm.	






<p>363/3 64</p>	<p>Elevation 8A-Grid B. Beam column joint underside of level 5</p> <p>DS 1 2.0%</p>	<p>Diagonal hairline cracks in column. Crack on LHS of beam column joint approx. 2 mm. Crack on RHS of beam column joint approx. 2.5 mm. 2 hairline cracks along beam span.</p>	
---------------------	---	---	---


			
365/3 66	Elevation 8A-Grid C. Beam column joint underside of level 5 DS 1 2.0%	Diagonal hairline cracking in column. Cracks on either side of beam column joint approx. 2.5 mm.	



			
367/3 68	Elevation 8A-Grid D. Beam column joint underside of level 5 DS 0 1 %	Column not accessible, only beam column joint. Crack on LHS of beam column joint approx. 0.3 mm Crack on RHS of beam column joint approx. 1.5 mm.	 

			
369/3 70	Elevation 8A-Grid E. Beam column joint underside of level 5 DS 1 2.0%	Diagonal hairline cracking in column. Cracking on either side of the beam column joint 1-2 mm.	 

			
<p>371/3 72</p>	<p>Elevation 8A-Grid F. Beam column joint underside of level 5</p>	<p>No access not exposed</p>	<p>looks relatively minor</p>
<p>373/3 74</p>	<p>Elevation 8A-Grid G. Beam column joint underside of level 5 DS 0 1 %</p>	<p>Diagonal hairline cracking in column. Spalling of concrete from column. Cracking either side of beam column joint approx. 1-1.5 mm wide.</p>	

			
375/3 76	Elevation 8A-Grid H. Beam column joint underside of level 5	No access at time of inspection	

378	Elevation 8A-Grid HA. Beam column joint underside of level 5 DS 1 2.0%	Hairline diagonal cracking in beam. Vertical crack at column face approx. 2 mm.	
-----	--	---	---


379	Elevation 1-Grid HA. Beam column joint underside of level 3 DS 1 2.0%	Vertical crack at column face approx. 5 mm wide. Diagonal cracking spreading from column face 0.3 mm wide. Transverse crack on underside of beam 5 mm wide. 6 cracks along span 0.2-0.3 mm. Loss of concrete to beam and column.	 
-----	--	--	--

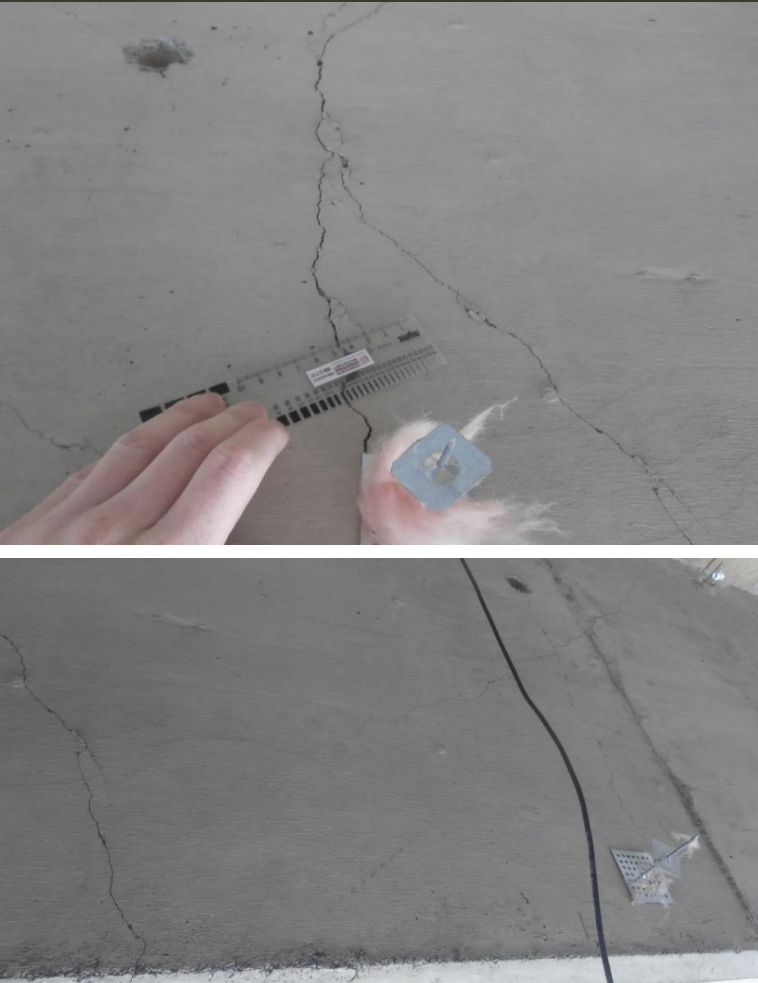



			A photograph showing significant structural damage to a concrete wall or ceiling. A large, jagged section of concrete has broken away, exposing a dark, fibrous material, likely rebar or a core of insulation. The remaining concrete surface is heavily cracked and crumbling.	
--	--	--	--	--



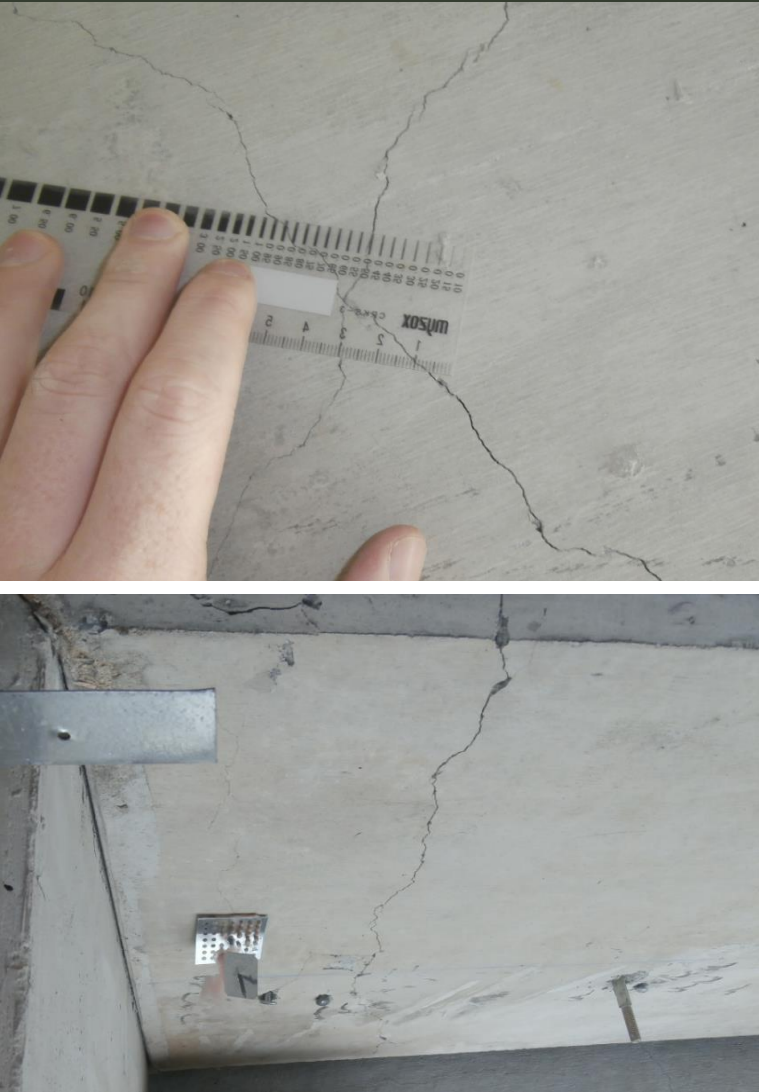
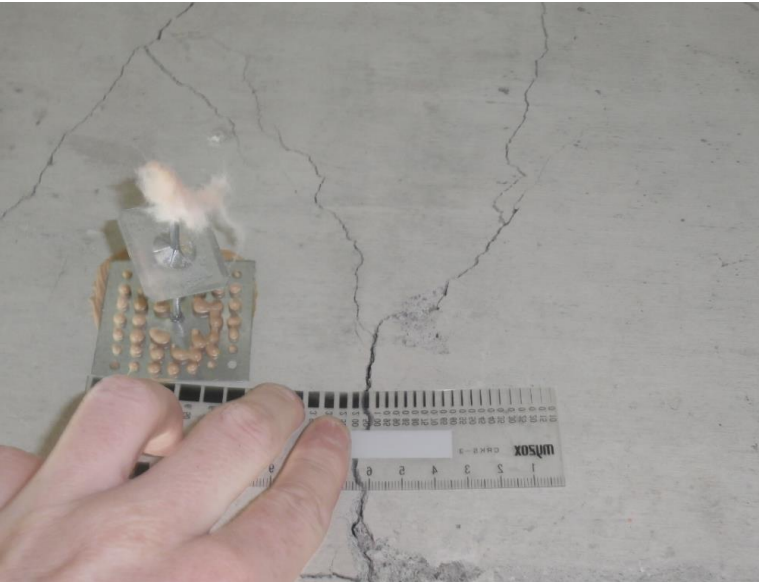
			The rightmost column of the table contains two photographs of concrete damage. The top photograph shows a close-up of a concrete surface with a large, irregularly shaped area of spalling or delamination, revealing a rough, porous interior. The bottom photograph shows a wider view of a concrete wall with several vertical and diagonal cracks. A small white tag is attached to the wall on the right side, and some faint markings are visible on the surface.
--	--	--	---

380/3 81	Elevation 1-Grid HA/KA. Beam column joint underside of level 3 DS 0 1 %	Diagonal cracking to beam column joint and column approx. 0.2 mm. Vertical cracking either side of beam column joint 0.3-1 mm. 5 hairline cracks along beam span.	
-------------	--	--	---

			
<p>382/3 83</p>	<p>Elevation 1-Grid KA. Beam column joint underside of level 3</p> <p>DS 1 2.0%</p>	<p>Diagonal cracking in column 0.2 mm. Vertical cracking either side of beam column joint 2.5 mm wide. Diagonal cracking spreading from beam column joint continuing to underside of beam 0.2-0.5 mm. 7 hairline cracks along beam.</p>	





			The table contains two photographs of concrete damage. The top photograph shows a vertical crack in a concrete wall, with two circular holes or indentations located below the crack. The bottom photograph shows a similar vertical crack in a concrete wall, with a ruler placed horizontally below it for scale. A hand is visible at the bottom of the ruler, pointing to the crack. The ruler is marked in centimeters and millimeters, and the crack is approximately 1.5 cm wide at the bottom.
--	--	--	--

			
<p>384/3 85</p>	<p>Elevation 1-Grid KA/N. Beam column joint underside of level 3</p> <p>DS 0 1 %</p>	<p>Diagonal hairline cracking in column.</p> <p>Diagonal cracking in each side of beam column joint spreading out into beam 0.2-1.5 mm wide.</p> <p>6 hairline cracks along beam span.</p>	





			The table contains three photographs of floor damage. The top photo shows a grey concrete floor with several cracks and a square metal grate with a hole in the center. The middle photo shows a similar floor with several white cables bundled together and running across it. The bottom photo shows the same floor with a ruler held against it for scale, showing the extent of the cracks and the metal grate.
--	--	--	--

			
386	Elevation 1-Grid N. Beam column joint underside of level 3 DS 1 2.0%	Vertical crack in beam at column face. Diagonal cracks in beam continuing to underside of beam approx. 2 mm. Spalling of column concrete. Crushing on concrete at column toe.	




			The rightmost column of the table contains two photographs stacked vertically. The top photograph shows a close-up of a concrete ceiling or wall corner with several prominent, jagged cracks. A small metal fastener is visible in the upper right corner. The bottom photograph shows a similar concrete surface with extensive cracking and a small metal fastener. A piece of white paper with a grid pattern is placed on the surface for scale. The overall appearance is one of significant structural damage to the concrete.
--	--	--	---

			
387	Elevation A-Grid 13. Beam column joint underside of level 5 DS 1 2.0%	Vertical crack at column face approx. 5 mm. Cracking 5 mm wide. Cracking to underside of beam. Diagonal cracks spread along the span of the beam.	





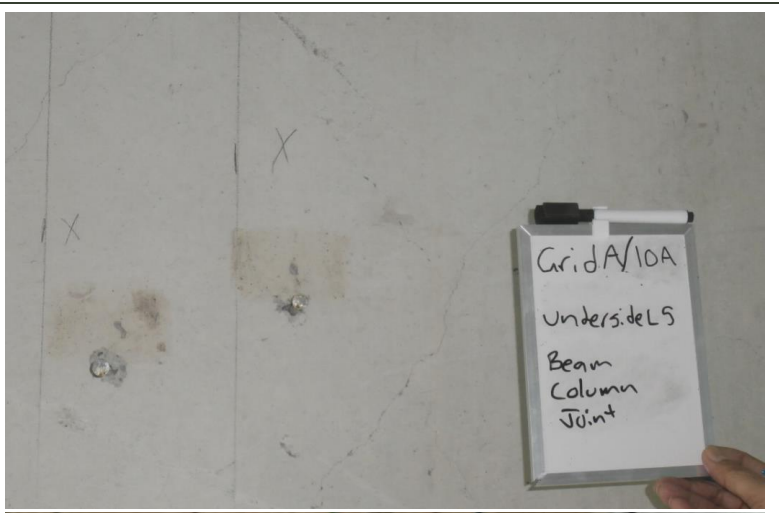
388

<p>288/3 89</p>	<p>Elevation A-Grid 13/10A. Beam column joint underside of level 5</p> <p>DS 1 2.0%</p>	<p>Diagonal cracking in column 0.3 mm. Diagonal cracking in beam column joint 1 mm wide. Vertical crack on RHS of beam column joint 2.5- 8 mm. Vertical crack on LHS of beam column joint 2 mm.</p>	
---------------------	---	---	---





			The rightmost column of the table contains three vertically stacked photographs. The top photograph shows a close-up of a crack in a light-colored concrete surface. A ruler is held horizontally across the crack, with a hand visible on the left side. The ruler has markings in centimeters and millimeters, with labels such as 4.50, 5.00, 5.50, 6.00, 6.50, 7.00, 7.50, 8.00, 8.50, 9.00, 9.50, and 10.00. The middle photograph shows a similar view of the crack and ruler, but from a slightly different angle, with a hand holding the ruler from below. The bottom photograph shows a wider view of the concrete surface, which appears to be a wall or ceiling. There is a horizontal crack and some discoloration or staining on the surface. A wooden floor is visible in the upper left corner of this photograph.
--	--	--	--

390/3 91	Elevation A-Grid 10A. Beam column joint underside of level 5 DS 1 2.0%	Diagonal cracking in column 0.3 mm wide. Vertical cracking either side of the beam column joint 2.5 mm wide. Diagonal cracking in beams either side of beam column joint 0.6 mm wide. Some spalling of concrete on underside of beam.
-------------	--	--







			<p>The table contains four photographs documenting structural damage to a concrete ceiling. The top photo shows a concrete surface with a circular mark and a small hole. The second photo shows a corner with significant cracking and spalling. The third and fourth photos are close-ups of a crack being measured with a ruler, showing a width of approximately 1.00 mm.</p>
--	--	--	---


			
<p>392/3 93</p>	<p>Elevation A-Grid 10A/8A. Beam column joint underside of level 5</p> <p>DS 1 2.0%</p>	<p>Diagonal hairline cracking in column. Diagonal cracking in beam column joint 0.6 mm wide. Vertical cracks either side of beam column joint 2 mm wide.</p>	








			The rightmost column of the table contains three vertically stacked photographs documenting structural damage. The top photograph shows a vertical crack in a concrete slab. The middle photograph shows a bundle of rebar protruding from the concrete, secured with white ties. The bottom photograph is a close-up of a crack in the concrete with a ruler placed alongside it for scale, showing the crack's width and depth.
--	--	--	---


			
394	Elevation A-Grid 8A. Beam column joint underside of level 5 DS 2 2.75%	Vertical crack at column face, continues under the beam. Approx. 5 mm separation. Diagonal cracking spreading from beam column joint 1-5 mm. Spalling of concrete in column.	





<p>395</p>	<p>Elevation HA-Grid 8A. Beam column joint underside of level 5 DS 1 2.0%</p>	<p>Vertical crack at column face approx. 2 mm.</p>	
<p>396/3 97</p>	<p>Elevation HA-Grid 8. Beam column joint underside of level 5</p>	<p>No access at time of inspection</p>	
<p>398/3 99</p>	<p>Elevation HA-Grid 7. Beam column joint</p>	<p>No access at time of inspection</p>	

	underside of level 5		
400/401	Elevation HA-Grid 6. Beam column joint underside of level 5 DS 0 1%	Diagonal hairline cracking in column. Vertical cracking either side of beam column joint 1 mm wide.	
402/403	Elevation HA-Grid 5. Beam column joint underside of level 5	Vertical cracking either side of beam column joint approx. 0.5 mm wide.	
404/405	Elevation HA-Grid 4. Beam column joint underside of level 5 DS 1 2.0%	Vertical crack LHS of beam column joint 2 mm wide. Vertical crack RHS of beam column joint 0.5 mm.	

			
406/4 07	Elevation HA-Grid 3. Beam column joint underside of level 5 DS 0 1 %	Vertical cracks either side of beam column joint 0.5-1 mm. Hairline diagonal cracks present in beam span.	



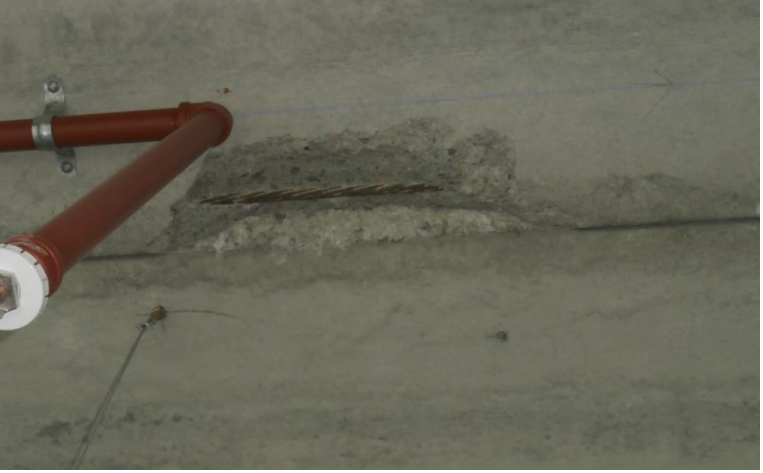
408/4 09	Elevation HA-Grid 2. Beam column joint underside of level 5 DS 1 2.0%	1.5 mm wide vertical crack LHS of beam column joint. Spalling of concrete at top of beam. 1 mm wide vertical crack RHS of beam column joint.	
-------------	---	---	---




			
410	Elevation HA-Grid 1. Beam column joint underside of level 5 DS 1 2.0%	Vertical crack at column face continuing to underside of beam approx. 5 mm. Spalling of concrete in column.	






			<p>The table contains three photographs documenting structural damage. The top photograph shows a corner where a concrete wall meets a concrete floor. A large, jagged crack runs along the wall, and a metal pipe is visible above the floor. The middle photograph shows a horizontal crack in a concrete wall, with a small electrical outlet and a light switch visible above it. The bottom photograph shows a close-up of a concrete floor with a prominent vertical crack and some surface staining.</p>
--	--	--	---

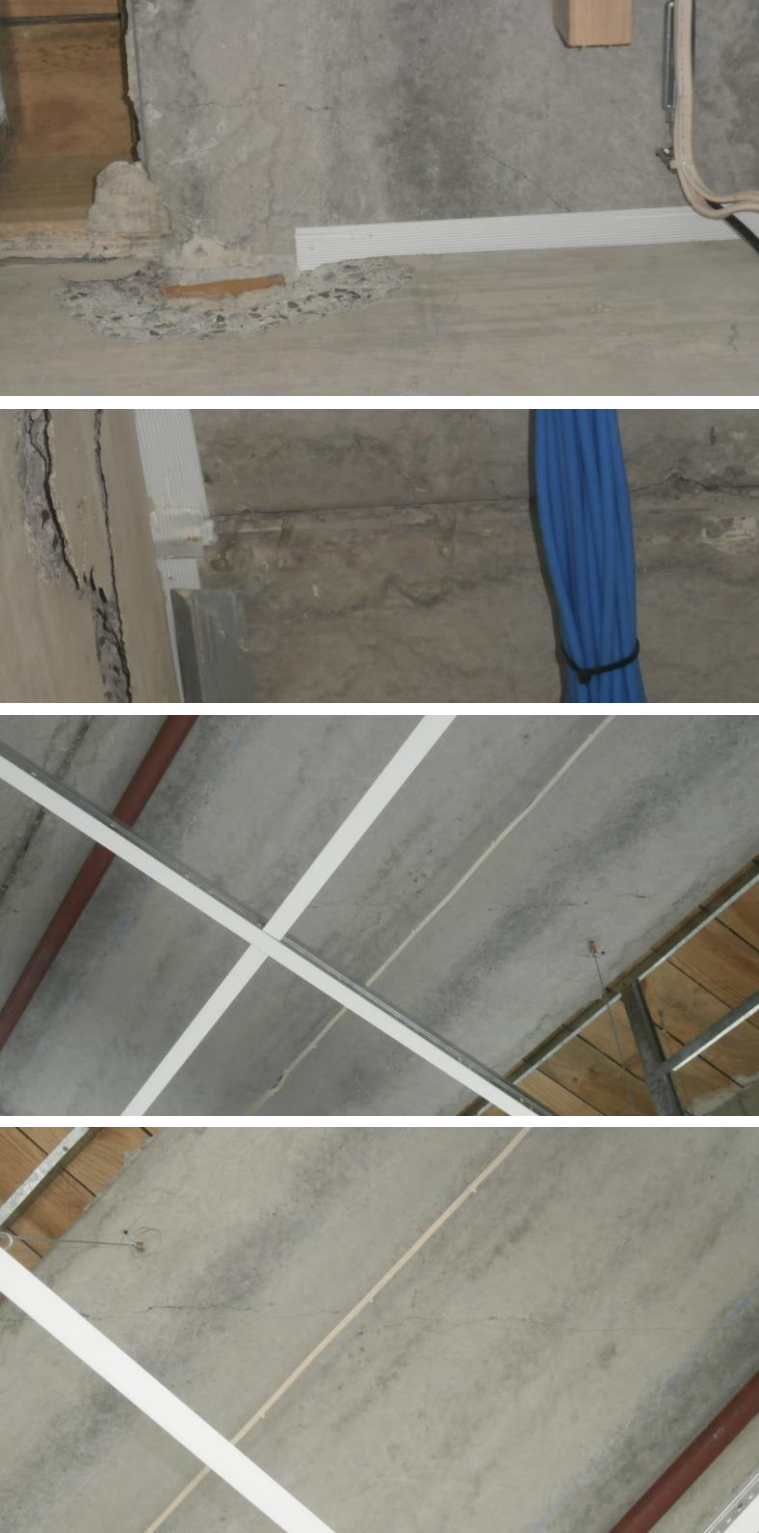


			
411-489	Frames on grid lines 13,10A,KA and N	Frames along these grid lines were not assessed.	
490	Dycore units Underside of level 5. Grid numbers between 1-2 and HA-KA.	Diagonal cracking in corner HA approx. 2 mm. Concrete loss in middle of slab exposing tendon.	 



491	Dycore units Underside of level 5. Grid numbers between 1-2 and KA-N.	Diagonal cracking in corner 1/N approx. 2 mm.	
492	Dycore units Underside of level 5. Grid numbers between 2-3 and HA-KA.	Concrete spalled at end on grid HA/2-3.	
493	Dycore units Underside of level 5. Grid numbers between 2-3 and KA-N.	No access at time of inspection.	
494	Dycore units Underside of level 5. Grid numbers between 3-8 and HA-KA.	Longitudinal crack from Grid point HA/4 along half span of slab.	
495	Dycore units	No access at time of inspection.	


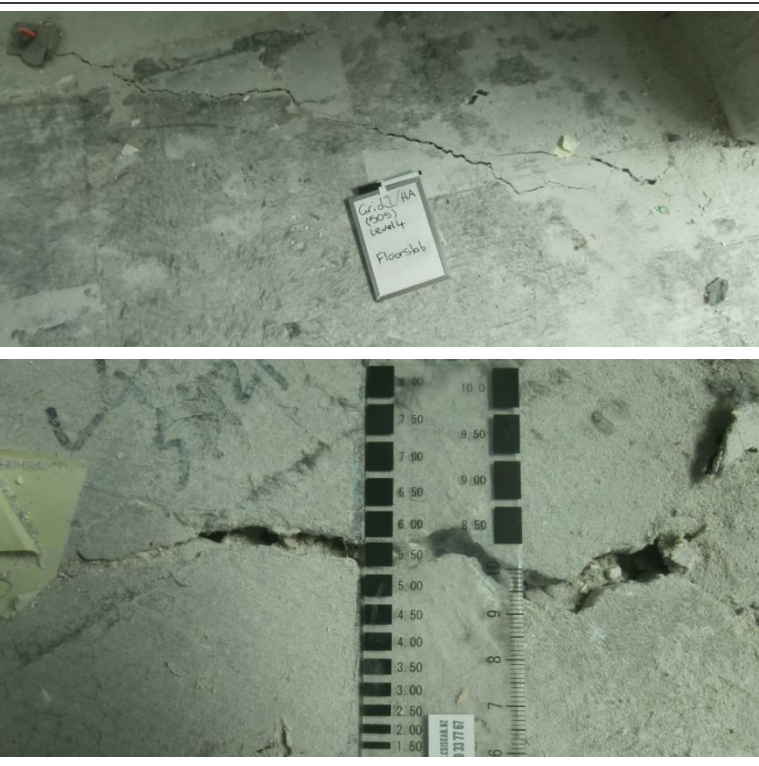
	Underside of level 5. Grid numbers between 3-8 and KA-N.		
496	Dycore units Underside of level 5. Grid numbers between 8-10A and H-KA.	No access at time of inspection.	
497	Dycore units Underside of level 5. Grid numbers between 8-13 and KA-N.	No access at time of inspection.	
498	Dycore units Underside of level 5. Grid numbers between 10A-13 and H-N.	No access at time of inspection.	
499	Dycore units Underside of level 5. Grid numbers between 10A-13 and C-H.	No access at time of inspection.	

<p>500</p>	<p>Dycore units Underside of level 5. Grid numbers between 8A-10A and C-H.</p>	<p>Longitudinal cracks between Grids F-G approx. 1.5 mm run as far as exposed.</p>	
<p>501</p>	<p>Dycore units Underside of level 5. Grid numbers between 10A-13 and B-C.</p>	<p>No access at time of inspection.</p>	
<p>502</p>	<p>Dycore units Underside of level 5. Grid numbers between 8A-10A and B-C.</p>	<p>Longitudinal crack from point 8A/C spanning approx. half the slab approx. 1.5 mm.</p>	

503	Dycore units Underside of level 5. Grid numbers between 10A-13 and A-B.	Diagonal cracking in corner A13 loss of concrete in beam. Beam damage in beam spanning grid line 10A, decrease in slab seating. Diagonal crack along mid span of slab.	 <p>The image block contains four photographs documenting structural damage. The top photo shows a corner where concrete has been lost from a beam. The second photo shows a beam with a vertical crack and a blue corrugated metal pipe nearby. The third and fourth photos show diagonal cracks in a concrete slab, with white and yellow markers used for measurement and identification.</p>
-----	--	---	---



			
504	Dycore units Underside of level 5. Grid numbers between 8A-10A and A-B.	Loss of concrete at hole in underside of Dycore. Suspected during installation. Diagonal cracking at corner A/8A.	



			
505	<p>Floor slab level 4. Grid numbers between HA-KA and 1-2.</p>	<p>Diagonal cracking spreading from corner column 1/HA 1-5.5 mm wide.</p> <p>9 mm transverse crack running along frame KA.</p> <p>Longitudinal crack running close to frame 2 approx. 1.5 mm.</p>	



			Three stacked photographs showing concrete damage. The top photo shows a corner with a crack and a green marker. The middle photo shows a crack with orange markings. The bottom photo shows a large area of spalled concrete.
--	--	--	--



			<p>The table contains four photographs documenting concrete damage. The top photograph shows a close-up of a vertical crack in a concrete surface, with a ruler and a scale placed horizontally above it for measurement. The middle photograph shows a wide view of a concrete slab with a prominent vertical crack. The bottom photograph is a close-up of a jagged, irregular crack in the concrete, with a ruler and scale placed vertically to its right.</p>
--	--	--	--

			
506	<p>Floor slab level 4. Grid numbers between KA-N and 1-2.</p>	<p>9 mm Transverse crack running along frame on grid KA.</p> <p>Diagonal cracking spreading from corner column 1/N 1.5-5 mm wide.</p> <p>Transverse cracking along outer frame on grid N approx. 1.5 mm wide.</p> <p>Diagonal cracking spreading from column 1/KA/N approx. 2 mm.</p>	



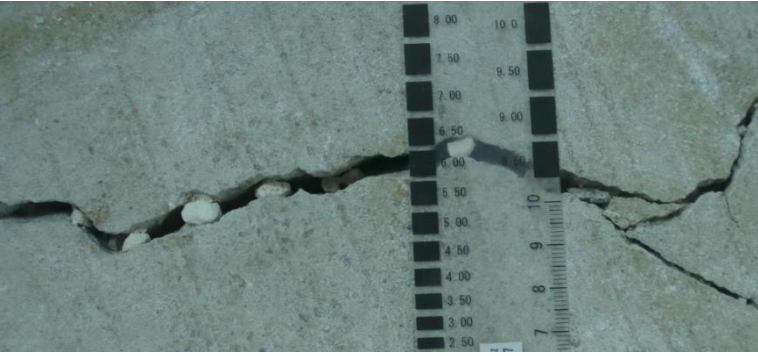

			
507 to 517	Floor slab level 4.	No access at time of inspection.	

<p>518</p>	<p>Floor slab level 4. Grid numbers between A-B and 8A-10A.</p>	<p>Longitudinal crack running along outer frame on grid A, 2.5 mm wide. Loss of cover concrete, reinforcement exposed. Vertical dislocation present. Longitudinal crack running along Grid B approx. 2 mm wide. Diagonal cracking spreading from corner column A/8A, largest crack 7.5 mm wide. Transverse crack running along internal frame at Grid 10A 4 mm wide.</p>
------------	--	--





			The table contains three photographs of a cracked concrete floor slab. The top photograph shows a wide, irregular crack in the concrete with a small white tag placed on the surface. The tag has handwritten text: "Grid A/B/A", "(518)", "Level 4", "Floor", and "Slab". The middle photograph is a close-up of the crack, showing a ruler placed across it for scale. The ruler is marked in centimeters and millimeters. The bottom photograph shows a wider view of the cracked area, with a small white tag on the floor and a metal cabinet visible in the background.
--	--	--	---

			
519	<p>Floor slab level 4. Grid numbers between A-B and 10A-13 .</p>	<p>Diagonal cracking spreading from corner column A/13 0.9-6 mm wide.</p> <p>Diagonal crack starting at column A/13/10A 1-9 mm wide with vertical dislocation.</p> <p>Longitudinal crack running along Grid B approx. 1.5 mm wide.</p> <p>Transverse crack along inner frame on Grid 10A 2 mm wide.</p>	  



			<p>The table contains three photographs documenting damage to a concrete floor slab. The top photograph shows a close-up of a crack in the slab with a clipboard placed on it for scale. The clipboard has handwritten text: "Grid A/130A (S19)", "Level 4", and "Floor Slab". A red pencil is also visible. The middle photograph shows a red spirit level placed on the slab next to a large, irregular hole where concrete has been removed. The bottom photograph shows a wider view of the slab with several cracks and a person's feet standing nearby for scale.</p>
--	--	--	---



			<p>The table contains three photographs documenting concrete damage. The top photograph is a close-up of a vertical crack in a concrete surface. A black ruler is placed horizontally above the crack, and a white ruler is placed horizontally below it. Handwritten in black marker on the concrete are the alphanumeric string 'L4GA10A/B' and the date '5/12/16'. The middle photograph shows a long, irregular crack on a light-colored concrete floor. A red marker with the letters 'WGA' is placed on the floor near the crack. A person's foot in a black boot is visible on the left side of the frame. The bottom photograph shows another view of a crack on a concrete floor, with a wooden beam visible in the background.</p>
--	--	--	--



			<p>The table contains three photographs documenting a crack in a concrete floor slab. The top photograph shows a wide view of the slab with a prominent crack running across it. The middle photograph is a close-up of a whiteboard with handwritten text: "Grid A/13 16A (S19)", "Level 4", and "Floor Slab", with a ruler placed next to the crack. The bottom photograph shows the whiteboard and ruler from a different angle, further highlighting the crack's path.</p>
--	--	--	--



			A photograph showing the lower legs and feet of a person walking on a light-colored concrete floor. The floor exhibits several prominent vertical and diagonal cracks, indicating structural damage. The person is wearing dark trousers and dark shoes.
--	--	--	--

Case Study 2

References

- ASCE, 2017, *Seismic Evaluation and Retrofit of Existing Buildings*, ASCE/SEI 41-17, American Society of Civil Engineers, Reston, Virginia.
- ATC, 1985, *Earthquake Damage Evaluation for California*, ATC-13, Applied Technology Council, Redwood City, California.
- ATC, 2020, *Resilient Repair Guide Source Report*, ATC-145-1, Applied Technology Council, Redwood City, California.
- Aurecon, 2017, *Kaikoura Earthquake Damage Report for Confidential Building*, Aurecon, Wellington, New Zealand.
- Bradley et al., 2017, "Ground motion and site effect observations in the Wellington region from the 2016 MW7.8 Kaikoura, NZ earthquake," *Bulletin of the New Zealand Society for Earthquake Engineering*, Vol. 50, No.2.
- Brooke, N., 2021, Personal Interview, August 12, 2021.
- CSI, 2020, "ETABS," Computers and Structures, Inc., v. 19.0.2, Berkeley, California.
- Dellow, et al., 2017, Landslides Caused by the MW7.8 Kaikoura Earthquake and the Immediate Response, *Bulletin of the NZSEE* Vol. 50, No. 2.
- FEMA, 2018, *Seismic Performance Assessment of Buildings*, FEMA P-58 prepared by the Applied Technology Council for the Federal Emergency Management Agency, Washington, D.C.
- Semmens, S, 2004, *NZS 1170.5 Site Subsoil Classification of Wellington City*, in Ninth Pacific Conference on Earthquake Engineering, Auckland, New Zealand.
- Standards New Zealand, 2004, *New Zealand Standard 1170.5*, Standards New Zealand, Wellington, New Zealand.